The Thesis Committee for Kevin Lee Moyer
Certifies that this is the approved version of the following thesis:

Assessment of Long-Term Corrosion Resistance of Recently Developed Post-Tensioning Components

APPROVED BY
SUPERVISING COMMITTEE:

Co-Supervisor: _____
Sharon L. Wood

Co-Supervisor: _____
John E. Breen

_____
Harovel G. Wheat

Assessment of Long-Term Corrosion Resistance of Recently Developed Post-Tensioning Components

by

Kevin Lee Moyer, B.S.C.E.

Thesis

Presented to the Faculty of the Graduate School of

The University of Texas at Austin

in Partial Fulfillment

of the Requirements

for the Degree of

Master of Science in Engineering

The University of Texas at Austin

August, 2012

Dedication

To my wife, family, and friends

Acknowledgements

There are many people I would like to thank. The most important person is my lovely wife, Holly. Without her, this journey would have not been possible. I know she will be glad to have her husband back and as she says, “I won’t be a school widow any longer.” I cannot say thank you enough to Dr. Breen. His timely answers to my questions helped keep the research going. I will miss the meetings where we talk about the project for a few minutes and the rest of the time was spent listening to you stories. Those meetings gave me a much needed break. To Dr. Wood and Dr. Wheat, thank you for taking the time to review this thesis and give me your suggestions. I must thank Michael Weyenberg. Without your help, I would not have been able to keep on schedule and not been able to finish this thesis on time. To the FSEL staff thank you for giving me a hand when I needed it. To my friends and family, thank you for your patience and understanding.

July 10, 2012

Abstract

Assessment of Long-Term Corrosion Resistance of Recently Developed Post-Tensioning Components

Kevin Lee Moyer, M.S.E.

The University of Texas at Austin, 2012

Co-Supervisor: Sharon L. Wood

Co-Supervisor: John E. Breen

The forensic analysis of fourteen post-tensioned beam specimens after six years of aggressive exposure testing is the focus of this thesis. Funding for this research came from TxDOT and FHWA. Current post-tensioning materials and construction practices have been deemed inadequate due to fairly recent corrosion failures. Recently developed post-tensioning components and systems were assessed to determine their suitability to prevent durability concerns that had been found in older structures. Testing was conducted on the following variables:

- Strand Type
- Duct Type
- Duct Coupler Type
- Anchorage Type
- Electrically Isolated Tendons

Non-destructive and destructive testing methods were used to study the specimens and were evaluated on their effectiveness in predicting corrosion. Service life analysis was done on a structure using the strands and ducts study in the project.

Galvanized duct showed substantial pitting and area loss. The majority of the plastic ducts had no observed damage. However, tendon grout chloride concentrations in most cases were extremely elevated with both galvanized and plastic ducts. This indicated that moisture had entered the duct, through either the couplers and/or grout vents. Except for strands from one specimen, the strands had minor corrosion with occasional mild pitting. The exception had heavy mild pitting confined to a small portion of the strand due to a hole in the duct. Backfill quality was good but it did not bond well with the base concrete. Therefore, moisture and chlorides entered the anchorage region. The electrically isolated tendon did not perform as well as expected. The grout chloride concentrations and level of corrosion damage were comparable to the concentrations and corrosion damage from the more conventionally protected specimens.

TABLE OF CONTENTS

List of Tables

List of Figures

CHAPTER 1

Introduction

1.1 Background

Post-tensioned concrete is widely used world-wide for the construction of various structures. For example, it is used in slab foundations to control the cracking of slabs that might experience differential settlement due to poor soil conditions. It is also used for bridge spans that are too long for conventional reinforced concrete beams. Some additional benefits of post-tensioned concrete are the increase of the cracking moment, which increases the durability of the concrete, better deflection control, and the post-tensioned sections can be mass produced, which lowers the cost of construction. However, while post-tensioning increases the cracking moment, it does not increase the ultimate strength of a post-tensioned element.

Post-tensioned sections are generally prestressed with high strength seven wire strands that keep the section completely in compression or sometimes just below the tensile strength of the concrete under design loads. The tendons, multiple strands, are stressed in a duct that has been precast into the concrete section and the duct can either be grouted (bonded tendon) or left un-grouted (unbonded tendon). The tendons bear against an anchorage plate and the strands are held in place by an anchor head and wedges. See Figure 1.1 for a detail of the components of a post-tensioning system.

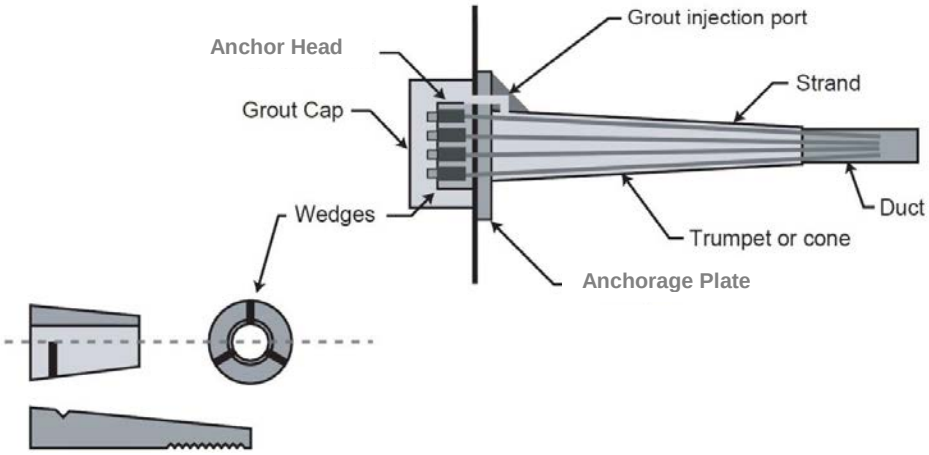

Figure 1.1: Detail of the Components of a Post-Tensioning System[28]

1.2 Durability

Durability of post-tensioned concrete is increased over that of reinforced concrete because the concrete is initially under compression and the precompressed tensile fibers have to completely overcome this compression before it can crack. Durability is also increased because of the many layers of protection that post-tensioned tendons have. The tendons are protected against corrosion by cover concrete, by the duct that they are stressed in, the grout they are encased in, and if strands are coated (such as with epoxy) this presents a final barrier. While under service loads the post-tensioned element might still have cracking due to overloads, bursting stresses in the anchorage region, and diagonal tension, which can affect the durability of the concrete. Another area of concern regarding durability, for segmental post-tensioned construction, is construction joints. All these factors that affect durability are a concern for chloride infiltration that promotes corrosion of the highly susceptible, very high strength wires. While cracking initially increases the corrosion rate from chloride infiltration, over time a specimen of the same concrete that is uncracked will eventually reach the same corrosion rate as the cracked specimen. See Figure 1.2 for a comparison of cracked and uncracked corrosion rates.

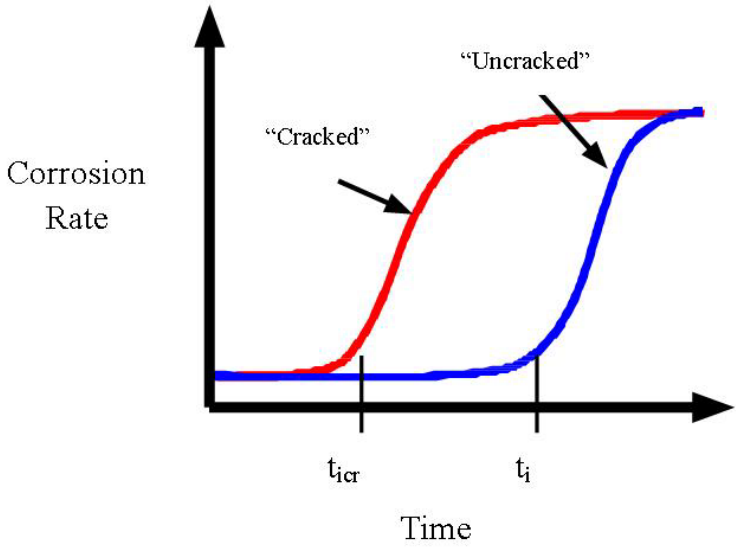

Figure 1.2: Over Time Corrosion is Similar in Cracked and Uncracked Concrete[8]

While the durability of post-tensioned concrete can be increased, it is not immune to the effects of corrosion. Post-tensioning strands are made of seven very high strength wires that have more surface area per volume than the comparable traditional reinforcement, which would lead to a greater corrosion rate. For this reason, corrosion in post-tensioned concrete is especially a major concern. Losing even a small area of strand could be unfavorable because post-tensioned elements have much less steel area than comparable traditional reinforced elements and the post-tensioning strands are initially stressed to between 60 and 75% of their ultimate strength. Depending on the redundancy of the structure and location of the tendon, corrosion of a tendon might ultimately lead to serviceability issues or even collapse of the structure.

1.3 Corrosion in Concrete

In 2002, it was estimated that corrosion in highway bridges in U.S. costs the American tax payer $8.7 billion per year[31]. For this reason and the safety of the public, many studies have been performed on the effects of corrosion on post-tensioned concrete.

There have been a few instances of post-tensioned structures failing or in danger of failing. One failure happened in West Glamorgan, Great Britain in December of 1985.

The structure was a post tensioned segmental bridge named the Ynysygwas Bridge built in 1952, the dawn of prestressed concrete. The failure was sudden and due to corrosion of very poorly protected longitudinal prestressing strands[32]. The Sunshine Skyway Bridge in Tampa, Florida, on the other hand, did not fail but severe corrosion was found on September 21, 2000 in the precast segments of the hollow piers[33](see Figure 1.3). The environment of high humidity and salt spray is conducive to this type of corrosion.

Figure 1.3: Tendon Corrosion in the Sunshine Skyway Bridge Piers[33]

Concrete and grout create an environment that is favorable to steel. The pH of the pore water in cured concrete is around 12 to 13. A pH this high will allow the formation of a passive layer which is primarily iron hydroxide. This passive layer creates a protective coating on the steel, which if undamaged will protect the steel from corrosion. See Figure 1.4 for the active –passive behavior of steel. Chloride infiltration will damage

this passive layer and induce pitting. There have been many theories on how chlorides destroy the passive layer. One of the theories is that the chlorides locally decrease the pH of the pore solution therefore destroying the passive layer promoting pitting. Another theory is the absorption of Cl^- will displace the O^{2-} from the passive layer eventually breaking down the passive layer. Finally, the introduction of chloride ions will lower the "interfacial surface tension", eventually resulting in cracks and flaws, which weaken the passive layer[34].

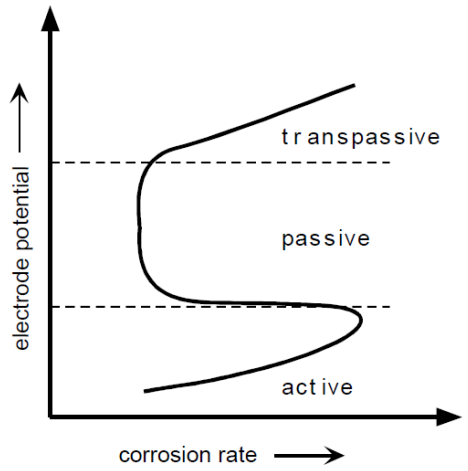

Figure 1.4: Active-Passive Behavior of Steel[6]

The corrosion of mild reinforcement and strands in concrete is detrimental to the durability of the concrete and therefore to the performance of the concrete. The corrosion product commonly known as rust has a greater volume then the iron that produced it. This increase in volume creates internal tensile forces in the concrete and ultimately leads to cracking. This cracking will lead to even more oxygen, moisture, and chlorides getting to the steel which will lead to further corrosion and further cracking. The electrochemical half- cell reactions of iron are governed by Equations 1.1 and 1.2[35]:

$Fe \rightarrow Fe^{2+} + 2e^-$ (anodic half-cell reaction) ***Equation 1.1***

$2H_2O + O_2 + 4e^- \rightarrow 4OH^-$ (cathodic half-cell reaction) ***Equation 1.2***

Rust, $Fe(OH)_3$, is formed through a number of reactions due to formation of an anode (oxidation) and a cathode (reduction) on the metal surface. See Figure 1.5 for a diagram of the corrosion process in steel. A summary of these reactions is shown in Equations 1.3 and 1.4[35].

$$2Fe + 2H_2O + O^2 \rightarrow 2\,Fe^{2+} + 4OH^- \rightarrow 2Fe(OH)_2$$ ***Equation 1.3***

This will further react to produce:

$$2Fe(OH)_2 + H_2O + 1/2O_2 \rightarrow 2\,Fe(OH)_3$$ ***Equation 1.4***

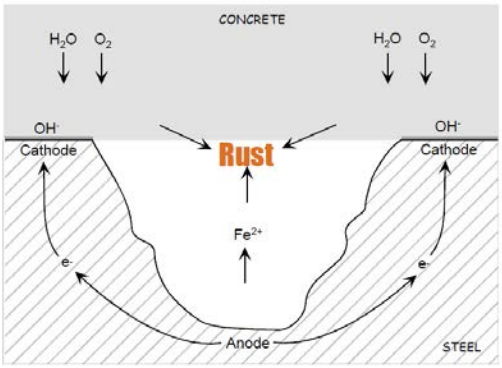

Figure 1.5: Corrosion of Steel in Concrete[6]

Post-tensioning strands are also susceptible to many other forms of corrosion, such as: crevice corrosion, pitting, stress corrosion cracking (SCC), hydrogen embrittlement, fretting fatigue, and corrosion fatigue cracking (CFC).

There are many solutions for improving corrosion resistance in post-tensioned concrete. Low permeability of concrete, proper grouting of tendons, and proper detailing are some of the solutions for reducing corrosion in post-tensioned concrete.

Low permeability of the concrete might not stop the egress of chloride ions into the concrete but it will substantially slow the egress of chlorides. Low permeability is usually controlled by using cementious materials to replace a portion of the cement and having a low water to cement ratio. A low water to cement ratio on the other hand

decreases the workability of the concrete so plasticizers need to be used to increase the workability.

Proper grouting of ducts is crucial to the protection of the tendons. If any voids are left in the duct due to bleed water and improper grouting procedures and if galvanized ducts are used, these voids will be attractive sites for corrosion of the ducts and eventual egress of chlorides to the tendon. This can be controlled using the proper grout and proper installation of the grout.

Proper detailing is another way to inhibit corrosion in post-tensioned structures. Placing the anchorage region away from drainage areas will slow the egress of chloride laden water into the anchorage region, a critical area for corrosion. The anchorage region is a critical area for corrosion due to the strands losing cross sectional area from the wedges and the crevices that the wedges create. Using the proper splice techniques at duct junctions is also crucial. If splices are not installed properly or the wrong type of splice is used, chlorides can infiltrate the duct.

1.4 Project Objective

The objective of TxDOT Project 0-4562 is to evaluate the long-term corrosion resistance of recently developed post-tensioning components and compare the results with more traditional systems (conventional strand encased in grout in galvanized steel duct). The project is being funded by the Texas Department of Transportation (TxDOT) and the Federal Highway Administration (FHWA). Passive and accelerated corrosion testing and mechanical testing were conducted on each strand type to determine their corrosion resistance and mechanical properties. Various strands, ducts, couplers, and protection systems are being evaluated in full scale beam specimens under aggressive exposure conditions. After four and six years of aggressive exposure, the full-scale beam specimens will be autopsied and the recently developed components will be evaluated to compare their performance with the traditional components.

1.5 Thesis Objectives and Scope

The objectives of this thesis are:

- To explain the justification for the design and testing methods for the specimens.
- To report the results of the passive and accelerated corrosion testing and mechanical testing.
- To assess the performance after six years of aggressive exposure to chlorides of epoxy coated mild steel components, post-tensioning ducts, strands, anchorages, and electrically isolated tendons of the final 14 specimens of Project 0-4562
- To present the results of the destructive testing and non-destructive monitoring of the specimens and assess the accuracy of the procedures.
- To present the analysis of the estimated construction cost increases of a typical segmental bridge related to the use each type of strand, duct, anchorage, and protection system
- To present the analysis of the service life estimates of a bridge that is using various combinations of each duct and strand type.
- To use the findings of the autopsies to develop recommendations for corrosion design.

The scope of this thesis includes:

- Analysis of non-destructive and destructive measurements taken during six years of aggressive exposure of the final 14 specimens of Project 0-4562.
- Autopsy and analysis of the final 14 specimens
- Recommendations based on the findings of this research for post-tensioned design

CHAPTER 2

Test Specimens

The basic design and construction details presented herein are based on Reference 1. Michael Ahern was the graduate research assistant who originally designed and constructed the specimens. He was assisted by Gregory Turco and Turco initiated exposure testing on some of the specimens.

2.1 Specimen Concept

A major factor in the design of the specimens was their size. The project needed a compact specimen that would produce comparative durability results in a timely fashion, the post-tensioning components were isolated, and cracking performance could be managed. Size was also a major factor due to the number of different component combinations, the limited amount of storage space for long term exposure, ease of handling during exposure and autopsies, and financial concerns.

Project 0-1405, the predecessor to present Project 0-4562, used large beams, which took up a considerable amount of space. The specimens consisted of identically dimensioned beams double stacked. The bottom beam, heavily reinforced, served as a reaction beam for the upper beam, which was post-tensioned to a range of levels and the focus of the project. The ponding region was the width of the beam, four feet long, and centered along the length of the specimen. The dimensions of the Project 0-1405 beams were 15 feet – 2 inches in length, 1.5 feet wide, and 2 feet tall. The ponding area was about 25% of the total top surface area of the beam. As well as having a ponding area, the specimens were sprayed on the dead end anchorage zone.

The Project 0-4562 specimens were designed using fewer materials but to approximate the same type and quantity of results as the previous project. The each Project 0-4562 specimen that utilized the conventional post-tensioning system had two ducts with three strands per tendon and a ponding area. The ponding area for Project 0-4562 specimens is three feet long, is centered along the length of the beam and is 50% of

the top surface area of the beam. The amount of exposed duct and strand of each specimen for both projects is comparable. Like the Project 0-1405 specimens, the Project 0-4562 specimens had their dead end anchorages sprayed with salt water but only ten of the 24 Project 0-4562 specimens were sprayed. Unlike the Project 0-1405 specimens, the Project 0-4562 specimens had all loads self-contained. Therefore, no reaction beam was needed. Figure 2.1 provides a comparison of the specimen sizes for the two different projects.

Figure 2.1: Project 0-1405 Specimens (Background) and Project 0-4562 Specimens (Foreground)[1]

The concrete surrounding the post-tensioning ducts of the Project 0-4562 specimens was pre-cracked before exposure and a reduced concrete cover was used to provide an aggressive environment for the research materials. The concrete cover at the apex of the duct was 1-3/8 inches. While post-tensioned concrete is often uncracked in usage, in order to provide direct access of moisture and chlorides to the post-tensioning components in these aggressive tests the specimens were designed to be cracked. Cracking was controlled in the ponding area by reducing the cross-section and moment of inertia, having a midsection lightly reinforced with longitudinal mild steel, and applying a uniform moment over the ponding area. The uniform moment was induced by applying an eccentric force with Dywidag bars through a conduit, PVC pipe, in the center of the

corbels. The target crack width within the ponding area was 0.010 inch. This width was based on the research on post-tensioned durability in Reference 5. A cracked specimen is shown in Figure 2.2.

Figure 2.2: Cracked Project Project 0-4562 Specimen[1]

Due to the extremely severe corrosion of the Project 0-1405 specimens' uncoated transverse reinforcement, with resulting substantial damage to the cover, and the possibility of the uncoated reinforcement corroding and interfering with the half-cell potential readings of the Project 0-4562 specimens, it was decided that epoxy coated reinforcement would be used for all reinforcement other than the post-tensioning tendons. Such epoxy coated non-prestressed reinforcement is widely used in U.S. bridge construction. It was also decided that plastic bar chairs would be used instead of metal for the management of concrete cover for the same reasons.

2.2 Specimen Description

The conventionally post-tensioned Project 0-4562 specimens were 6 feet in length and the fully encapsulated Project 0-4562 specimens were 7 feet in length. Both types were 17 inches wide. Over the midsection of the specimens the depth was 15 inches and at the corbels the depth was 27 inches. As mentioned before, the corbels had a PVC conduit precast into them for Dywidag bars that were used for the application of an eccentric axial live load to crack the specimens. Railroad springs were used to keep the

eccentric Dywidag force reasonably constant throughout the duration of the exposure period.

The conventional post-tensioned specimens had two tendons that ran the length of the specimen whereas the fully encapsulated specimens had one tendon. The fully encapsulated specimens had only one tendon due to spacing constraints caused by the size of the anchorage components. Each tendon consisted of 3 strands with sizes 0.5 inch or 0.6 inch diameter. The 0.6 inch strands were the stainless steel and stainless steel clad, all others were 0.5 inch. The 0.6 inch strands were used because of availability limitations. See Reference 1 for a more comprehensive description of the design process.

2.3 Specimen Notation

Only 24 of the 28 concrete specimens initially constructed underwent exposure testing because of difficulty in procuring electroplated galvanized strand. Three of the four unexposed specimens are still in dry storage. The fourth specimen was autopsied by McCool[2] in 2010 as a control specimen. The identification system shown in Figure 2.3 and used for the specimens is based on the casting group and the types of components that the specimen contains. A complete list of the specimens is contained in Appendix A.

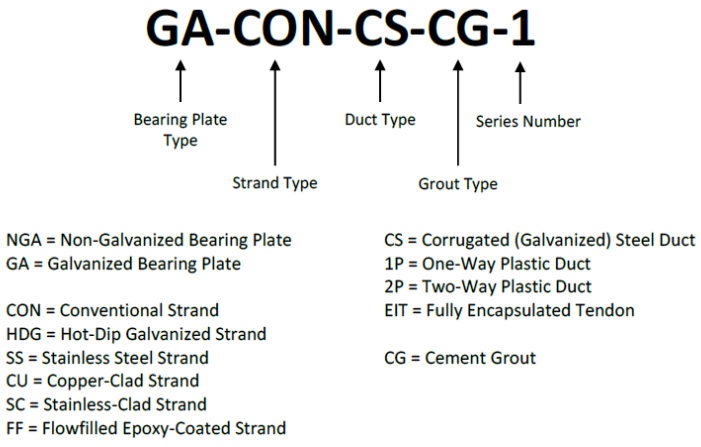

Figure 2.3: Specimen Identification System[1]

For simplicity, the specimens were referred to by the series number and the specimen in that series. Such as, specimen 4.1 is in series 4 and is the first specimen in that series and is also identified as NGA-SS-1P-CG-4.

2.4 Specimen Variables

The findings from References 5, 6, 7, and 8, Project 0-1405, concluded that the then common post-tensioning practices and materials were not providing adequate corrosion protection. Because of these inadequacies, Project 0-4562 was conceived to find and evaluate recently developed post-tensioning components. In 2003, an assembly of various members of the post-tensioning community met at Ferguson Structural Engineering Laboratory (FSEL) to identify new materials and industry trends to be evaluated. From this assembly, a list of post-tensioning components was compiled. See Table 2.1 for the list of specimens and their components. The list of suppliers is contained in the Appendix B.

Table 2.1: Final Specimen Matrix [2]

Duct	Prestressed – Strand Type						Non-Prestressed
	Conventional	Hot Dip Galvanized	Copper Clad	Stainless Clad	Stainless	Flowfilled	
Galvanized	G – 1.4 NG -1.1 G – T.2 NG – T.1	NG – 2.2	NG – 1.2	NG – 1.3	NG – 4.1		
One-Way Ribbed Plastic	NG – 2.3	NG – 3.4	NG – 2.4		NG – 4.2		
Two-Way Ribbed Plastic	G – 5.1* NG – 3.1*	NG – 3.2*	NG – 3.3*	NG – 5.2*	NG – 5.3*		
Fully Encapsulated	NG – 7.1* NG- 7.2*	NG – 7.3*				NG – 7.4*	
None							black – 4.4 epoxy – 4.3

G = Galvanized Bearing Plate; NG = Non-galvanized Bearing Plate
= Autopsy performed in March 2010 = Autopsy performed in March 2012
* = Dead end anchorage exposure
Note: For each specimen with plastic ducts, one duct is coupled and the other is continuous
For specimens with galvanized ducts, both ducts were continuous

2.4.1 Strand Type

Out of the seven types of strands initially proposed for evaluation only six were available for evaluation. The electroplated galvanized strands were not able to be provided by any supplier. The list of strand types used is as follows:

- Conventional
- Hot Dip Galvanized
- Stainless Steel
- Stainless Clad
- Copper Clad
- Flow Filled, Epoxy Coated

All strands were seven wire and 0.5 inch, except for the stainless steel and stainless clad strands. The stainless steel and stainless clad strands were 0.6 inch. Due to the size of the stainless and stainless clad, special bearing plates had to be milled. Special wedges had to be obtained for the flow filled strands so the strands would not slip during stressing operations. The interstitial space of the hot dip galvanized is not coated with zinc due to the galvanizing process, thus leaving the interstitial space unprotected. Furthermore the galvanizing process reduces the tensile strength of the strand to approximately 240 ksi.

2.4.2 Duct Type

Both galvanized steel and plastic ducts were used in this project. The plastic duct can be made out of polyethylene or polypropylene. Three types of plastic duct were used: General Technologies, Inc. (GTI) two-way and one-way ribbed, polypropylene[10], and VSL one-way ribbed, polypropylene[9]. See Figure 2.4 for the types of ducts used in the project. The size of the duct type used in the project was based on the smallest coupler available for that duct type.

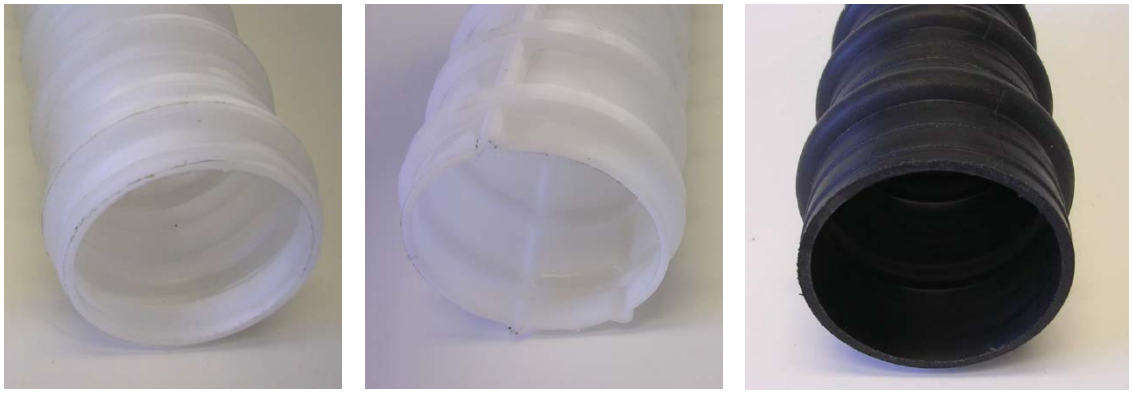

(a) ***(b)*** ***(c)***

Figure 2.4: GTI 76mm One-Way Ribbed (a), GTI 85mm Two-Way Ribbed, and VSL PT-Plus Plastic Duct (c) [1]

2.4.3 Coupler Type

Previous post-tensioning durability research conducted at FSEL showed that splicing galvanized duct was not effective in preventing chloride infiltration into the grout. Therefore, the galvanized ducts in this series were not spliced. One of the two plastic ducts in each specimen with plastic duct was spliced with its corresponding coupler at midspan. Three types of couplers were used:

- GTI slip-on 76mm (GTI two-way duct) (Figure 2.5 a)
- GTI slip-on 85mm (GTI two-way duct) (Figure 2.5 b)
- GTI snap-on (GTI one-way duct) (Figure 2.5 c)
- VSL snap-on (VSL one-way duct) (Figure 2.5 d)

The GTI two-way duct only allows a slip-on coupler due to the longitudinal ribs. The slip-on couplers were sealed against the duct with heat shrink sleeves. The VSL one-way duct did not have grout vents pre-installed at the time of casting so the project team had to fabricate vents. The VSL one-way couplers also had heat shrink sleeves installed.

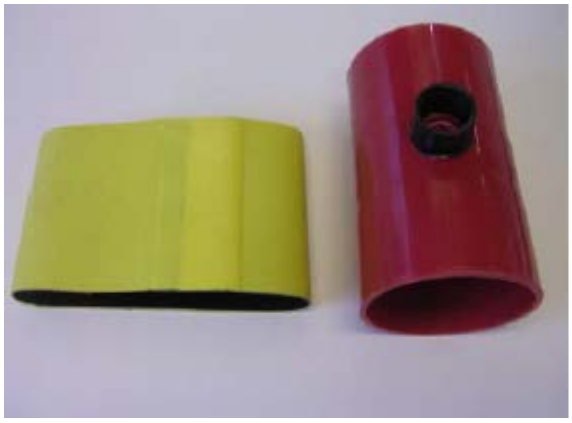

(a) GTI 76mm Slip-On

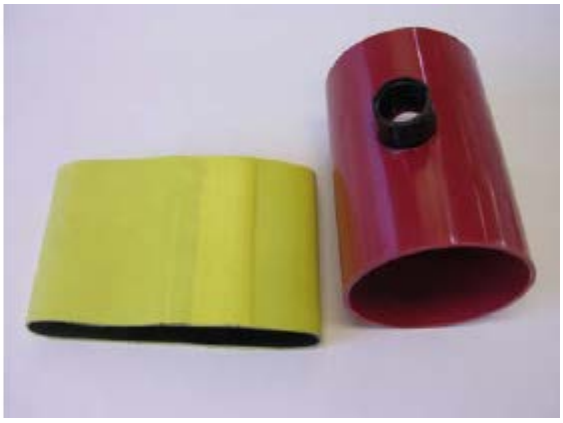

(b) GTI 85mm Slip-On

(c) GTI 76mm Snap-On

(d) VSL PT-Plus Snap-On

Figure 2.5: Couplers [1]

2.4.4 Anchorage Type

Due to availability issues the original anchor head, VSL E5-3, was not able to be used. Instead, a VSL E5-7 anchor head was used. The VSL E5-7 is a seven strand anchor head whereas VSL E5-3 is a three strand bearing plate. Therefore, the four unused holes had to be filled with epoxy. The encapsulated tendons did not use this type of anchor head. Both hot-dip galvanized and non-galvanized versions of the anchorage plate were used.

2.4.5 Fully Encapsulated System

The fully encapsulated system achieves electrically isolated tendons (EIT) by using specialty components, such as:

- An isolating insert between the anchor head and bearing plate
- Plastic duct, couplers, and bearing trumpet
- Permanent plastic isolation cap sealing the anchorage

EIT means that the tendon is isolated from the surrounding concrete. VSL supplied the components for this system.

2.5 Construction Procedure

The development of practical and efficient methods for production of practical research specimens was the aim of the construction process. Refer to Reference 1 for a detailed description of the construction process.

2.5.1 Specimen Fabrication

To control concrete variation and conserve floor space in the lab, two sets of wood forms containing two specimens each were built so that four specimens could be concreted at the same time. See Figure 2.6 for completed formwork. Because the live end needed the extra room for stressing operations, the end walls were the only walls that differed in their construction, Figure 2.7.

Figure 2.6: Form Work [1]

Figure 2.7: End Walls, Dead (Left) and Live (Right)[1]

As mentioned before, epoxy coated mild reinforcement was used and was provided by ABC Coating, Inc., Waxahatchie, Texas. The cages were assembled using coated wire instead of conventional wire ties for fear that the conventional wire ties would damage the epoxy coating. See Figure 2.8 for a completed cage. To maintain the proper cover, plastic chairs were attached to the bottom of the cage before cage was placed into the form work.

Figure 2.8: Passive Reinforcement Cage[1]

Ducts were cut to length using a grinder for steel ducts or a power miter saw for plastic ducts. For uncoupled ducts, a hole was drilled at the apex of the duct and through one wall and a vent installed. For a detailed schematic of the vent connection, refer to Figure 2.9. The couplers that did not have a vent pre-installed, GTI slip-on and VSL PT-Plus, had to have vents installed in them. The modifications for the GTI-slip-on coupler were performed by the company but the VSL PT-Plus modifications were performed by the research team. The diameters of the one-way and two-way GTI plastic duct and the VSL PT-Plus plastic duct were too large to fit inside the cone of the anchorage plate of the conventional post-tensioning system. Therefore, these ducts were slipped over the anchorage plate cone and sealed to the anchorage plate cone with duct tape (Figure 2.10). The galvanized duct had a diameter small enough to fit inside the cone of the anchorage plate of the conventional post-tensioning system.

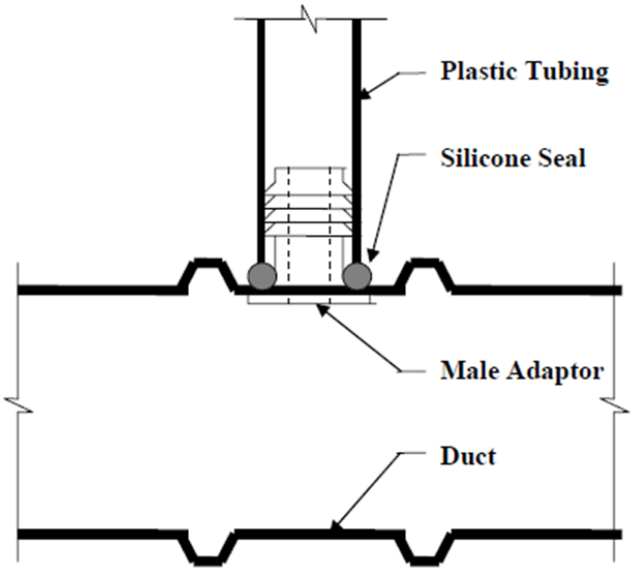

Figure 2.9: Grout Vent Connection [1]

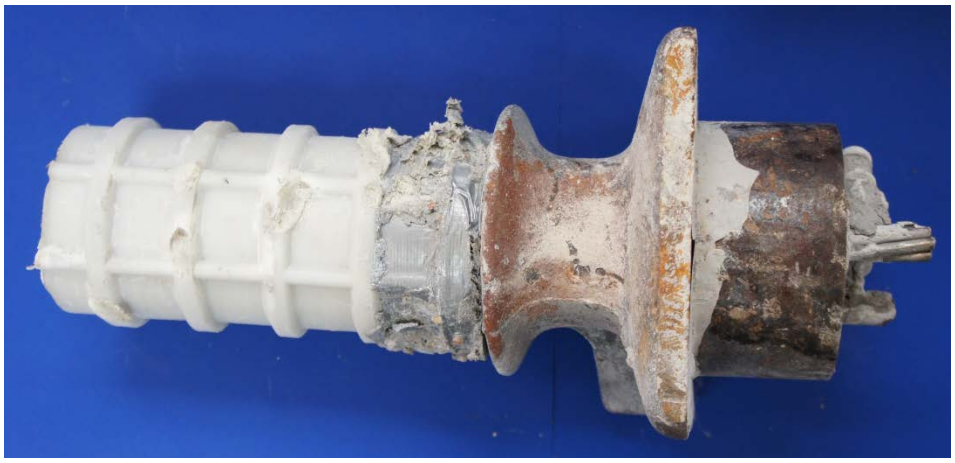

Figure 2.10: GTI Two-Way Plastic Duct Slipped Over the Anchorage Plate Cone

The strands were delivered as continuous rolls ranging from 2.4 feet to 6 feet in diameter. Before cutting, a roll of strand was placed into a steel safety enclosure lined with plywood, bottoms and sides, and foam pipe insulation at the metal edges of the cage. The lining of the cage was to protect the coated strands from damage. The strands were then cut into 8 feet lengths using a grinder.

Concrete was provided by Capitol Aggregates and placed using a one cubic yard bucket and over-head crane. Vibrators were used to consolidate the concrete in the form work. Nine, 6 inch x 12 inch, cylinders were prepared from each batch of concrete. In order to monitor strength gain, three cylinders were tested at 7, 14, and 28 days.

2.5.2 Post-Tensioning

It was essential that the post-tensioning strands be stressed but the level at which they were stressed was not important. Therefore, the strands were only stressed to a small percentage of their guaranteed ultimate strength (GUTS). The trial specimens were prestressed to 25% GUTS but the crack widths that were achieved were on the order of 0.005 inch, which were narrower than the target crack width of 0.010 inch. This led to lowering the prestress to 15% GUTS for the remainder of the specimens for better crack control. For specimens with 0.6 inch strands the level of prestress was reduced to 12.8% GUTS. 12.8% GUTS was used instead of 15% GUTS because the force from the Dywidag bar would not be able to overcome the prestress level in the section to produce cracking. A monostrand ram with power seating capabilities was used to stress the strands. Figure 2.11 shows the prestressing setup.

Figure 2.11: Prestressing Setup [1]

Stress losses due to seating, shortening, friction, relaxation, creep, and shrinkage were taken into account during the design process. Seating losses were taken seriously because the length of the tendon was short. Therefore, any losses from seating would

negate any prestress force that was gained. Seating losses were minimized be using power seating and by over stressing the strand. Shortening losses were assumed to be negligible because of the low level of prestressing but to minimize the possibility of shortening losses the strands were alternately stressed between the two tendons. Friction losses were ignored since the ducts were short and the angle of change was only 10 degrees in the negative direction. Relaxation losses were also ignored because the initial stress on the tendon was less than 55% of yield strength. Creep losses would be low since the level of prestress was so low and the maturity of the concrete at time of prestressing was elevated. Shrinkage losses were neglected due to the maturity of the concrete at the time of prestressing.

2.5.3 Grouting

As per Reference 13, grouting was completed within 48 hours of prestressing. Sika Grout 300 PT, a non-bleed, high flow, sand free grout, was used to grout the ducts. The sequence of the grouting procedure was adapted from VSL. Grout was placed into the duct with a hand pump. Figure 2.12 shows the grouting of a specimen by a member of the research team. To prevent the loss of grout through the gaps of the wedges, temporary grout caps were used. After grouting, the anchorages were coated using TxDOT Type V or VII epoxy and then the anchorage pockets were backfilled with Masterflow 928 mortar.

Figure 2.12: Grouting in Progress[1]

2.5.4 Live Load Application

As discussed earlier, a Dywidag bar through the precast conduits in the corbels was used to apply a live load to the specimen. A data acquisition system was used to monitor the specimen during live load application. The bars were incrementally stressed and between loadings cracks were checked. Once the target crack width of 0.010 inch in the ponding area of the specimen was reached, the load application was halted. The load was kept constant through duration of the project time frame through the use of railroad springs on the dead end of the specimen and the load was "locked" into place by tightening a Dywidag nut on the live end on the specimen, Figure 2.13. Unintentional cracks on the reentrant corners of the corbels were observed on some of the specimens and were sealed using the same pre-mixed concrete patch used in the backfill operations. The cracks along the side of the specimen in the ponding area were sealed with an epoxy.

Figure 2.13: Dywidag Assembly, Dead End (Left) and Live End (Right)[1]

CHAPTER 3

Strand Properties

All content in this chapter comes from research conducted by either Sean Mac Lean[3] or Ryan Kalina[4] and published in CTR Technical Report 0-4562-3[13].

3.1 Mechanical Properties

For a more comprehensive description of the mechanical tension testing of the project strands refer to Reference 13.

Tension mechanical testing was performed on the Project 0-4562 strand types to determine if the mechanical properties of the new strand types would meet specifications for use in post-tensioning applications. The tension testing was performed on each strand type to determine the breaking strength, yield strength, and the modulus of elasticity for each type of strand. To have a standard of comparison, conventional low-relaxation strands were tested along with the new strand types.

A literature review was performed to determine a safe and reliable test method that could be repeated easily because of the large number of tension tests that needed to be performed. Premature failure was one of the main issues that needed to be addressed when devising a viable way of tension testing the strands. The strands can fail prematurely due to one or more of the wires failing. This can happen either from failure of the grip applying equal pressure to all seven wires in the strand and/or from defects in the strands. Defects in the strands are an issue because of the high stresses the strands experience and can come from the manufacturing process or from the testing machine grips.

After the extensive literature review, it was decided that a new gripping method needed to be developed. Instead of the grips bearing directly against the strands, it was decided to epoxy one inch circular metal tubing to the ends on which the grips bear. Reference 14 does not specify the length of the strand or a requirement for grip length.

Instead it specifies that the distance between the grips needs to be 36 inches. For this reason, various grip lengths were tested and the grip length was determined to be 18 inches for the 0.5 inch strands and 28 inches for the 0.6 inch strands. Before the epoxy was applied to the strand and tubing, both had to be thoroughly cleaned. At first the tubing and strand were cleaned with acetone and rags but after debonding between the epoxy and strand, it was decided that the ends of the strands would be sand blasted and then cleaned. For casting, an adjustable jig was made that could cast three strands at a time, Figure 3.1.

Figure 3.1: Adjustable Casting Jig [13]

After casting, the strands were tested in a SATEC Systems, Inc. load controlled testing machine. The testing machine was load controlled not strain controlled. Therefore, the strands were loaded at an approximate rate of 0.1 kips per second and the strain had to be measured using an extensometer. One strand out of the three strands tested for each strand type was tested to failure to determine the failure load without the extensometer attached to the strand. Then the extensometer was attached to the remaining two strands and loaded until the data was satisfactory. Then the extensometer was removed and strand was loaded to failure. The 0.6 inch diameter conventional, 0.5 inch diameter conventional, and epoxy coated strands met all requirements of Reference 15 for both ultimate and yield strengths for low and normal relaxation strands. The stainless steel, stainless clad, and copper clad strands did not meet any of the strength requirements of Reference 15. Table 3.1 shows the results of the testing for ultimate and yield strength and if the strand type met strength provisions of Reference 15.

Table 3.1: Ultimate and Yield Stength Testing Results [13]

			Ultimate Strength			Yield Strength		
Strand Type	Nominal Diameter (in)	Area (in^2)	Breaking Strength (kip)	Met Grade 250 Req.	Met Grade 270 Req.	Yield Strength (kip)	Met Grade 250 Req.	Met Grade 270 Req.
Conventional	0.5	0.153	43.0	Yes	Yes	37.3	Yes	Yes
Epoxy Coated	0.5	0.153	43.7	Yes	Yes	37.8	Yes	Yes
Conventional	0.6	0.217	61.5	Yes	Yes	56.1	Yes	Yes
Hot dip Galvanized	0.5	0.153	40.9	Yes	No	34.5	Yes	No
Stainless Clad (nominal area)	0.6	0.217	57.5	Yes	No	50.6	Yes	No
Stainless Clad (steel area)	0.5	0.153	57.5	Yes	Yes	50.6	Yes	Yes
Stainless Steel	0.6	0.217	48.9	No	No	39.8	No	No
Copper Clad (nominal area)	0.5	0.144	25.9	No	No	22.3	No	No
Copper Clad (steel area)	0.438	0.108	25.9	No	No	22.3	No	No

3.2 Active Corrosion Testing

The content in this section comes from References 13. For a more comprehensive description of the test set-up and testing procedures see References 3 and 4.

To better understand the corrosive nature of the strands used in Project 0-4562, active corrosion tests were performed on strands encased in grout, SikaGrout 300PT, to mimic the conditions that the strands might experience in the field. The active corrosion tests that were performed on the specimens were linear polarization resistance (LPR) and potentiodynamic. These types of tests were performed on both uncracked and cracked specimens to determine the corrosion potential and time to corrosion for the each strand type. The corrosion potential was determine by using the potentiodynamic and LPR

testing methods. Since polarization resistance and time to corrosion are related, the values for each strand type obtained from the LPR testing were used to obtain a comparative time to corrosion.

Encasing the strands in grout was accomplished by milling clear PVC pipe and inserting the strand in the milled PVC pipe and placing grout around the strand. The PVC pipe was milled to ensure the same amount of grout cover on each size of strand, 0.5 inch and 0.6 inch diameter, and that the clear PVC pipe could be removed from the exposure area of the specimen. See Figure 3.2 for an example of a cracked specimen. After the specimens cured for 28 days in a fog room, the cracked specimens were cracked using the pre-cracking device shown in Figure 3.3 and testing was then performed on both uncracked and cracked specimens. The electrolyte used in the testing of the specimens was a five percent by weight chloride solution. See Figure 3.4 for testing set-up.

Figure 3.2: Cracked Active Corrosion Test Specimen [4]

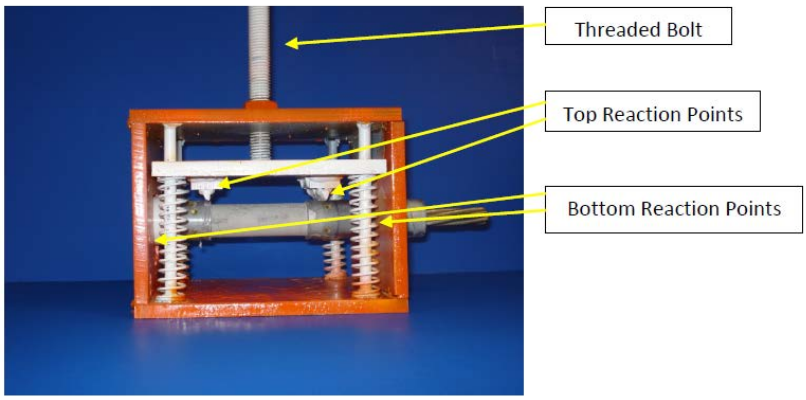

Figure 3.3:Pre-Cracking Device [4]

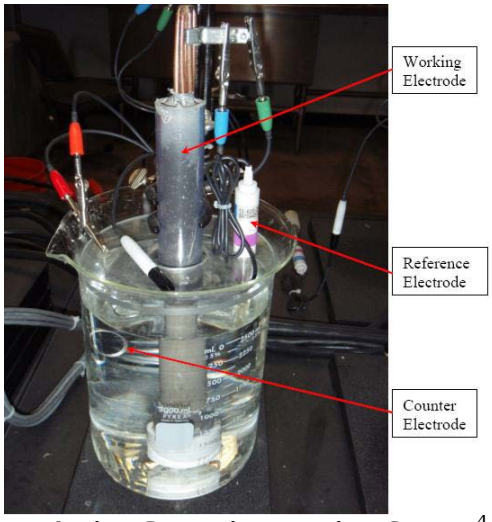

Figure 3.4: Active Corrosion Testing Set-up [4]

3.2.1 Uncracked Grout

The LPR and potentiodynamic testing on the uncracked specimens were performed by Mac Lean[3]. Six strand types were tested:

- Flow filled epoxy coated 0.5 in. dia.
- Conventional 0.6 in. dia.
- Hot dip Galvanized 0.5 in. dia.
- Stainless clad 0.6 in dia.
- Stainless Steel 0.6 in. dia.
- Copper clad 0.5 in. dia.

Ten potentiodynamic tests and ten LPR tests were performed on each strand type. In order to acquire any results from the flow filled epoxy coated strand specimens, the epoxy coating had to be intentionally damaged. Hot-dip galvanized had the most active corrosion potential and the stainless clad had the most noble corrosion potential. See Table 3.2 for the results from the LPR testing. According to the comparative results of the polarization resistance values, the epoxy coated strand performed the best, as expected, and the conventional strand performed the worst.

Table 3.2: Uncracked Specimen LPR testing results [13]

Strand Type	Conventional	Copper Clad	Flow Filled Epoxy Coated	Hot Dip Galvanized	Stainless Clad	Stainless Steel
Avg. Polarization Resistance, $R_{p\ AVG}$ ($k\Omega cm^2$)	10.82	11.68	1000	20.06	92.72	100.5
Vs. Conventional	1.00	1.08	92.4	1.85	8.57	9.28
Avg. Corrosion Potential, $E_{corr\ AVG}$ (mV vs. SCE)	-601	-298	-409	-687	-201	-243

3.2.2 Cracked Grout

The LPR and potentiodynamic testing on the cracked specimens was performed by Kalina[4].

The specimens were cracked to model actual field conditions, because the grout normally cracks when the strands are released after stressing operations. Cracking allows the chlorides from the electrolyte to reach the strands quicker. Six strand types were tested:

- Flow filled epoxy coated
- Conventional
- Hot dip Galvanized
- Stainless clad
- Stainless Steel
- Copper clad

Three potentiodynamic tests and three LPR tests were performed on each strand type. Unlike Reference 3's flow filled epoxy coated specimens, Reference 4's flow filled epoxy coated specimens were not intentionally damaged. Hot-dip galvanized had the most active corrosion potential and the stainless steel had the most noble corrosion potential. See Table 3.3 for the results from the LPR testing. According to the

comparative results of the polarization resistance values, the epoxy coated strand performed the best, as expected, and the hot dip galvanized strand performed the worst.

Table 3.3: Cracked Specimen LPR Testing Results [13]

Strand Type	Conventional	Copper Clad	Flow Filled Epoxy Coated	Hot Dip Galvanized	Stainless Clad	Stainless Steel
Avg. Polarization Resistance, $R_{p\ AVG}$ ($k\Omega cm^2$)	22.48	3.68	144163	2.69	93.37	89.95
Vs. Conventional	1.00	0.16	6413	0.12	4.15	3.99
Avg. Corrosion Potential, $E_{corr\ AVG}$ (mV vs. SCE)	-333	-343	-207	-805	-258	-207

3.3 Passive Corrosion Testing

Information in this section comes from Reference 13. For a more detailed description of the testing processes and set-ups refer to Reference 4.

Passive corrosion testing was performed to determine the corrosion properties of the six strand types of the project. The type of passive corrosion testing used entails monitoring the potential and current while the strands are exposed to a five percent by weight chloride solution. Two types of exposures were monitored. One exposure type was the strands were completely exposed to the chloride solution using a wet/dry cycle. The other was the strands were encased in grout, SikaGrout 300 PT, and continuously exposed to the chloride solution.

3.3.1 Exposed Strands

The exposed strand testing was conducted over a period of six months. Three strands of each strand type were tested. The strands underwent a wet/dry cycle consisting of one week wet and three weeks dry. At the end of each dry cycle the strands were

removed from their containment vessel and visually rated. Refer to Table 3.4 for the rating system. The strands were weighed before exposure was started and after the completion of the testing period.

Table 3.4: Corrosion rating System [13]

Rating	Description
1	As received from manufacturer and completely clean from any corrosion products
2	No signs of corrosion at any level, or there might be small spots of rust material present
3	Small blisters, superficial but widely spread corrosion, pitting is unusual
4	Small blisters, uniform corrosion or initial signs of wide pitting in centralized areas
5	Large blisters, trail of blisters does not exceed 2-in. (51-mm.), deep and wide pitting is visible, corrosion products and pitting does not affect more than 50% of steel area
6	Large blisters, trail of blisters along the strand exceeds 2-in. (51-mm.), deep and wide pitting cover most of the strand surface, corrosion products and pitting affect over 50% of the steel surface, and several forms of corrosion are present simultaneously
7	High levels of corrosion with visible large areas of steel lost

The strands were cut to length using an abrasive blade chop saw, the ends were ground using a bench grinder, cleared of any debris and defects, and had the ends exposied. The strands were then inserted into their respective vessels for exposure. Refer to Figure 3.5 for a view of strand in the exposure vessel and the exposure set-up.

Figure 3.5: Strand in Exposure Vessel (Right) and Exposure Set-up (Left) [4]

The results at the end of testing were not surprising. As expected the epoxy coated flow filled strand (EC) performed the best and the conventional strand (CN) performed the worst. The EC had an average weight loss of 0.60 grams and an average corrosion rating of 1.5, whereas the CN had an average weight loss of 10.13 grams and an average corrosion rating of 7.0. See Table 3.5 for final results of the testing and Figure 3.6 for the appearance of the strand after six months of exposure.

Table 3.5: Final Results of the Passive Corrosion Testing [13]

	Epoxy Coated	Stainless Clad	Stainless Steel	Galvanized	Copper Clad	Conventional
	EC	SC	SS	GV	CC	CN
AVG 6 Month Rating	1.5	1.5	1.7	2.0	3.0	7.0
vs. EC	1.00	1.00	1.13	1.33	2.00	4.67
AVG Weight Loss	0.60	1.07	1.10	2.03	1.03	10.13
vs. EC	1.00	1.78	1.83	3.39	1.72	16.89

- EC – Epoxy Coated Flow-Filled
- SC – Stainless Steel Clad
- SS – Stainless Steel
- GV – Hot Dip Galvanized
- CC – Copper Clad
- CN - Conventional

Figure 3.6: Appearance of Strands after Six Months of Exposure [13]

3.3.2 Grouted Strands

The specimens used in this testing were comparable to the ones used in the accelerated corrosion testing performed Reference 3. Instead of the strand having one end exposed to allow the connection for the application of potential, both ends were epoxied and the strand was fully encapsulated in grout with a copper wire sticking out of one end to facilitate taking potential and current readings. Figure 3.7 shows all of the completed specimens. After the specimens were cast and the grout had cured for 28 days in a fog room, the specimens were placed in a five percent by weight chloride solution. The specimens were exposed to the chloride solution for a total of four months but data were collected for only the last three months. See Figure 3.8 for the set-up of the test mechanism. Only five of the six strand types were used in this testing procedure because the epoxy coated flow-filled strand performed so well in the research performed in Reference 3.

Figure 3.7: Completed Specimens for Passive Corrosion Testing [13]

Figure 3.8: Completed Passive Corrosion Test Set-up [4]

After exposure to the chloride solution for one month, data acquisition commenced. The reason for the month of no data acquisition was for the specimens to develop a constant corrosion potential (E_{corr}). Twice daily potential and current readings were taken by two separate multiplexers and recorded by a data logger. Some source of error was observed after a period of time had elapsed. The readings were becoming less negative over time, which indicated that the specimens were becoming nobler instead of more active. Because of this trend all the specimens were examined after one week of data acquisitions and that potential was considered E_{corr}. The corrosion tendency of all the strand types followed the emf table. The strand with the most corrosion tendency for this type of test was the galvanized strand. The least corrosion tendency for this type of test was the stainless steel clad strand. To see the E_{corr} for each specimen type, refer to Table 3.6.

Table 3.6: Corrosin Potential for Each Strand Type [13]

	CN	CC	GV	SC	SS
E_{corr} (mV_{SCE})	-875	-370	-1025	-360	-475

- SC – Stainless Steel Clad
- SS – Stainless Steel
- GV – Hot Dip Galvanized
- CC – Copper Clad
- CN – Conventional

3.4 Over All Performance

The information in this section is contained in Reference 13.

If the mechanical and corrosion properties of the strands are compared, it will help determine the best strand for post-tensioning of prestressed bridges. Table 3.1 clearly indicates that conventional and epoxy coated strands meet the criteria for ultimate strength of Grade 250 and Grade 270 strands. Conversely, the stainless steel and copper clad did not meet the criteria for ultimate strength of Grade 250 and Grade 270 strands. The stainless clad strand did meet ultimate strength requirements for Grade 250 strand but because the stainless clad is a clad material the cladding must be considered, it did not meet the requirements for Grade 270 strand.

Table 3.7 shows the rankings for corrosion resistance of the strands tested for each type of test performed, where 1 indicates the best corrosion resistance and 6 the worst corrosion resistance. As previously stated the epoxy coated strand was excluded from the passive corrosion testing of grouted strand because it had outperformed the other strand types during active corrosion testing. The epoxy coated strand outperformed the other strands that were tested, followed by stainless steel and stainless clad strands, then copper clad and hot dip galvanized strands, and lastly the conventional strand performed the worst.

Table 3.7: Strand Rankings Based of Corrosion Resistance [13]

Test	**Best 1**	**2**	**3**	**4**	**5**	**Worst 6**
Half-Cells	SS	SC	CC	GV	CN	N/A
Exposed Strand	EC	SC	SS	CC	GV	CN
Grouted Strand	EC	CC	SS	CN	GV	N/A
Accelerated (Uncracked)	EC	SC	SS	GV	CC	CN
Accelerated (Cracked)	EC	SC	SS	CN	CC	GV
Overall	EC	SC	SS	CC	GV	CN

- EC – Epoxy Coated
- SC – Stainless Steel Clad
- SS – Stainless Steel
- GV – Hot Dip Galvanized
- CC – Copper Clad
- CN – Conventional

When the corrosion resistance characteristics and Grade 250 requirements are combined for each strand type, the epoxy coated strand was the best and in descending order stainless clad strand, hot dip galvanized strand, and conventional strand. For the combined corrosion resistance characteristics and Grade 270 requirements for each strand type, only two strand types could be compared, the epoxy coated strand and conventional strand, with the epoxy coated performing the best. For a detailed comparison see Table 3.8.

Table 3.8: Combined Ranks Based on both Corrosion Resistance and Mechanical Properties [13]

Grade	**Best 1**	**2**	**3**	**Worst 4**
250	EC	SC	GV	CN
270	EC	CN	-	-

CHAPTER 4

Experimental Procedure

4.1 Long-Term Exposure Set-Up

Ten of the 24 specimens were autopsied after four years of exposure in 2010 by McCool[2]. The remaining 14 specimens underwent six years of exposure testing outside on the north end of FSEL. The exposure process consisted of wet and dry exposure periods. The wet exposure period involved pouring salt solution in the ponding area and keeping the salt solution level constant throughout the wet exposure period. Seven of the 14 remaining specimens had their dead end anchorage region sprayed with salt solution. Throughout the exposure testing period, the specimens underwent non-destructive monitoring. A few of the Project 0-4562 specimens are shown in Figure 4.1.

Figure 4.1: Project 0-4562 Specimens Undergoing Exposure Testing

4.1.1 Ponding Cycle

The wet exposure period lasted for two weeks and entailed placing a 3.5 percent by weight salt solution in the ponding area. Before 2007, Reference 16 required that the concentration of the salt solution be 3.5 percent by weight but when it changed in 2007 to 3 percent by weight, to stay consistent with the previous exposure periods the project did not change the concentration. The flexural cracks in the sides of the specimens in the ponding area were sealed with epoxy to prevent leakage during the wet exposure period. At the end of the wet exposure period, the ponding area was rinsed out and dried with a sponge in preparation for a two week dry exposure period. Except for a few periods where the wet/dry exposure did not happen, this process was administered monthly until exposure testing was completed.

The following information comes from Reference 2. To help maintain proper solution levels in the ponding area during wet exposure period and keep the ponding area dry during dry exposure periods, "roofs" were made out of Polygal®, a cellular polycarbonate. The roofs were designed to maintain a snug enough fit on the specimen to minimize evaporation and rainwater intrusion but not too snug to restrict fresh air from reaching the cracks in the ponding area. The roof components were connected together with construction adhesive and attached to the specimens with Velcro®. To see a covered specimen, refer to Figure 4.1[2]. Due to ultraviolet rays, which are notorious for breaking down plastics, the Velcro® needed to be occasionally replaced and towards the end of exposure testing the roofs were held down with ropes running longitudinally along the specimen. The ultraviolet rays also made the construction adhesive brittle and the roofs had to be re-assembled with aluminum tape.

4.1.2 Anchorage Spray Cycle

At the beginning of each wet exposure period, some of the specimens had their dead end anchorage region sprayed for six hours with the same salt solution that was used in the ponding area. These specimens will be referred to as the dripper specimens in this document[2]. In 2010, three of the ten dripper specimens were autopsied[2]. The remaining seven dripper specimens were autopsied for this report. The spray system was a closed-

loop system, in which the salt solution was pumped from a small reservoir into a network of piping and then out of 45-degree sprinkler heads on to the dead end anchorage region of the dripper specimens. Then a network of gutters channeled the salt solution back into the small reservoir. The salt solution used for the wet exposure period and the spraying operations was stored in a 1000 gallon tank. The small reservoir was filled from the bulk storage tank and solution level was kept constant with a float valve. Refer to Figure 4.2 for the spray system and bulk storage tank. This system was efficient at minimizing losses from run-off and the number of times that the salt solution needed to be mixed.

Figure 4.2: Spray System [2] ***(Left) and Bulk Storage Tank (Right)***

In 2010, the spray system was in ill repair. The pump was inoperable due to the corrosive effects of the salt solution and the original reservoir and piping network had been damaged by ultraviolet radiation. To continue the exposure of the dead end anchorage region of the remaining dripper specimens the spray system needed to be upgraded. The spray system was upgraded with a new pump and any broken piping was repaired. The bulk storage tank was added at the same time with the help of the FSEL technicians[2], Figure 4.2.

4.2 Monitoring During Exposure Testing

Most of the non-destructive methods that were used to monitor the Project 0-4562 specimens were the same methods that were used on the Project 0-1405 specimens. The non-destructive methods used in both projects were visual examination and half-cell potential measurements. AC Impedance was only performed on the Project 0-4562

specimens with electrically isolated tendons. At the end of exposure testing just before autopsies, chloride penetration measurements were taken as a destructive test.

4.2.1 Visual Examination

Periodically during exposure testing, visual examinations were conducted on the specimens. The specimens were checked for spalling, corrosion staining, further or new cracking, and efflorescence on the sides of the specimens.

4.2.2 Half-Cell Potential Readings

Half-cell potential readings were conducted on the specimens at the end of each wet exposure period to ensure that the pore spaces had enough moisture to effectively take half-cell potential readings. Since corrosion is an electrochemical process in which electrons are transferred from an anode to a cathode, a potential can be read for either the anodic or cathodic reactions. These reactions are known as half-cell reactions. When iron oxidizes in concrete, the reaction of interest is the anodic reaction. The half-cell potential is the difference between the anodic potential and the potential of a reference electrode with a known potential. The probability of corrosion and the time to corrosion can be estimated from the half-cell potential[17]. The standard method for gathering and interpreting the half-cell potentials of steel in concrete is summarized in Reference 18. This method is intended primarily for uncoated reinforcing steel in concrete[18] but because few methods were available for monitoring bonded post-tensioned tendons Project 0-1405 employed this method to monitor its specimens. Because of the success that Project 0-1405 had with this monitoring method it was implemented for Project 0-4562 even though the specimens contained both prestressing strand and epoxy coated rebar[1]. Note that specimens 4.4 and 4.3 did not have half-cell potential readings taken because the specimens contained only epoxy coated and/or uncoated steel reinforcement.

After the ponding area was rinsed and dried of salt solution at the end of the wet exposure period, half-cell potential readings were taken using a saturated calomel reference electrode (SCE) connected to a voltmeter. The half-cell readings were taken by wetting the ponding area with soapy water and placing the tip of a SCE on a sponge in

the ponding area. The soapy water was used as conduction medium in which the flow of current is improved and the sponge serves as a permeable barrier between the SCE and the concrete. As well as being connected to the SCE, the voltmeter was connected to a wire that had been attached to the live end of each tendon. In the ponding area, a grid of measurement points was set up and readings were taken at these points by touching the tip of the SCE to the sponge (refer to Figure 4.3). To account for each tendon separately, potential readings were taken and recorded while the voltmeter was connected to the tendon in question on three rows of measurement points over that tendon. Then the voltmeter was connected to the other tendon and potential readings were taken and recorded on the three rows of measurement points over that tendon. For the grid of measurement points refer to Figure 4.4. Since the specimens 7.2, 7.3, and 7.4 only had one tendon, readings were taken at every measurement point while the voltmeter was connected to the tendon.

Figure 4.3: Taking Half-Cell Potential Readings [2]

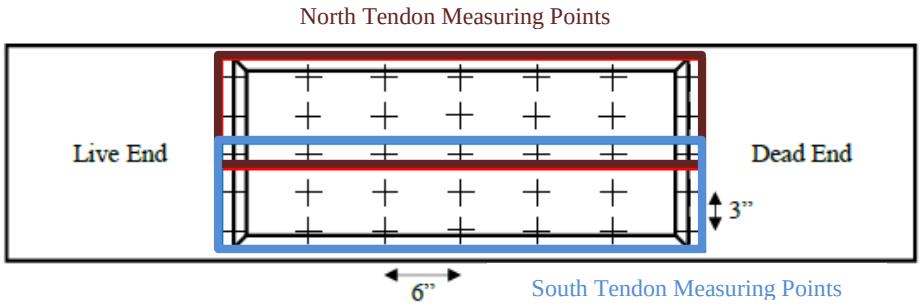

Figure 4.4: Half-Cell Measurement Points[2]

4.2.3 AC Impedance Readings

AC Impedance readings were taken on the 7-series (electrically isolated tendons) specimens in conjunction with half-cell potential readings at the end of each wet exposure period. AC impedance can be an effective way of detecting defects in the duct of a fully encapsulated tendon. The plastic duct acts as a capacitor that is in parallel with a resistor, the grout and concrete, with a high resistance[20]. A post-tensioned electrically isolated tendon can be monitored using AC impedance throughout its life to detect defects in the duct. Defects in ducts can lead to chloride, moisture, and/or oxygen infiltration and therefore corrosion. The defects can be detected when changes in capacitance and resistance are noted during monitoring[19]. Because changes in capacitance and resistance can be monitored over time AC impedance is a suitable monitoring procedure for the 7-series specimens, which are electrically isolated tendon (EIT) specimens.

The 7-series specimens were constructed with two wire leads. One was connected to the tendon and the other was connected to uncoated steel bars that ran longitudinally along each side of the tendon (see Figure 4.5). Uncoated steel bars were used to increase conductivity. A BK Model 885/886 LCR meter was used to take AC impedance readings. Figure 4.6 shows how the BK Model 885/886 LCR meter was connected. Originally the resistance, capacitance, and loss factor were read and recorded from the meter at the 1 kHz frequency. However, due to the odd resistance readings that McCool[2] was getting, McCool contacted Dr. Hans-Rudolf Ganz. Dr. Ganz suggested that the readings be taken by one of two methods:

1. Readings taken at the 100 Hz frequency[21].
2. Connecting a DC voltmeter to the tendon and uncoated steel bars and measuring the voltage, then connecting a DC current source, battery charger, to the tendon and uncoated steel bars and measuring the voltage and current. The voltage difference was then divided by the current to get the resistance[21].

The writer f this series did both of these methods for six wet/dry cycles and the readings from method 1 were comparable to method 2, so the writer of this series continued to take readings using method 2.

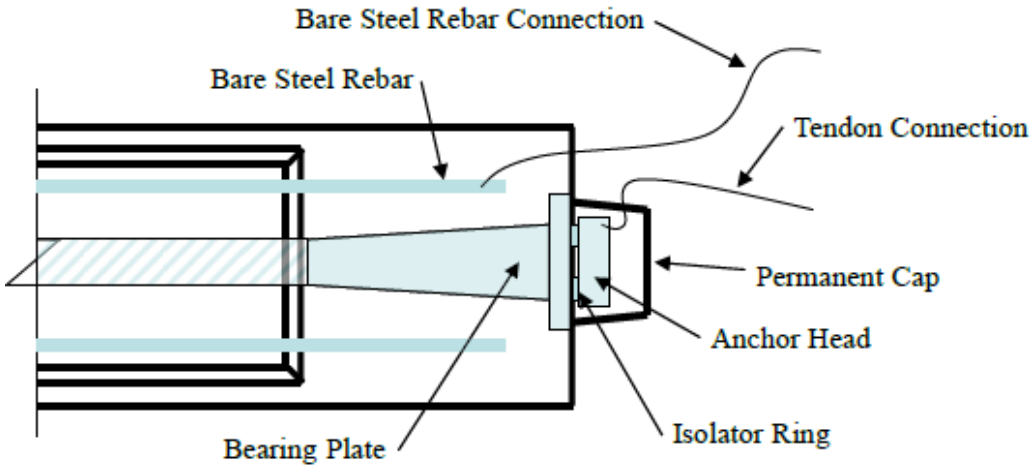

Figure 4.5: Electrically Isolated Tendon Detail [1]

Figure 4.6: BK Model 885/886 LCR Meter Connected to Specimen[2]

4.2.4 Chloride Content

At the end of exposure testing, samples of concrete and grout were taken from all 14 specimens to determine the extent of chloride penetration. The samples of concrete and grout were tested for chloride content using the CL-200 Chloride Test System by James Instrument, shown in Figure 4.7. This chloride testing system is a variation of acid-soluble test summarized in Reference 22. To confirm the accuracy of this chloride testing system, a sample of concrete powder from the top surface of specimen 1.3 at a depth of 0.5 inches was sent to Tourney Consulting Group, Kalamazoo, Michigan for testing in accordance with Reference 22. The results confirmed the CL-200 results.

Figure 4.7: Chloride Content Measurement Setup[2]

4.2.4.1 Surface Chloride Penetration

Samples of concrete powder were taken at all locations at depths of 0.5 and one inch. The concrete powder was obtained using a hammer drill, as shown in Figure 4.8. After drilling to the required depth, a sample of concrete powder was taken and the hole was thoroughly cleaned to prevent cross contamination. Except for the 7-series specimens, all the concrete powder samples from the top surface of the ponding area were taken at two inches, in the live end direction, from the transverse centerline (Figure 4.9). The 7-series had concrete samples obtained from the top surface of the ponding area at the transverse centerline. Except for the 7-series specimens, all specimens had the concrete powder samples taken from the dead end anchorage zone, five inches from the top surface of the specimen (Figure 4.10). The dripper specimens had concrete powder samples taken from the live end anchorage zone, six inches from the top surface of the specimen. The 7-series specimens had concrete powder samples taken from both the live and dead end anchorage zone, six inches from the top surface of the specimen. The

distances from the top surface of the specimen correspond with the center of the anchorage pockets.

Figure 4.8: Concrete Powder Extraction with Hammer Drill

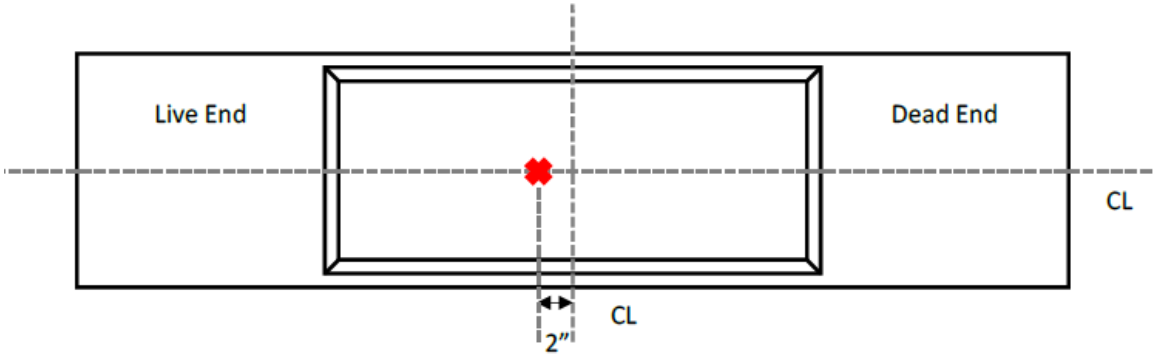

Figure 4.9: Top Surface Concrete Powder Sample Location [2]

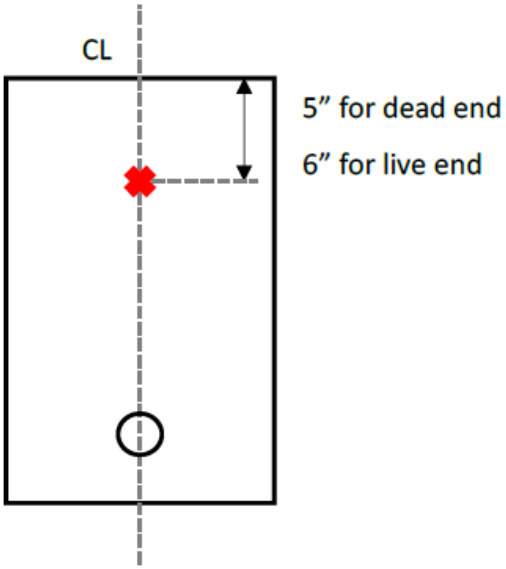

Figure 4.10: Anchorage Zone Concrete Powder Sample Location [2]

4.2.4.2 Grout Chloride Content

Samples of grout from the post-tensioning (PT) ducts were obtained after all the PT components had been removed from the specimens and the duct had been removed from the tendon. All specimens had grout samples taken from the anchorage plate. To obtain grout samples for the anchorage plates, the duct had to be cut from the anchorage plate using an abrasive blade cut-off saw to get to the grout contained in the anchorage plate and then a hammer drill was used to extract grout powder ensuring that the strands were not damaged (Figure 4.11). The specimens with galvanized ducts had grout samples

removed every two inches in the area in which the duct had deteriorated due to corrosion. Except for the 7-series specimens, the specimens with plastic duct had grout samples taken from the midspan of the tendon which was the location of the grout vents and splices. The 7-series had grout samples removed from the grout vent region and the midspan of the tendon. The grout samples were obtained from the tendon using a clean hammer and chisel and care was taken to obtain pieces of grout from the entire depth of the tendon (Figure 4.12). After all grout samples were obtained, the grout was ground using a mortar and pestle (Figure 4.12).

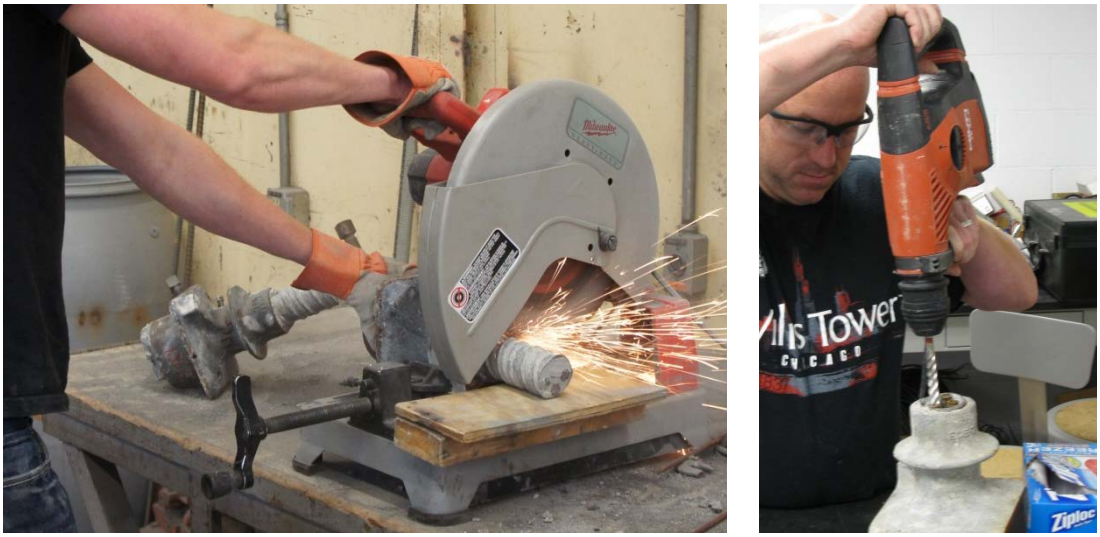

Figure 4.11: Cutting Duct from the Anchorage Plate (Left) and Extracting Grout from Anchorage Plate (Right)

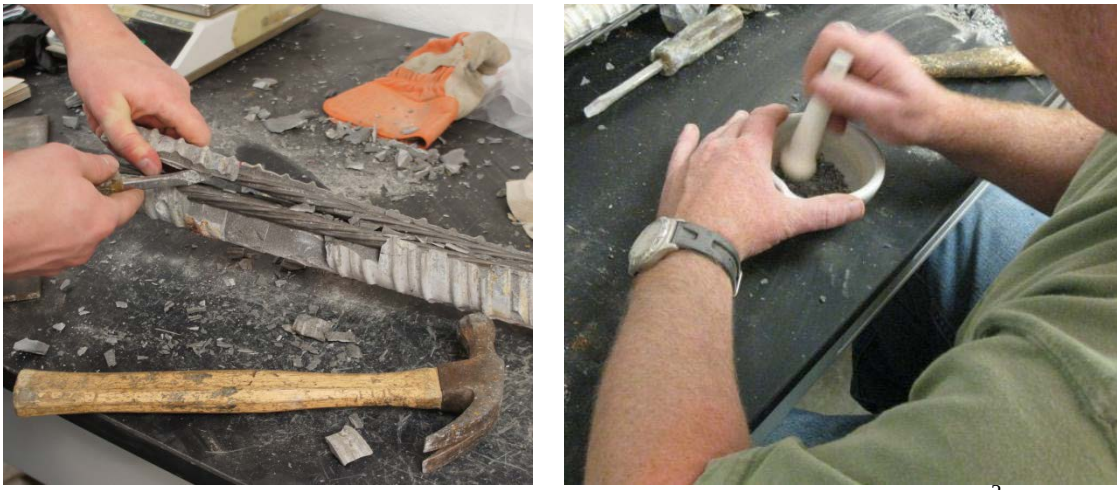

Figure 4.12: Grout Sample Extraction (Left) and Grinding Grout Sample [2] (Right)

CHAPTER 5

Exposure Test Results and Analysis

On March 1, 2006, exposure testing began on all 24 specimens. On March 1, 2010, exposure testing finished for 10 of the 24 specimens, which was 1460 days of exposure[2]. Autopsy results for these specimens were reported in Reference 2. On March 1, 2012, exposure testing finished for the 14 remaining specimens, which was 2192 days of exposure. Even though there were gaps in the data due to logistical issues during the six years of exposure testing, readings for the half-cell potentials and the AC impedance generally happened monthly. As mentioned in Chapter 4, concrete and grout samples were removed from the specimens at the ends of the exposure testing periods to test for chloride content.

5.1 Half-Cell Potential Data and Analysis

Even though the half-cell potential method outlined Reference 18 is for uncoated reinforcing steel, the method was used to determine the half-cell corrosion potentials for the grouted strands in the Project 0-4562 specimens. The method might be useful in determining if corrosion has been induced and estimating the time to corrosion but does not estimate the rate of corrosion. It should also be noted that the half-cell potential readings can only detect localized corrosion[18]. Specimens 4.4 and 4.3 did not have half-cell potential readings taken because the specimens were reinforced only with epoxy coated and/or uncoated conventional reinforcement.

Reference 18 defines the probability of corrosion based on the half-cell potential readings with respect to a copper-copper sulfate reference electrode. The half-cell potential readings from Reference 18 were converted to the standard saturated calomel electrode (SCE) (Table 5.1), which is the reference electrode used in the project to take half-cell potential readings. As discussed before, strictly speaking the half-cell potential readings of the project specimens would only be valid for uncoated reinforcing steel but were used to determine if they correlate with actual corrosion as found in the autopsies.

Table 5.1: Probability of Corrosion[18]

Potential	Probability of Corrosion
More positive than -123 mV vs. SCE	Less than 10%
-123 to -273 mV vs. SCE	Uncertain
More negative than -273 mV vs. SCE	Greater than 90%

Contour plots of the final readings taken on February 29, 2012, day 2192, the final day of exposure testing, can be seen in Figure 5.1. The contour maps are an overhead view of the ponding area with the live end on the left, the dead end on the right, and the north tendon at the top. The contour plots for Specimens 3.3, 4.1, and 5.1 show a marked disparity in half-cell potential readings between the north and south tendon. The north tendon had more negative half-cell potential readings than the south tendon. This disparity in half-cell potentials might be an indication of the coupler of the spliced north duct allowing more infiltration of chlorides into the tendon than the continuous south duct. The south duct had a grout vent that was installed by drilling a hole into the apex of the duct and inserting a grout vent in the hole (Figure 2.9), whereas the coupler of the spliced north duct had a grout vent installed by the manufacturer. This chloride infiltration might increase the half-cell potential readings. In Specimens 7.2 and 1.1 a marked difference between the ends and the center portion of the ponding area can be seen. This might be because at the ends of the ponding area the tendons are further away from the surface due to increased cover over the tendons outside the ponding area. This indicates that accuracy of the half-cell potential readings decrease as the distance between the reading surface and the steel increases[16].

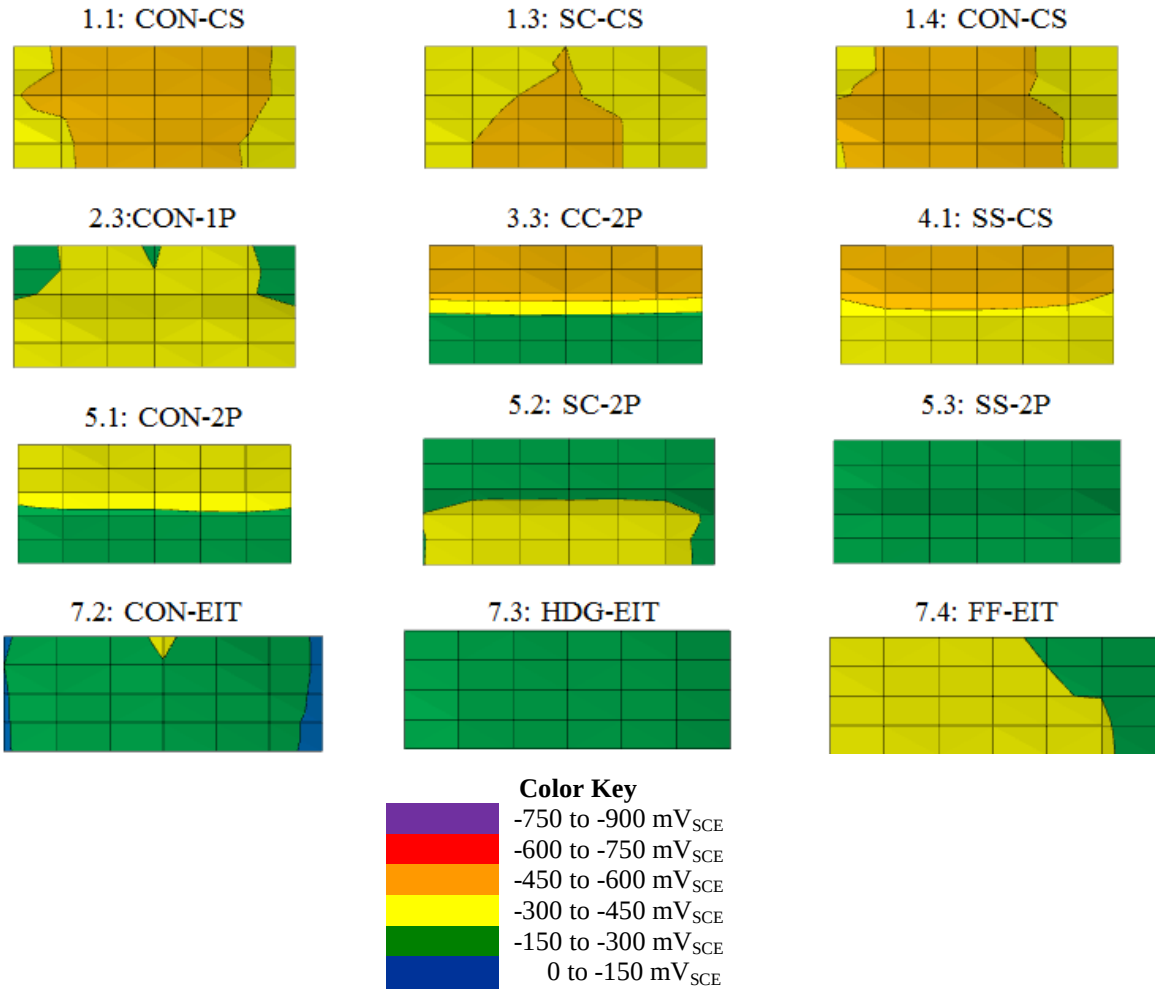

CON = Conventional Strand
CC = Copper-Clad Strand
HDG = Hot-Dip Galvanized Strand
SS = Stainless Steel Strand
SC = Stainless Clad Strand
FF = Flow Filled Epoxy Coated Strand

CS = Corrugated (Galvanized) Steel Duct
1P = 1-Way Plastic Duct
2P = 2-Way Plastic Duct
EIT = Electrically Isolated Tendon

Figure 5.1: Final Half-Cell Potential Contour Plots

Averages of the final half-cell potential readings for all tendons are shown in Figure 5.2.

Except for Specimen 7.2 and Specimen 5.1's south tendon, all the tendons with conventional strands and flow filled epoxy coated strand, had an average final half-cell potential more negative than -273 mV, which signifies that there is a 90% chance that the

strands in the tendon are corroded. Specimen 7.2 had electrically isolated tendon (EIT) and Specimen 5.1 had two-way plastic duct. This accounts for why Specimen 7.2 had an average final half-cell potential in the uncertainty range for corrosion but it does not account for why there was a disparity between the north and south tendon of Specimen 5.1. The difference in average final half-cell potential between the north and south tendon of Specimen 5.1 might be because of how the grout vents were installed (see Chapter 2) and might signify that there are more chloride ions in the north duct thus increasing the average final half-cell potential. Surprisingly, Specimen 7.4 with the flow filled epoxy coated strand had an average final half-cell potential that was in the greater than 90% chance of corrosion range. This is unusual because Specimen 7.4 had an EIT and had flow filled epoxy coated strands within the tendon which was expected to have an average final half-cell potential in the less than 10% chance of corrosion or corrosion uncertain range. This might be an indication that the duct has been penetrated and moisture, oxygen, and/or chlorides have entered the system increasing the half-cell potential and possibly inducing corrosion. It might also indicate that corrosion of the uncoated or epoxy coated steel reinforcement has elevated the half-cell potential.

All the tendons with the non-conventional strands cannot be effectively evaluated using the half-cell potential limits and probability of corrosion in Reference 18 because they are not entirely made of steel or are not made of steel at all. However, the average final half-cell potentials can be compared with the active corrosion potential from the LPR testing of cracked specimens from Reference 13 (Table 3.3 and Figure 5.2). The active corrosion potential from the LPR testing of cracked specimens were -343 mV vs. SCE for copper clad strand, -805 mV vs. SCE for hot dip galvanized strand, -258 mV vs. SCE for stainless clad strand, and -207 mV vs. SCE for stainless steel strand[13]. If the values from the LPR testing of cracked specimens are used, than Figure 5.2 is much more informative when evaluating the average final half-cell potential for the non-conventional strands.

All the tendons with stainless clad strands (north and south tendons of specimens 1.3 and 5.2) had average final half-cell potentials at or more negative than the active

corrosion potential from the LPR testing of cracked specimen. This might signify that chlorides may have entered the tendons because the ducts are not as water tight as expected and/or the epoxy coated mild reinforcement is corroding and elevating the half-cell potentials. The half-cell potentials from each tendon of a specimen were close except that the half-cell potentials of Specimens 1.3, galvanized duct, and 5.2, 2-way plastic duct, were not close. Half-cell potentials for the tendons of Specimen 1.3 were more negative, -423 (north tendon) and -436 (south tendon) mV vs. SCE. This might signify that the corrosion from the galvanized duct and/or chlorides have entered the tendon and elevated the half-cell potential. This should NOT be alarming for two reasons. One reason is when chloride levels increase usually there is a corresponding increase in half-cell potential. The other reason is stainless steel is usually very resistant to corrosion when in a chloride environment.

All the tendons with stainless steel strands (north and south tendons of Specimens 4.1 and 5.3) were at or more negative than the corrosion potential from the LPR testing of cracked specimens. Like the tendons with stainless clad strands, this might signify that chlorides may have entered the tendons because the ducts are not as water tight as expected and/or the epoxy coated mild reinforcement is corroding and elevating the half-cell potentials. This should not be alarming for two reasons. One reason is when chloride levels increase usually there is a corresponding increase in half-cell potential. The other reason is stainless steel is very resistant to corrosion when in a chloride environment. There was some disparity between the north and south tendons of Specimen 4.1. This disparity might indicate that the duct of the north tendon might be more severely corroded thus allowing more chlorides to enter the tendon and increasing the final average half-cell potential. The north tendon of Specimen 4.1 had an average final half-cell potential that was significantly more negative, -530 mV vs. SCE, than the south tendon, -378 mV vs. SCE, of specimen 4.1. The average of the average final half-cell potential for specimen 4.1 (-454 mV vs. SCE) was significantly more negative than from specimen 5.3 (-238 mV vs. SCE). This might be from the corrosion of the zinc in the

galvanized ducts of Specimen 4.1. The corrosion of the zinc in the galvanized duct might be elevating the final half-cell potentials of Specimen 4.1.

The copper clad strand in the north tendon in Specimen 3.3 was significantly more negative and the south tendon in Specimen 3.3 was less negative than the active corrosion potential from the LPR testing of cracked specimens. Like Specimen 5.1, this disparity in average final half-cell potential between the north and south tendon of Specimen 3.3 might be because of how the grout vents were installed (see Chapter 2) and might signify that there are more chloride ions in the north duct thus increasing the average final half-cell potential.

The final average half-cell potential of the galvanized strands in Specimen 7.3 is significantly less negative than the corrosion potential from the LPR testing of cracked specimens. There might be two possible reasons for this. One the EIT system is working as hoped, fully isolating the tendon, and the zinc in the galvanized coating has not started to corrode. This is unlikely and it should become clearer why it is unlikely after reviewing the AC impedance data and chloride concentrations of the tendons. The other reason is the zinc in the galvanized coating has corroded away and the underlying steel is corroding. This might be the case and will become clearer after reviewing the data from the maximum monthly half-cell potentials for the exposure testing period.

Some of the elevated average half-cell potentials might have been affected by corrosion of the galvanized duct, corrosion of the epoxy coated conventional reinforcement and/or chloride infiltration of the duct. All of these would elevate half-cell potentials and skew the data.

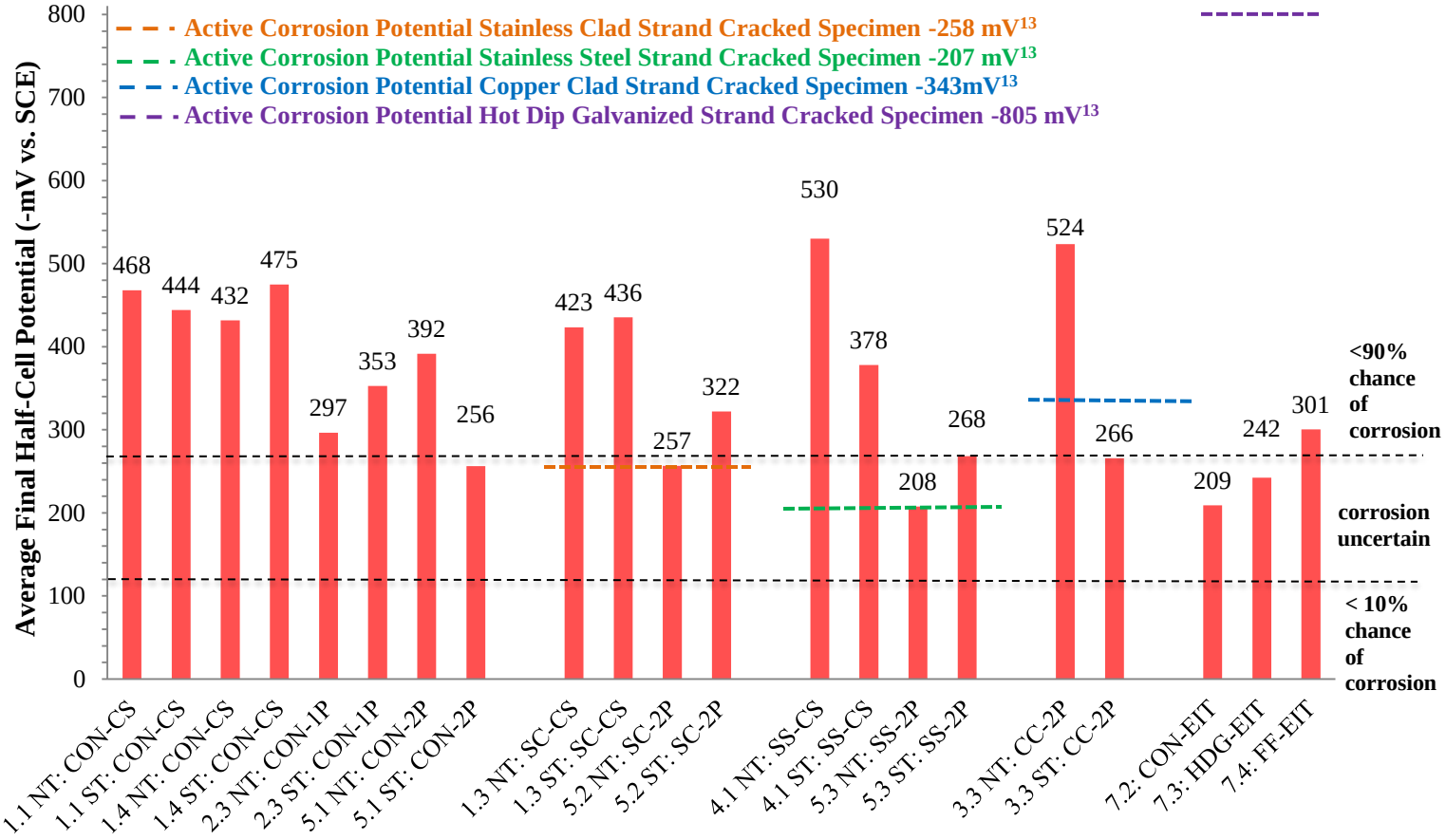

Figure 5.2: Average Final Half-Cell Potential Readings

Figure 5.3 shows the monthly maximum half-cell potential reading of conventional and flow filled epoxy coated strands for the exposure testing period. It was decided that the maximum half-cell potential readings for each tendon would be graphed instead of just the maximum half-cell potential readings for the whole specimen because it was noticed that some of the tendons in the same specimen had major disparities in half-cell potential readings periodically during the exposure testing period. All the conventional strand and flow filled epoxy coated strand tendons at some point during the exposure testing period had maximum half-cell potential readings in the greater than 90% probability of corrosion range. Surprisingly, even for the fully encapsulated Specimens, 7.2 and 7.4, the maximum half-cell potential readings at some point were in the greater than 90% chance of corrosion range. These fully encapsulated specimens should not have half-cell potentials this negative unless there was a defect in the duct which allowed moisture, oxygen, and/or chlorides to enter the tendon or corrosion in the epoxy coated conventional reinforcement thus elevating the half-cell potentials and possibly inducing corrosion. Since there was essentially no corrosion found in the strands from the main autopsy region during inspection of the tendon, a defect in the duct is assumed to have allowed moisture, oxygen and/or chlorides into the tendon. The south tendon of Specimen 1.1 had the most negative maximum half-cell potential reading, which was -799 mV vs. SCE and Specimen 7.2 had the least negative maximum half-cell potential reading of -171 mV vs. SCE. If the type of duct is used to evaluate the maximum half-cell potentials, then Specimens 1.1 and 1.4, which had galvanized duct, consistently had the most negative maximum half-cell potentials for the majority of the exposure period. This might be from the corrosion of the zinc in the galvanized coating of the duct contributing the half-cell potentials.

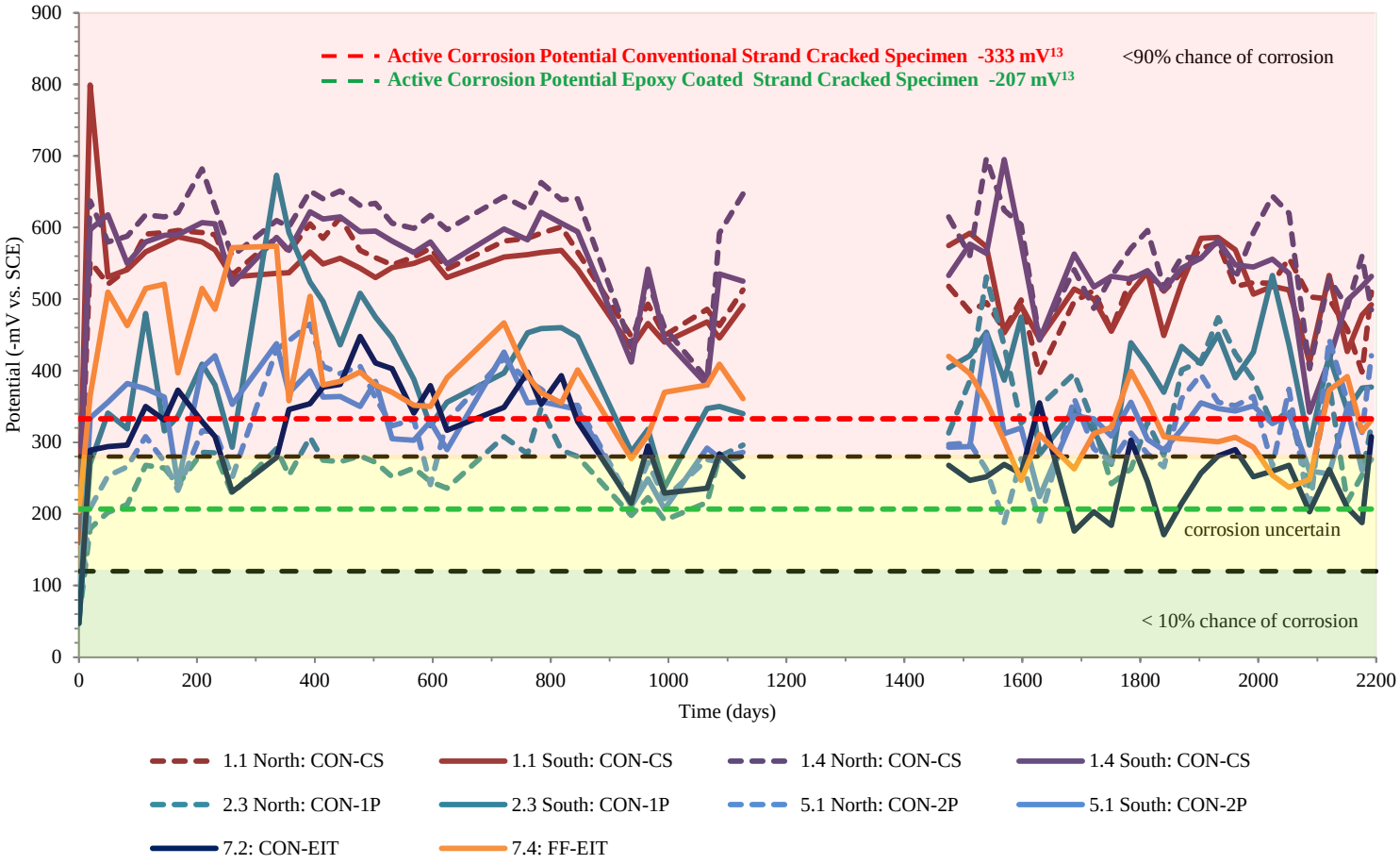

Figure 5.3: Monthly Maximum Half-Cell Potential Readings for Conventional Strand and Flow Filled Epoxy Coated Strand for the Exposure Testing Period

Figure 5.4 shows the maximum monthly half-cell potential readings for stainless clad and stainless steel strand tendons for the exposure testing period. As mentioned previously, the limits of Reference 18 are not effective at evaluating the non-conventional strands but if the corrosion potentials determined in the LPR testing of cracked grouted specimens performed for Reference 13 are used as a limit, a comparison can be made. The active corrosion potentials from the LPR testing of cracked specimens for stainless clad and stainless steel strands were -258 mV vs. SCE and -207 mV vs. SCE, respectively[13]. For all of the exposure testing period, the tendons in galvanized duct were more negative than their active corrosion potentials. As mentioned before, this might be from the corrosion of the zinc in the galvanized coating of the duct and/or chlorides have entered the tendon, thus elevating the half-cell potential. The tendons in the plastic duct had maximum half-cell potentials around their active corrosion potentials. There is not much disparity over the majority of exposure testing period in the maximum half-cell potentials between the north and south tendon of a specimen, as there was in some of the specimens containing conventional strand.

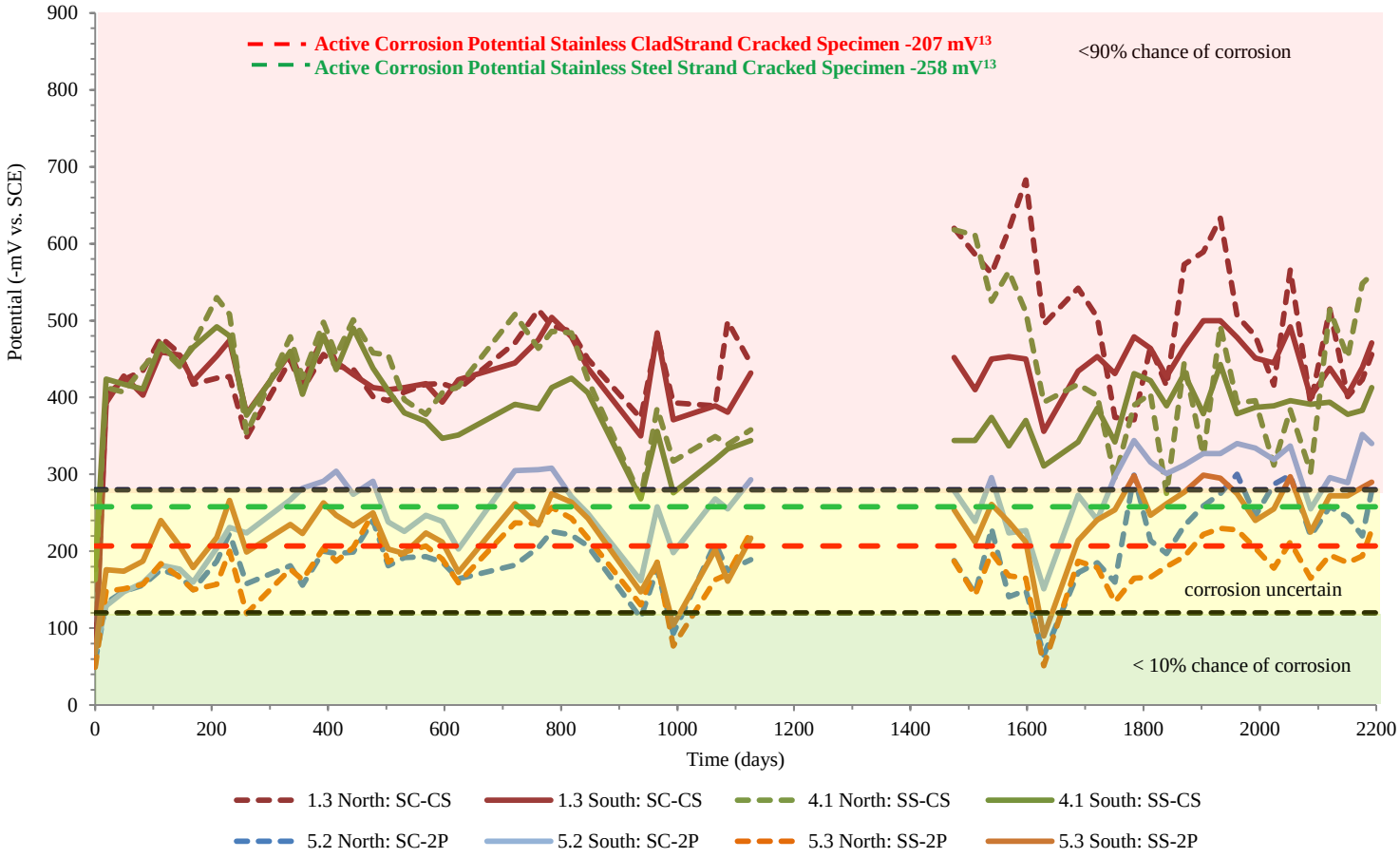

Figure 5.4: Monthly Maximum Half-Cell Potential Readings for Stainless Clad and Stainless Steel Strands for the Exposure Testing Period

Figure 5.5 shows the maximum monthly half-cell potential readings for copper clad and hot dip galvanized strand tendons for the exposure testing period. As mentioned previously, the limits in Reference 18 are not effective at evaluating the non-conventional strands but if the corrosion potentials determined in the LPR testing of cracked grouted specimens performed for Reference 13 are used as a limit, a comparison can be made. The active corrosion potentials from the LPR testing of cracked specimens for copper clad and hot dip galvanized strands were -343 mV vs. SCE and -805 mV vs. SCE, respectively[13]. The tendon in Specimen 7.3 initially had maximum half-cell potentials that were more negative than the corrosion potential for hot dip galvanized strand but the potential dropped significantly after about 1000 days of exposure testing. This drop in half-cell potential might be from the depletion of the zinc in the galvanized coating due to corrosion and the initiation of corrosion of the underlying steel. The specimen that had tendons with copper clad strand, Specimen 3.3, had maximum half-cell potentials that were less negative than the corrosion potential from the LPR testing of cracked specimens until about day 1500 of the exposure testing for the south tendon and about day 1550 of the exposure testing for the north tendon. This spike in maximum half-cell potential might be from chlorides reaching the strands in the tendon and raising the half-cell potential of the copper clad strands. There was some disparity of maximum half-cell potentials between the tendons of Specimen 3.3 towards the end of the exposure testing period. This disparity might be from the grout vent of coupler of the spliced north duct allowing more chlorides into the tendon than the grout vent in the south duct thus elevating the half-cell potential to a greater extent. The grout vent of the coupler was installed by the manufacturer of the coupler and the grout vent in the continuous south duct was installed be the research team that designed and constructed the Project 0-4562 specimens.

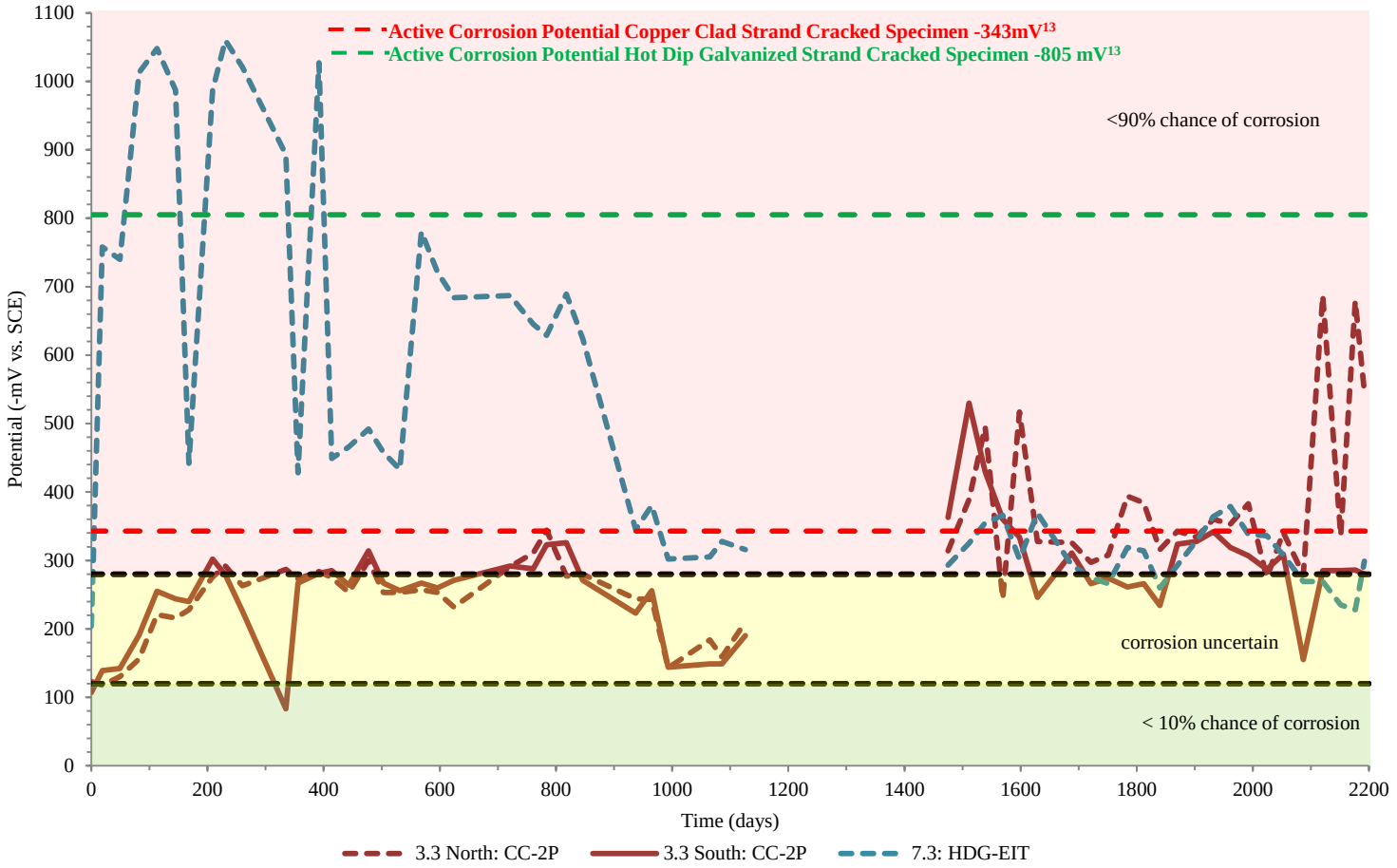

Figure 5.5: Monthly Maximum Half-Cell Potential Readings for Copper Clad and Hot Dip Galvanized for the Exposure Testing Period

To estimate the days to initiation of corrosion, the half-cell potential for greater than 90% chance of corrosion from Reference 18 was used for the conventional and flow filled epoxy coated strands and the corrosion potentials from Reference 13 were used for the non-conventional strands. See Figure 5.6 for the approximate days to the initiation of corrosion. All of the tendons within galvanized duct that had conventional strands had corrosion initiated at 19 days. The estimated days to corrosion varied from 19 to 209 for the tendons within plastic duct that contained conventional strand. All of the tendons in galvanized duct that contained stainless clad and stainless steel had estimated days to corrosion of 19. Most of the tendons within plastic duct containing stainless clad and stainless steel had an estimated 231 days to corrosion. The outlier was Specimen 5.3's south tendon which had estimated days to corrosion of 748. The tendons with copper clad strand performed the best, Specimen 3.3's south and north tendon. The south tendon did not initiate corrosion until 1475 days and the north tendon did not initiate corrosion until day 748. The tendons within the encapsulated specimens did not perform as well as expected. Specimens 7.2 and 7.4 had corrosion initiated at about 19 days and Specimen 7.3 had corrosion initiated at about 82 days.

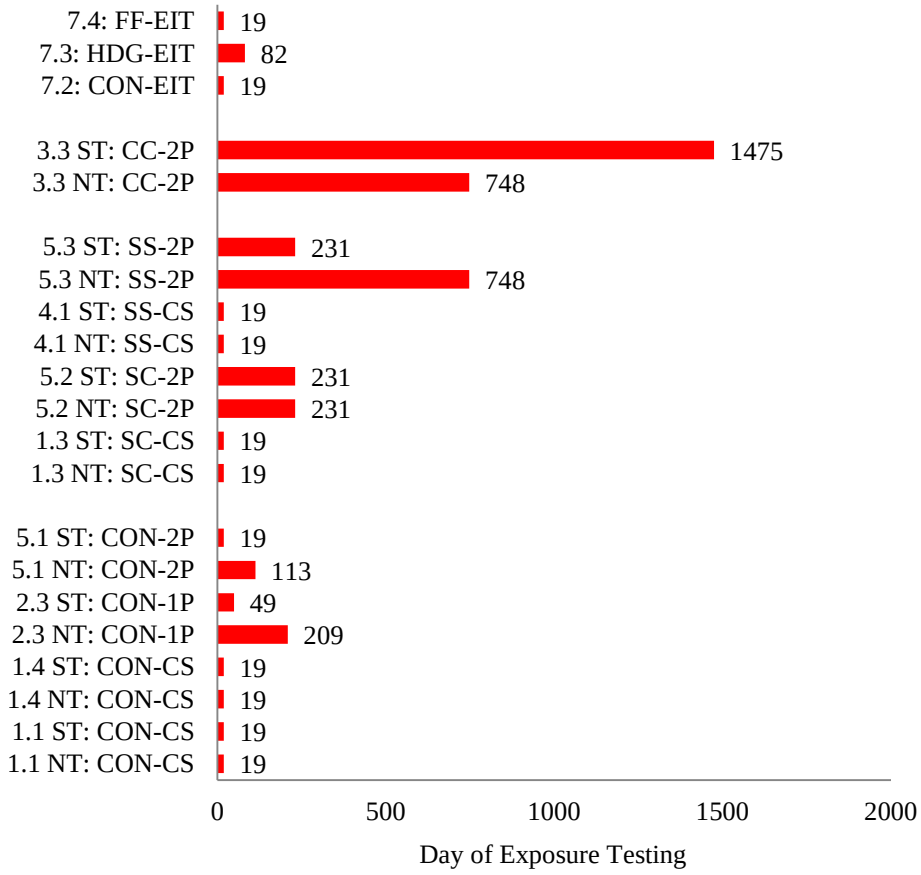

Figure 5.6: Approximate Days to the Initiation of Corrosion

The analysis of the half-cell potentials suggests that the tendons in galvanized duct did not perform well. This might be due to a few reasons. One is that galvanized duct is not a water tight duct. The corrugation of the duct allows moisture, oxygen, and/or chlorides to enter the tendon even if the duct is not corroded. The other reason is once the zinc in the galvanized coating and underlying steel has corroded to the point at which a hole has formed in the duct, moisture, oxygen, and/or chlorides are free to enter the tendon. The tendons in plastic duct performed only marginally better. This might be due to the ducts not being completely water tight at the coupler of the spliced duct and the grout vent of the continuous duct. Surprisingly, the EIT's did not perform as well as expected. This might be due to the duct having a defect thus causing a breach in the

system and allowing moisture, oxygen, and/or chlorides to enter the tendon. One possible reason for elevated half-cell potentials is the corrosion of the galvanized duct and/or the epoxy coated conventional reinforcement elevating the half-cell potential.

When the data from the autopsies are compared to the half-cell potentials for each tendon a more definitive analysis can be made. For the EIT's, the analysis of the AC impedance and the data from the autopsies might help determine why the half-cell potentials were elevated and why corrosion might have been initiated so early in the exposure testing period.

Just as in any testing procedure, errors can skew data. A few errors might have been made during the half-cell potential monitoring. Reference 18 has exact specifications for the concentration of wetting solution, the procedure for wetting the surface, the size of the porous medium, and temperature corrections for the half-cell potentials readings[18]. It is suspected that these specifications for a majority of the exposure testing may not been strictly followed and because of the lack of maintenance records it is not known how this affected the data. Another error is that the researcher should wait for the potential reading to stabilize for each measurement. There had been lapses in half-cell potential readings during the six year exposure testing period due to turn-over of graduate research assistants and miscommunication with FSEL staff.

5.2 AC Impedance Data and Analysis

The fully encapsulated Specimens 7.2, 7.3, and 7.4 had resistance, capacitance, and loss factor measured each month during exposure testing, which had conventional, hot dip galvanized, and flow filled epoxy coated strands, respectively. There were a few outliers in the data for these measurements that were several orders of magnitude higher than the rest of the data and were omitted from the analysis.

Resistance and specific resistance measurements are shown in Figure 5.7. The limiting value for resistance is that it must be greater than $0.01K\Omega$. This resistance limit signifies a short circuit has occurred between the strand and the conventional reinforcement and is not electrically isolated due to a defect in the duct or short-circuit at

the anchorage[19]. The resistances for the specimens were significantly higher than 0.01kΩ over the entire exposure testing period so it can be assumed that the system did not short circuit. As expected, the resistance steadily increased over the exposure testing period because resistance should increase with age[19]. During the exposure testing period, there were times in which the resistance dropped to relatively low resistances, which signified that moisture had entered the duct[19]. The threshold specified by Reference 19 for specific resistance is 500 kΩ-m[19] but the threshold specified by the Reference 22 is 50 kΩ-m[22]. Specific resistance is the resistance times the length of the tendon. This indicates that the system is monitorable over the long term[19]. The standard in Reference 22 is newer than the standard in Reference 19. This standard from Reference 22 was implemented because it was found that the limit set by Reference 19 was nearly unattainable in the field[22]. For the entire exposure testing period, the specific resistance calculations fell well below the Reference 19 limit and for the majority of the exposure period the specific resistance was below the Reference 22 limit. Therefore, the long-term monitorability is questionable for the specimens.

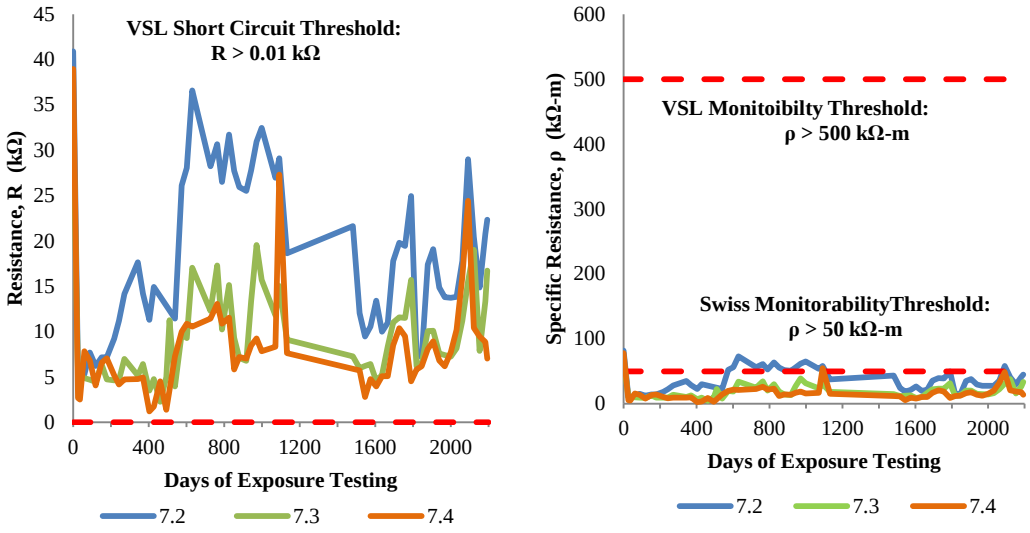

Figure 5.7: Resistance (Left) and Specific Resistance (Right) for Specimens 7.2, 7.3, and 7.4

Figure 5.8 shows the calculated specific capacitance for the exposure testing period of specimens 7.2, 7.3, and 7.4. Specific capacitance was calculated by dividing the

measured capacitance by the length of the tendon, which was two meters. The monitorability threshold specified by Reference 19 is that the specific capacitance shall be 2.35 nF/m or below[19]. Specimen 7.2 and 7.3 had specific capacitances above the threshold for monitorability for the majority of the exposure testing period. This suggests that the monitorability of Specimens 7.2 and 7.3 are suspect. Specimen 7.4 had specific capacitances that were at or below the limit for monitorability for majority of the exposure testing period, which indicates that the system was somewhat monitorable. All specimens had elevated periods of specific capacitance at about the end of the first year for three months of exposure testing and for over a year at the end of exposure testing.

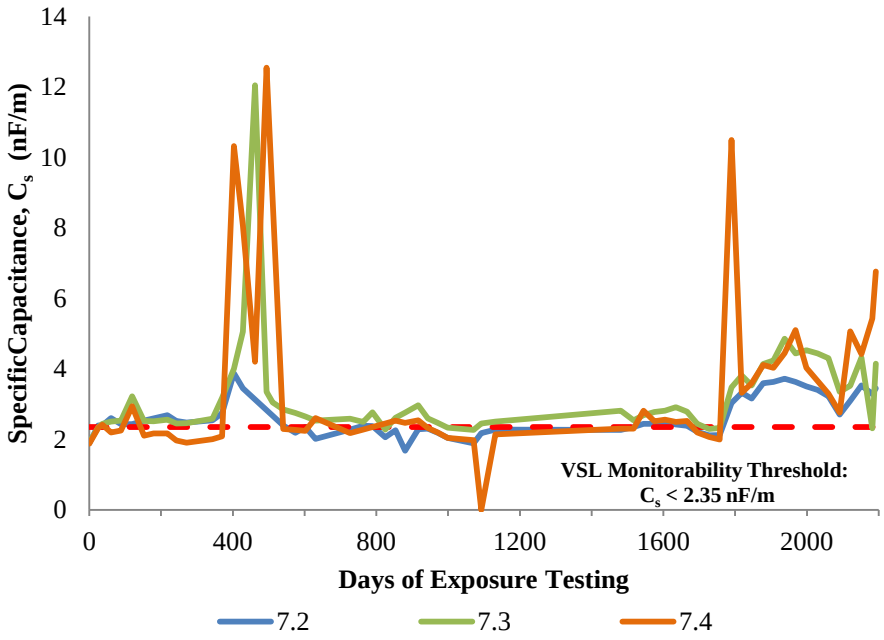

Figure 5.8: Specific Capacitance for Specimens 7.2, 7.3, and 7.4

Figure 5.9 shows the loss factors measured for Specimens 7.2, 7.3, and 7.4 for the exposure testing period. Reference 19 sets the maximum limit for monitorability for the loss factor at 0.01[19]. All specimens were above this limit for the entire exposure testing period, which indicates that the specimens were not monitorable.

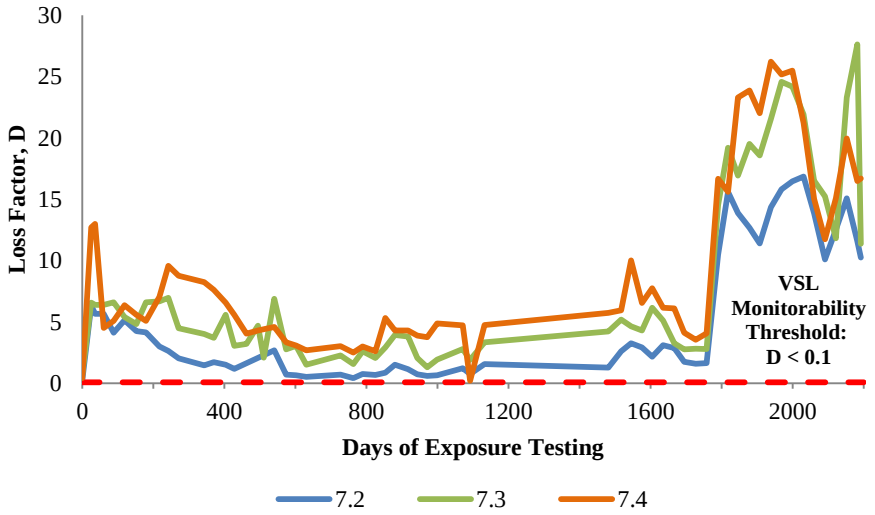

Figure 5.9: Loss Factors for Specimens 7.2, 7.3, and 7.4

The AC impedance data suggests monitorability of Specimens 7.2, 7.3, and 7.4 is questionable. The resistance data indicates that none of the 7-series specimens experienced a short circuit during the exposure testing period but the drops in resistance imply that at some point moisture had entered the duct through a defect and therefore moisture, oxygen and/or chlorides might have entered the tendon. There were signs of moisture when the tendons were cut from all the anchorages of the 7-series when grout samples were obtained for chloride concentration testing. Even with the humid climate in Austin, the readings should not have much variability from month to month. Changing the frequency to 100 Hz, as suggested in Reference 21, did not change the variability in the data. This further suggests that the measuring device used does not comply with accepted standards for measuring AC impedence[21].

5.3 Chloride Penetration Data and Analysis

As mentioned in Chapter 4, grout and concrete powder samples were taken on all specimens to test for their chloride content. The chloride limit for corrosion of 0.033% by weight of concrete used in this report comes from Reference 5. This limit might not be the actual corrosion limit for chlorides because the true limit may vary with cementious material content[17]. Also, the chloride corrosion limit from Reference 5 might not be an effective limit for evaluating corrosion of the non-conventional strands because the chloride levels that initiate corrosion might differ from strand type to strand type. However, the 0.033% by weight of concrete limit will be used for analysis of concrete and grout samples to provide continuity with References 2 and 5. Another reason why the 0.033% by weight of concrete threshold will be used instead of percent by weight of cementious material is because the cementious material content could not be determined exactly from the grout and anchorage backfill concrete due to material property concerns and due to limited availability of records for the concrete used to make the specimens.

5.3.1 Chloride Concentrations of Exterior Concrete

Figure 5.10 shows the chloride contents of the concrete powder extracted from the top surface of the ponding area. As mentioned in Chapter 4, all samples, except for the 7-series specimens, were extracted from top surface of the ponding area at two inches, in the live end direction, from the transverse centerline (Figure 4.9). The 7-series had concrete samples obtained from the top surface of the ponding area at the transverse centerline. All specimens had concrete samples taken at the extraction sites from a depth of 0.5 and 1 inch. As expected, all samples from the 0.5 inch depth had chloride contents well above the 0.033% corrosion limit. There was some scatter in chloride content among the samples taken at 0.5 inch depth. The chloride content ranged from 0.220% to 1.700%. The two specimens with the highest chloride content at the 0.5 inch depth were Specimen 2.3 (1.700%) and Specimen 7.4 (1.330%). These high chloride contents might be from micro cracking in the concrete allowing more chlorides to reach that depth. At

the 1 inch depth, all samples, except the sample from Specimen 4.1, had chloride contents above the 0.033% corrosion limit. The chloride content at the 1 inch depth were well grouped with a range of 0.020% (Specimen 4.1) to 0.187% (Specimen 3.3) with outliers at 0.46% (Specimen 7.2) and 1.180% (Specimen 2.3). Specimen 7.4 had chloride contents nearly equal for both depths, 0.47% (0.5 inch) and 0.46% (1 inch). This might be from a micro crack that ran the depth of the hole thus allowing nearly the same amount of chlorides to reach the 1.0 inch depth as did the 0.5 inch depth. It should be noted that a portion of the sample from the depth of 0.5 inch in top surface of Specimen 1.3 was sent to Tourney Consulting Group, Kalamazoo, Michigan had a chloride concentration of 0.542% by weight of concrete for testing in accordance with Reference 22. Material from the same sample tested at FSEL had a chloride concentration of 0.67% by weight of concrete using the James Instrument CL-200 Chloride Test System for chloride detection. It can be assumed that the results from the CL-200 Chloride Test System are fairly accurate because these chloride concentrations are in general agreement.

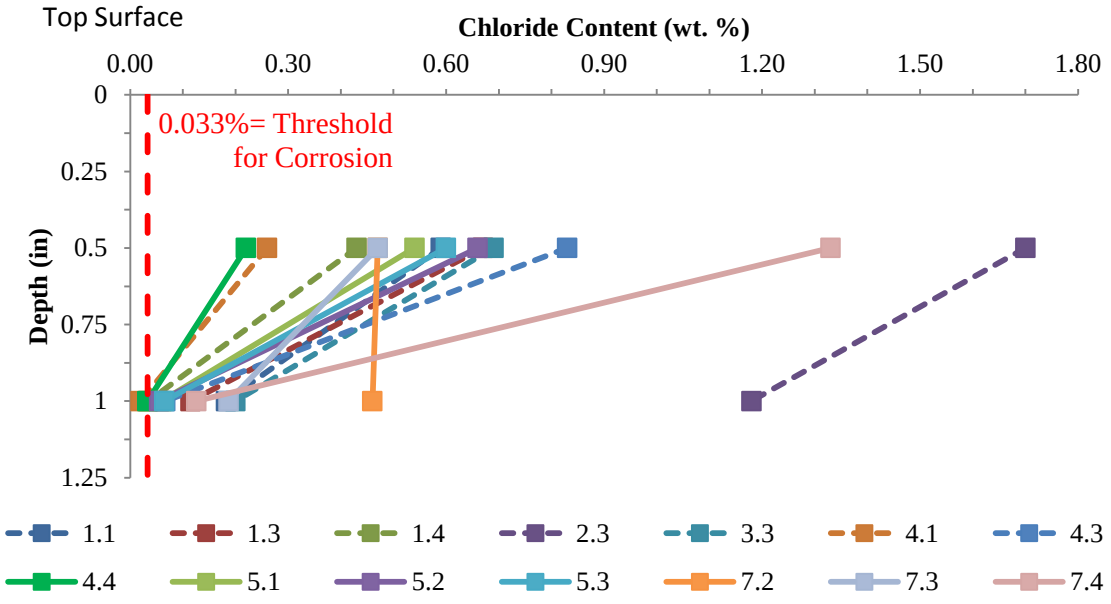

Figure 5.10: Chloride Content of Top Surface Concrete Samples

Figure 5.11 shows the chloride contents of the concrete powder extracted from the dead end anchorage region of the non-dripper specimens. Concrete powder samples from the dead end anchorage region were taken at 5 inches from the top surface of the specimen at a depth of 0.5 and 1 inch (Figure 4.10). As expected, most of the concrete samples from both depths had chloride contents below the corrosion limit. The two samples that were above the corrosion limit were both from a depth of 0.5 inch and were from Specimens 4.3 (0.28%) and 4.4 (0.143%). These outliers might be because these specimens did not have pour-backs because they were only reinforced with conventional epoxy coated and uncoated steel reinforcement and the concrete surface were scaled. Therefore when the ponding area was emptied at the end of the wet exposure period, salt may have adhered to the end of the specimen and traveled into the pore space of the concrete.

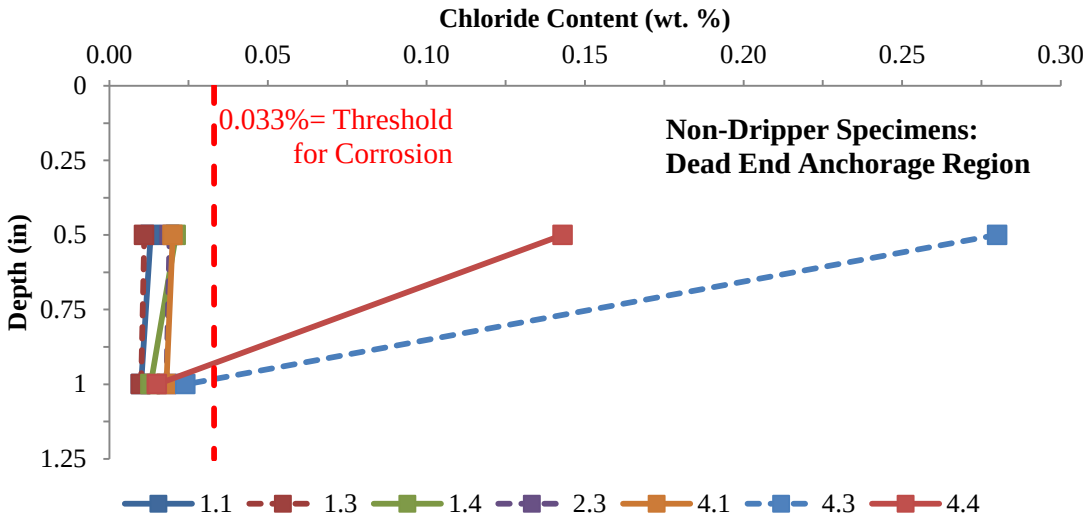

Figure 5.11: Chloride Content Non-Dripper Specimens' Dead End Anchorage Region

Figure 5.12 shows the chloride contents of the concrete powder extracted from the dead and live end anchorage regions of the dripper specimens. Except for the 7-series specimens, all specimens had the concrete powder samples taken from the dead end anchorage zone, five inches from the top surface of the specimen (Figure 4.10). The dripper specimens had concrete powder samples taken from the live end anchorage zone,

six inches from the top surface of the specimen. The 7-series specimens had concrete powder samples taken from both the live and dead end anchorage zone, six inches from the top surface of the specimen. At all extraction sites, samples were taken at depths 0.5 and 1 inch. Surprisingly, samples from the dead anchorage regions of Specimens 5.1, 5.2, and 5.3, which were the ends that received salt solution spray, did not have chloride contents above the corrosion limit. This might be due to the concrete of the pour backs being well consolidated causing the concrete to have lower permeability then the other dead end pour backs. Another interesting observation is the chloride contents of the live end anchorage regions of Specimens 7.2, 7.3, and 7.4 had chloride contents above the corrosion limit. This might be from the cracking over the vent spout in the anchorage region that had been observed during the visual inspection before autopsy, elevating the chloride content. As expected, samples from the dead end anchorage region of Specimens 3.3, 7.2, 7.3, and 7.4 had chloride levels that exceeded the corrosion limit but the chloride levels in the 7-series specimens were higher. This higher chloride content of the 7-series specimens might be for the same reason as the dead end anchorage region of the same specimens. Another anomaly is the chloride content of the concrete sample taken from the dead end anchorage region of Specimen 7.2 increased with depth. Again this might be due to the cracking over the dead end anchorage region.

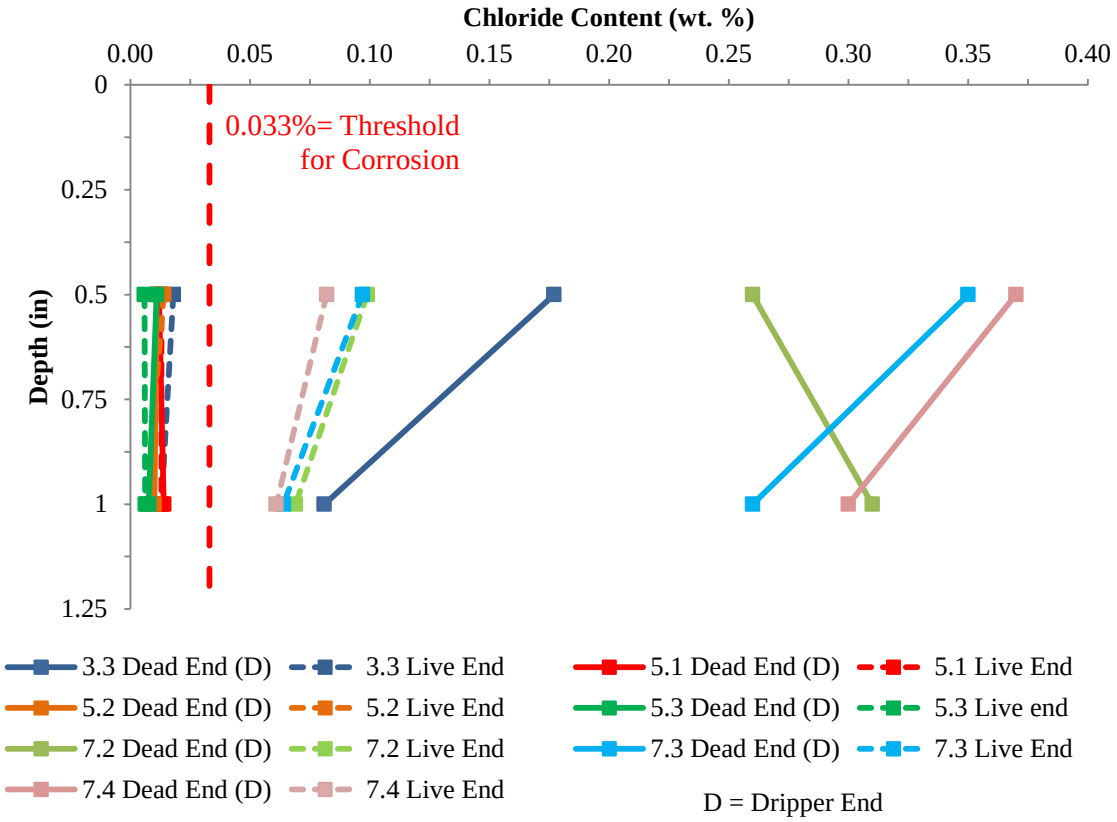

Figure 5.12: Chloride Content for the Live and Dead Ends of the Dripper Specimens

The elevated levels of chlorides in the top surface of the ponding area could be an indication of various factors but two things are prominent. One possible reason is the concrete in the ponding area was not finished and/or not properly consolidated, which would have increased the permeability of the concrete thus allowing chlorides to infiltrate the concrete faster. The other reason is the surface of the ponding area was in poor condition and micro cracks might have been present at the extraction site, even though care was taken to not drill where visible cracking had occurred. Regardless of the reason for the elevated chloride levels, the presence of large, deep cracks induced by the exterior eccentric load would have allowed sufficient amounts of chlorides to reach the duct to allow for corrosion and increase the probability of corrosion. Therefore the amount of chlorides infiltrating through the pore space of the concrete would be negligible.

5.3.2 Chloride Concentrations of Grout

As mentioned in Chapter 4, grout samples were taken from all anchorage plates of each tendon at both dead and live ends. For tendons in galvanized duct, additional samples were taken every 2 inches in regions where the galvanized ducts were deteriorated. For tendons in plastic duct, except for the 7-series specimens, grout samples were taken at midspan of the tendon. For the 7-series specimens, grout samples were taken from the regions where grout vents were located and at midspan of the tendon. It should be mentioned that the grout used in this Project 0-4562, SikaGrout 300 PT, might have been contaminated with chlorides to a level very near the chloride limit before the grout was placed in the tendons. Reference 25 limits the chloride concentration of SikaGrout 300 PT to 0.04% by weight of cementious material[25]. Assuming 65% of the SikaGrout 300 PT is cementious material, the limit for chloride concentration would be 0.026% by weight of grout. This is below but close to the limit of 0.033% by weight of grout used in this report. It should be noted that chloride concentration limit for corrosion of conventional steel from Reference 5 might not be the chloride limit for corrosion of the non-conventional stand types.

Figure 5.13 shows the chloride concentrations of the tendons that contained conventional strands, except for the tendon in Specimen 7.2. All tendons had chloride concentrations along the whole length of tendon above the corrosion limit of 0.033% by weight of grout. This is consistent with the average half-cell potential readings at the end of exposure testing being more negative or close to the greater than 90% probability of corrosion half-cell potential readings that these tendons had. As expected, the chloride concentrations were greater at midspan than in the anchorages. This might be because the chlorides would take longer to get to the anchorages because the chloride ions would have to travel through the interstitial space between the gout and the duct and/or interstitial space between the grout and the strand. The chloride concentrations at the anchorages were all somewhat equivalent. Surprisingly, the tendons from Specimen 2.3 had the highest chloride contents for this grouping. North tendon had 0.880% by weight of grout and the south tendon had 0.940% by weight of grout. The tendons in specimen

2.3 were 2-way plastic ducts. This might indicate that the ducts are not water tight and freely allowed chlorides to enter the tendon earlier than the other ducts. Another interesting observation is the tendons from Specimen 5.1 had chloride concentrations comparable to the chloride concentrations from the tendons in galvanized duct. The ducts that encased the tendon in Specimen 5.1 were 2-way plastic duct, as well. Again, the water tightness of the couplers and grout vents of the plastic ducts are in question. The north tendon of Specimen 1.4 had the lowest chloride concentration at midspan. The disparity in the average final half-cell potentials between the north and south tendons of Specimen 5.1 do not correspond to the difference in chloride concentrations at midspan of the same tendons. The south tendon had chloride concentrations greater than the north tendon and midspan, whereas the average final half cell-potentials (Figure 5.2) suggest that the north tendon should have had the higher chloride concentrations. Therefore, the disparity in the average final half-cell potentials might be from corrosion of the epoxy coated steel reinforcement located closer to the north duct elevating the half-cell potentials. The live end side of the south tendons in Specimens 1.1 and 1.4 had chloride concentrations that were far greater than the chloride concentrations of the dead end side of the tendons. Specimens 1.1 and 1.4 had tendons with galvanized duct. This difference in chloride concentrations between the live and dead ends of the south tendons of Specimens 1.1 and 1.4 might be from the cracks on the live end over the south tendons of the ponding area in the concrete allowing more chlorides to reach the live end of the tendons then the dead ends. On the other hand, the chloride concentrations of the north tendons of Specimens 1.1 and 1.4 dropped significantly away from the midspan of the tendon. The elevated chloride concentrations of the tendons would make the average final half-cell potentials more negative but the average final half-cell potentials for the tendons with galvanized duct, Specimens 1.1 and 1.4, were more negative than the potentials from the tendons with plastic duct. This would suggest that the corrosion of the zinc in the galvanized duct as well as the chlorides were contributing to the average final half-cell potential of the tendons in Specimens 1.1 and 1.4. The level of chlorides in the tendons is consistent with the corrosion observed during autopsies.

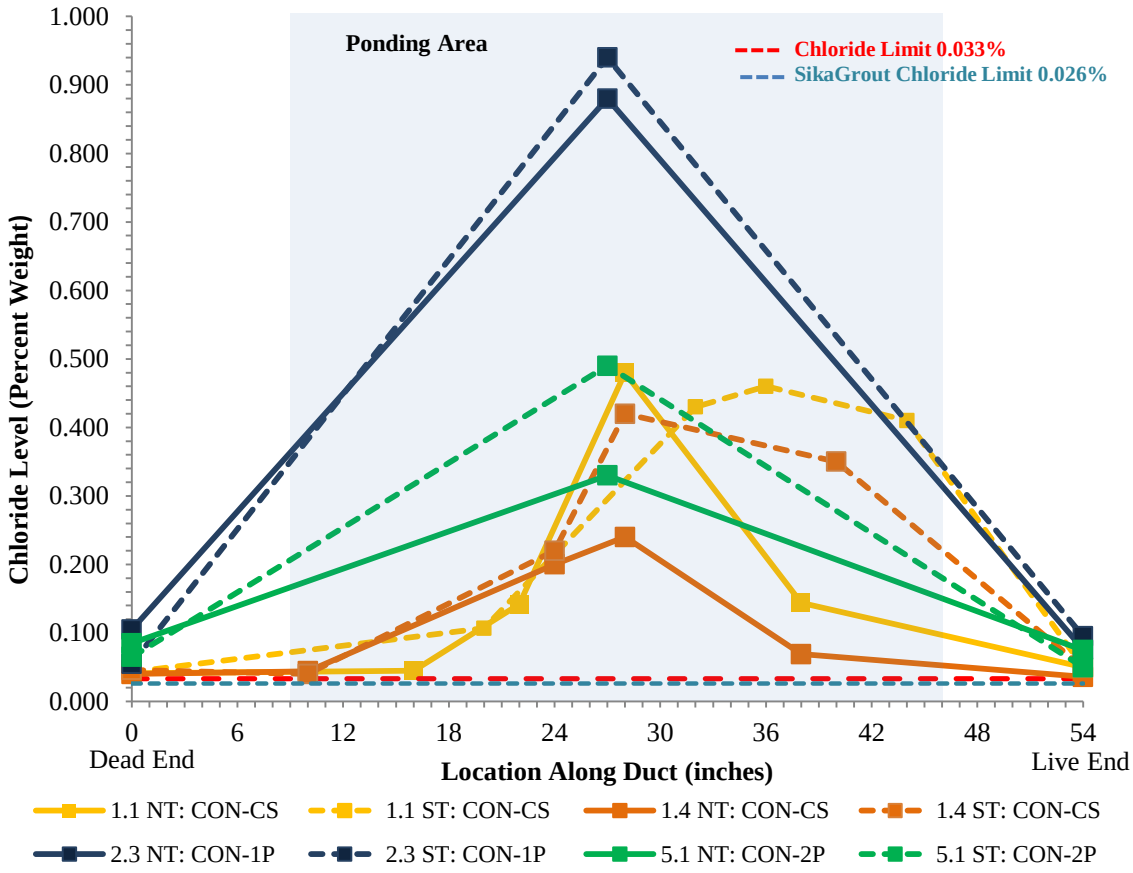

Figure 5.13: Chloride Concentrations for Tendons Containing Conventional Strands, Expect Specimen 7.2

Figure 5.14 shows the chloride concentrations for the tendons containing stainless clad, stainless steel, or copper clad strands. Along the length of all tendons, the chloride concentrations exceeded the 0.033% by weight corrosion limit. Except for the south tendon of Specimen 3.3, this would explain why the average final half-cell potentials were at or more negative than the strand types active corrosion potentials. As expected, the chloride concentrations at midspan were higher than the chloride concentrations at the anchorages. Like mentioned previously, this might be because the chlorides would take longer to get to the anchorages because the chloride ions would have to travel through the interstitial space between the gout and the duct and/or interstitial space between the grout

and the strand. The chloride concentrations on the dead end were well grouped whereas the chloride concentrations at the live end ranged from 0.033% (north tendon Specimen 5.2) to 0.220% (north tendon Specimen 3.3) by weight of grout. All the tendons from Specimens 1.3 and 4.1 and the north tendons of Specimens 5.2 and 5.3 were well grouped at the live end region. The south tendon of Specimen 3.3 had the highest chloride concentration at midspan in this grouping, 0.480% by weight of grout. The lowest chloride concentration at midspan is from the south tendon of Specimen 3.3, 0.220% by weight of concrete. Surprisingly, the difference in levels of chlorides between the north and the south tendons of Specimen 3.3 does not correspond to the difference in average final half-cell potentials experienced by the tendons of Specimen 3.3. The greater chloride concentrations in the south tendon of Specimen 3.3 suggest that the lab installed grout vent did not work as well as the manufactured installed grout vent on the coupler at keeping out chlorides. This would also suggest that corrosion in the epoxy coated steel reinforcement might be contributing more to the average final half-cell potentials of the north tendon than the south tendon. The difference in chloride concentrations between the north and south tendons of Specimens 5.2 and 5.3 corresponds well with the disparity between the average final half-cell potentials of the tendons. This suggests that the coupler on the north duct did not work as well at keeping out chlorides as the lab installed grout vent on the south duct. The tendons of Specimens 5.2 and 5.3 were encased in plastic duct. Again, the majority of the tendons with plastic duct had chloride concentrations at midspan greater than the tendons with galvanized ducts. Again, this calls into question the ability of the plastic duct couplers to keep out moisture, oxygen, and/or chlorides. To reiterate, when the comparison of the chloride concentration and the average final half-cell potentials are made it can be shown that presence of chlorides and the corrosion of the zinc in the galvanized duct would elevate the average final half-cell potentials.

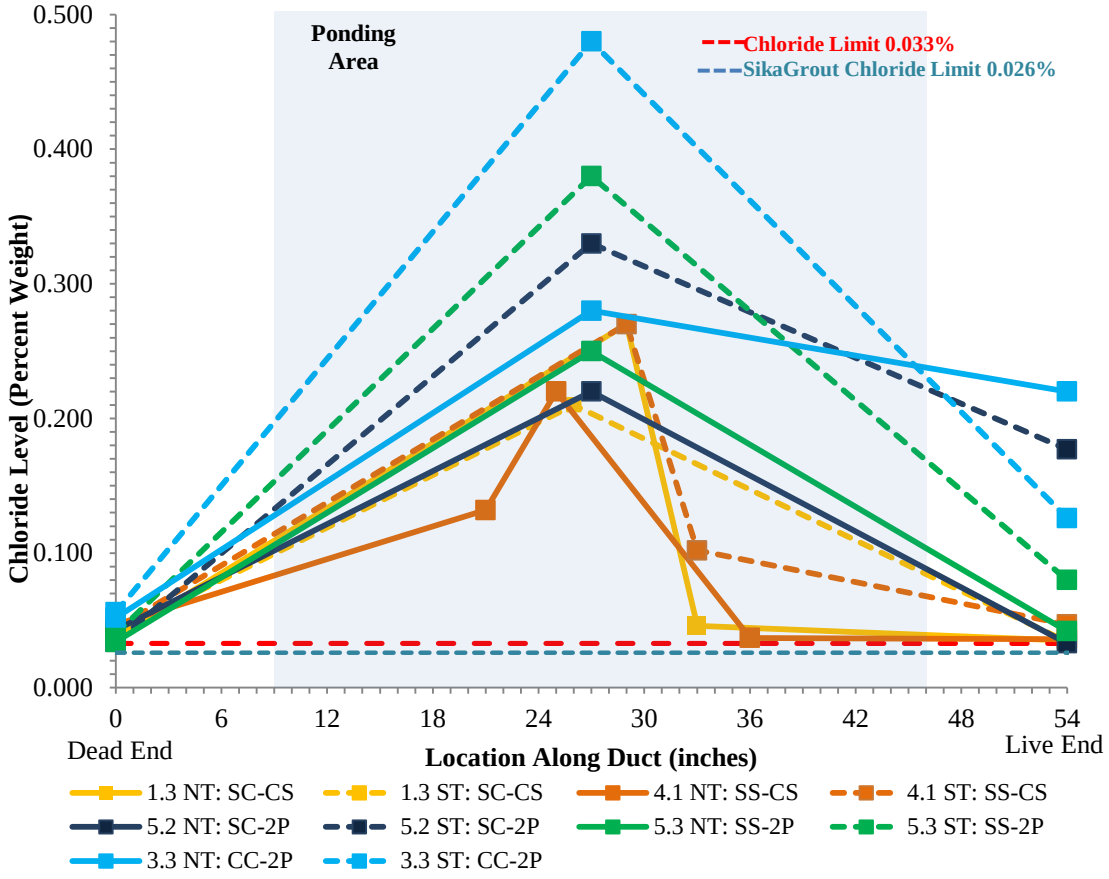

Figure 5.14: Chloride Concentrations for Tendons Containing Stainless Clad, Stainless Steel, or Copper Clad Strands

Figure 5.15 shows the chloride concentrations of the tendons in the 7-series specimens. The chloride levels at midspan were at or just below the 0.033% by weight of grout limit for corrosion and were smaller than the rest of the sample locations but were higher than Sika limit of 0.026% by weight of grout[25]. The chloride concentration being below the rest of the sample location was expected because the integrity of the duct at midspan was not breached due to a splice and/or grout vent and it was at the apex of the duct. The chloride concentrations being above the Sika limit is troublesome and suggests that grout may have been contaminated before it was placed in the tendon. For most of the tendons, the chloride concentrations at the locations of the splices were higher than the rest of the locations. This suggests that the splices are not water tight and corresponds to the AC impedance data. The AC impedance data indicated that there

might be a defect in the duct which allowed moisture, oxygen, and/or chlorides into the duct. There was moisture observed in the anchorage region when the tendons were cut from the anchorage to obtain grout samples for the chloride concentration testing. The chloride concentration at the dead end anchorage zone of the tendon of Specimen 7.2 was higher than the dead end splice region. This can be explained. During the autopsy of Specimen 7.2, the duct at the splice region had a crack and one of the stands was found to have severe pitting in the same location. This suggests that the concentration of chlorides in this region would be extremely elevated. No definitive reason can be given for the lower chloride concentrations of the grout in the region where the crack in the duct of Specimen 7.2 was observed. It should be noted that chlorides do not cause corrosion but contribute to corrosion process by breaking down the passive layer and raising the pH in the region of the corrosion. Except for Specimen 7.4, the chloride concentrations do not correspond to the average final half-cell potentials for the tendon with conventional strands, Specimen 7.2, or with the active corrosion potential for tendon with hot dip galvanized, Specimen 7.3. Specimen 7.4 had an average half-cell potential that was more negative than the greater than 90% probability of corrosion half-cell potential and had chloride concentrations above the corrosion limit of 0.033% chlorides by weight of grout. The tendon in Specimen 7.4 had flow filled epoxy coated strands and during autopsy the strand was found to have minimal corrosion in the main autopsy region. This suggests that the elevated average final half-cell potentials were possibly from the corrosion of the uncoated steel reinforcement that was used to conduct AC impedance readings and/or the corrosion of epoxy coated steel reinforcement.

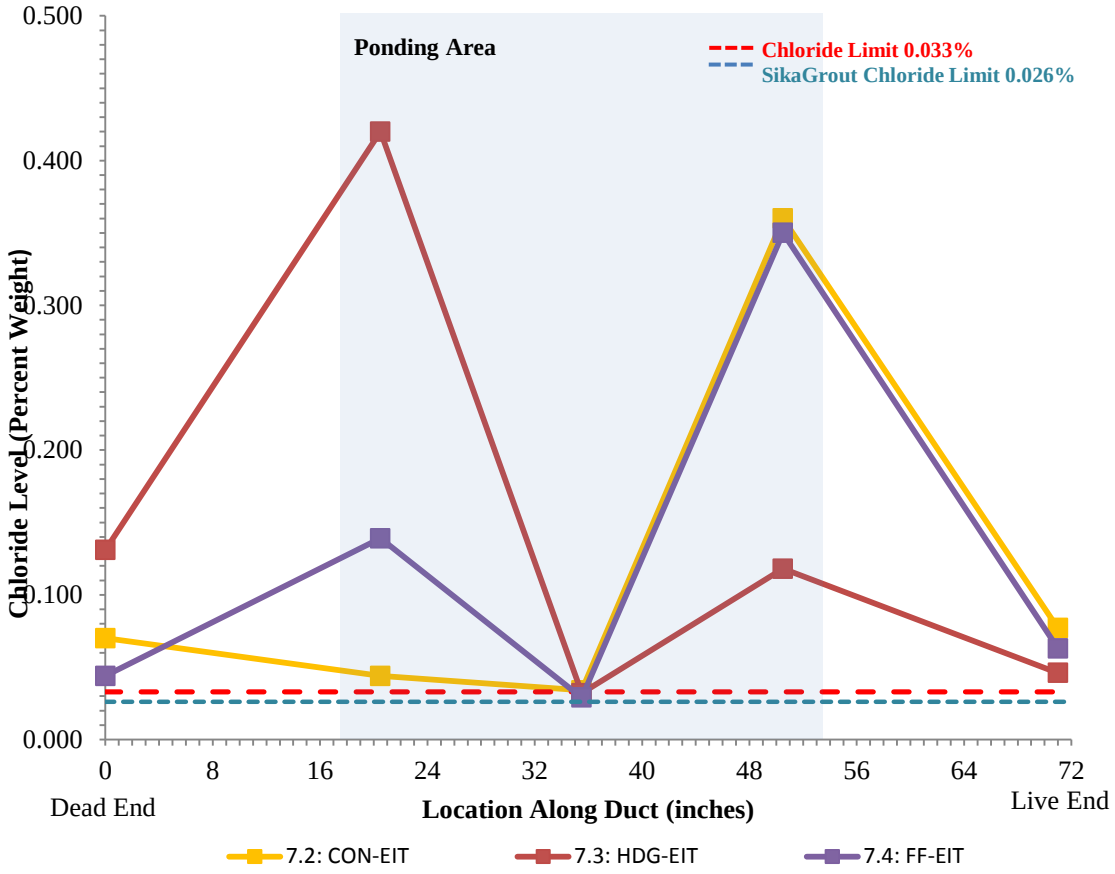

Figure 5.15: Chloride Concentrations of Tendons in the 7-Series Specimens

The majority of the chloride concentrations in the tendons correspond with the average final half-cell potentials of the tendons. The disparity between the chloride concentrations of the tendons in plastic and galvanized duct reinforces the suggestion that corrosion of the zinc in the galvanized coating of the galvanized ducts contributed to the average final half-cell potential readings. The disparities in the comparison between half-cell potentials and chloride concentrations of tendons in the same specimen suggest that the epoxy coated steel reinforcement was corroded. Corrosion of the epoxy coated steel reinforcement was observed during autopsy.

The testing errors for chloride concentration for both the concrete and grout could have occurred. One error could have come from cross contamination during the extraction of the concrete or even when the grout was being ground in the mortar and

pestle, even though care was taken to prevent cross contamination. Another error could have occurred when using the CL-200 Chloride Test System. The testing device does not give an instantaneous chloride concentration. So, if the researcher does not wait for the reading from the device to stabilize then the wrong concentration will be recorded. Another error that might occur when using this device is the device should be calibrated every 2 hours. If not the device could give erroneous concentrations.

CHAPTER 6

Forensic Analysis

6.1 Autopsy Procedure

After exposure testing was completed on March 1, 2012, the final 14 specimens were autopsied. First, the exteriors were examined for signs of distress, new and further cracking, and staining. Following the visual inspection, all mild reinforcement, ducts, and post-tensioning tendons and anchorages were extracted from the specimens and examined for signs of corrosion. The post-tensioning anchorages from the dead ends of non-dripper specimens and from the live and dead ends of the dripper specimens were then examined.

6.1.1 Final Visual Examination

The procedures of Reference 24 were used to examine the visible surfaces of each specimen for cracking, surface flaws, discoloration and corrosion staining, and efflorescence. Each specimen was photographed before it was unloaded and autopsied. Surface cracks in the ponding area were measured, marked, photographed, and mapped using a crack scope, crack comparator, grid, and camera (Figure 6.1). The cracks were traced with a marker for visibility and photographed from approximately four feet above the center line of the ponding area.

Figure 6.1: Crack Mapping and Crack Measuring Tools

The measurements from the crack mapping were used to determine a crack rating for the specimen. The crack rating in Equation 6-1 was adapted from Reference 5 and was used to numerically compare the extent of cracking between specimens.

$$Crack\ Rating = \sum_{i=1}^{m} w_i^{avg} \times l_i \qquad \textbf{\textit{Equation 6-1}}$$

Where,

$w^{avg}{}_i$ = average crack width for crack i at the end of exposure testing

l_i = crack length at end of exposure testing period for crack i

m = number of longitudinal and transverse cracks within the main autopsy region

i = crack under consideration

A beam with a single transverse crack across the 18 inch face with an average width of 0.015 inch would have a rating of 0.27.

The crack width and crack rating for each specimen will be given in Section 6.2 and will be analyzed in Chapter 7.

6.1.2 Specimen Unloading

From the research conducted in Reference 2, it was decided to unload the specimens by cutting the Dywidag bars with an oxy-acetylene torch and place a large concrete block in front of the live end to control the possible explosive unloading of the Dywidag bar. Figure 6.2 shows cutting the Dywidag bar to unload specimen.

Figure 6.2: Cutting Dywidag Bar to Unload Specimen

6.1.3 Cutting Beams and Removal of Reinforcing Elements

Specimen blocks were cut from each specimen using a walk behind gas powered concrete saw with water cooled 26 inch diamond blade by cutting longitudinally along both sides of the specimen (Figure 6.3). Figure 6.3 also shows the locations of the cut lines and the main autopsy region. The resulting specimen blocks for all the specimens except the 7-series specimens were 72 inches long by 18 inches wide by approximately 9 inches deep. The 7-series specimens were the same width and depth but were 84 inches in length. The specimen block depths varied by about five inches because the walk behind saw tended to stray from a straight line while cutting. The resulting specimen blocks were stacked until the mild reinforcement and post-tensioning components could be removed from them (Figure 6.4). The specimen blocks then had their mild reinforcement and post-tensioning components removed by carefully chipping the concrete away from the items of interest with an electric jack-hammer (Figure 6.5). The

chipping was done carefully to minimize the damage to the items. During the chipping operations the longitudinal mild reinforcement and tendons were cut twice in the main autopsy region of the specimen blocks using a dry blade gas powered hand held concrete saw (Figure 6.5). Both cuts were made 21 inches from the longitudinal centerline of the main autopsy region (ponding area plus three inches on either side) towards the dead and live end of the specimen blocks, respectively. The longitudinal mild reinforcement and tendons measured approximately 42 inches in length after cutting. The hand held saw was used to cut the longitudinal mild reinforcement and the tendons during chipping operations instead of the walk behind saw because the research team feared that the water from the walk behind saw would force more chlorides into the tendon. The mild reinforcement and post-tensioning components were moved indoors to the clean room at FSEL immediately after removal to prevent any further corrosion (Figure 6.6). The size of the main autopsy regions were similar to the ones used in References 5 and 7 for Project 0-1405 but the length of the main autopsy region was shortened by 30 inches because of the compact nature of the Project 0-4562 specimens[2].

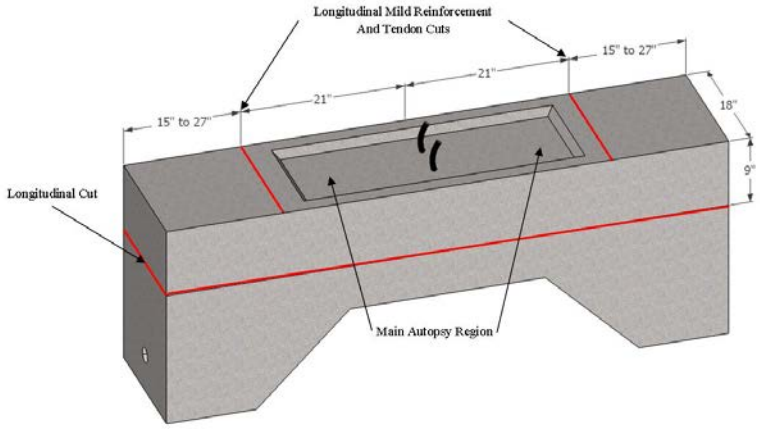

Figure 6.3: Longitudinal Cut Made on Side of Specimen (Top) and Cut Diagram (Bottom)

Figure 6.4: Stacked Specimen Blocks Awaiting Removal of Mild Reinforcement and Post-Tensioning Components

Figure 6.5: Chipping Post-Tensioning Components and Mild Reinforcement from Specimen Blocks (Kevin Moyer on the left and Michael Weyenberg on the right)

Figure 6.6: Storage of the Mild Reinforcement and Post-Tensioning Components in the Clean Room at FSEL

6.1.4 Removal of Post-Tensioning Anchorages

The post-tensioning components from the dead and live anchorage regions were carefully chipped away from the surrounding concrete with an electric jack-hammer. For most specimens, the anchorage plates and anchorage heads were able to be removed largely intact but a few were cut by the wet saw due to the deviation of the saw during cutting operations (Figure 6.7). All of the tendons, except for the tendons from the 7-series specimens, removed from the anchorage regions were approximately 14 inches long. The tendons from the anchorage regions of the 7-series specimens were approximately 18 inches long. The anchorage components were moved indoors to the clean room at FSEL immediately after removal to prevent further corrosion (Figure 6.6).

Figure 6.7: Damage from Saw of the South Dead End Anchorage of Specimen 5.2

6.1.5 Disassembly of Post-Tensioning Tendons

After removal from the main autopsy region, the ducts were removed from the tendon to expose the underlying grout by cutting both sides of the duct longitudinally with an electric grinder. Then the grout was examined for any corrosion staining, cracks, voids, and differential coloration. For galvanized duct, samples of grout were taken every two inches in regions where the duct had deteriorated due to corrosion. Grout was removed from the plastic ducts only at midspan if no damage in the duct was observed at any other location. The electrically isolated tendons had grout removed only from the

grout vent region and at midspan if no damage in the duct was observed at another location. Care was taken to ensure that a representative sample of grout was taken from the entire depth of the tendon. After grout samples were taken, the strands, except for the strands from specimen 7.4, were carefully removed from the grout and then the exterior was examined for any signs of corrosion. The flow-filled epoxy coated strands from Specimen 7.4 had to have their epoxy coating removed after the strands were removed from the grout and the then exteriors of the strands were examined for signs of corrosion. Removal of the epoxy coating was accomplished by applying an industrial paint remover on the epoxy coating. Then the paint remover coated strands were encased in aluminum foil for seven days. After seven days, the epoxy was stripped from the strands and the then exterior of the strands were examined for signs of corrosion. The wires of the all strands were carefully separated from each other using a screwdriver so that the interstices could be examined for corrosion (Figure 6.8). Throughout the process extensive photographs were taken at each step.

Figure 6.8: Separating Wires of the Strand Using a Screwdriver[2]

To start the process of removing the strands from the anchorage zones, the tendon had to be cut from the anchorage plate to expose the grout in the anchorage plate. Then grout samples were carefully taken from the anchorage plate using a small hammer drill ensuring that the strands were not damaged. Grout samples were taken from all anchorage plates of a specimen (Figure 4.11). The same process was used to remove the strands from the tendon cut from the anchorage plate as was used to remove the strands

from the tendon cut from the main autopsy region. After grout samples were taken from the anchorage plate, the anchorages were disassembled. The anchorage plate had to be halved using an oxy-acetylene torch. Care was taken to ensure that the strands did not become damaged during the cutting process. The strands were then removed from the anchor head by using an oxy-acetylene torch with a rosebud tip to heat up the anchor head and then the strands were hammered out. Note, some strands had to be cut flush with the dead end anchor head because the strands were too flexible and the wedges had expanded to such an extent that they would not easily release from the anchor head.

6.1.6 Element Rating System

The numerical rating system outlined in Reference 8 for Project 0-1405 was used to evaluate and compare corrosion damage among the metal components inside each Project 0-4562 specimen. Reference 8 did not have a numerical rating system for plastic duct or the epoxy coating of the prestressing strand. A numerical rating system was developed in Reference 2 for the plastic duct[2]. A numerical rating system was developed for the epoxy coating of the flow filled epoxy coated prestressing strands by the author.

Epoxy Coated Steel Bar Rating System

The longitudinal epoxy coated and/or uncoated steel bars for each specimen were divided up into 21 sections with each section being two inches (Figure 6.9). The transverse epoxy coated steel bars had a horizontal and vertical region. The horizontal region was divided up into 6 sections each being 2 inches long and the vertical section was divided up into 2 sections each being 3 inches long (Figure 6.9). Both sides of each bar type were rated separately using Table 6.1 and the ratings were combined. Note, the steel bars in Reference 8 were not epoxy coated steel bars but the numerical rating system will be useful in comparing the corrosion damage between each Project 0-4562 specimen.

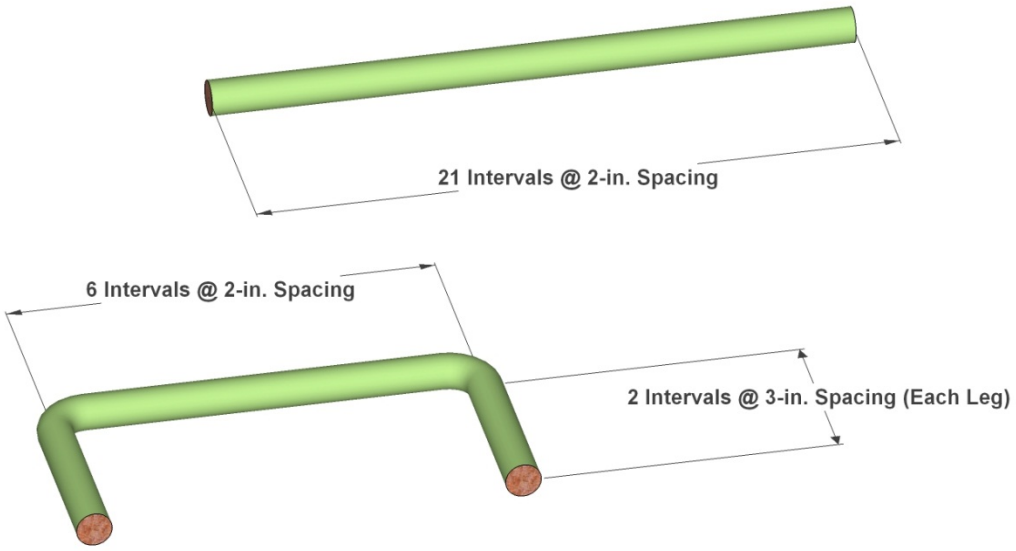

Figure 6.9: Spacing Layout for Longitudinal and Transverse Bars[2]

Table 6.1: Epoxy Coated Steel Bars Numerical Rating System[2]

Code	Meaning	Description	Rating
NC	No Corrosion	No evidence of corrosion	0
D	Discoloration	No evidence of corrosion, but some discoloration from original color	1
L	Light	Surface corrosion on less than one half of the interval, no pitting is present. Surface corrosion can be removed using a cleaning pad	2
M	Moderate	Surface corrosion on more than one half of the interval, no pitting. **AND/OR** Any Corrosion which cannot be removed using cleaning pad	4
P	Pitting	Pit is visible to the unaided eye	8
AR	Area Reduction	Measurable reduction in bar cross-sectional area due to corrosion	R^2

R = Estimated cross-sectional area reduction in percent

To distinguish if a section had a rating of L or M, a 3M Scotchbrite™ scratch pad was used to scrub the section with a pressure equivalent to the pressure needed to remove

dried food particles from a pot or pan. The AR rating was determined by measuring the area loss with a micrometer and converting it to a percentage of the total cross sectional area. The highest possible rating an interval can achieve is 10,000. This indicates that the bar has lost the entire cross section.

Equation 6-2 gives the rating for one longitudinal bar.

$$R_{bar} = \sum_{i=1}^{21}\left(R_{top,i} + R_{bottom,i}\right) \qquad \textbf{\textit{Equation 6-2}}$$

Equation 6-3 gives the rating for both longitudinal bars.

$$R_{total} = \sum_{n=1}^{2} R_{bar,n} \qquad \textbf{\textit{Equation 6-3}}$$

Where,

$R_{top,i}$ = corrosion rating on top bar surface, interval i

$R_{bottom,i}$ = corrosion rating on bottom bar surface, interval i

$R_{bar,n}$ = total bar corrosion rating, bar n

i = interval, 1 to 21

n = bar number, 1 to 2 (for the 7-Series specimens n=4)

Equation 6-4 gives the generalized corrosion rating in units of average rating per foot of bar.

$$R_{gen,bar} = \frac{R_{total}}{2 \times 3.5} \qquad \textbf{\textit{Equation 6-4}}$$

Note: 2×3.5 in the denominator is the total length in feet of the longitudinal bars.

Equation 6-5 gives the total rating for an individual transverse bar.

$$R_{stirrup} = \sum_{i=1}^{10}\left(R_{top,i} + R_{bottom,i}\right) \qquad \textbf{\textit{Equation 6-5}}$$

Equation 6-6 gives the total rating for all seven transverse bars in the main autopsy region.

$$R_{total} = \sum_{n=1}^{7} R_{stirrup,n} \qquad \textbf{\textit{Equation 6-6}}$$

Where,

$R_{top,i}$ = corrosion rating on top bar surface, interval i

$R_{bottom,i}$ = corrosion rating on bottom bar surface, interval i

$R_{stirrup,n}$ = total bar corrosion rating, bar n

i = interval, 1 to 10

n = stirrup number, 1 to 7

Equation 6-7 gives the generalized transverse corrosion rating for the transverse bars in the main autopsy region. It is used to compare transverse bar corrosion between specimens.

$$R_{gen,stirrup} = \frac{R_{total}}{7 \times 2} \qquad \textbf{\textit{Equation 6-7}}$$

Note: 7×2 in the denominator is the total length in feet of the transverse bars in the main autopsy region.

Prestressing Strand Rating System

All the wires of the strands from the main autopsy region, six outer and one inner, were divided up into 21 intervals of two inches length per interval. The wires of the strands from the anchorage zone were divided up into 2 inch length intervals as well, with the number of intervals varying due to the system type. The wires were numerically evaluated using the method outlined in Reference 8, which is shown in Table 6.2. This system of evaluation does not take into account the type of metal or metals that the strands are made of. Therefore a direct comparison cannot be made between strand types but the corrosion rating can be compared to the chloride concentration and the half-cell potentials of the tendons that contained the same strand type.

Table 6.2: Prestressing Strand Numerical Rating System[8]

Code	Meaning	Description	Rating
NC	No Corrosion	No evidence of corrosion	0
D	Discoloration	No evidence of corrosion, but some discoloration from original color	1
L	Light	Surface corrosion on less than one half of the interval, no pitting is present. Surface corrosion can be removed using a cleaning pad	2
M	Moderate	Surface corrosion on more than one half of the interval, no pitting. **AND/OR** Any Corrosion which cannot be removed using cleaning pad	4
P1	Mild Pitting	Broad shallow pits with a maximum pit depth not greater than 0.02 in.	8
P2	Moderate Pitting	Pitting where the maximum pit depth ranged between 0.02 in. and 0.04 in.	16
P3	Severe Pitting	Pitting where the maximum pit depth is greater than 0.04 in.	32

The same type of cleaning pad and process used for the epoxy coated steel bars was used on the strands to distinguish between ratings L and M. A micrometer was used to measure the pit depths. The highest possible rating that an interval can attain is 224. This signifies that every wire in a strand has severe pitting.

Equation 6-8 calculates the corrosion rating for an individual strand.

$$R_{strand} = \sum_{i=1}^{21}\left(n_i \times R_{outer,i} + R_{inner,i}\right) \qquad \textbf{\textit{Equation 6-8}}$$

The total corrosion rating for all strands in one duct is given by Equation 6-9:

$$R_{total} = \sum_{n=1}^{3} R_{strand,n} \qquad \textbf{\textit{Equation 6-9}}$$

Where,

$R_{outer,i}$ = corrosion rating on outer wires, interval i

n_i = number of corroded outer wires in interval i

$R_{inner,i}$ = corrosion rating on inner wire, interval i

n = strand number, 1 to 3

i = interval, 1 to 21 for main autopsy region

Equation 6-10 gives the generalized corrosion rating for the strands in units per foot of strand. This generalized corrosion rating will be used to compare strands of the same type.

$$R_{gen,strand} = \frac{R_{total}}{3 \times 3.5} \qquad \textit{Equation 6-10}$$

Note: 3 × 3.5 in the denominator is the total length in feet of the strands.

Before the epoxy coating was stripped off the epoxy coated strand, the coating was evaluated using Table 6.3. This was done to evaluate the condition of the epoxy coating before the strand was rated for corrosion. The rating system is a hybrid of the plastic duct rating system. Holes were measured using a micrometer. The highest rating that an interval can receive is 2400. This signifies that the entire outer coating is gone in that interval and the outer wires are total exposed.

Table 6.3: Epoxy Coating of Prestressing Strand Numerical Rating System

Code	Meaning	Description	Rating
ND	No Defect	No evidence of any defect in the epoxy coating	0
S	Scratch	Slight surface scratches on epoxy coating	4
G	Gouge/Deep Scratch	Epoxy coating is gouged or deeply scratched but underlying strand is not visible with the unaided eye	16
H	Hole in Epoxy Coating	Hole gouged in epoxy coating of strand and underlying strand is visible	$32+A_h$

A_h =Estimated area of hole(s) in mm^2.

Equation 6-11 calculates the epoxy condition rating for an individual strand.

$$R_{epoxy} = \sum_{i=1}^{21} R_{epoxy,i} \qquad \textbf{\textit{Equation 6-11}}$$

The total epoxy condition rating for all strands in one duct is given by Equation 6-12:

$$R_{total} = \sum_{n=1}^{3} R_{epoxy,n} \qquad \textbf{\textit{Equation 6-12}}$$

Where,

$R_{epoxy,i}$ = epoxy condition rating, interval i

n = strand number, 1 to 3

i = interval, 1 to 21 for main autopsy region

Equation 6-13 gives the generalized epoxy condition rating for the strands in units per foot of strand.

$$R_{gen,epoxy} = \frac{R_{total}}{3 \times 3.5} \qquad \textbf{\textit{Equation 6-13}}$$

Note: 3 × 3.5 in the denominator is the total length in feet of the strands.

Galvanized Duct Rating System

The galvanized ducts from the main autopsy region were divided up into 21 intervals each interval being two inches long and the ducts from the anchorage zone were divided up into two inch intervals with the number of intervals varying between post-tensioning systems. The top and bottom of the duct had their inside and outside evaluated using the method outlined in Reference 8. Table 6.4 shows the rating system used to numerically evaluate the galvanized ducts. Holes were measured using a micrometer. The maximum an individual interval can achieve is 8,139, which indicates that the duct is total corroded over the entire interval.

Table 6.4: Galvanized Duct Numerical Rating System[8]

Code	Meaning	Description	Rating
NC	No Corrosion	No evidence of corrosion	0
D	Discoloration	No evidence of corrosion, but some discoloration from original color	1
L	Light	Surface corrosion on less than one half of the interval, no pitting is present.	2
M	Moderate	Surface corrosion on more than one half of the interval, no pitting is present	4
S	Severe	Corrosion completely covers the interval **AND/OR** Presence of Pitting	8
H	Hole Through Duct	Hole corroded through duct Used in conjunction with ratings D, L, M, and S	$32+A_h$

A_h =Estimated area of hole(s) in mm^2.

Equation 6-14 gives the corrosion rating for the entire duct.

$$R_{total} = \sum_{i=1}^{21}\left(R_{top,outer,i} + R_{bottom,outer,i} + R_{top,inner,i} + R_{bottom,inner,i}\right)$$

Equation 6-14

Where,

$R_{top,outer,i}$ = top outer surface corrosion rating, interval i

$R_{bottom,outer,i}$ = bottom outer surface corrosion rating, interval i

$R_{top,inner,i}$ = top inner surface corrosion rating, interval i

$R_{bottom,inner,i}$ = bottom inner surface corrosion rating, interval i

i = interval, 1 to 21 for main autopsy region, 1 to 3 or 4 for anchorages

Equation 6-15 gives the generalized corrosion rates for an individual duct. This generalized corrosion rating will be used to compare individual ducts

$$R_{gen,duct} = \frac{R_{total}}{3.5}$$

Equation 6-15

Note: The 3.5 in denominator is the total length of duct in the main autopsy region.

Plastic Duct Rating System

The plastic ducts from the main autopsy region were divided up into 21 intervals each interval being two inches long. The ducts from the anchorage zone were divided up into two inch intervals with the number of intervals varying due to the type of post-tensioning system. The top and bottom of the ducts had their inside and outside evaluated using the method outlined in Reference 2. Table 6.5 shows the rating system used to numerically evaluate the plastic ducts. Holes and gouges were measured using a micrometer. The maximum an individual interval can achieve varies with duct diameter and rages from 9,436 to 13,612, which indicates that the duct is absent over the entire interval. Equations 6-14 and 6-15 give the damage rating and generalized damage rating for the entire duct, respectively.

Table 6.5: Plastic Duct Numerical Rating System[2]

Code	Meaning	Description	Rating
ND	No Defect	No evidence of any defect in the epoxy coating.	0
G	Gouge/Scratching	Gouges or scratches are present on the duct walls.	R^2
H	Hole Through Duct	Hole Present in Duct. Used in Conjunction with ratings ND and G.	$32+A_h$

R = Estimated cross-sectional area reduction in percent

A_h =Estimated area of hole(s) in mm^2.

6.2 Results of Forensic Analysis

Presented in this section are the results of the forensic analysis for each specimen. All bars, ducts, and strands are pictured with a measuring tape. For the longitudinal bars, ducts, and strands, the distance on the measuring tape correlates to the distance from the dead end of the components. For the components from the anchorage region, the distance on the measuring tape correlates to the distance from the end of the component closest to the outside end of the specimen. Figure 6.10 shows the designation criteria for the components from the main autopsy region. The components from the anchorage region are designated by north or south side and live or dead end depending on their location in the specimen. All rating plots for this chapter have the dead end on the left of the main

autopsy region and for the anchorage region the left side of the plot is the outside end of the component. For crack map figures of the main autopsy region, the left side of the figure is the dead end of the main autopsy region and the bottom of the figure is the north side.

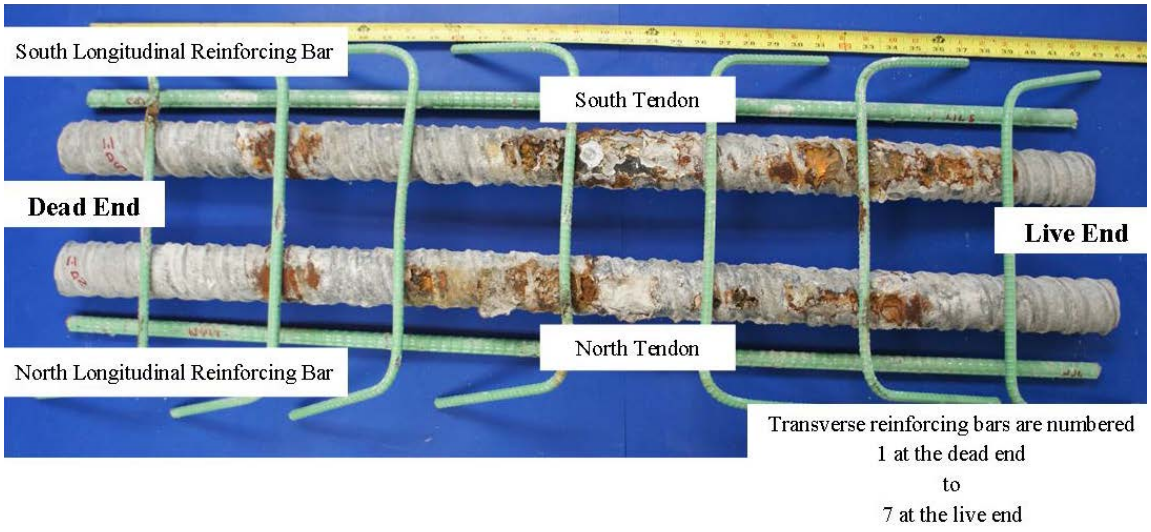

Figure 6.10: Designation Criteria for Components from the Main Autopsy Region

All plots in this section were formatted in a similar manner to References 2, 5, and 7. This was done to assist in the comparison of data from these References.

6.2.1 Specimen 1.1: Non-Galvanized Anchorage, Conventional Strand, Corrugated Galvanized Steel Duct

Figure 6.11: Specimen 1.1 Main Autopsy Region and Grout Vents

Table 6.6: Specimen 1.1 Summary of Main Autopsy Region Corrosion Ratings

Component	Maximum	Total	Generalized
Longitudinal Bars	4	28	4
Transverse Bars	12	95	7
North Duct	2829	15985	4567
South Duct	4144	23985	6853
North Strands	42	782	74
South Strands	48	699	67

6.2.1.1 Appearance

The surface of Specimen 1.1 had medium scaling over the majority of the exterior. Aggregate was visible in many locations, especially along the edges of the ponding area and sides of the specimen. The surface of the ponding area had medium scaling as well (Figure 6.11). There was a puddle of hardened grout about 2 inches in diameter approximately in the center of the ponding area. This puddle of hardened grout is from overflow during grouting operations. The base of the south grout vent had rust staining (Figure 6.11). This is an indication of corrosion inside the specimen. The backfill mortar in the live end anchorage pockets was separating from the concrete. This indicates that the mortar did not adhere well to the base concrete.

There were cracks present at the re-entrant corners of the corbel on both sides of the live end. These cracks were not present after live load application[1]. Therefore, the cracks had not been sealed with mortar or epoxy. The ponding area of Specimen 1.1 had 3 large transverse cracks that ran from the north to the south side of the specimen (Figure 6.12). The average crack width was approximately 0.01 inches. The crack rating for Specimen 1.1 was 0.42. See Figure 6.13 for the crack data from Specimen 1.1.

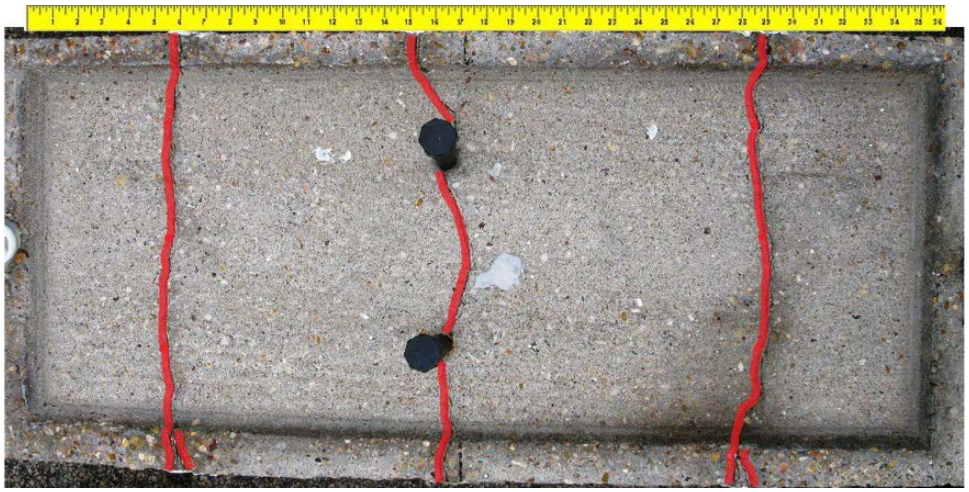

Figure 6.12: Specimen 1.1 Crack Map of Ponding Area

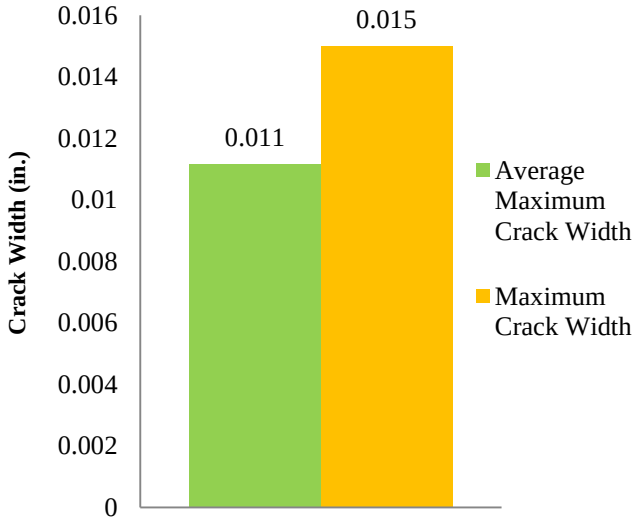

Figure 6.13: Crack Data for Specimen 1.1

6.2.1.2 Longitudinal and Transverse Bars

The north and south longitudinal bars had slight damage from when the bars were extracted from the specimen (Figure 6.14). Rust stains were also evident at locations where the transverse bars were tied to the longitudinal bars (Figure 6.14). This staining is from corrosion of the tie wire used to attach the transverse reinforcement to the longitudinal bars and NOT from the longitudinal bar itself. The south longitudinal bar had a spot of moderate corrosion on the longitudinal rib of the bar at approximately 23 inches from the dead end of the bar (Figure 6.14). Figure 6.20 shows the longitudinal bar's corrosion ratings and Table 6.6 shows the summary of the corrosion ratings for the longitudinal bars.

Figure 6.14: Extraction Damage, Rust Staining, and Moderate Corrosion of South Longitudinal Bar of Specimen 1.1

Transverse bars #1, #2, #3, #6, and #7 had damage from when they were extracted from the specimen. All the transverse bars had rust staining from corrosion of the tie wire used to attach the transverse bars to the longitudinal bars and to attach the ducts to the transverse bars. The staining is also from the corrosion of the galvanized duct. There was moderate corrosion on one of the vertical legs of bar #2 (Figure 6.15) and on the horizontal portion of bar #6. There was pitting on the horizontal portion of bar #4

(Figure 6.15). Bars #2, #4, and #6 had the highest rating, 19, 20, and 20, respectively. If any of the transverse bars were to have corrosion it would be these bars because of their close proximity to the induced deep cracks. The end bars, #1 and #7, had the lowest corrosion rating, 8 and 5, respectively. This was expected because these bars are outside the ponding area and should have had little to no exposure to chloride, moisture, and oxygen due to no evidence of cracks and increased concrete cover. Figure 6.20 shows the transverse bar's corrosion ratings and Table 6.6 shows the summary of the corrosion rating for the transverse bars.

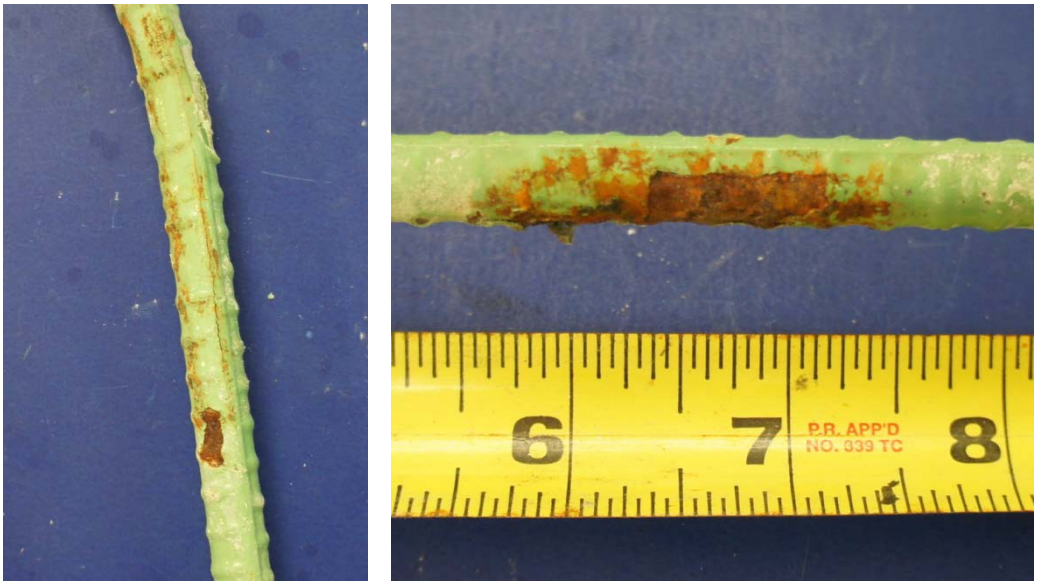

Figure 6.15: Moderate Corrosion on Vertical Leg of bar #2 (Left) and Pitting on Horizontal Portion of bar #4 (Right) of Specimen 1.1

6.2.1.3 Ducts

Both the north and south ducts had localized severe corrosion damage. This damage resulted in holes in the ducts. The top of the north duct had large holes at midspan and at intervals of approximately 6 inches until about the quarter points of the duct (Figure 6.16). The bottom of the north duct had moderate corrosion centered at midspan and at approximately 32 inches from the dead end of the duct (Figure 6.16). Except for the holes, the top inner surface of the north duct was in reasonably good shape with only a few locations of light corrosion next to where holes had occurred and at the

live and dead ends. The bottom inner surface of the north duct had no signs of corrosion. The top of the south duct had large holes at midspan and at the quarter points of the south duct (Figure 6.17). The bottom of the south duct had small holes at about the quarter points and moderate corrosion damage at midspan (Figure 6.17). The top inner surface of the south duct had no signs of corrosion at locations where no holes had occurred. The bottom inner surface of the south duct had light corrosion at midspan. The holes experienced by both the north and south ducts indicate that voids in the grout had formed along the top of the duct. The light corrosion observed on the bottom inner surface of the south duct might be from the chlorides traveling in the interstitial space between the grout and the duct after the holes had formed. Figure 6.20 shows the corrosion ratings for the ducts and Table 6.6 shows the summary of the corrosion ratings for the ducts.

Figure 6.16: Hole on the Top at Midspan (Left) and Moderate Corrosion on the Bottom at Midspan of the North Duct of Specimen 1.1(Right)

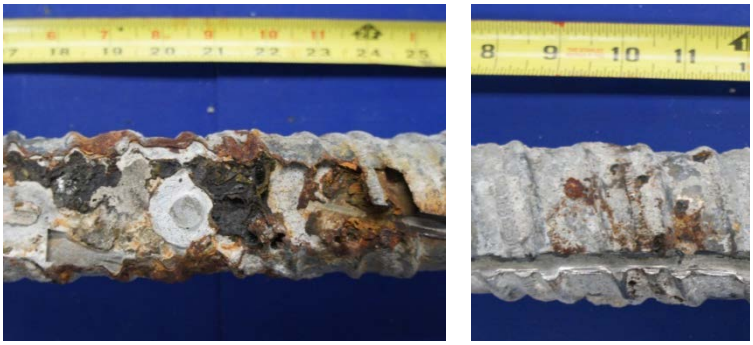

Figure 6.17: Hole on the Top at Midspan (Left) and Small Hole on the Bottom at the Dead End Quarter Point of Specimen 1.1 (Right)

6.2.1.4 Grout

Only a few transverse cracks and no longitudinal cracks were observed during examination of grout from the north and south grouts of Specimen 1.1. Staining from corrosion of the duct was observed at locations where corrosion had caused holes in both the north and south duct. Small voids in the grout were observed in the flutes at the top of both the north and south duct along the entire length of the each duct (Figure 6.18). These voids measured approximately 0.75 inch long and were as wide as the flute width.

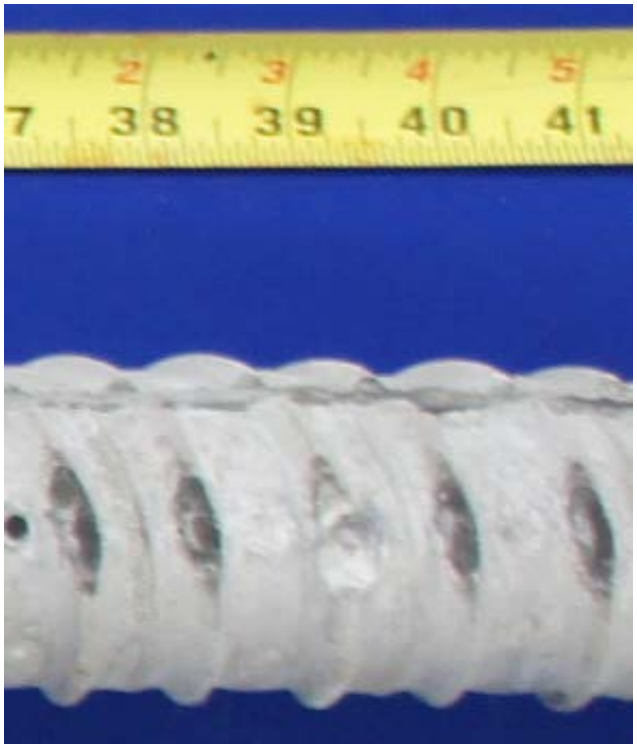

Figure 6.18: Observed Flute Voids in the Grout of the North Tendon of Specimen 1.1

The chloride concentrations were discussed in depth in Chapter 5. All the chloride concentrations were well above the 0.033% by weight of grout limit for corrosion. See Figure 5.13 for the results of the chloride concentration testing. As expected, the highest chloride concentration for the north tendon was at midspan and was 0.480% by weight of grout. The highest chloride concentration for the south tendon was not at midspan as

expected but at 36 inches from the dead end and was 0.460% by weight of grout. As expected, the anchorage regions had the lowest chloride concentrations. This might be because the chlorides would take longer to migrate to the anchorages because the chloride ions would have to travel through the interstitial space between the grout and the duct and/or the interstitial space between the grout and the strand.

6.2.1.5 Strands

The three strands in the north tendon had only minor damage. Discoloration was observed on many intervals on all the outer wires but only a few of the intervals had light corrosion. The entire length of two of the inner wires had moderate corrosion and the third inner wire had light corrosion along the enter length. This is an indication that moisture, oxygen, and chlorides had reached the strands. Corrosion ratings over the entire length of the three north strands were relatively uniform. The live end had the lowest ratings with an average of 32 and the midspan region had the highest ratings with an average of 39.

The three strands from the south tendon fared marginally better. Discoloration was observed on many intervals on all the outer wires but a few of the intervals experienced light corrosion. The inner wire of all three strands had light corrosion on most of the intervals but a few successive intervals of one strand had moderate corrosion. Again, this is an indication that moisture, oxygen, and chlorides had reached the strands. The corrosion ratings over the entire length of the three south strands were relatively uniform. An interval at midspan had the highest corrosion rating of 48 and as expected, the live and dead ends had the lowest corrosion ratings with an average of 31.

Figure 6.19 shows the condition of a typical strand and the condition of an unraveled strand. Figure 6.20 shows the corrosion ratings for the strands and Table 6.6 shows the summary of the corrosion ratings for the strands.

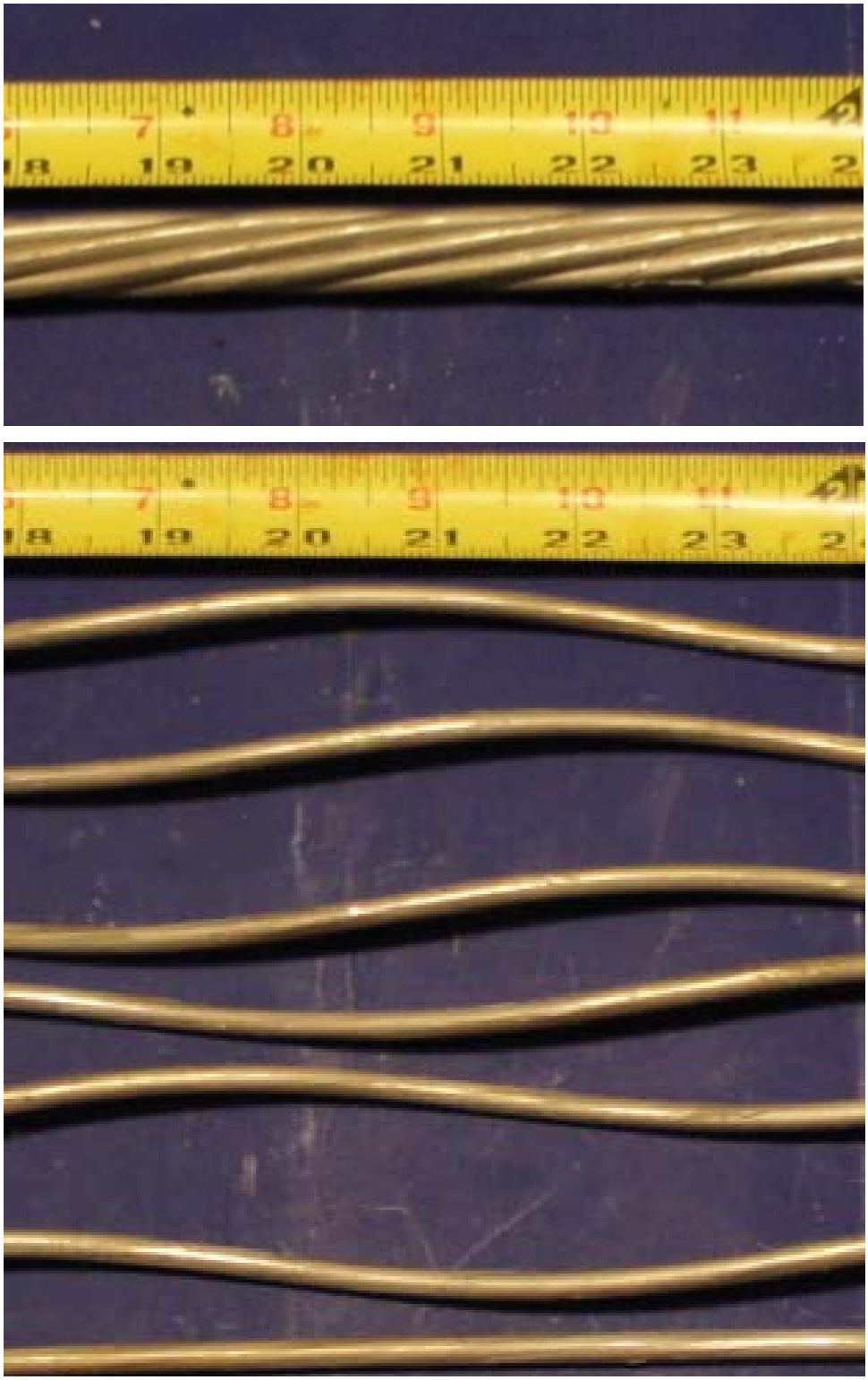

Figure 6.19: Typical Strand (Left) and Unraveled Strand (Right) from Specimen 1.1

Figure 6.20: Corrosion Rating Plots for Main Autopsy Region of Specimen 1.1

6.2.1.6 Dead End Anchorages

Most of the epoxy applied to the anchorage components before the anchorage cavity was backfilled had debonded from the anchorage components. The exposed faces of the north and south anchorage plate had light surface corrosion over approximately 80% of their surface but the embedded portion had no visible signs of corrosion (Figure 6.21). The sides of the north anchor head were primarily corrosion free with only light surface corrosion near the interface of the anchorage plate and anchor head but the sides of the south anchor head had no visible corrosion. The exposed face of the north and south anchor heads were corrosion free (Figure 6.21). However, the unexposed face of the north and south anchor heads had minimal spots of light corrosion. The ducts were not sealed to the anchorage plates with duct tape[1].

Figure 6.21: Dead End South Side Anchorage Assembly (Left) and Exposed Face of Anchor Head and Anchorage Plate (Right)from Specimen 1.1

Table 6.7: Specimen 1.1 Summary of Dead End Anchorage Region Corrosion Ratings

Component	Maximum	Total	Generalized
North Duct	6	11	16
South Duct	4	8	12
North Strands	37	199	66
South Strands	34	178	59

Both the north and south ducts from the dead end had no visible corrosion on their outer surface. The bottom inside surface of the north duct had light surface corrosion on two intervals. The inside of the south duct had no visible signs of corrosion. Figure 6.24

shows the corrosion ratings for the anchorage region ducts and Table 6.7 shows the summary of the corrosion ratings for the anchorage region ducts.

The grout from the north and south dead end tendons had no visible transverse or longitudinal cracks. The grout from both tendons had voids and signs of "bubbling" in the area of the flutes of the ducts along the length of the top surface (Figure 6.22). The grout from both tendons showed signs of segregation along the length of the anchorage region. Figure 6.22 shows grout and the ducts from the north and south anchorage region.

Figure 6.22: Dead End North Tendon Duct and Grout (Top) and Dead End South Tendon Duct and Grout (Bottom) from Specimen 1.1

The outer wires of the strands from the dead end of the north and south tendon had discoloration and light corrosion over the length of the stands. The inner wires had light corrosion over the total length of the strand. The wedges were intact and showed no visible signs of corrosion. Figure 6.23 shows a typical wedge, strand and an unraveled stand. Figure 6.24 shows the corrosion ratings for the anchorage region strands and Table 6.7 shows the summary of the corrosion ratings for the anchorage region stands.

Figure 6.23: Typical Wedge (Top), Strand (Middle), and Unraveled Stand (Bottom) for the Dead End Anchorage Region of Specimen 1.1

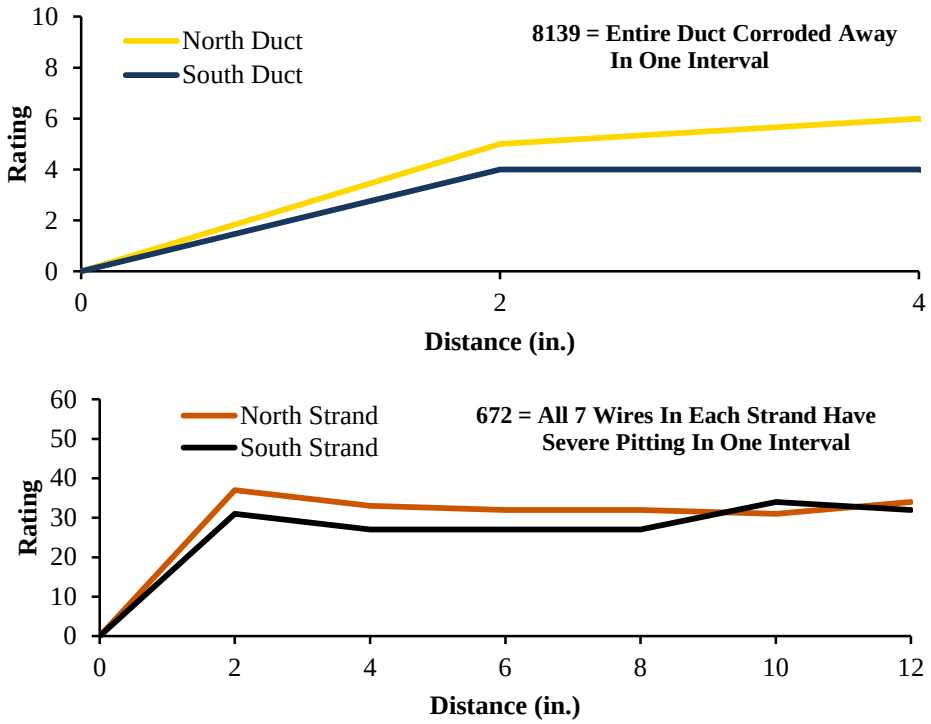

Figure 6.24: Corrosion Rating Plots for Dead End Anchorage Region of Specimen 1.1

6.2.2 Specimen 1.3: Non-Galvanized Anchorage, Stainless Clad Strand, Corrugated Steel Duct

Figure 6.25: Specimen 1.3 Main Autopsy Region and Grout Vents

Table 6.8: Specimen 1.3 Summary of Main Autopsy Region Corrosion Ratings

Component	Maximum	Total	Generalized
Longitudinal Bars	4	12	1.7
Transverse Bars	3	61	4
North Duct	3008	5445	1556
South Duct	2527	3062	875
North Strands	2	8	1
South Strands	3	23	2

6.2.2.1 Appearance

The surface of Specimen 1.3 had medium scaling over the majority of the exterior. Aggregate was visible in many locations, especially along the edges of the ponding area and sides of the specimen. The surface of the ponding area had medium scaling as well as small shallow depressions that had developed during casting of the specimen. The base of the south grout vent had rust staining. This is an indication of corrosion inside the specimen. The base of the backfill mortar in the dead end anchorage pocket was separating from the concrete. This indicates that the mortar did not adhere well to the base concrete.

There was a crack present at the re-entrant corner of the corbel on the north side of the dead end (Figure 6.26). This crack was not present after live load application[1].

Therefore, the crack had not been sealed with mortar or epoxy. The ponding area of Specimen 1.3 had 1 large transverse crack that ran from the north to the south side of the specimen (Figure 6.27). The average crack width was 0.007 inch. The crack rating for Specimen 1.3 was 0.071. See Figure 6.28 for the crack data from Specimen 1.3.

Figure 6.26: Crack at the Re-Entrant Corbel Corner on the North Side of the Dead End of Specimen 1.3

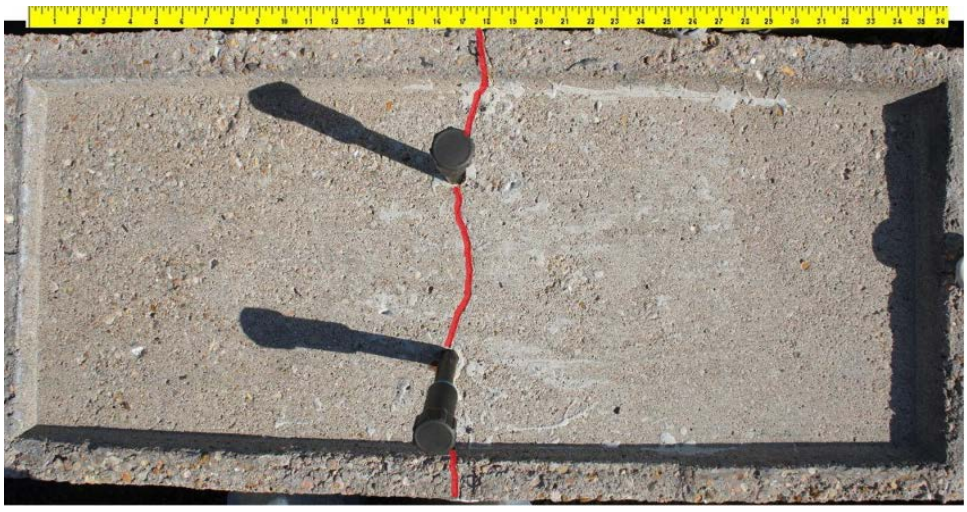

Figure 6.27: Specimen 1.3 Crack Map of Ponding Area

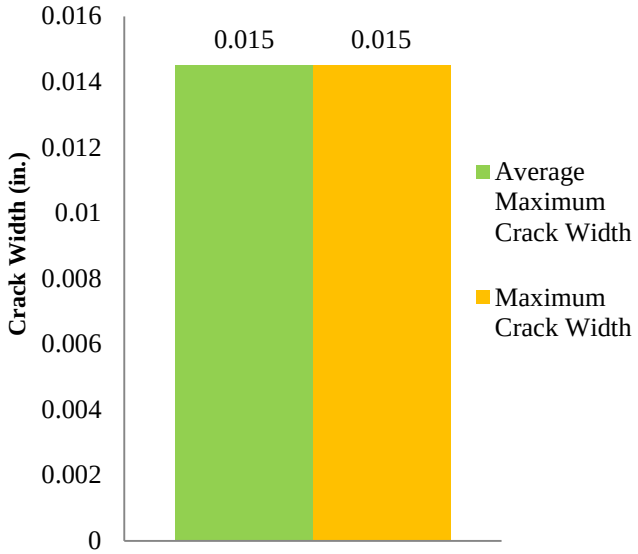

Figure 6.28: Crack Data for Specimen 1.3

6.2.2.2 Longitudinal and Transverse Bars

The north and south longitudinal bars had slight damage from when the bars were extracted from the specimen. Rust stains were also evident at locations where the transverse bars were tied to the longitudinal bars. This staining is from corrosion of the tie wire used to attach the transverse reinforcement to the longitudinal bars and NOT from the longitudinal bar itself. The north and south longitudinal bars had a spot of light corrosion at approximately 10 and 16 inches, respectively, from the dead end of the bar. Figure 6.32 shows the longitudinal bar's corrosion ratings and Table 6.8 shows the summary of the corrosion ratings for the longitudinal bars.

All the transverse bars had damage from when they were extracted from the specimen. All the transverse bars had rust staining at least somewhere over the length of the bar from corrosion of the tie wire used to attach the transverse bars to the longitudinal bars and to attach the duct to the transverse bars. The staining is also from the corrosion of the galvanized duct. There was light corrosion on part of the horizontal portion of transverse bars #2, #3, #5 and #6. Transverse bars #4 and #5 had the highest ratings, 17 and 12, respectively. The end bars, #1 and #7, both had the lowest corrosion rating of 5. This was expected because these bars are outside the ponding area and should have had

little to no exposure to chloride ions due to increased concrete cover and no signs of cracked concrete. Figure 6.32 shows the transverse bar's corrosion ratings and Table 6.8 shows the summary of the corrosion rating for the transverse bars.

6.2.2.3 Duct

Both the north and south ducts had localized severe corrosion damage. This damage resulted in holes in the ducts. The top of the north duct had a large hole at midspan (Figure 6.29). The bottom of the north duct had a hole at midspan and pitting in the intervals adjacent to the hole. The top inner surface of the north duct had light corrosion on one interval and discoloration on intervals without holes. The bottom inner surface of the north duct had evidence of light corrosion on seven intervals scattered along the length of the duct. The top of the south duct had a large hole at midspan (Figure 6.29). The bottom of the south duct had a small hole at midspan and pitting in the adjacent intervals. The top inner surface of the south duct had a few intervals with light corrosion. The bottom inner surface of the south duct had no visible signs of corrosion. The holes experienced by both the north and south ducts indicate that voids in the grout had formed along the top of the duct. Figure 6.32 shows the corrosion ratings for the ducts and Table 6.8 shows the summary of the corrosion ratings for the ducts.

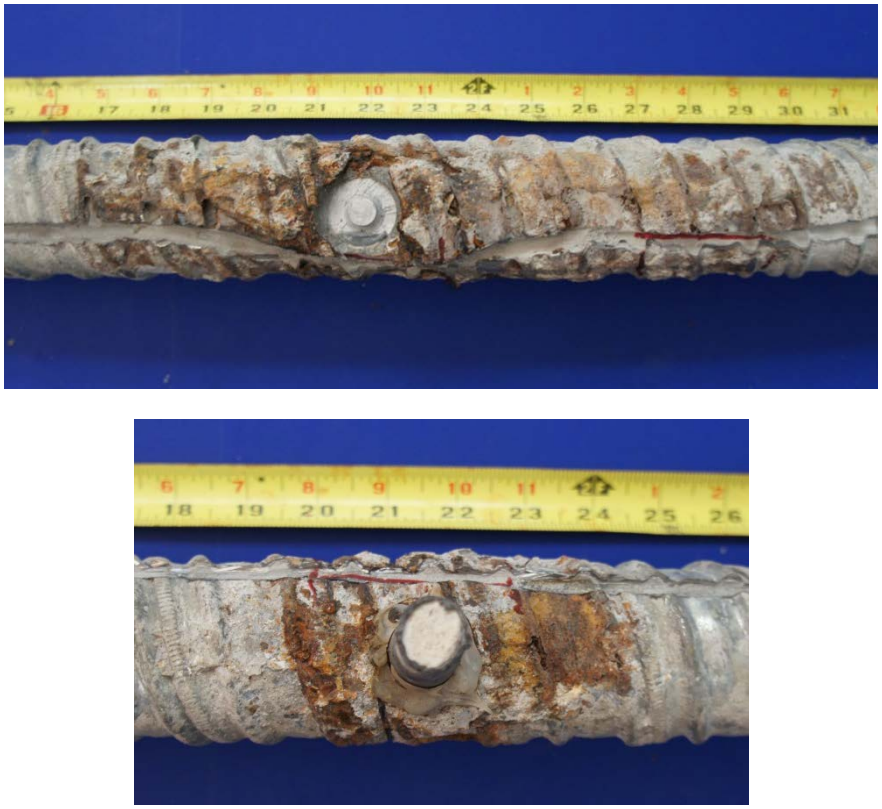

Figure 6.29: Holes in Top of North (Top) and South (Bottom) of Duct of Specimen 1.3 Caused by Corrosion

6.2.2.4 Grout

No transverse or longitudinal visible cracks were observed during examination of grout from the north and south gouts of Specimen 1.3. Staining from corrosion of the duct was observed at locations where corrosion had caused holes in the both the north and south duct (Figure 6.30). Voids in the grout were observed in the flutes at the top of both the north and south duct along the entire length of the each duct. These voids measured approximately 0.75 inch long and were as wide as the flute width of the duct (Figure 6.30). A portion of the strands at the bottom of both tendons was not entirely covered with grout at midspan of the south duct and the majority of the length of the north tendon (Figure 6.30). The coloration of the grout for both tendons was light gray at the ends and transitioned to darker gray at midspan.

Figure 6.30: Staining on Grout from North Tendon (Top) and Exposed Strands on the Bottom of South Duct (Bottom) of Specimen 1.3

The chloride concentrations were discussed in depth in Chapter 5. All the chloride concentrations were above the 0.033% by weight of grout limit for corrosion. See Figure 5.14 for the results of the chloride concentration testing. As expected, highest chloride concentrations for the north and south tendons were at midspan and were 0.270% and 0.210% by weight of grout, respectively. As expected, the anchorage regions had the lowest chloride concentrations. This might be because the chlorides would take longer to migrate to the anchorages because the chloride ions would have to travel through the interstitial space between the grout and the duct and/or interstitial space between the grout and the strand.

6.2.2.5 Strands

As expected, the stainless clad strands of the north and south tendons were essentially defect free. Minimal discoloration was observed on the outer wires of two

strands. One strand was from the north tendon and the other was from the south tendon. The entire length of the inner wires of 5 of the 6 strands had no visible corrosion. The one strand with corrosion had a small spot of light corrosion at midspan. The small spot of corrosion might have been from corrosion product from the duct that had migrated to the strand through micro cracking of the grout because there was no hole in the cladding of any of the strands in that duct to suggest that the corrosion product came from the underlying steel. Figure 6.31 shows a typical stainless clad strand from Specimen 1.3. Figure 6.32 shows the corrosion ratings for the strands and Table 6.8 shows the summary of the corrosion ratings for the strands.

Figure 6.31: Typical Stainless Clad Strand from Specimen 1.3

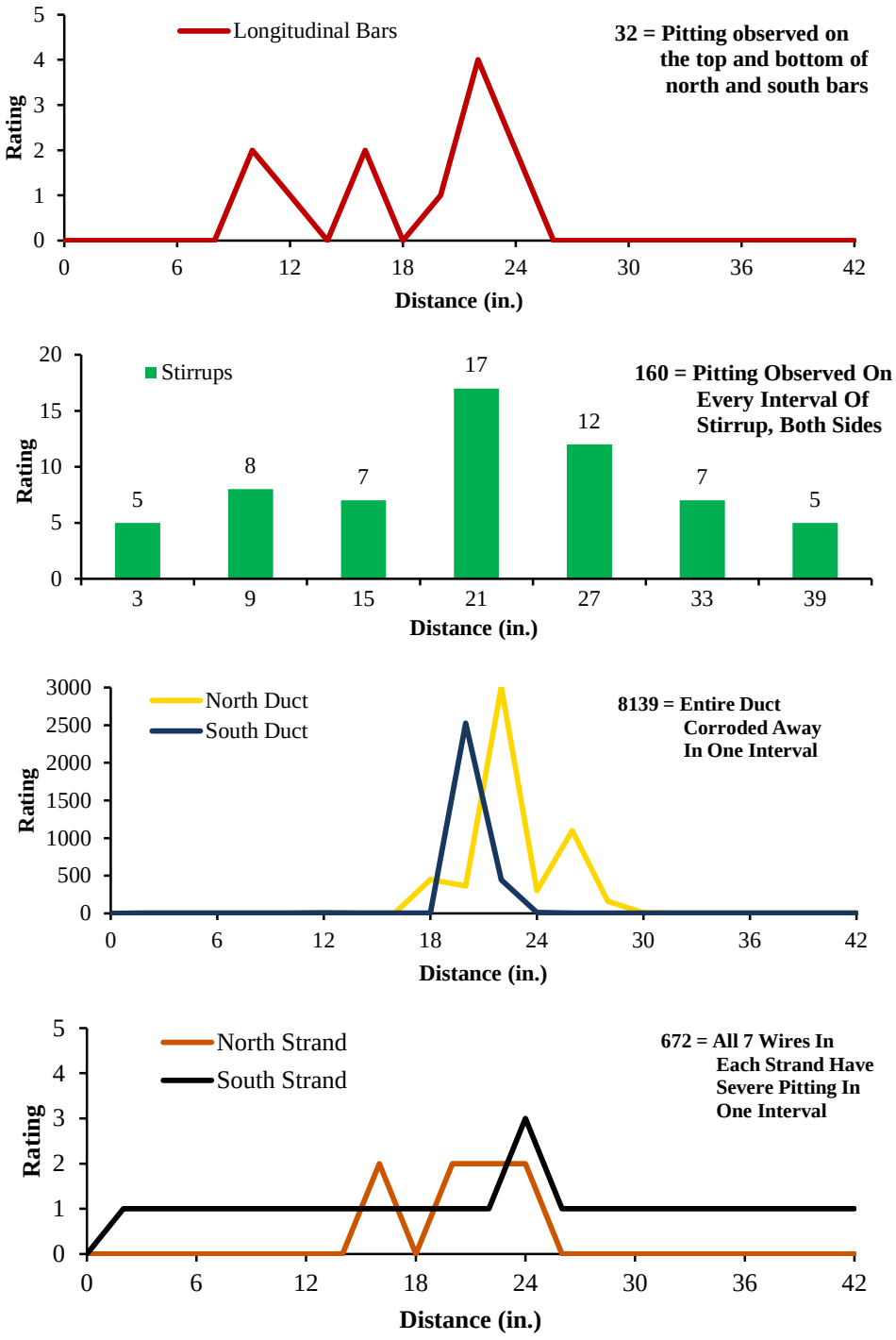

Figure 6.32: Corrosion Rating Plots for Main Autopsy Region of Specimen 1.3

6.2.2.6 Dead End Anchorages

The majority of the epoxy applied to the anchorage components before the anchorage cavity was backfilled had debonded from the anchorage components of both tendons. The exposed faces of the north and south anchorage plate had light surface corrosion on their surface. The embedded portion of the south anchorage plate had light corrosion on the bottom (Figure 6.33). However, the embedded portion of the north anchorage plate had no visible signs of corrosion (Figure 6.33). The sides of the north and south anchor head had light surface corrosion (Figure 6.33). The exposed face of the north and south anchor heads had moderate surface corrosion on portions of its surface (Figure 6.33). The unexposed faces had light surface corrosion on the outer ring where the grout had not come into contact with anchor head (Figure 6.33). The ducts were not sealed to the anchorage plates with duct tape[1].

Figure 6.33: Light Surface Corrosion on Anchorage Components: Bottom of Anchorage (Top Left), Exposed Surface of Anchorage Plate and Head (Top Right), and Unexposed Surface of Anchor Head (Bottom) of Specimen 1.3

Table 6.9: Specimen 1.3 Summary of Dead End Anchorage Region Corrosion Ratings

Component	Maximum	Total	Generalized
North Duct	5	13	19
South Duct	4	12	18
North Strands	8	8	3
South Strands	0	0	0

The south duct from the dead end had no visible corrosion on its outer or inner surface. The north duct from the dead end had light surface corrosion on one interval and had no visible signs of corrosion on the rest of the intervals. Figure 6.35 shows the corrosion ratings for the anchorage region ducts and Table 6.9 shows the summary of the corrosion ratings for the anchorage region ducts.

The grout from the north and south dead end tendons had no visible transverse or longitudinal cracks. The grout from both tendons had voids and signs of "bubbling" in the area of the flutes of the ducts along the length of the top surface. The grout from both tendons did not show signs of segregation along the length of the anchorage region.

The majority of the intervals for outer wires of the strands from the dead end of the north and south tendon had no visible signs of corrosion or discoloration. The one outlier was on one strand at the interval closest to where the tendon was cut from the main autopsy region and the outer wires showed discoloration but no corrosion. Except for one interval of one strand, the inner wire was corrosion free and no discoloration was observed. The one interval had a small spot of light corrosion. This spot of light corrosion of the inner wire and discoloration of the outer wires might have come from when the tendon was cut from the main autopsy region. The wedges were intact and showed light surface corrosion on the outer surface (Figure 6.34). Figure 6.35 shows the corrosion ratings for the anchorage region strands and Table 6.9 shows the summary of the corrosion ratings for the anchorage region stands.

Figure 6.34: Light Surface Corrosion on Wedge from Specimen 1.3

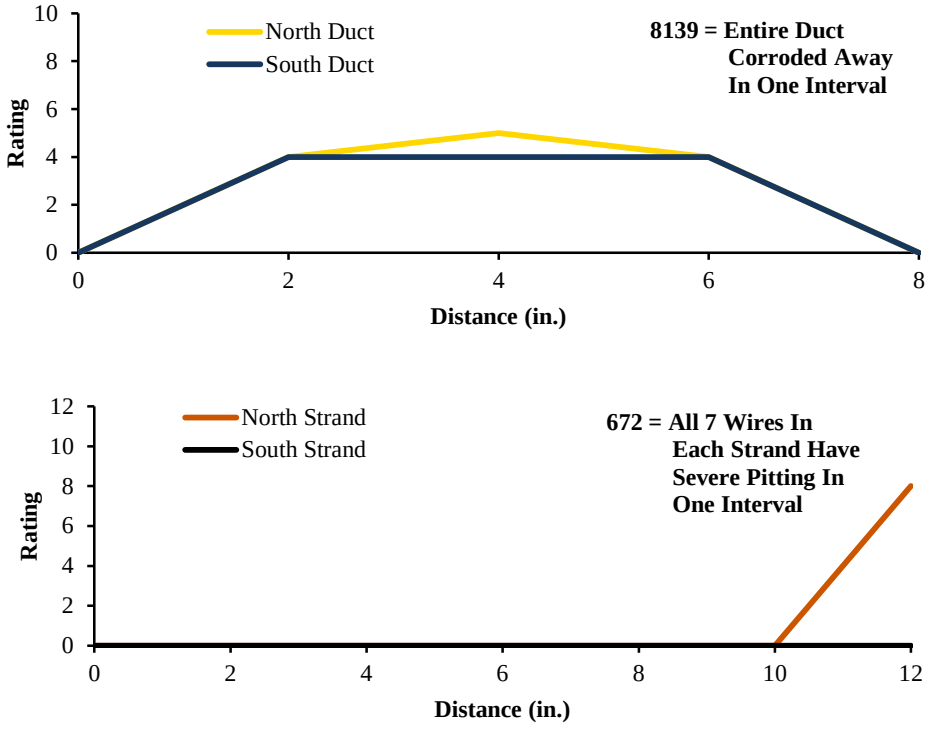

Figure 6.35: Corrosion Rating Plots for Dead End Anchorage Region of Specimen 1.3

6.2.3 Specimen 1.4: Galvanized Anchorage, Conventional Strand, Corrugated Galvanized Duct

Figure 6.36: Specimen 1.4 Main Autopsy Region and Grout Vents

Table 6.10: Specimen 1.4 Summary of Main Autopsy Region Corrosion Ratings

Component	Maximum	Total	Generalized
Longitudinal Bars	4	30	4
Transverse Bars	8	57	4
North Duct	3219	18109	5174
South Duct	3493	14786	4225
North Strands	49	854	81
South Strands	47	844	80

6.2.3.1 Appearance

The surface of specimen had medium scaling and shallow depressions were present over the majority of the exterior (Figure 6.37). Aggregate was visible in many locations, especially along the edges of the ponding area and sides of the specimen. The surface of the ponding area had medium scaling. Rust staining was observed at the base of the south grout vent and along a portion of a transverse crack located in the live end portion of the ponding. This is an indication of corrosion inside the specimen. The backfill

mortar in the live end anchorage pocket was separating from the concrete (Figure 6.37). This indicates that the mortar did not adhere well to the base concrete.

Figure 6.37: Separation of the Backfill Mortar of the Live End Anchorage Pocket from the Base Concrete of Specimen 1.4

There were cracks present at the re-entrant corbel corners on both sides of the dead end and live end (Figure 6.37). These cracks were not present after live load application[1]. Therefore, the cracks had not been sealed with mortar or epoxy. The ponding area of Specimen 1.4 had 4 large transverse cracks that ran from the north to the south side of the specimen and 2 longitudinal cracks in the live end of the ponding region (Figure 6.38). The average crack width was 0.006 inch. The crack rating for Specimen 1.4 was 0.50. See Figure 6.39 for the crack data from Specimen 1.4.

Figure 6.38: Specimen 1.4 Crack Map of Ponding Area

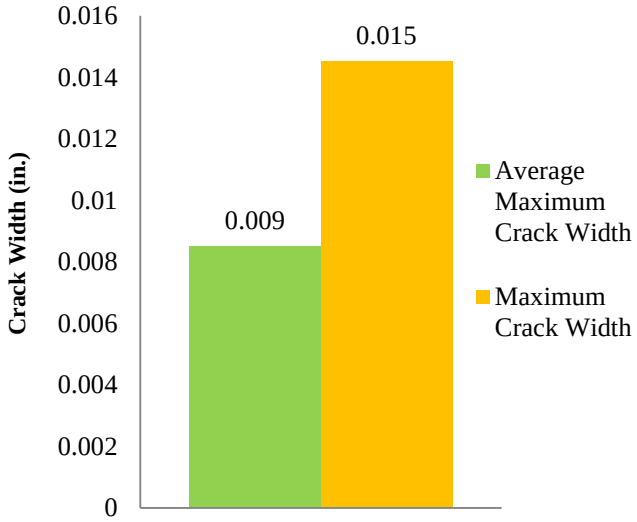

Figure 6.39: Crack Data for Specimen 1.4

6.2.3.2 Longitudinal and Transverse Bars

The north and south longitudinal bars had slight damage from when the bars were extracted from the specimen. Rust stains were also evident at locations where the transverse bars were tied to the longitudinal bars. This staining is from corrosion of the tie wire used to attach the transverse reinforcement to the longitudinal bars and NOT from the longitudinal bar itself. The north and south longitudinal bars had visible signs

of corrosion. Figure 6.44 shows the longitudinal bar's corrosion ratings and Table 6.10 shows the summary of the corrosion ratings for the longitudinal bars.

Transverse bars #1, #4, #6, and #7 had damage from when they were extracted from the specimen. All the transverse bars had rust staining at least somewhere over the length of the bar from corrosion of the tie wire used to attach the transverse bars to the longitudinal bars and to attach the duct to the transverse bars. The staining is also from the corrosion of the galvanized duct. There was moderate corrosion observed on the corner of bar #4 (Figure 6.40) and light corrosion observed on the corner of bar #5. Transverse bar #4 had the highest rating of 21. The end bars, #1 and #3, both had the lowest corrosion rating of 2. This was expected for bar #1 because this bar was outside the ponding area and should have had little to no exposure to chloride ions. Figure 6.44 shows the transverse bar's corrosion ratings and Table 6.10 shows the summary of the corrosion rating for the transverse bars.

Figure 6.40: Moderate Corrosion on the Corner of Transverse Bar #4 from Specimen 1.4

6.2.3.3 Duct

Both the north and south ducts had localized severe corrosion damage. This damage resulted in holes in the ducts. The top outer surface of the north duct had large holes at midspan and around the live end quarter point of the duct and had discoloration and light to moderate corrosion (Figure 6.41). The bottom outer surface of the north duct had discoloration, light to moderate corrosion, pitting, and a small hole at midspan. The

top inner surface of the north duct had discoloration and pitting adjacent to the holes. Except at the ends, the bottom inner surface of the north duct had pitting along the entire length. The top outer surface of the south duct had large holes on the live end side of midspan and one centered at approximately 33 inches from the dead end and had small holes centered at approximately 3 inches and 15 inches from the dead end. The bottom outer surface of the south duct had a small hole centered approximately 31 inches from the dead end (Figure 6.41). The top inner surface of the south duct had one interval with pitting adjacent to the small hole centered at 5 inches from the dead end and had intervals with discoloration and moderate corrosion. The bottom inner surface had pitting almost the entire length of the duct as well as discoloration and light to moderate corrosion. The holes experienced by both the north and south ducts indicate that voids in the grout had formed along the top of the duct and a large void was evident in the south tendon that spanned approximately 60% of length of the tendon (Figure 6.42). The pitting observed on the bottom inner surface of the north and south duct might be from the chlorides traveling in the interstitial space between the grout and the duct after the holes had formed. Figure 6.44 shows the corrosion ratings for the ducts and Table 6.10 shows the summary of the corrosion ratings for the ducts.

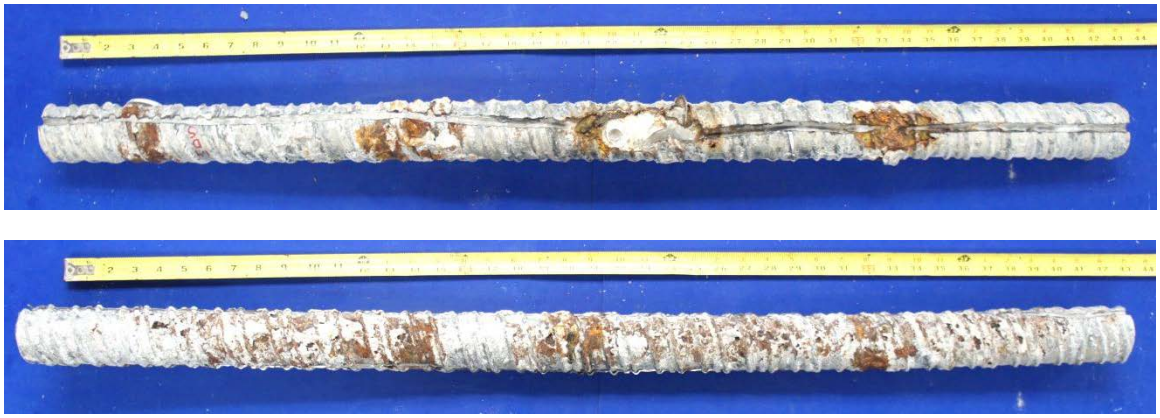

Figure 6.41: Specimen 1.4 Top of North Duct (Top) and Bottom of South Duct (Bottom)

6.2.3.4 Grout

No transverse or longitudinal visible cracks were observed during examination of grout from the north and south tendons of Specimen 1.4. Staining from corrosion of the duct was observed at locations where corrosion had caused holes in the both the north and south duct. Small voids in the grout were observed in the flutes along the entire length of the top of both the north and south tendons and large voids were present at mid span of both the north and south tendons with the void in the south tendon spanning approximately 60% of the length (Figure 6.42). The small voids measured approximately 0.75 inch long and were as wide as the flute width.

Figure 6.42: Large Void in Grout of South Tendon from Specimen 1.4

The chloride concentrations were discussed in depth in Chapter 5. All the chloride concentrations were above the 0.033% by weight of grout limit for corrosion. See Figure 5.13 for the results of the chloride concentration testing. As expected, the highest chloride concentration for the north and south tendons were at midspan and were 0.420% and 0.240%, respectively, by weight of grout. As expected, the anchorage regions had the lowest chloride concentrations. This might be because the chlorides would take longer to migrate to the anchorages because the chloride ions would have to travel through the interstitial space between the grout and duct and/or interstitial space between the grout and strand.

6.2.3.5 Strand

The three strands in the north tendon had only minor damage. Moderate corrosion was observed on most of the intervals on at least one of the outer wires (Figure 6.43) but

a few of the intervals had discoloration. The entire length of all three of the inner wires had light corrosion. Corrosion ratings over the entire length of the three north strands were relatively uniform. The live end had the lowest ratings of 28. The highest corrosion rating of 43 was not at midspan but at an interval centered at approximately 15 inches from dead end.

The three strands from the south tendon had only minor damage, as well. Discoloration was observed on many intervals on all the outer wires but a few of the intervals experienced moderate corrosion (Figure 6.43). The inner wire of two of the three strands had light corrosion along the entire length and one strand had light corrosion along half of its length and discoloration on the remaining length of the wire. The corrosion ratings over the entire length of the three south strands were relatively uniform. The highest corrosion rating of 40 was not at midspan but on two intervals centered at eight inches from the dead end and the live end had the lowest corrosion rating with an average of 28.

Figure 6.44 shows the corrosion ratings for the strands and Table 6.10 shows the summary of the corrosion ratings for the strands.

Figure 6.43: Specimen 1.4 Moderate Corrosion on Outer Wire from a Strand in North Tendon (Top) and on Outer Wire from a Strand in South Tendon (Bottom)

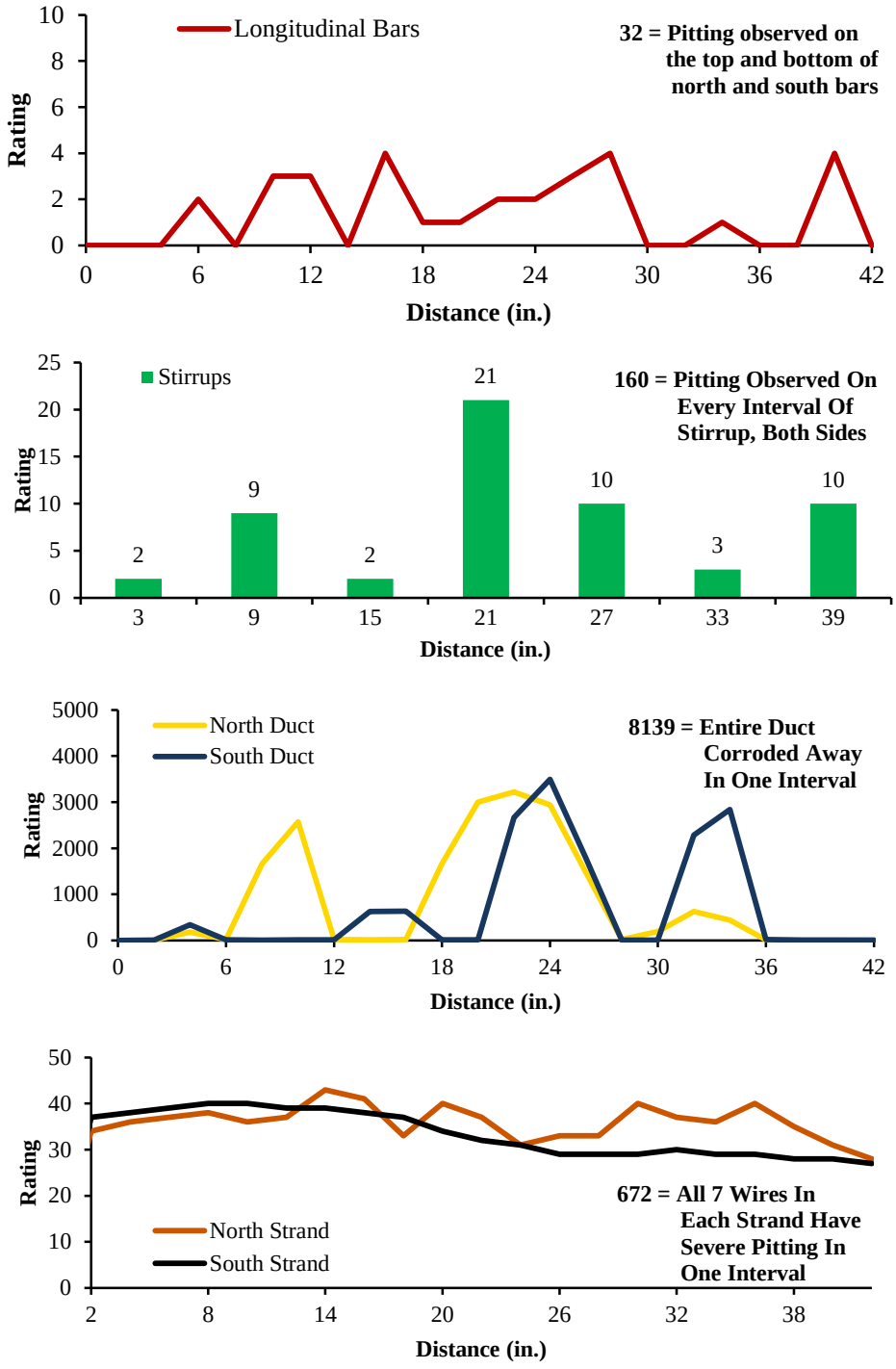

Figure 6.44: Corrosion Rating Plots for Main Autopsy Region of Specimen 1.4

6.2.3.6 Dead End Anchorages

The majority of the epoxy applied to the anchorage components before the anchorage cavity was backfilled had debonded from the anchorage components. Portions of both the exposed faces of the north and south anchorage plate had light surface corrosion on their surface. The embedded portion of the north anchorage plate had no visible signs of corrosion but the embedded portion of the south anchorage plate had light corrosion on the bottom of the bearing surface. The sides of the north and south anchor heads were primarily corrosion free with only light surface corrosion near the interface of the anchorage plate and anchor head. The exposed face of the south anchor head was corrosion free but the exposed face of the north anchor head had small spots of light corrosion (Figure 6.45). The unexposed face of the north and south anchor heads had light surface corrosion. The ducts were not sealed to the anchorage plates with duct tape[1].

Figure 6.45: Light Surface Corrosion of Exposed Face of North Anchor Head from Specimen 1.4

Table 6.11: Specimen 1.4 Summary of Dead End Anchorage Region Corrosion Ratings

Component	Maximum	Total	Generalized
North Duct	6	10	15
South Duct	7	13	19
North Strands	30	151	50
South Strands	30	150	50

The north and south ducts from the dead end anchorage region had light corrosion in one interval of the bottom outer surface of the duct. The bottom inside surface of the north duct had light surface corrosion on one interval. The inside of the south duct had light surface corrosion on two intervals. Figure 6.46 shows the corrosion ratings for the anchorage region ducts and Table 6.11 shows the summary of the corrosion ratings for the anchorage region ducts.

The grout from the north and south dead end tendons had no visible transverse or longitudinal cracks. The grout from both tendons had voids and signs of "bubbling" in the area of the flutes of the ducts along the length of the top surface. The grout from both tendons showed signs of segregation along the length of the anchorage region.

The outer wires of the strands from the dead end anchorage region of the north and south tendon had discoloration and light corrosion over the length of the wires. One of the inner wires had light corrosion over the majority of its length and another inner wire had discoloration on half of its length and light corrosion on the other half. The other inner wires were primarily discolored with some light corrosion. The wedges were intact and showed no visible signs of corrosion. Figure 6.46 shows the corrosion ratings for the anchorage region strands and Table 6.11 shows the summary of the corrosion ratings for the anchorage region stands.

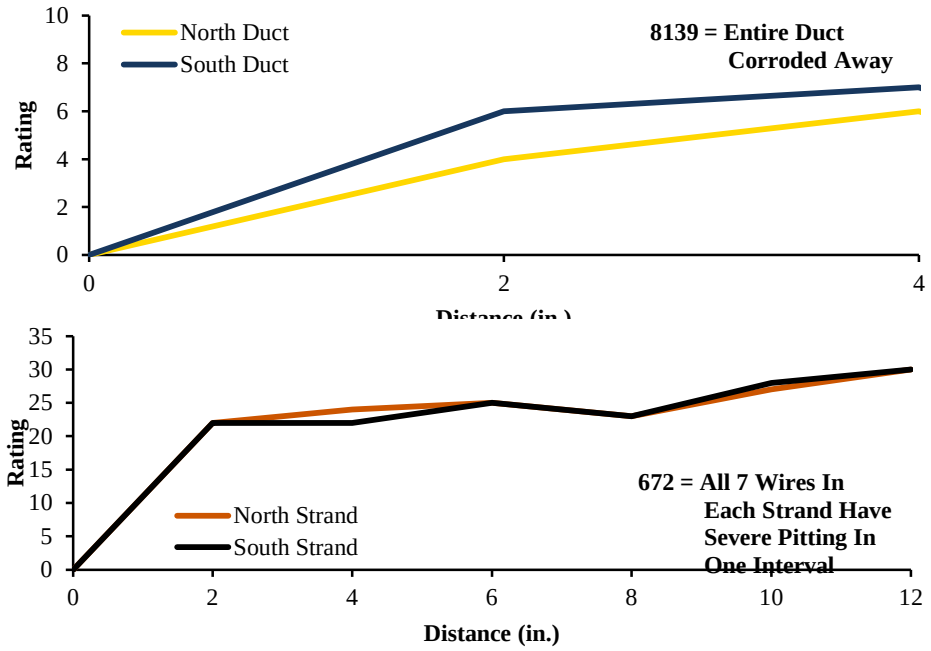

Figure 6.46: Corrosion Rating Plots for Dead End Anchorage Region of Specimen 1.4

6.2.4 Specimen 2.3: Non-Galvanized Anchorage, Conventional Strand, One-way Plastic Duct

Figure 6.47: Specimen 2.3 Main Autopsy Region and Grout Vents

Table 6.12: Specimen 2.3 Summary of Main Autopsy Region Corrosion Ratings

Component	Maximum	Total	Generalized
Longitudinal Bars	4	21	3
Transverse Bars	8	68	5
North Duct	10	20	6
South Duct	10	60	17
North Strands	49	854	81
South Strands	45	802	76

This specimen was not grouted until 5 days after prestressing[1].

6.2.4.1 Appearance

The surface of Specimen 2.3 had medium scaling over the majority of the exterior. Aggregate was visible in many locations, especially along the edges of the ponding area and sides of the specimen. The surface of the ponding area had medium scaling as well (Figure 6.47). No rust stains were observed during examination. The backfill mortar of the dead and live end anchorage pockets were separating from the concrete. This indicates that the mortar did not adhere well to the base concrete.

There were cracks present at the re-entrant corbel corners on both sides of the dead and live end. These cracks were not present after live load application[1]. Therefore, the cracks had not been sealed with mortar or epoxy. The ponding area of Specimen 2.3 had 3 large transverse cracks that ran from the north to the south side of the specimen and longitudinal cracks located on the north and south side of the ponding area (Figure 6.48). The average crack width was 0.008 inch. The crack rating for Specimen 2.3 was 0.63. See Figure 6.1 for the crack data from Specimen 2.3.

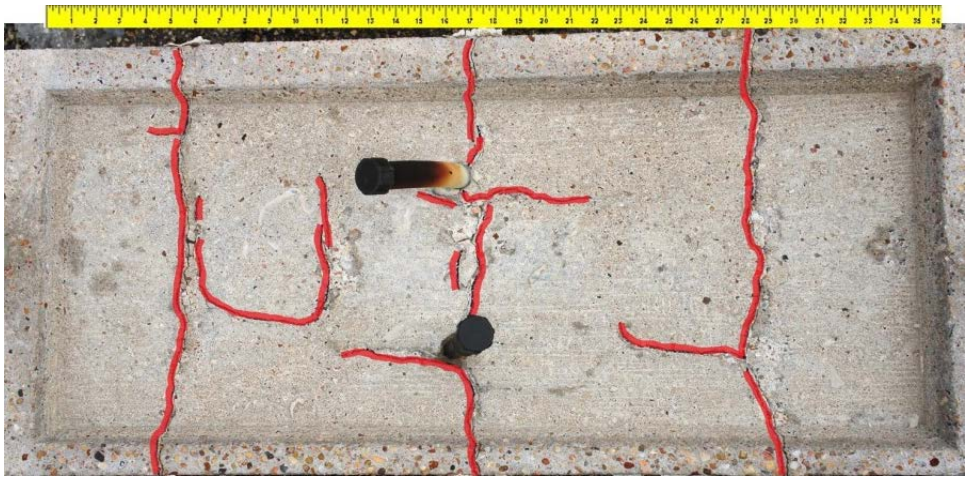

Figure 6.48: Specimen 2.3 Crack Map of Ponding Area

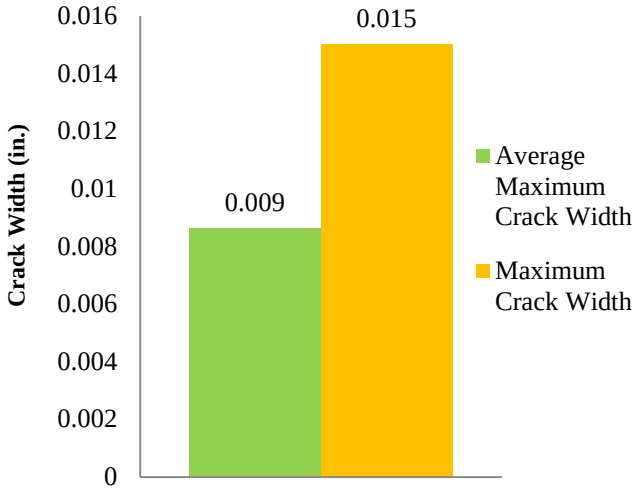

Figure 6.49: Crack Data for Specimen 2.3

6.2.4.2 Longitudinal and Transverse Bars

The north and south longitudinal bars had slight damage from when the bars were extracted from the specimen. Rust stains were evident at locations where the transverse bars were tied to the longitudinal bars. This staining is from corrosion of the tie wire used to attach the transverse reinforcement to the longitudinal bars and NOT from the longitudinal bar itself. Figure 6.54 shows the longitudinal bar's corrosion ratings and Table 6.12 shows the summary of the corrosion ratings for the longitudinal bars.

Transverse bars #1, #2, #4, and #7 had damage from when they were extracted from the specimen. All the transverse bars had rust staining at least somewhere over the length of the bar from corrosion of the tie wire used to attach the transverse bars to the longitudinal bars and to attach the duct to the transverse bars. All transverse bars had either light or moderate corrosion or both. There was moderate corrosion observed on bars #1, #3, #6, and #7 (Figure 6.50) and light corrosion observed on bars #2, #3, #4, #5, and #6. Transverse bar #6 had the highest rating of 24. Bar #4 had the lowest corrosion rating of 5. This wasn't expected because the bar was from the center of the ponding area and directly under a crack. Figure 6.54 shows the transverse bar's corrosion ratings and Table 6.12 shows the summary of the corrosion rating for the transverse bars.

Figure 6.50: Moderate Corrosion on Transverse Bar #3 of Specimen 2.3

6.2.4.3 Duct

The entire outer surface of the north duct had a chalky white residue. No corrosion staining was observed on the outer or inner surface of the duct. The inner bottom surface

of the north duct had slight gouges on the dead end of midspan. This indicates that one or more of the strands caused damage either when the strands were being threaded through the duct or one of the strands or stands were rubbing against the north duct when the strands were being stressed. In either case, the integrity of the duct was not compromised. Indications of voids were observed on the top inner surface of the duct along the entire length (Figure 6.51). No damage was observed on the coupler. Grout was observed inside the coupler but outside the seal (Figure 6.51). This indicates that the seals of the coupler were not water tight and allowed the grout to escape from inside the duct. Thus, in reverse, it could have been a pathway for moisture, oxygen, and/or chlorides to enter the duct.

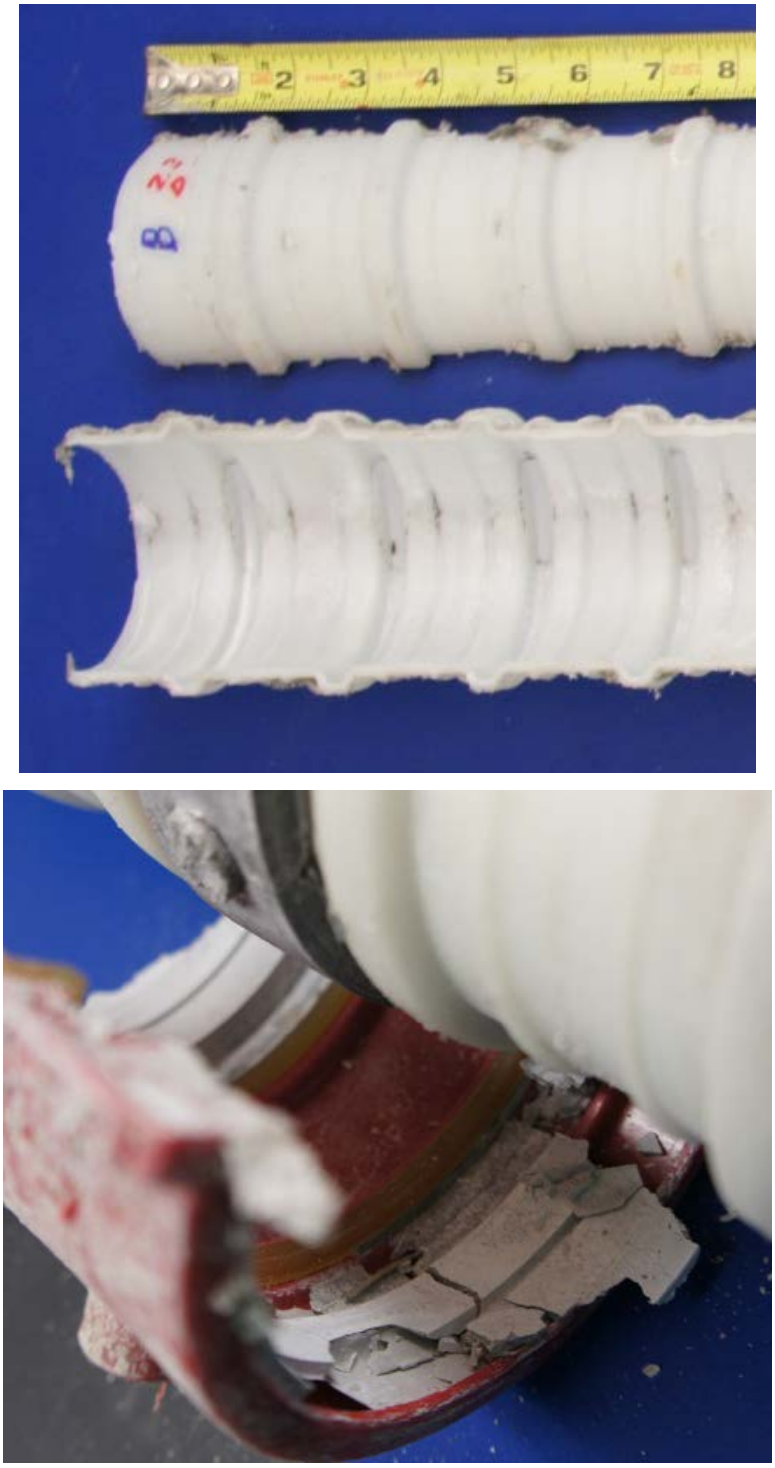

Figure 6.51: Evidence of Voids in Grout of North Tendon (Top) and Grout inside the Coupler but outside the Seals of North Duct (Bottom) of Specimen 2.3

The damage and appearance of the south duct was similar to the north duct. The entire outer surface of the south duct had a chalky white residue. The inner bottom surface of the south duct had slight gouges over a large length of the midspan. Again, this indicates that one or more of the strands caused damage either when the strands were being threaded through the duct or possibly one of the strands or stands were rubbing against the duct when the strands were being stressed. In either case, the integrity of the duct was not compromised. The silicone that was used to seal the grout vent to the south duct was found to have debonded from the duct. It is not known if this happened during extraction or when the concrete was placed. Chloride levels indicate that the latter is the more valid explanation.

Figure 6.54 shows the damage ratings for the ducts and Table 6.12 shows the summary of the damage ratings for the ducts.

6.2.4.4 Grout

No transverse or longitudinal visible cracks were observed during examination of grout from the north and south grouts of Specimen 2.3. No staining of the grout was observed on either the north or south tendon. Small voids in the grout were observed in the flutes along the entire length of the top of both the north and south tendons (Figure 6.52). The small voids measured approximately 1.5 inch long and were as wide as the flute width. Segregation of the grout was observed on the live and dead end of both the north and south tendon (Figure 6.52). Portions of the strands were visible in the grout on the bottom of the north and south tendon (Figure 6.52).

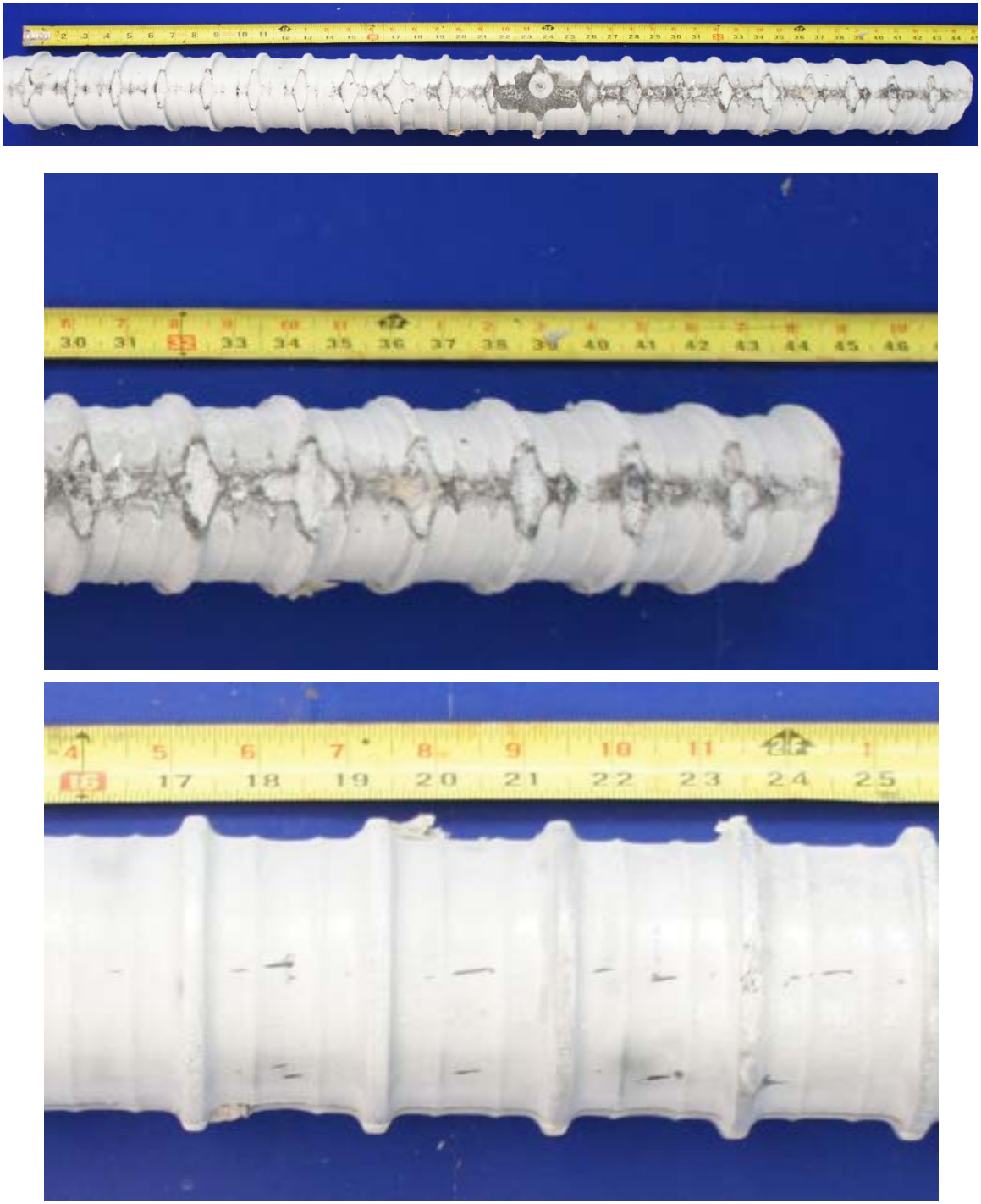

Figure 6.52: Voids in Grout (Top), Segregation of Grout (Middle), and Strands Visible in Grout (Bottom) in the South Tendon of Specimen 2.3

The chloride concentrations were discussed in depth in Chapter 5. All the chloride concentrations were well above the 0.033% by weight of grout limit for corrosion. See Figure 5.13 for the results of the chloride concentration testing. As expected, the highest chloride concentration for the north and south tendons were at midspan and were 0.880% and 0.940%, respectively, by weight of grout. As expected, the anchorage regions had the lowest chloride concentrations. This might be because the chlorides would take longer to migrate to the anchorages because the chloride ions would have to travel through the interstitial space between the grout and duct and/or interstitial space between the grout and strand.

6.2.4.5 Strands

Light corrosion was observed on many intervals on all the outer wires of the north strands but a few of the intervals had moderate corrosion (Figure 6.53). The entire length all the inner wires of the north strands had light to moderate corrosion over their entire length (Figure 6.53). Corrosion ratings over the entire length of the three north strands were relatively uniform. The lowest corrosion rating of 35 was on 3 successive intervals located at the dead end quarter point and one interval at midspan. The highest corrosion rating was 49 and was located at approximately 28 inches from the dead end.

Light corrosion was observed on many intervals on all the outer wires of the south strands but a few of the intervals had moderate corrosion (Figure 6.53). The inner wire of all three strands had light corrosion on some of the intervals and the rest of the intervals had moderate corrosion (Figure 6.53). The corrosion ratings over the entire length of the three south strands were relatively uniform. The highest corrosion rating was 47 and was located on the interval centered at 32 inches from the dead end. The lowest rating was 35 and located on an interval centered at 4 inches from the dead end.

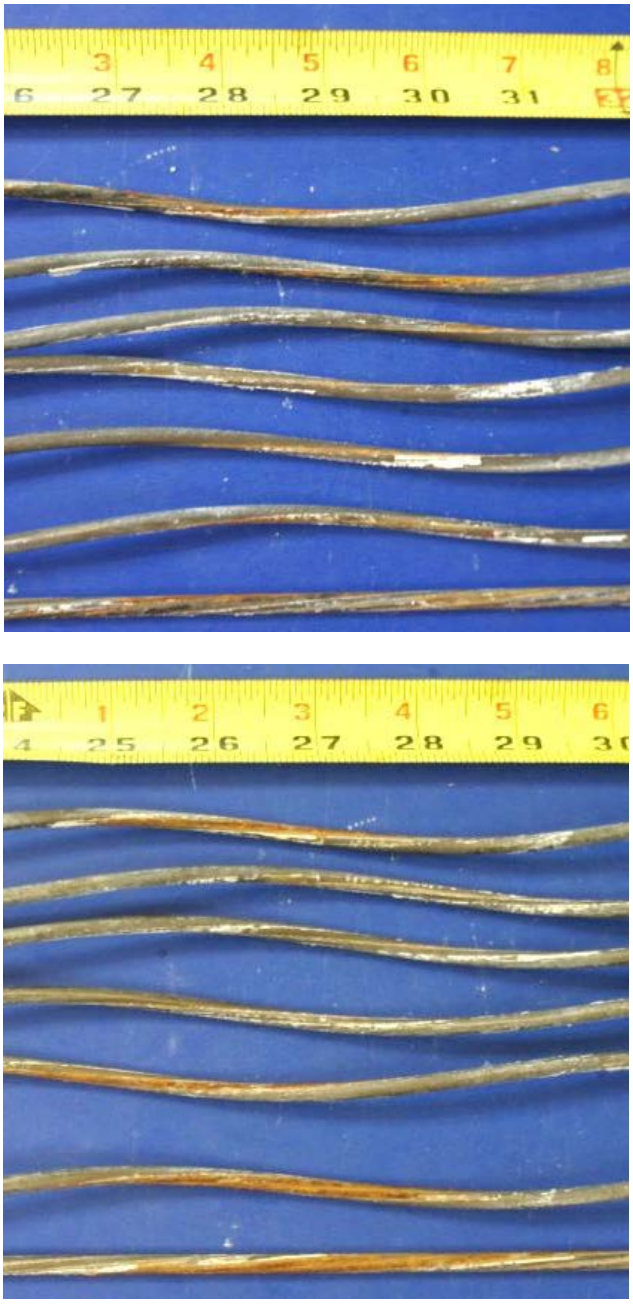

Figure 6.53: Moderate Corrosion on Outer and Inner Wires of Strands from the North (Top) and South (Bottom) Tendon of Specimen 2.3

Figure 6.54 shows the corrosion ratings for the strands and Table 6.12 shows the summary of the corrosion ratings for the strands.

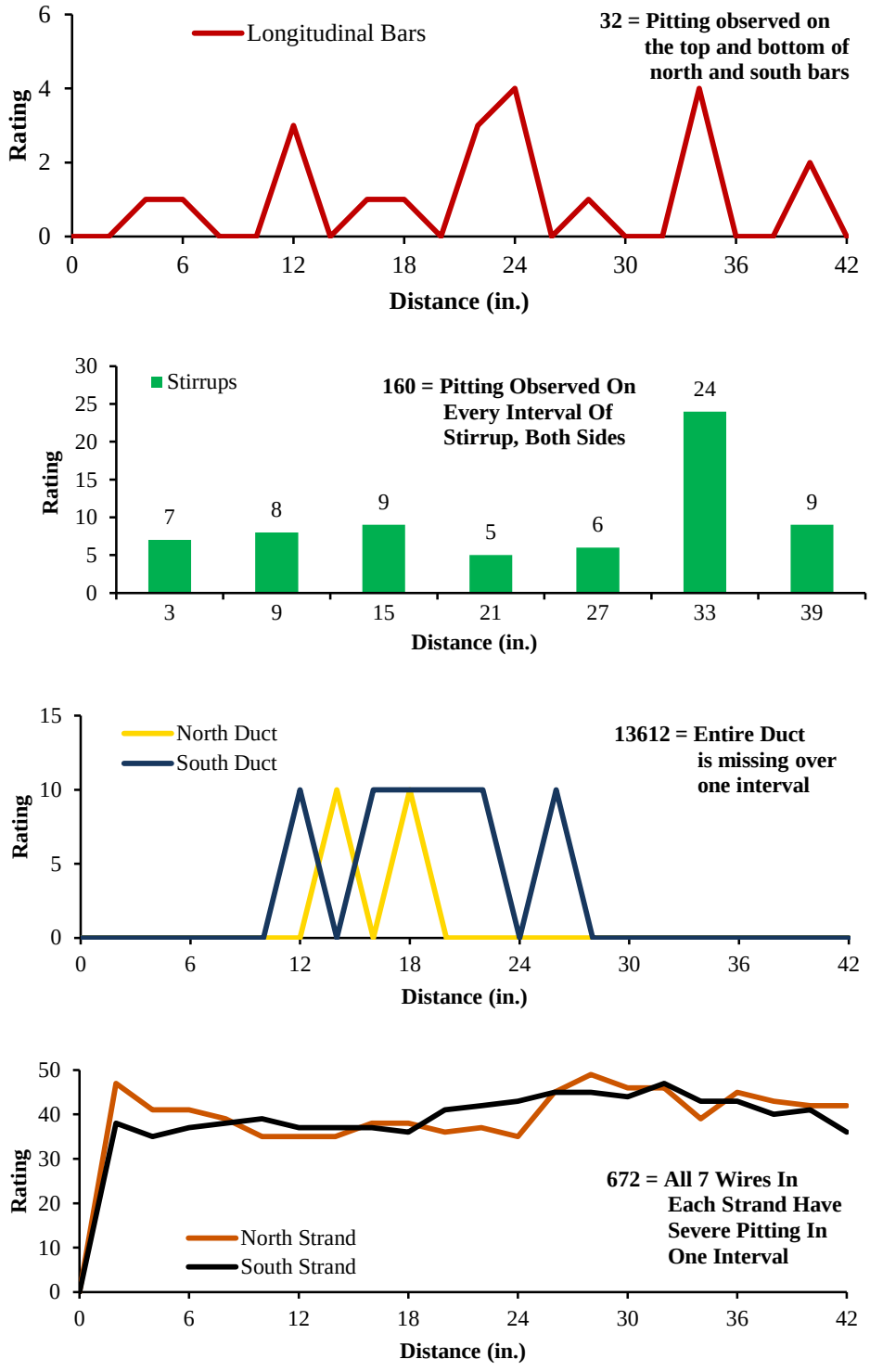

Figure 6.54: Corrosion Rating Plots for Main Autopsy Region of Specimen 2.3

6.2.4.6 Dead End Anchorages

All of the epoxy applied to the both anchor heads before the anchorage cavity was backfilled had debonded from the anchorage components of both tendons. The majority of the epoxy on the anchorage plate was still bonded to the exposed surface. The exposed faces of the north and south anchorage plate had light surface corrosion on their surface. The embedded portion of both anchorage plates had moderate corrosion and pitting on the bottom and moderate corrosion where the duct was taped to the anchorage plate using duct tape (Figure 6.55). The sides and exposed face of the north and south anchor head had spots of light surface corrosion. The unexposed face of the north and south anchor heads had light surface corrosion.

Figure 6.55: Moderate Surface at South Dead End Interface of Duct and Anchorage Plate of Specimen 2.3

Table 6.13: Specimen 2.3 Summary of Dead End Anchorage Region Corrosion Ratings

Component	Maximum	Total	Generalized
North Duct	0	0	0
South Duct	0	0	0
North Strands	101	412	137
South Strands	30	168	56

The north and south ducts no had visible signs of damage or staining. There were indications of voids in the grout of the north and south tendon along the length of the duct in the anchorage region from the flutes of the duct. Figure 6.57 shows the damage ratings

for the anchorage region ducts and Table 6.13 shows the summary of the damage ratings for the anchorage region ducts.

The grout from the north and south dead end tendons had no visible transverse or longitudinal cracks. The grout from both tendons had voids and signs of "bubbling" in the area of the flutes of the ducts along the length of the top surface. The grout from both tendons did not show signs of segregation along the length of the anchorage region.

There was mild pitting observed on two of the north strands outer wires (Figure 6.56). The inner wires of the same strands had mild pitting observed as well (Figure 6.56). The other north strand had light to moderate corrosion on its outer wires and the inner wire had light corrosion along its length. The three strands from the south tendon had discoloration and light corrosion on their outer wires and moderate corrosion along the entire length of their inner wires. Figure 6.57 shows the corrosion ratings for the anchorage region strands and Table 6.13 shows the summary of the corrosion ratings for the anchorage region stands.

Figure 6.56: Mild Pitting on Inner and Outer Wires of a Strand from the Dead End Anchorage Region of Specimen 2.3

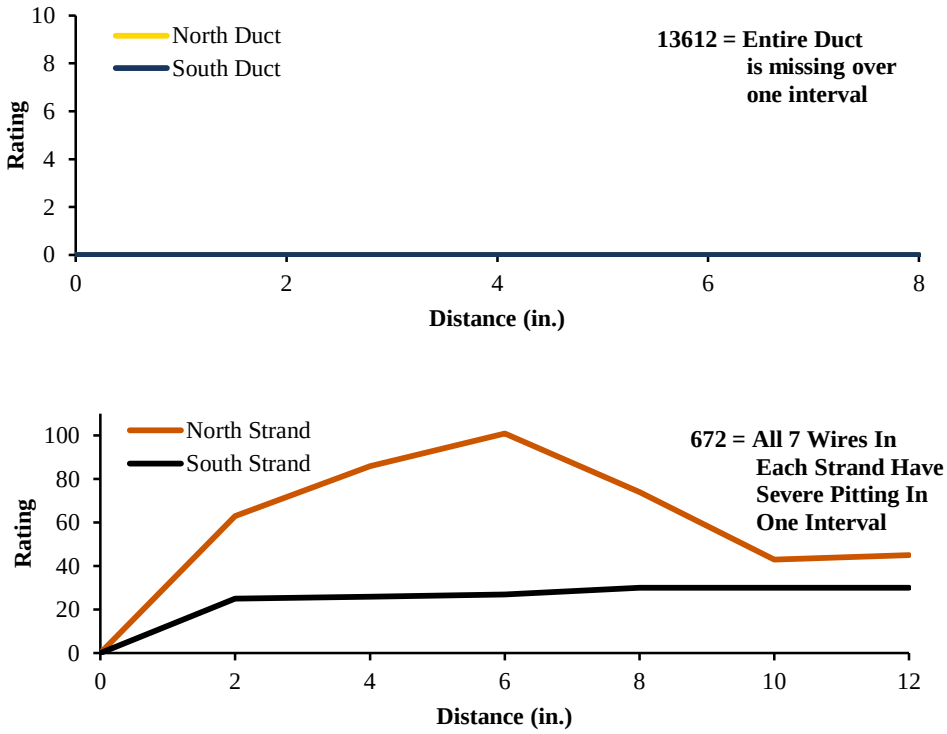

Figure 6.57: Corrosion Rating Plots for Dead End Anchorage Region of Specimen 2.3

6.2.5 Specimen 3.3: Non-Galvanized Anchorage, Copper Clad Strand, Two-way Plastic Duct

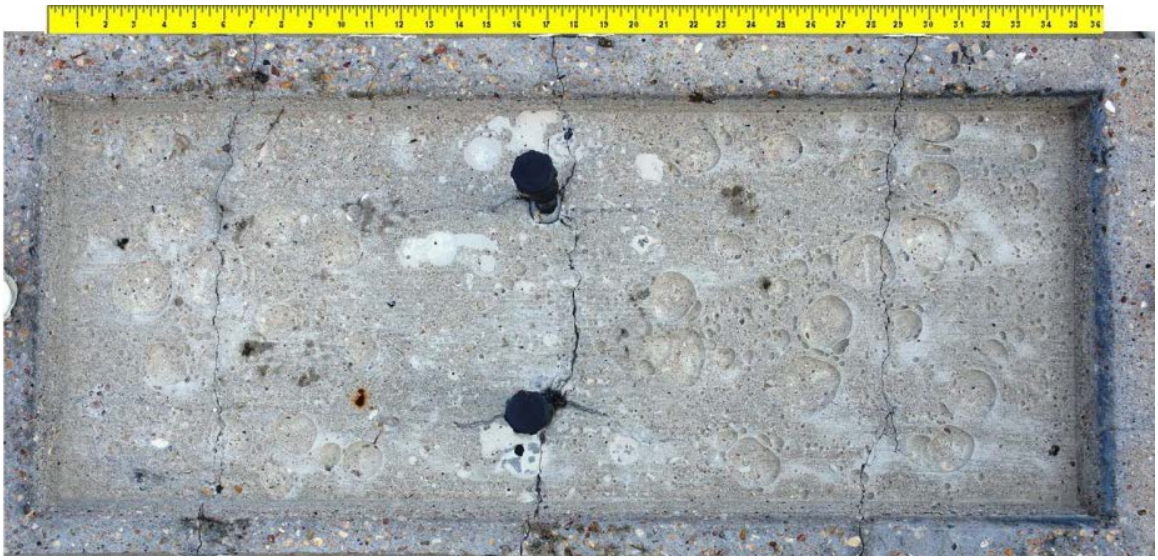

Figure 6.58: Specimen 3.3 Main Autopsy Region and Grout Vents

Table 6.14: Specimen 3.3 Summary of Main Autopsy Region Corrosion Ratings

Component	Maximum	Total	Generalized
Longitudinal Bars	10	37	5
Transverse Bars	8	73	5
North Duct	10	70	20
South Duct	10	30	9
North Strands	22	444	42
South Strands	21	441	42

This specimen received dead end spray exposure during the exposure testing period.

6.2.5.1 Appearance

The surface of Specimen 3.3 had medium scaling over the majority of the exterior. Aggregate was visible in many locations, especially along the edges of the ponding area and sides of the specimen. The surface of the ponding area had medium scaling as well and had medium sized shallow depressions from bleed water pockets when the ponding area was formed during casting (Figure 6.58). A small rust stain from a tie wire that did

not have any concrete cover was observed in the ponding area on the dead end north side (Figure 6.58). The backfill mortar live end anchorage pocket was separating from the base concrete. This indicates that the mortar did not adhere well to the base concrete.

There were cracks present at the re-entrant corbel corners on both sides of the live end and efflorescence was observed coming from the crack (Figure 6.59). These cracks were not present after live load application[1]. Therefore, the cracks had not been sealed with mortar or epoxy. The ponding area of Specimen 3.3 had 3 large transverse cracks that ran from the north to the south side of the specimen and 1 small transverse crack on the dead end south side that ran from the edge of the specimen to approximately the center line of the south duct. The longitudinal cracks observed were located on the north and south side of the ponding area over the top of the corresponding tendons (Figure 6.60). This cracking might have been caused by the differential shrinkage or expansion because the duct and concrete have different thermal coefficients and the concrete in this region had decreased cover. The average crack width was 0.008 inch. The crack rating for Specimen 3.3 was 0.72. See Figure 6.61 for the crack data from Specimen 3.3.

Figure 6.59: Efflorescence from Re-entrant Crack on North side of Specimen 3.3 Live End

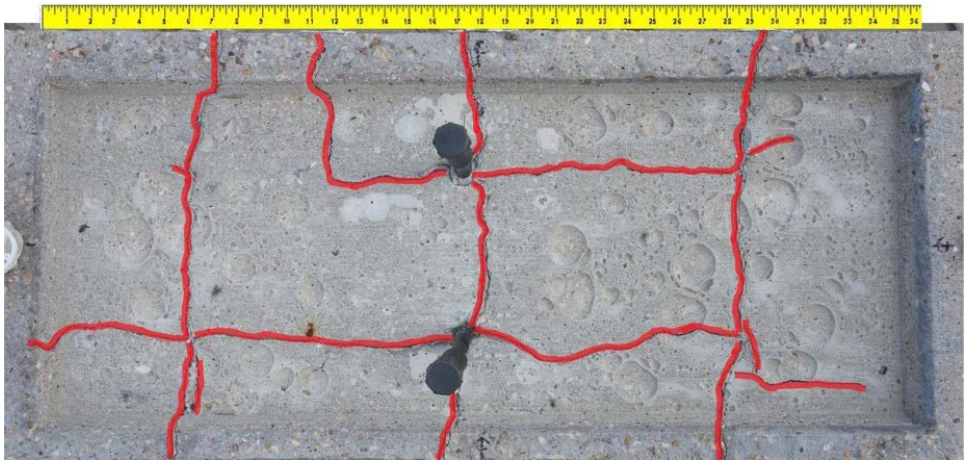

Figure 6.60: Specimen 3.3 Crack Map of Ponding Area

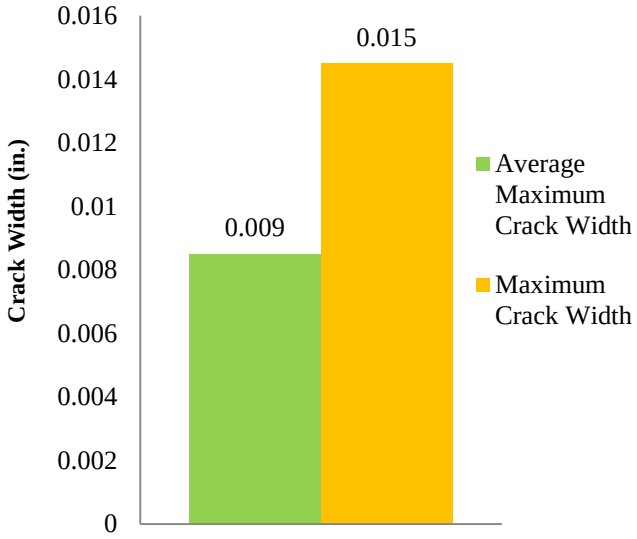

Figure 6.61: Crack Data for Specimen 3.3

6.2.5.2 Longitudinal and Transvers Bars

The north and south longitudinal bars had slight damage from when the bars were extracted from the specimen. Rust stains were also evident at locations where the transverse bars were tied to the longitudinal bars. This staining is from corrosion of the tie wire used to attach the transverse reinforcement to the longitudinal bars and NOT from the longitudinal bar itself. Moderate corrosion was observed on both the north and

south longitudinal bars. The north bar had moderate corrosion at the dead end and the south bar had moderate corrosion at the dead end quarter point (Figure 6.62). Figure 6.67 shows the longitudinal bar's corrosion ratings and Table 6.14 shows the summary of the corrosion ratings for the longitudinal bars.

Figure 6.62: Moderate Corrosion at the Dead End Quarter Point of Specimen 3.3 South Longitudinal Bar

All transverse bars had damage from when they were extracted from the specimen. All the transverse bars had rust staining at least somewhere over the length of the bar from corrosion of the tie wire used to attach the transverse bars to the longitudinal bars and to attach the duct to the transverse bars. Light corrosion was observed on at least one interval of bars #1, #2, #3, #4, and #7 and moderate corrosion observed on at least one interval of bars #1, #3, #4, and #6. Surprisingly, bar #1 had the highest rating of 17. This was surprising because bar #1 was outside the ponding area and should not have been exposed to oxygen and/or chlorides because of the increased cover and the fact that the concrete was not cracked. Bar #4 had the next highest rating of 15. Bars #2 and #7 had

the lowest rating of 4. Figure 6.67 shows the transverse bar's corrosion ratings and Table 6.14 shows the summary of the corrosion rating for the transverse bars.

6.2.5.3 Duct

The entire outer surface of the north duct had a chalky white residue. No corrosion staining was observed on the outer or inner surface of the duct. The inner bottom surface of the north duct had slight gouges on successive intervals in the dead end side of midspan and one interval on the live side of midspan. This indicates that one or more of the strands caused damage either when the strands were being threaded through the duct or one of the strands or stands were rubbing against the duct when the strands were being stressed. In either case, the integrity of the duct was not compromised. Indications of voids were observed on the top inner surface of the duct along the entire length. No damage was observed on the coupler, grout vent, or heat shrink wrap used to seal the coupler/duct interface (Figure 6.63). However, the heat shrink wrap did not bond well to the coupler or duct (Figure 6.63). This might indicate why chloride levels were elevated.

Figure 6.63: Coupler and Heat Shrink Wrap from North Duct of Specimen 3.3

The damage and appearance of the south duct was similar to the north duct. The entire outer surface of the south duct had a chalky white residue. The inner bottom and top surface of the north duct had slight gouges. The top inner surface had gouges at the dead end of the duct and the inner bottom surface had gouges at approximately the dead end quarter point. Again, this indicates that one or more of the strands caused damage

either when the strands were being threaded through the duct or possibly one of the strands or stands were rubbing against the duct when the strands were being stressed. In either case, the integrity of the duct was not compromised. The silicone that was used to seal the grout vent to the south duct was found to have debonded from the duct (Figure 6.64). It is not known if this happened during extraction or when the concrete was placed. Chloride levels indicate that the latter is the more valid explanation.

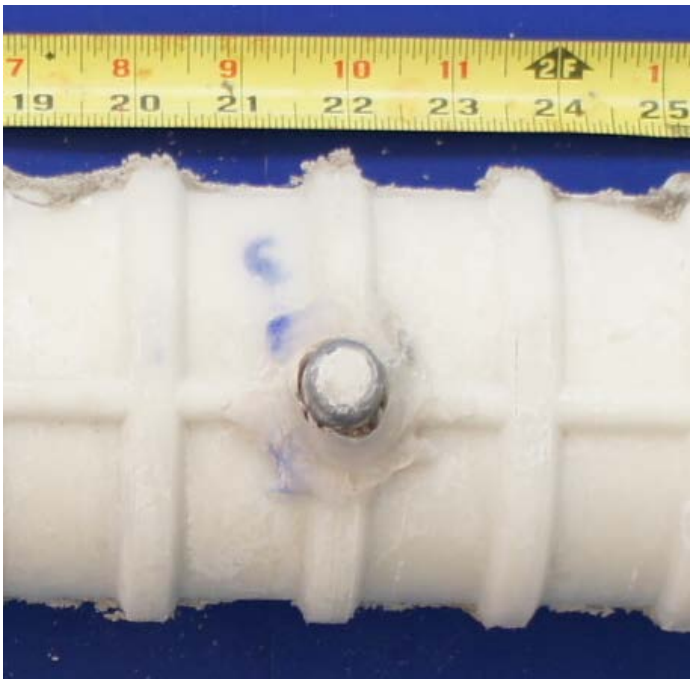

Figure 6.64: Silicone Debonded from Grout Vent of South Duct from Specimen 3.3

Figure 6.67 shows the damage ratings for the ducts and Table 6.14 shows the summary of the damage ratings for the ducts.

6.2.5.4 Grout

No transverse or longitudinal visible cracks were observed during examination of the grout from the north and south tendons of Specimen 3.3 but when chloride samples were being taken transverse cracks became evident (Figure 6.65). No staining of the grout was observed on either the north or south tendon. Small voids in the grout were

observed in the flutes along the entire length of the top of both the north and south tendons. The small voids measured approximately 1.5 inch long and were as wide as the flute width. Segregation of the grout was observed on the live and dead end of both the north and south tendon. The coloration of the grout from the north tendon was dark grey at the ends and transitioned to light grey at midspan (Figure 6.65). A white crystalline powder was observed on the grout on the bottom of the entire length of the south tendon and on the bottom of the north tendon at midspan (Figure 6.65).

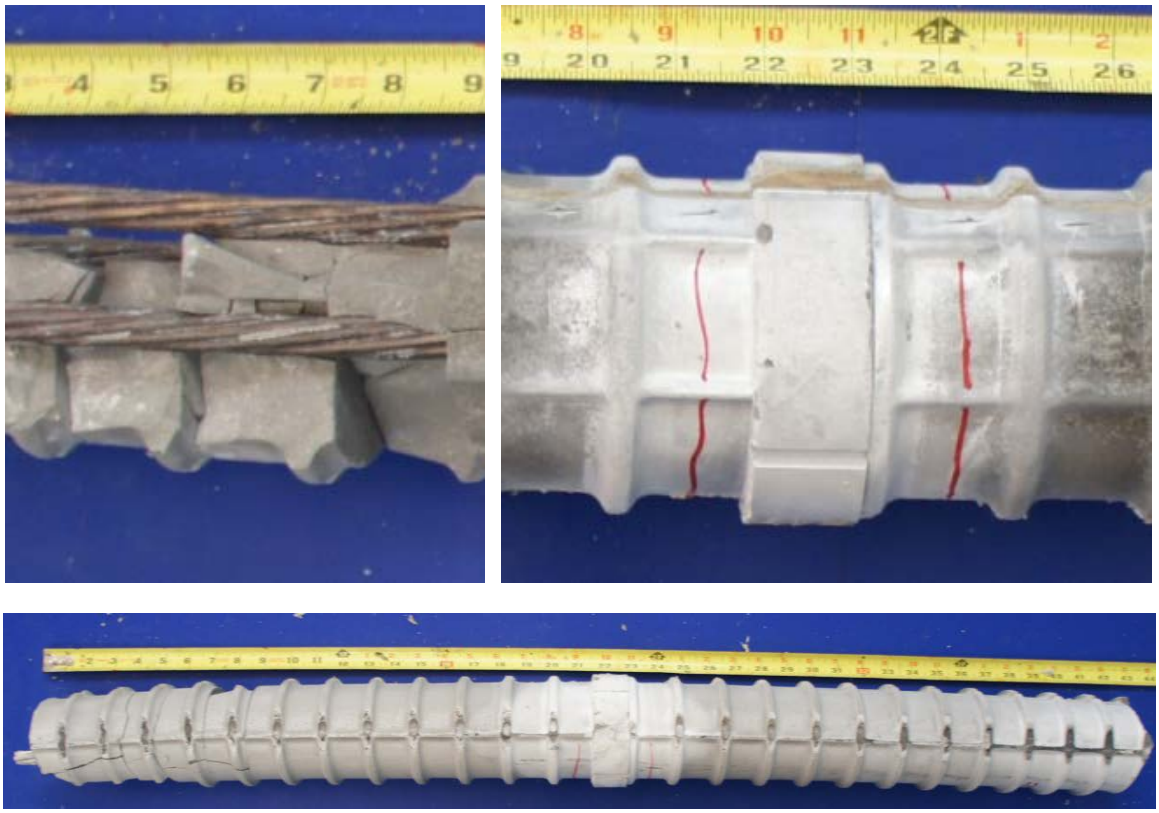

Figure 6.65: Transverse Cracks (Top Left), White Crystalline Powder (Top Right) and Color Transition (Bottom) of Specimen 3.3 North Tendon

The chloride concentrations were discussed in depth in Chapter 5. All the chloride concentrations were above the 0.033% by weight of grout limit for corrosion. See Figure 5.14 for the results of the chloride concentration testing. As expected, the highest chloride concentration for the north and south tendons were at midspan and were 0.280% and

0.480%, respectively, by weight of grout. As expected, the anchorage regions had the lowest chloride concentrations. This might be because the chlorides would take longer to migrate to the anchorages because the chloride ions would have to travel through the interstitial space between the grout and duct and/or interstitial space between the grout and strand.

6.2.5.5 Strand

All the wires from the strands in the north and south tendons of Specimen 3.3, except for a few intervals, had a very dark brown discoloration over the majority of their length (Figure 6.66). The few intervals had small spots of reddish color corrosion product and were given the rating of 2 for light corrosion because it was easily removed from the surface with the scouring pad. The very dark brown discoloration was from the passivation of the copper cladding and was not considered corrosion. There were no visible signs of the steel core corroding. Figure 6.67 shows the damage ratings for the ducts and Table 6.14 shows the summary of the damage ratings for the ducts.

Figure 6.66: Very Dark Brown Discoloration of Copper Cladding on Strand from Specimen 3.3

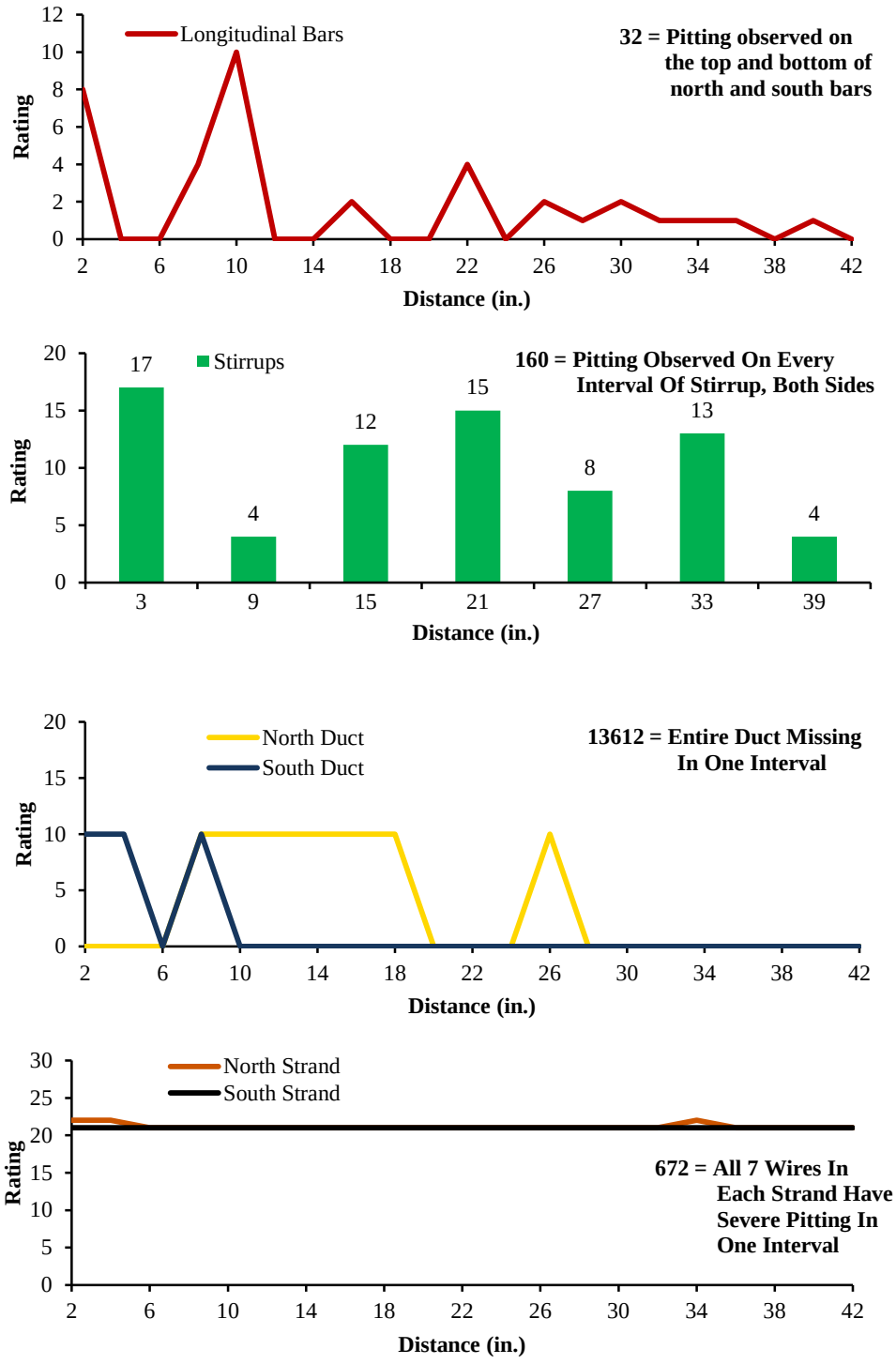

Figure 6.67: Corrosion Rating Plots for Main Autopsy Region of Specimen 3.3

6.2.5.6 Dead and Live End Anchorages

The majority of the epoxy applied to the anchorage components from the dead end before the anchorage cavity was backfilled had debonded from the anchorage components of both tendons. The exposed faces of the north and south anchorage plates from the dead end had light surface corrosion on the majority their surface. The majority of the surface of the bottom of the north and south anchorage plates and the north and south duct/anchorage plate interfaces from the dead end had light surface corrosion (Figure 6.68). The exposed faces of the north and south anchor heads from the dead end had spots of light surface corrosion. The north and south sides of the anchor heads from the dead end had light surface corrosion at the interface of the anchor head and anchorage plate. The unexposed face of the north and south dead end anchor heads had light surface corrosion.

Figure 6.68: Light Surface Corrosion on Bottom of the North Dead End Anchorage Plate from Specimen 3.3

The majority of the epoxy applied to the anchorage heads from the live end before the anchorage cavity was backfilled had debonded from the anchorage components of both tendons. Most of the epoxy applied to the exposed surface of the anchorage plates from the live end before the anchorage cavity was backfilled was still bonded to the

surface. The exposed faces of the north and south anchorage plates from the live end had light surface corrosion in the locations were the epoxy had debonded. The majority of the surface of the bottom of the north and south anchorage plates and the north and south duct/anchorage plate interfaces from the live end had light surface corrosion. The exposed faces of the north and south anchor heads from the dead end had no visible signs of corrosion. The north and south sides of the anchor heads from the live end had light surface corrosion at the interface of the anchor head and anchorage plate. The unexposed face of the north and south live end anchor heads had light surface corrosion.

Table 6.15: Specimen 3.3 Summary of Dead and Live End Anchorage Region Corrosion Ratings

	Dead End Anchorage			Live End Anchorage		
Component	Maximum	Total	Generalized	Maximum	Total	Generalized
North Duct	10	10	30	10	10	30
South Duct	10	10	30	10	10	30
North Strands	27	136	45	23	153	44
South Strands	23	130	43	23	151	43

The north and south ducts from the dead end had slight gouging. This indicates that one or more of the strands caused damage either when the strands were being threaded through the duct or one of the strands or stands were rubbing against the duct when the strands were being stressed. There was no staining on either duct. There were indications of voids in the grout of the north and south tendon along the length of the top of the duct in the dead end anchorage region from the flutes of the duct.

The north and south ducts from the live end had slight gouging. This indicates that one or more of the strands caused damage either when the strands were being threaded through the duct or one of the strands or stands were rubbing against the duct when the strands were being stressed. In either case, the integrity of the duct was not compromised. There was no staining on either duct. There were indications of voids in the grout of the north and south tendon along the length of the top of the duct in the live end anchorage region from the flutes of the duct.

Figure 6.70 shows the damage ratings for the dead and live anchorage region ducts and Table 6.15 shows the summary of the damage ratings for the dead and live anchorage region ducts.

The grout from the north and south dead end tendons had no visible transverse or longitudinal cracks. The grout from both tendons from the dead end had voids and signs of "bubbling" in the area of the flutes of the ducts along the length of the top surface. Concrete was observed in the grout of the dead end of the south tendon (Figure 6.69). This might be an indication that the duct tape that was used to seal the connection of the duct and anchorage plate was not suitable to create a water tight seal.

Figure 6.69: Concrete in Grout from the Dead End of the North Tendon of Specimen 3.3

The grout from the north and south live end tendons had no visible transverse or longitudinal cracks. The grout from both tendons from the live end had voids and signs of "bubbling" in the area of the flutes of the ducts along the length of the top surface.

Similar to the outer wires of the strands from the ponding area, the outer wires of the strands in both the north and south dead end anchorage region had very dark brown

discoloration over most of their lengths with a few spots of reddish colored light corrosion. The inner wires of the strand from the north and south tendons from the dead end had the same discoloration as the outer wires. Two of the inner wires (one from north tendon and one from the south tendon) had a spot of reddish colored light corrosion. Four of the outer wires from the north tendon had spots of reddish colored light corrosion in the indentions made by the wedge anchors. This was not "rust" but the same reddish colored light corrosion observed in the wires from the ponding area.

The outer wires of the strands in both the north and south live end anchorage region had very dark brown discoloration over most of their lengths with a few spots of reddish colored light corrosion, similar to the discoloration and corrosion of the dead end outer wires. The inner wires of the strand from the north and south tendons had the same discoloration as the outer wires. Four of the outer wires from the north tendon had spots of reddish colored light corrosion in the indentions made by the wedge anchors. Two other outer wires had the same reddish colored light corrosion not in the region if the wedge anchors.

Figure 6.70 shows the corrosion ratings for the dead and live anchorage region strands and Table 6.15 shows the summary of the corrosion ratings for the dead and live anchorage region strands.

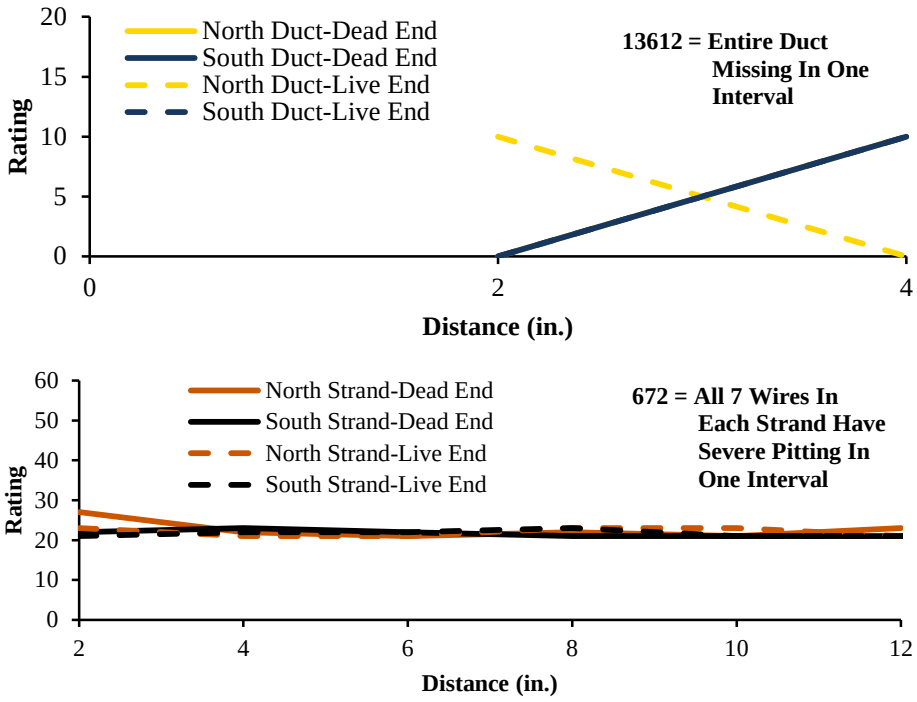

Figure 6.70: Corrosion Rating Plots for Dead and Live End Anchorage Regions of Specimen 3.3

The anchorage components from the live and dead ends had experienced similar damage. So, it can be assumed that the dead end anchorage spray did not make a difference when it came to the damage that was observed. However, the chloride data suggests that the spray system did increase the chloride concentrations in the backfill mortar to a level that was above the chloride limit for corrosion. In spite of this, the similar damage in the live and dead anchorage components suggests that chlorides did not migrate far enough into the backfill mortar to cause damage.

6.2.6 Specimen 4.1: Non-Galvanized Anchorage, Stainless Steel Strand, Corrugated Steel Duct

Figure 6.71: Specimen 4.1Main Autopsy Region and Grout Vents

Table 6.16: Specimen 4.1 Summary of Main Autopsy Region Corrosion Ratings

Component	Maximum	Total	Generalized
Longitudinal Bars	2	8	1.1
Transverse Bars	3	32	2.3
North Duct	2924	6488	1854
South Duct	2728	6629	1894
North Strands	2	4	0.4
South Strands	2	7	0.7

6.2.6.1 Appearance

The surface of Specimen 4.1 had medium scaling over the majority of the top surface and ponding area. The rest of the exterior had no scaling but had small shallow depressions from air voids that had developed against the formwork during casting. Small rust stains were observed in the ponding area at the base of north and south grout vents. The backfill mortar from the dead and live end anchorage pockets were separating from the base concrete. This indicates that the mortar did not adhere well to the base concrete.

There were cracks present at the re-entrant corbel corners on both sides of the dead end and efflorescence was observed coming from the cracks. These cracks were not present after live load application[1]. Therefore, the cracks had not been sealed with mortar or epoxy. The repairs to the cracks from the application of live load on both sides of the live end re-entrant corbel corners were in good repair but moisture was observed around the edge of the repair (Figure 6.72). The ponding area of Specimen 4.1 had 1 large transverse crack that ran from the north to the south side of the specimen and 4 small transverse cracks on the edge of the ponding area (2 on the north side and 2 on the south side) (Figure 6.73). The average crack width was 0.006 inch. The crack rating for Specimen 4.1 was 0.06. See Figure 6.74 for the crack data from Specimen 4.1.

Figure 6.72: Moisture Observed around the Edge of North Live End Re-entrant Corbel Corner Crack of Specimen 4.1

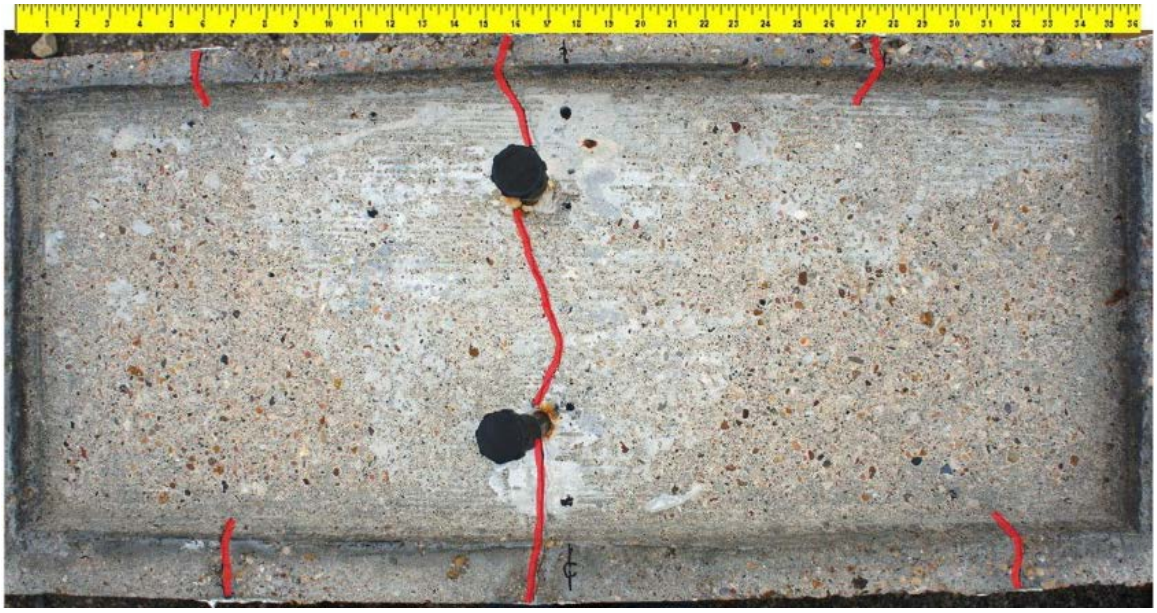

Figure 6.73: Specimen 4.1 Crack Map of Ponding Area

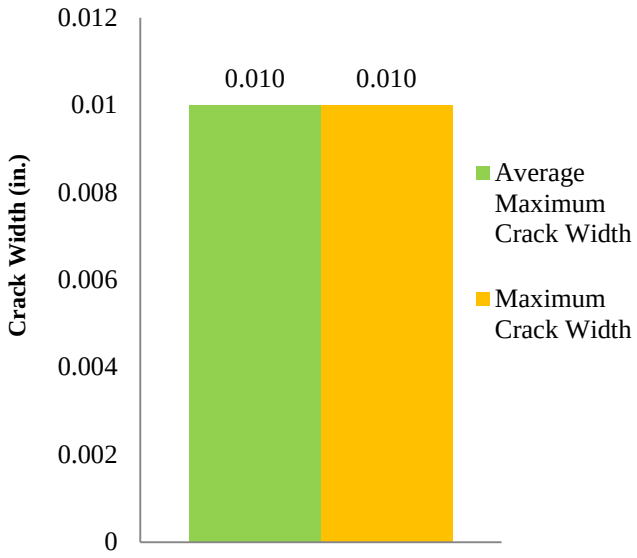

Figure 6.74: Crack Data for Specimen 4.1

6.2.6.2 Longitudinal and Transverse Bars

The north and south longitudinal bars had slight damage from when the bars were extracted from the specimen (Figure 6.75). Rust stains were also evident at locations where the transverse bars were tied to the longitudinal bars. This staining is from corrosion of the tie wire used to attach the transverse reinforcement to the longitudinal bars and NOT from the longitudinal bar itself. The south longitudinal bar had a spot of light corrosion at approximately 34 inches from the dead end of the bar. Figure 6.79 shows the longitudinal bar's corrosion ratings and Table 6.16 shows the summary of the corrosion ratings for the longitudinal bars.

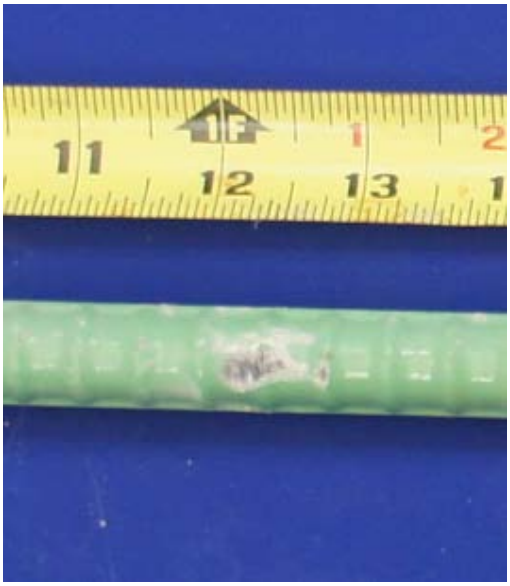

Figure 6.75: Extraction Damage to South Longitudinal Bar from Specimen 4.1

All the transverse bars had damage from when they were extracted from the specimen. All the transverse bars had rust staining from corrosion of the tie wire used to attach the transverse bars to the longitudinal bars and to attach the ducts to the transverse bars. The staining is also from the corrosion of the galvanized duct. Light corrosion was observed on all the bars except bars #1 and #7. Bars #2 and #5 had the highest ratings of 8 and 9, respectively. The end bars, #1 and #7, had the lowest corrosion rating of 1. This was expected because these bars are outside the ponding area and should have had little

to no exposure to chloride ions. Figure 6.79 shows the transverse bar's corrosion ratings and Table 6.16 shows the summary of the corrosion rating for the transverse bars.

6.2.6.3 Duct

Both the north and south ducts had localized severe corrosion damage. This damage resulted in holes in the ducts. The top of the north duct had a large hole at midspan (Figure 6.76). The bottom outer surface of the north duct had light corrosion at midspan. The top inner surface of the north duct had light corrosion on the live and dead ends. The bottom outer surface of the north duct had light corrosion at midspan. The bottom inner portion of the north duct had light corrosion spanning from approximately 12 inches to approximately 30 inches. The top of the south duct had a large hole at midspan. The top outer surface of the south duct had light corrosion in intervals adjacent to the large hole at midspan. The bottom outer surface of the south duct had moderate corrosion at approximately midspan and light corrosion periodically over the length of the duct. The top inner surface of the south duct had no visible signs of corrosion on intervals that did not have holes. The bottom inner portion of the south duct had moderate corrosion at approximately 24 inches and had light corrosion on the adjacent intervals. The holes experienced by both the north and south ducts indicate that voids in the grout had formed along the top of the duct. Figure 6.79 shows the corrosion ratings for the ducts and Table 6.16 shows the summary of the corrosion ratings for the ducts.

Figure 6.76: Hole on the Top at Midspan of the North Duct from Specimen 4.1

6.2.6.4 Grout

No cracking in the grout could be observed because the grout fell apart when the ducts were removed from the tendon due to the highly curved nature of the strands (Figure 6.78). Staining from corrosion of the duct was observed at locations where corrosion had caused holes in both the north and south duct. Because the grout fell apart, a rust stain that was observed on the grout will be shown in Figure 6.77 still encased in the duct. Small voids in the grout were observed in the flutes along the entire length of the top of both the north and south tendons and large voids were present at mid span of both the north and south tendons. The small voids measured approximately 0.75 inch long and were as wide as the flute width.

Figure 6.77: Staining on Gout from Specimen 4.1

The chloride concentrations were discussed in depth in Chapter 5. All the chloride concentrations were above the 0.033% by weight of grout limit for corrosion. See Figure 5.14 for the results of the chloride concentration testing. As expected, the highest chloride concentration for the north and south tendons were approximately at midspan and were 0.220% and 0.270%, respectively, by weight of grout. As expected, the anchorage regions had the lowest chloride concentrations. This might be because the chlorides would take longer to migrate to the anchorages because the chloride ions would have to

travel through the interstitial space between the grout and duct and/or interstitial space between the grout and strand.

6.2.6.5 Strand

The three strands in the north and south tendons had no visible corrosion. Minimal discoloration was observed on the outer wires. The discoloration was located primarily at the locations of the holes in the duct. The inner wires had no visible signs of discoloration or corrosion. See Figure 6.78 for a typical stainless steel strand. This outcome was expected because of the corrosion resistance properties of stainless steel. The grout did not adhere well to the strands. Because the grout did not adhere well to the strands, when the tendons were cut the strands retracted into the grout. The strands had a highly curved shape (Figure 6.78). Figure 6.79 shows the corrosion ratings for the strands and Table 6.16 shows the summary of the corrosion ratings for the strands.

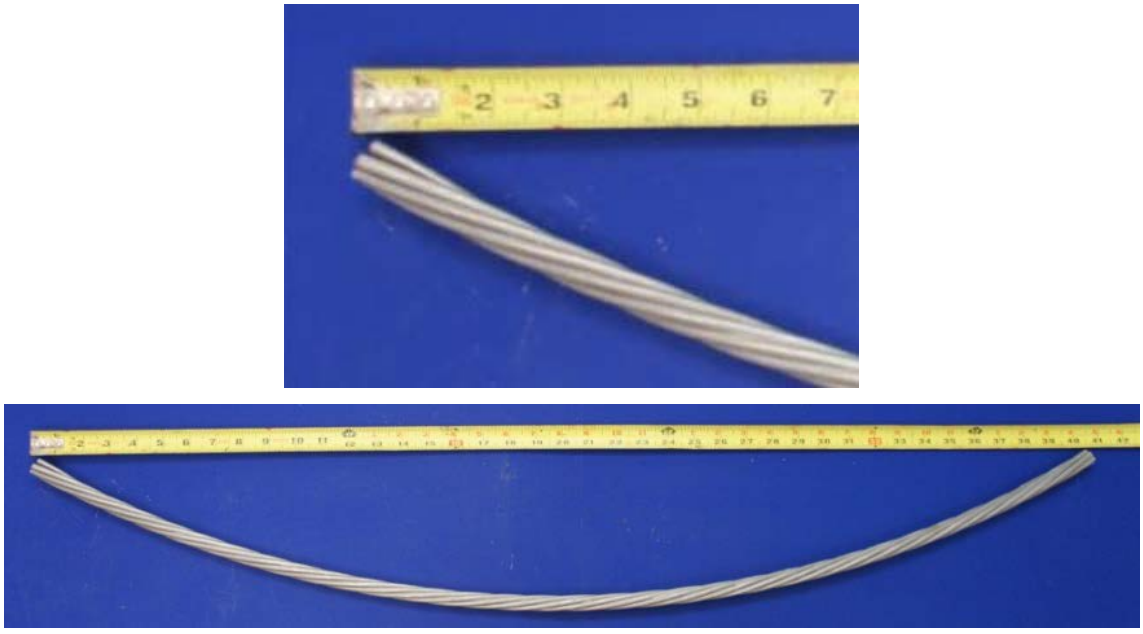

Figure 6.78: Typical Stainless Steel Strand (Top) and Arched Strand (Bottom) from Specimen 4.1

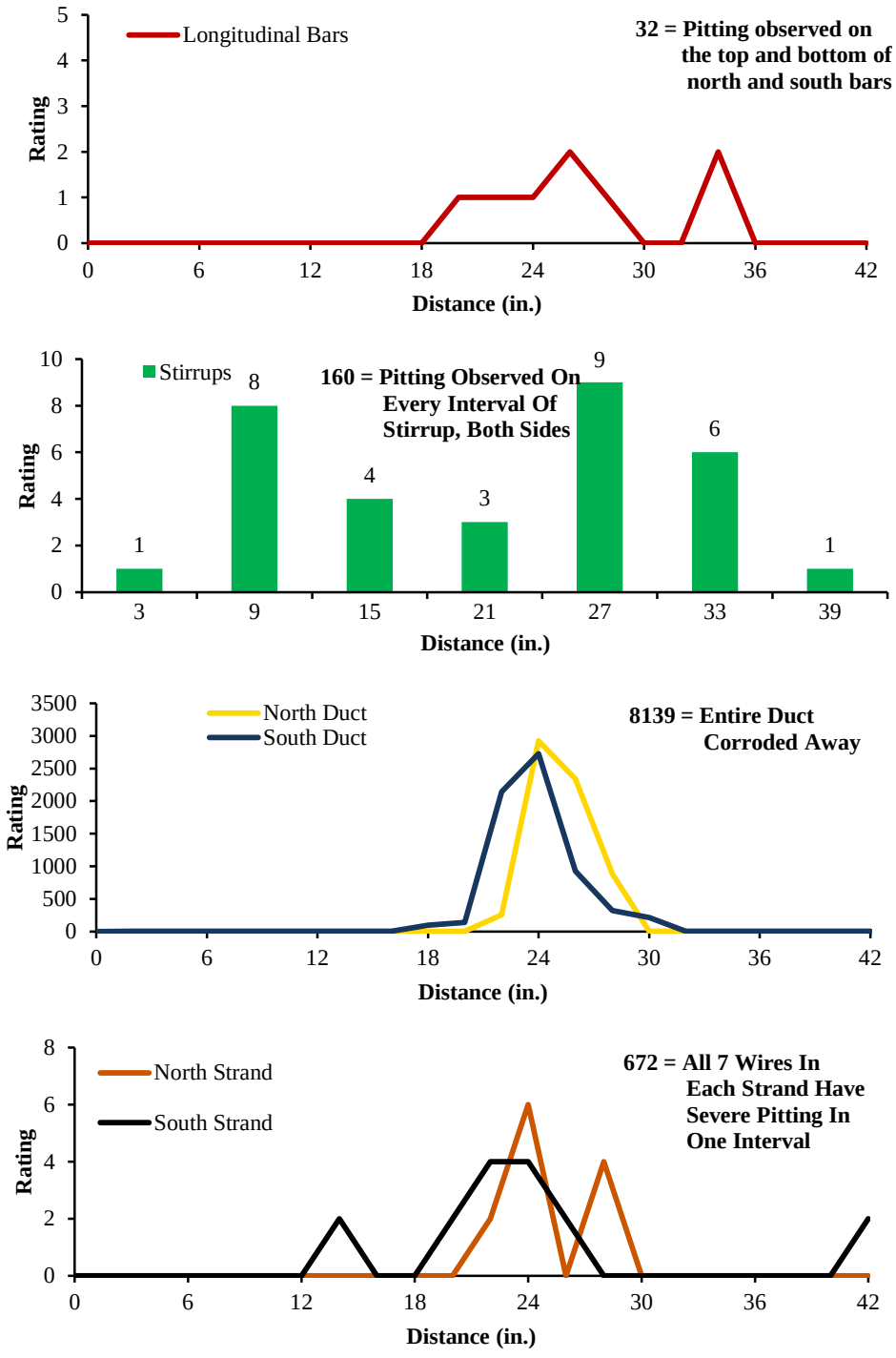

Figure 6.79: Corrosion Rating Plots for Main Autopsy Region of Specimen 4.1

6.2.6.6 Dead End Anchorage

Except for a few spots at the interface of the anchorage plate and anchor head, all the epoxy applied to the anchorage components from the dead end before the anchorage cavity was backfilled had debonded from the anchorage components of both tendons. The exposed faces of the north and south anchorage plates from the dead end had light surface corrosion on the majority their surface. The majority of the bottom surface of the north and south anchorage plates and the north and south duct/anchorage plate interfaces from the dead end had light surface corrosion. The exposed face of the north and south anchor heads from the dead end had a few spots of light surface corrosion. The unexposed faces of the north and south anchor heads had light surface corrosion on the majority of their surface. The sides of the north and south anchor heads had light surface corrosion over the majority of their surface. The unexposed face had light surface corrosion on the outer ring where the grout had not come into contact with the anchor head (Figure 6.80).

Figure 6.80: Corrosion on Unexposed Face of an Anchor Head from Specimen 4.1

Table 6.17: Specimen 4.1 Summary of Dead End Anchorage Region Corrosion Ratings

Component	Maximum	Total	Generalized
North Duct	7	13	19
South Duct	6	10	15
North Strands	21	56	19
South Strands	21	63	21

The north duct from the dead end had light corrosion on its inner and outer surface of the duct and bottom outer surface. The south duct from the dead end had light corrosion on its top and bottom outer surface. There were indications of voids in the grout on the top of the north and south tendon along the length of the duct in the anchorage region from the flutes of the duct. Figure 6.82 shows the corrosion ratings for the anchorage region ducts and Table 6.17 shows the summary of the corrosion ratings for the anchorage region ducts.

It could not be determined if the grout from either the north or south duct had transverse or longitudinal cracks because the grout fell apart when the grout was removed from the duct due to the curved nature of the stainless steel strands. The grout from both tendons had voids and signs of "bubbling" in the area of the flutes of the ducts along the length of the top surface. It could not be determined if the grout had segregated because the grout fell apart.

All outer and inner wires of the strands from the north and south tendons had discoloration in the region of the wedge anchors and in the south strands in the region close to where the tendon was cut so grout could be extracted from the anchorage region (Figure 6.81). However, the north strands had discoloration in the same region on all the inner wires but not on all the outer wires. This discoloration in the wedge anchor region is more than likely from when the anchor heads had to be heated to remove the strands. The discoloration where the tendon had to be cut to extract grout from the anchorage might be from the strand being heated during cutting of the tendon. The wedges from the north tendon were intact and had no visible signs of corrosion. However, the wedges from the south tendon were intact but had light surface corrosion on the exterior surface.

Figure 6.82 shows the corrosion ratings for the anchorage region strands and Table 6.17 shows the summary of the corrosion ratings for the anchorage region stands.

Figure 6.81: Discoloration of Stainless Steel Wires from the South Tendon in the Dead End Anchorage of Specimen 4.1

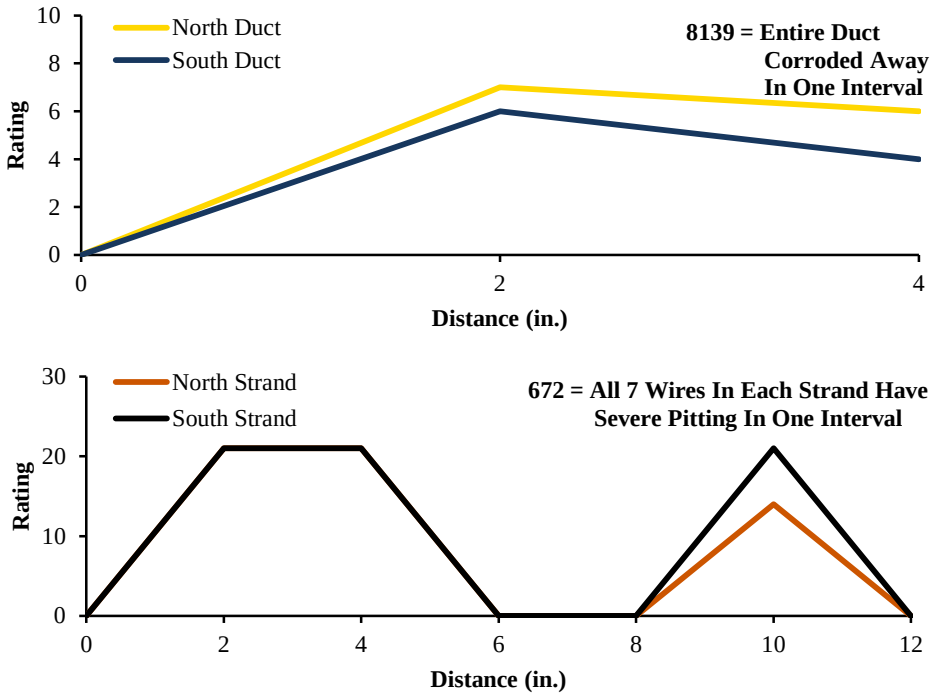

Figure 6.82: Corrosion Rating Plots for Dead Anchorage Region of Specimen 4.1

6.2.7 Specimen 4.3: Non-Prestressed, Epoxy Coated Steel Reinforcing Bars

Figure 6.83: Specimen 4.3 Main Autopsy Region and Grout Vents

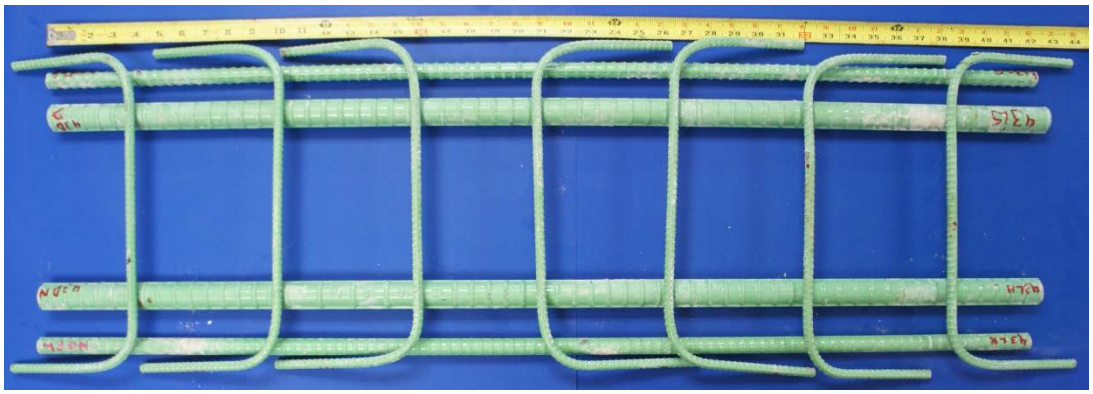

Figure 6.84: Steel Reinforcement Layout for Specimen 4.3

Table 6.18: Specimen 4.3 Summary of Main Autopsy Region Corrosion Ratings

Component	Maximum	Total	Generalized
#4 Epoxy Coated Longitudinal Bars	5	19	2.7
#8 Epoxy Coated Longitudinal Bars	5	20	2.9
Transverse Bars	8	69	4.9

6.2.7.1 Appearance

The surface of Specimen 4.3 shown in Figure 6.83 had medium scaling over the majority of the top surface and the edges of the ponding area. The ponding area had shallow to deep depressions from air voids that formed under the form that was used to create the ponding area when the specimen was cast. The rest of the exterior had no scaling but had small shallow depressions from bleed water voids that had developed against the formwork during casting.

No cracks were present at the re-entrant corners on both sides of the dead and live end. Unlike the other specimens with prestressing the live load applied to this specimen was not as large. Therefore, the re-entrant corbel corners did not crack[1]. The ponding area of Specimen 4.3 had 4 large transverse cracks that ran from the north to the south side of the specimen and 1small transverse crack on the edge of the ponding area at midspan and on the north side of the ponding area (Figure 6.85). The average crack width was 0.008 inch. The crack rating for Specimen 4.3 was 0.32. See Figure 6.86 for the crack data from Specimen 4.3.

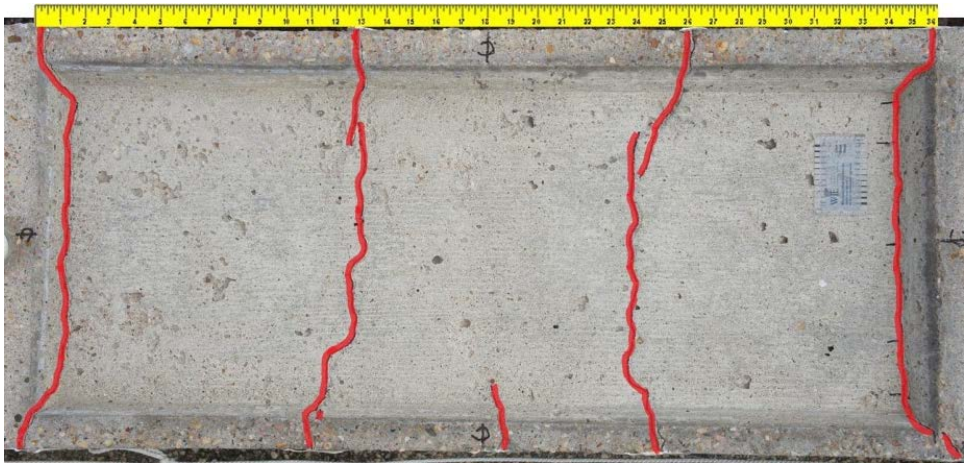

Figure 6.85: Specimen 4.3 Crack Map of Ponding Area

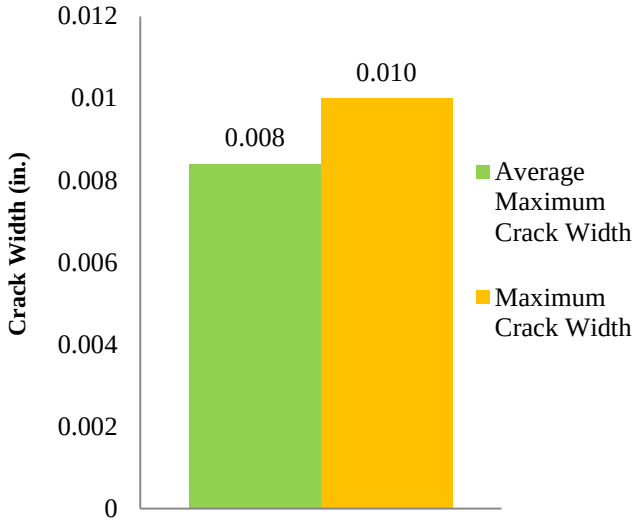

Figure 6.86: Crack Data for Specimen 4.3

6.2.7.2 Longitudinal and Transverse Bars

The north and south #4 longitudinal bars had slight damage from when the bars were extracted from the specimen. Light corrosion was observed on the dead end of the north #4 longitudinal bar. Rust stains were also evident at locations where the transverse bars were tied to the longitudinal bars. This staining is from corrosion of the tie wire used to attach the transverse reinforcement to the longitudinal bars and NOT from the longitudinal bar itself. Figure 6.89 shows the #4 longitudinal bar's corrosion ratings and Table 6.18 shows the summary of the corrosion ratings for the #4 longitudinal bars.

The north and south #8 longitudinal bars had slight damage from when the bars were extracted from the specimen. Light and moderate corrosion was observed on the dead end of the north #8 longitudinal bar (Figure 6.87). Rust stains were also evident at locations where the transverse bars were tied to the longitudinal bars. This staining is from corrosion of the tie wire used to attach the transverse reinforcement to the longitudinal bars and NOT from the longitudinal bar itself. Figure 6.89 shows the #4 longitudinal bar's corrosion ratings and Table 6.18 shows the summary of the corrosion ratings for the longitudinal bars.

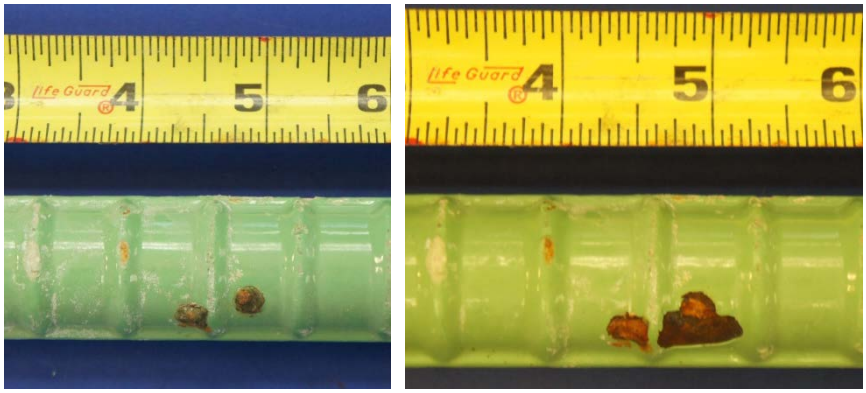

Figure 6.87: "Bubbles" in Epoxy Coating (Left) and Moderate Corrosion under "Bubbles" (Right) at the Dead End of North #8 Bar of Specimen 4.3

All the transverse bars, except #5, had damage from when they were extracted from the specimen. All the transverse bars had rust staining from corrosion of the tie wire used to attach the transverse bars to the longitudinal bars. Moderate corrosion was observed on bars #6 and #7 on the horizontal portion of the transverse bar (Figure 6.88). Bars #6 and #7 had the highest ratings of 20 and 29, respectively. The #1 transverse bar had the lowest corrosion rating of 6. This was expected because this bar was outside the ponding area and should have had little to no exposure to chloride ions but the #7 bar should have had one of the lowest ratings for the same reason. Figure 6.89 shows the transverse bar's corrosion ratings and Table 6.18 shows the summary of the corrosion rating for the transverse bars.

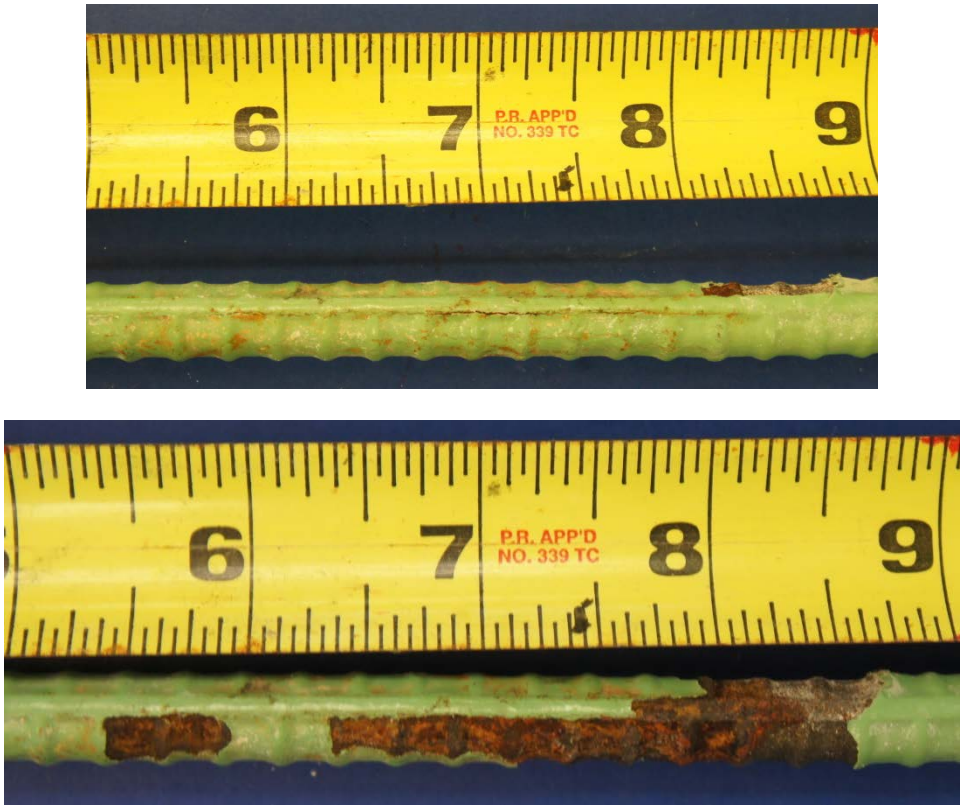

Figure 6.88: Crack in Epoxy Coating along the Longitudinal Rib (Top) and Moderate Corrosion at the Crack along the Longitudinal Rib (Bottom) on #6 Transverse Bar from Specimen 4.3

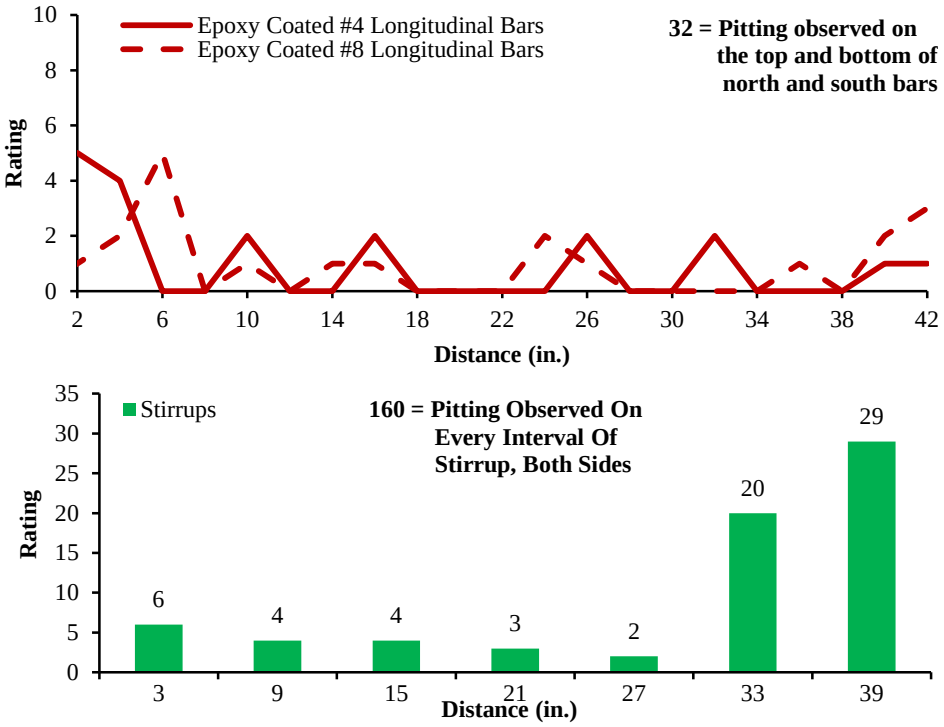

Figure 6.89: Corrosion Rating Plots for Main Autopsy Region of Specimen 4.3

6.2.8 Specimen 4.4: Non-Prestressed, Epoxy Coated and Uncoated Steel Reinforcing Bars

Figure 6.90: Specimen 4.4 Main Autopsy Region and Grout Vents

Figure 6.91: Steel Reinforcement Layout for Specimen 4.4

Table 6.19: Specimen 4.4 Summary of Main Autopsy Region Corrosion Ratings

Component	Maximum	Total	Generalized
#4 Epoxy Coated Longitudinal Bars	3	18	2.6
#8 Uncoated Longitudinal Bars	32	342	49
Transverse Bars	8	99	7.1

6.2.8.1 Appearance

The surface of Specimen 4.4 had medium scaling over the majority of the top surface and the edge of the ponding area. The ponding area had shallow to deep depressions from bleed water voids that formed under the form that was used to create the ponding area when the specimen was cast. The rest of the exterior had no scaling but had small shallow depressions from bleed water voids that had developed against the formwork during casting. Rust staining was observed on the north side towards the live end of the ponding area in the location of the #8 uncoated longitudinal steel reinforcing bar (Figure 6.90). This rust stain indicated that the #8 uncoated steel bar was corroded.

No cracks were present at the re-entrant corbel corners on both sides of the dead and live end. Unlike the other specimens with prestressing the live load applied to this specimen was not as large. Therefore, the re-entrant corbel corners did not crack[1]. The ponding area of Specimen 4.4 had 3 large transverse cracks that ran from the north to the south side of the specimen and 3 small transverse cracks that extended from the edge of the ponding area to about the transverse centerline of the ponding area (Figure 6.92). Two longitudinal cracks were observed on the north side towards the live end of the ponding area (Figure 6.92). This crack was also located over the north #8 uncoated longitudinal bar and might have been caused by the corrosion of the north #8 uncoated longitudinal bar creating expansive forces thus cracking the concrete. The average crack width was 0.007 inch. The crack rating for Specimen 4.4 was 0.54. See Figure 6.93 for the crack data from Specimen 4.4.

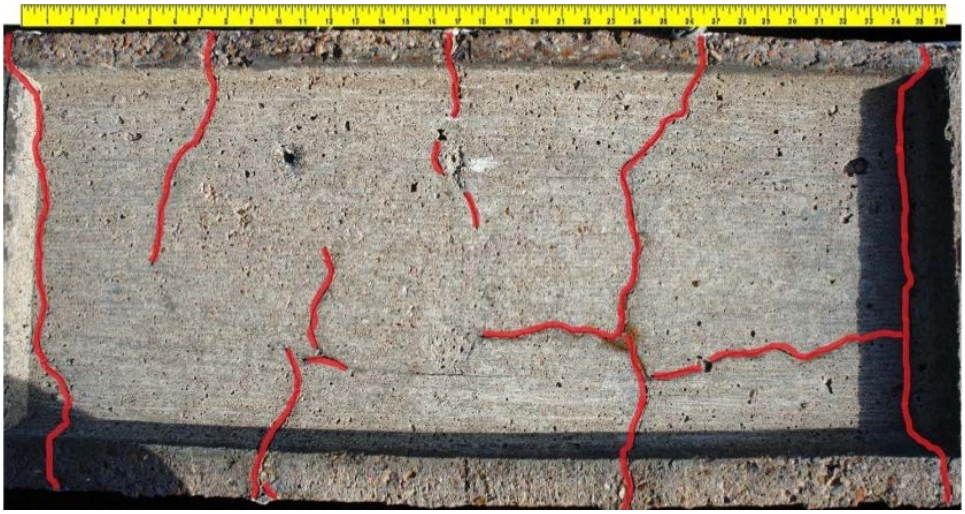

Figure 6.92: Specimen 4.4 Crack Map of Ponding Area

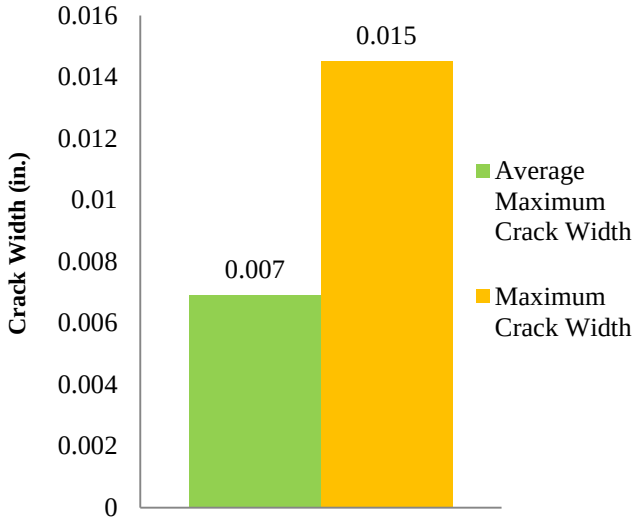

Figure 6.93: Crack Data for Specimen 4.4

6.2.8.2 Longitudinal and Transverse Bars

The north and south #4 epoxy coated longitudinal bars had slight damage from when the bars were extracted from the specimen. No visible corrosion was observed on either bar. Rust stains were evident at locations where the transverse bars were tied to the longitudinal bars. This staining is from corrosion of the tie wire used to attach the transverse reinforcement to the longitudinal bars and NOT from the longitudinal bar

itself. Figure 6.95 shows the #4 epoxy coated longitudinal bar's corrosion ratings and Table 6.19 shows the summary of the corrosion ratings for the #4 epoxy coated longitudinal bars.

The north and south #8 uncoated longitudinal bars had slight damage from when the bars were extracted from the specimen. The north and south bars had extensive pitting, moderate corrosion, and light corrosion along their lengths (Figure 6.94). The pitting was located at locations were transverse cracks were observed. This indicates that moisture, oxygen, and chlorides reached the depth of the bars. The light and moderate corrosion was normally located on intervals adjacent to the areas of pitting. Figure 6.95 shows the #8 uncoated longitudinal bar's corrosion ratings and Table 6.19 shows the summary of the corrosion ratings for the #8 uncoated longitudinal bars.

Figure 6.94: Moderate and Light Corrosion (Top) and Pitting (Bottom) on South #8 Uncoated Bar from Specimen 4.4

All the transverse bars had damage from when they were extracted from the specimen. All the transverse bars had rust staining from corrosion of the tie wire used to attach the transverse bars to the longitudinal bars and from the corrosion of the #8 uncoated longitudinal bars. Moderate corrosion was observed on bars #1, #3, and #6. Light corrosion was observed on all the bars except #7. Bars #1 and #3 had the highest

corrosion ratings of 23 and 25, respectively. The #1 bar having the second highest corrosion rating was unexpected because it was from outside the ponding area and should not have been exposed to chlorides, moisture, and oxygen. The #2 and #4 transverse bars had the lowest corrosion rating of 8. Figure 6.95 shows the transverse bar's corrosion ratings and Table 6.19 shows the summary of the corrosion rating for the transverse bars.

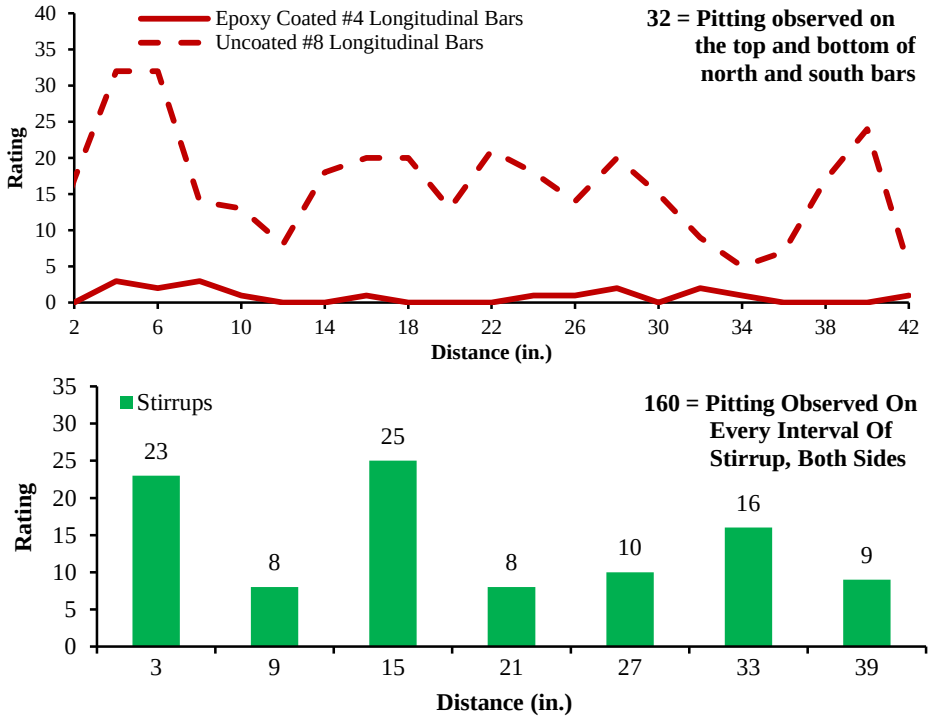

Figure 6.95: Corrosion Rating Plots for Main Autopsy Region of Specimen 4.4

6.2.9 Specimen 5.1: Galvanized Anchorage, Conventional Strand, Two-way Plastic Duct

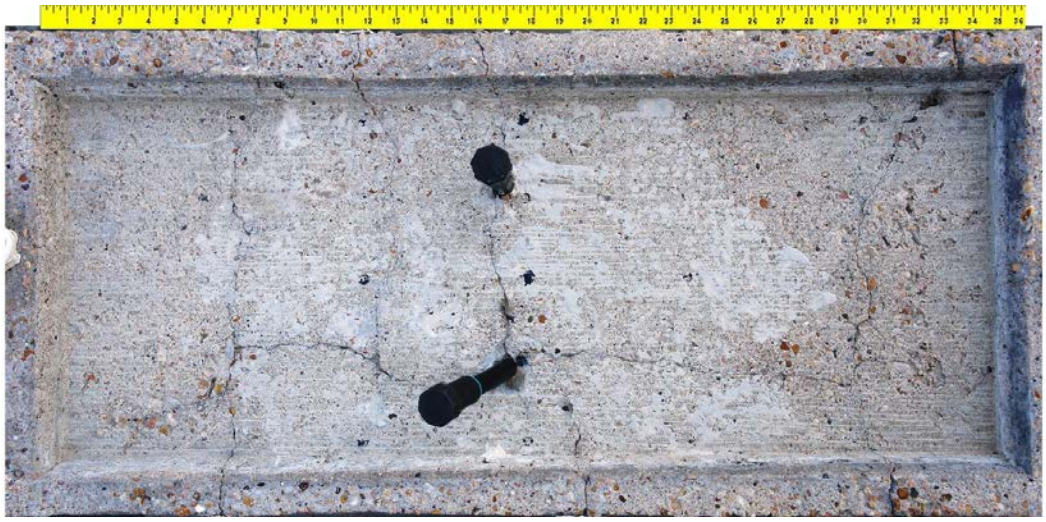

Figure 6.96: Specimen 5.1 Main Autopsy Region and Grout Vents

Table 6.20: Specimen 5.1 Summary of Main Autopsy Region Corrosion Ratings

Component	Maximum	Total	Generalized
Longitudinal Bars	4	24	3.4
Transverse Bars	8	75	5.4
North Duct	10	30	8.6
South Duct	10	110	31
North Strands	39	726	69
South Strands	39	757	72

This specimen received dead end spray exposure during the exposure testing period.

6.2.9.1 Appearance

The surface of Specimen 5.1 had medium scaling on the top surface and on the edges and parts of the ponding area. Small shallow depressions were observed on the sides of the specimen where bleed water was trapped between the concrete and formwork during casting. The backfill mortar live end anchorage pocket was separating from the base concrete. This indicates that the mortar did not adhere well to the base concrete.

The repairs to the cracks from the application of live load on both sides of the live end re-entrant corbel corners were in good repair. No cracks on the dead end re-entrant corbel corners were observed. The ponding area of Specimen 5.1 had 2 large transverse crack that ran from the north to the south side of the specimen and 4 small transverse cracks on the edge of the ponding area (1 on the north side and 2 on the south side that extended to the area of the north tendon) (Figure 6.97). A longitudinal crack was observed in the location of the north tendon and ran the majority of the length of the ponding area. This crack might have formed because the plastic duct and concrete have different thermal coefficients. Therefore, any heating or cooling of the specimen would cause differential shrinkage or expansion between the duct and concrete. The concrete also had decreased cover in this region further exacerbating the cracking. However, this does not explain why no longitudinal cracking was observed over the south tendon. The average crack width was 0.007 inch. The crack rating for Specimen 5.1 was 0.54. See Figure 6.74 for the crack data from Specimen 5.1.

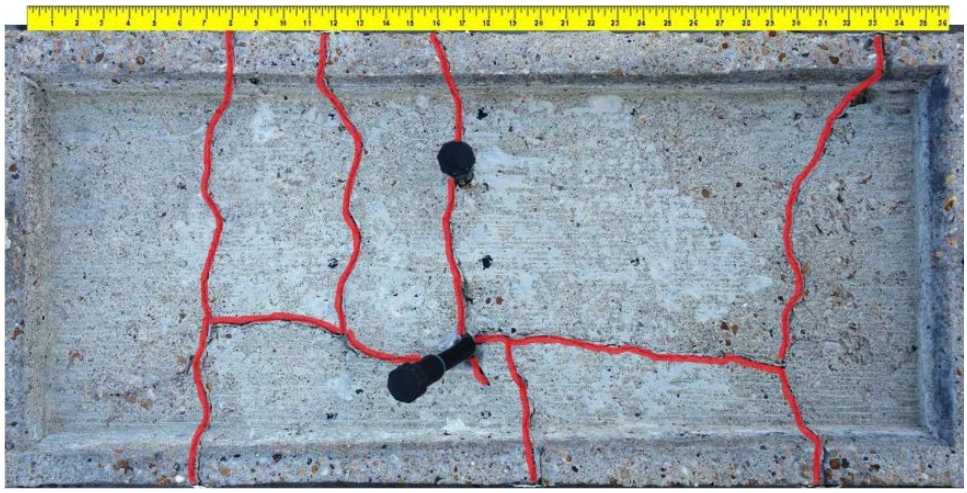

Figure 6.97: Specimen 5.1 Crack Map of Ponding Area

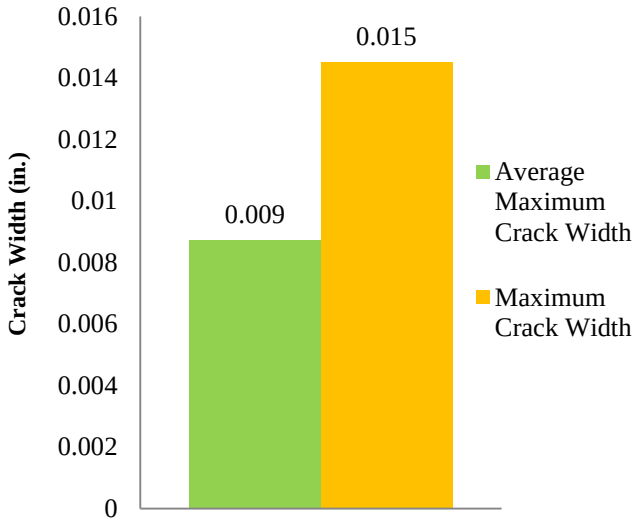

Figure 6.98: Crack Data for Specimen 5.1

6.2.9.2 Longitudinal and Transverse Bars

The north and south longitudinal bars had slight damage from when the bars were extracted from the specimen. Rust stains were also evident at locations where the transverse bars were tied to the longitudinal bars (Figure 6.99). This staining is from corrosion of the tie wire used to attach the transverse reinforcement to the longitudinal bars and NOT from the longitudinal bar itself. Figure 6.103 shows the longitudinal bar's corrosion ratings and Table 6.20 shows the summary of the corrosion ratings for the longitudinal bars.

Figure 6.99: Rust Stain on North Longitudinal Bar from Specimen 5.1

All transverse bars had damage from when they were extracted from the specimen. All the transverse bars had rust staining at least somewhere over the length of the bar from corrosion of the tie wire used to attach the transverse bars to the longitudinal bars and to attach the duct to the transverse bars. Light corrosion was observed on at least one interval on all bars and moderate corrosion observed on at least one interval of bars #2, #4, and #6. Bar #6 had the highest rating of 21. Bar #4 had the next highest rating of 15. Bars #1 and #7 had the lowest ratings of 4 and 7, respectively. Figure 6.103 shows the transverse bar's corrosion ratings and Table 6.20 shows the summary of the corrosion rating for the transverse bars.

6.2.9.3 Duct

The entire outer surface of the north duct had a chalky white residue. No corrosion staining was observed on the outer or inner surface of the duct. The inner bottom surface of the north duct had slight gouges on the successive intervals on the dead end side of midspan. This indicates that one or more of the strands caused damage either when the

strands were being threaded through the duct or one of the strands or stands were rubbing against the duct when the strands were being stressed. In either case, the integrity of the duct was not compromised. Indications of voids were observed on the top inner surface of the duct along the entire length. No damage was observed on the coupler, grout vent, or heat shrink wrap used to seal the coupler/duct interface. However, the heat shrink wrap did not bond well to the coupler or duct. This might indicate why chloride levels were elevated.

The entire outer surface of the south duct had a chalky white residue. The inner bottom surface of the north duct had slight gouges over 50% of the length of the duct. Again, this indicates that one or more of the strands caused damage either when the strands were being threaded through the duct or possibly one of the strands or stands were rubbing against the duct when the strands were being stressed. In either case, the integrity of the duct was not compromised. Indications of voids were observed on the top inner surface of the duct along the entire length. The silicone that was used to seal the grout vent to the south duct was found to have debonded from the duct. It is not known if this happened during extraction or when the concrete was placed. Chloride levels indicate that the latter is the more valid explanation. Figure 6.100 shows the top outer and bottom inner surfaces at midspan of the south duct.

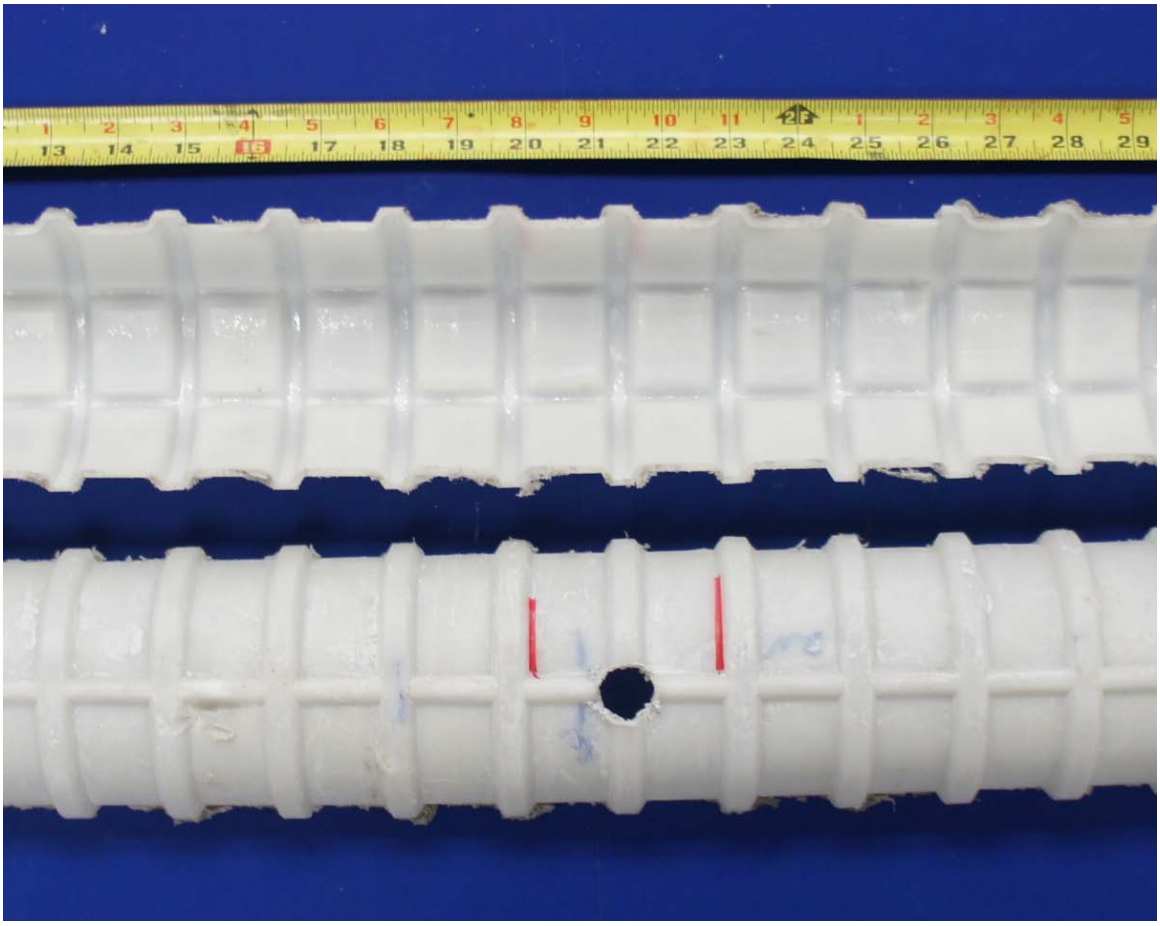

Figure 6.100: Top Outer (Bottom) and Bottom Inner Surfaces at Midspan of the South Duct from Specimen 5.1

Figure 6.103 shows the damage ratings for the ducts and Table 6.20 shows the summary of the damage ratings for the ducts.

6.2.9.4 Grout

No transverse or longitudinal visible cracks were initially observed during examination of grout from the north and south tendons of Specimen 5.1 but when chloride samples were being taken transverse cracks became evident. No staining of the grout was observed on either the north or south grouts. Small voids in the grout were observed in the flutes along the entire length of the top of both the north and south tendons. The small voids measured approximately 1.5 inch long and were as wide as the

flute width. The coloration of the grout from the north tendon was dark grey at the ends and transitioned to light grey at midspan. A silver crystalline powder was observed on the grout on the bottom of the entire length of the south tendon (Figure 6.101).

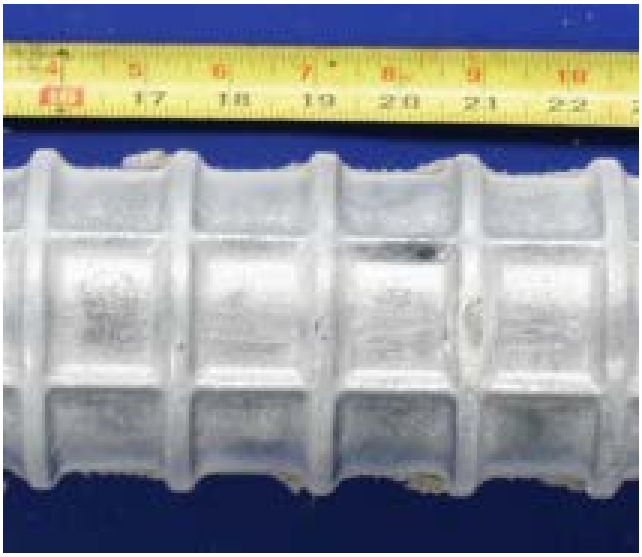

Figure 6.101: Silver Crystalline Powder on Bottom of South Tendon from Specimen 5.1

The chloride concentrations were discussed in depth in Chapter 5. All the chloride concentrations were well above the 0.033% by weight of grout limit for corrosion. See Figure 5.13 for the results of the chloride concentration testing. As expected, the highest chloride concentration for the north and south tendons were at midspan and were 0.880% and 0.940%, respectively, by weight of grout. As expected, the anchorage regions had the lowest chloride concentrations. This might be because the chlorides would take longer to migrate to the anchorages because the chloride ions would have to travel through the interstitial space between the grout and duct and/or interstitial space between the grout and strand.

6.2.9.5 Strand

The three strands in the north tendon had only minor damage. Light corrosion was observed on the majority of the outer and inner wire intervals (Figure 6.102). This is an

indication that moisture, oxygen, and chlorides had reached the strands and corresponds to the chloride concentrations discussed in Chapter 5. The live end had the lowest ratings with an average of 32. The highest rating of 39 was at approximately 32 inches from the dead end.

Figure 6.102: Light Corrosion on a North Strand from Specimen 5.1

The corrosion observed on the south strands was similar to the damage that was observed on the north strands. The outer and inner wires of the strands had light corrosion on the majority of their intervals. Again, this is an indication that moisture, oxygen, and chlorides had reached the strands and corresponds with the chloride concentrations discussed in Chapter 5. Two intervals had the highest corrosion rating of 39, one at 14 inches from the dead end and one at 22 inches from the dead end. The live end had the lowest corrosion ratings with an average of 32.

Figure 6.103 shows the corrosion ratings for the strands and Table 6.20 shows the summary of the corrosion ratings for the strands.

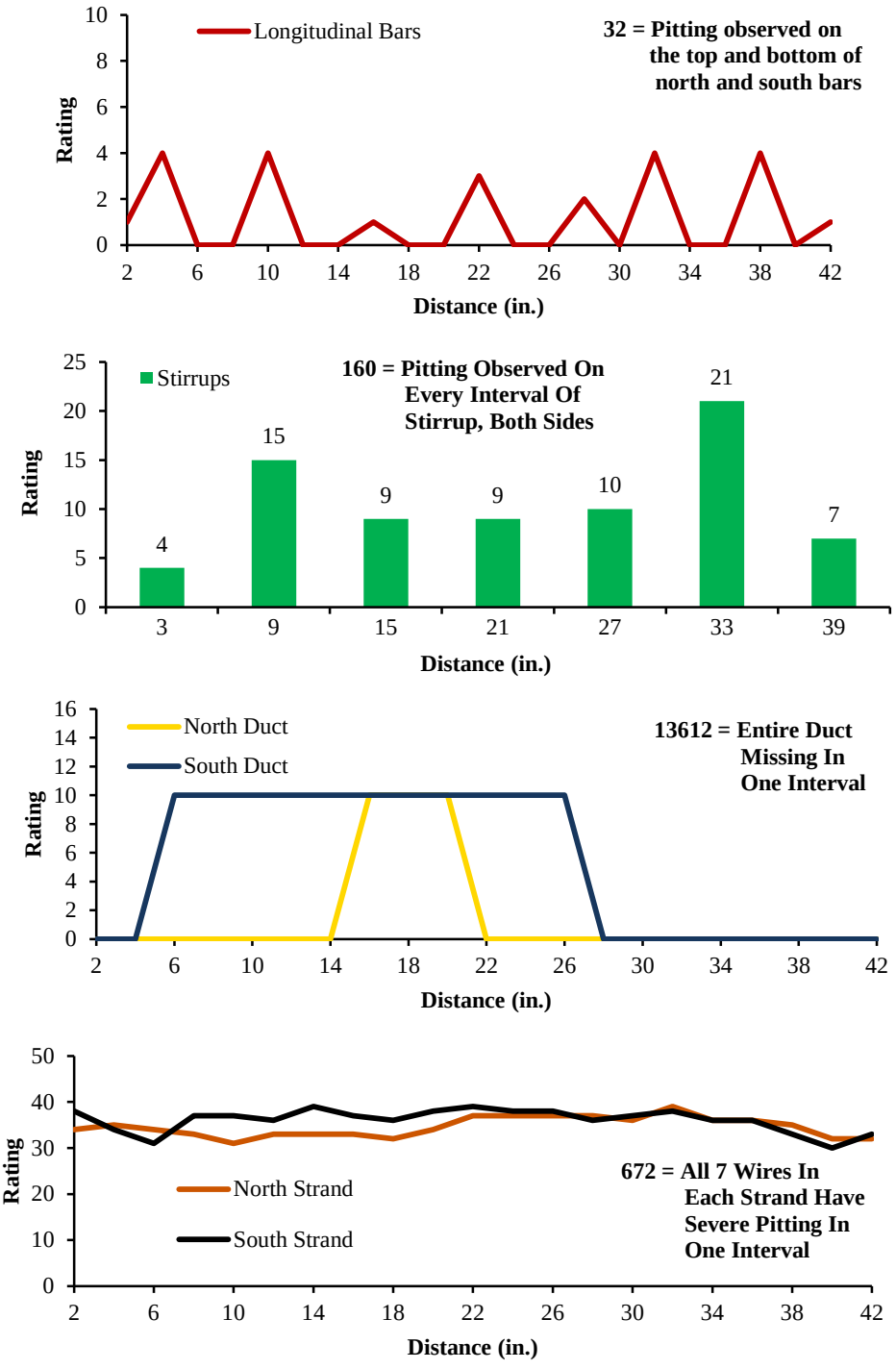

Figure 6.103: Corrosion Rating Plots for Main Autopsy Region of Specimen 5.1

6.2.9.6 Dead and Live End Anchorages

The majority of the epoxy applied to the anchorage from the dead end before the anchorage cavity was backfilled had debonded from the anchorage components of both tendons. The exposed faces of the north and south anchorage plates from the dead end had no visible corrosion. Moderate corrosion was observed on the bottom of the embedded portion of the north and south anchorage plates. This corrosion was located where the duct tape was used to seal the duct to the north and south anchorage plates and on the bottom of the north anchorage plate. The exposed faces of the north anchor head from the dead end had spots of light surface corrosion. The exposed face of the south anchor head from the dead end had no visible signs of corrosion. The sides of the north and south anchor heads from the dead end had light surface corrosion at the interface of the anchor head and anchorage plate. The unexposed face of the north and south dead end anchor heads had light surface corrosion.

The majority of the epoxy applied to the anchorage heads from the live end before the anchorage cavity was backfilled had debonded from the anchorage components of both tendons. Most of the epoxy applied to the exposed surface of the anchorage plates from the live end before the anchorage cavity was backfilled had been still bonded to the surface. The exposed faces of the north and south anchorage plates from the live end had light surface corrosion in the locations were the epoxy had debonded (Figure 6.104). The embedded portion of the north anchorage plate from the live end had moderate corrosion where duct tape was used to seal the duct to the anchorage plate. The embedded portion of the south anchorage from the live end had no visible signs of corrosion. The exposed faces of the north and south anchor heads from the dead end had no visible signs of corrosion. The sides of the south anchor head from the live end had light surface corrosion at the interface of the anchor head and anchorage plate. The sides of the north anchor head had no visible signs of corrosion. The unexposed face of the north and south live end anchor heads had light surface corrosion.

Figure 6.104: Light Surface Corrosion where Epoxy had Debonded from Exposed Face of North Live End Anchorage Plate from Specimen 5.1

Table 6.21: Specimen 5.1 Summary of Dead and Live End Anchorage Region Corrosion Ratings

	Dead End Anchorage			Live End Anchorage		
Component	Maximum	Total	Generalized	Maximum	Total	Generalized
North Duct	10	30	60	10	30	60
South Duct	10	30	60	10	30	60
North Strands	34	187	53	50	214	61
South Strands	32	156	45	29	180	51

The north and south ducts from the dead end had slight gouging along their entire length. This indicates that one or more of the strands caused damage either when the strands were being threaded through the duct or one of the strands or stands were rubbing against the duct when the strands were being stressed. There was no staining on either duct. There were indications of voids in the grout of the north and south tendon along the length of the top of the duct in the dead end anchorage region from the flutes of the duct.

The north and south ducts from the live end had slight gouging along their entire length. This indicates that one or more of the strands caused damage either when the strands were being threaded through the duct or one of the strands or stands were rubbing against the duct when the strands were being stressed. In either case, the integrity of the duct was not compromised. There was no staining on either duct. There were indications of voids in the grout of the north and south tendon along the length of the top of the duct in the live end anchorage region from the flutes of the duct.

Figure 6.105 shows the damage ratings for the dead and live anchorage region ducts and Table 6.21 shows the summary of the damage ratings for the dead and live anchorage region ducts.

The grout from the north and south dead end tendons had no visible transverse or longitudinal cracks. The grout from both tendons from the dead end had voids and signs of "bubbling" in the area of the flutes of the ducts along the length of the top surface. The segregation was observed in the grout from the north south dead end tendons.

The grout from the north and south live end tendons had no visible transverse or longitudinal cracks. The grout from both tendons from the live end had voids and signs of "bubbling" in the area of the flutes of the ducts along the length of the top surface. The same silver crystalline powder found on the grout of the south tendon was evident on the grout from the live end of the south tendon.

The outer wires of the strands from the north and south, dead and live end anchorage regions had discoloration over most of their intervals. The intervals without discoloration had light corrosion. The inner wires of the strands from the north and south dead and live end anchorage region had light corrosion on the majority of their intervals and discoloration on the rest. The wedges from both anchorage regions and both tendons were intact and had light surface corrosion on their outer surface. Figure 6.105 shows the corrosion ratings for the dead and live anchorage region strands and Table 6.21 shows the summary of the corrosion ratings for the dead and live anchorage region strands.

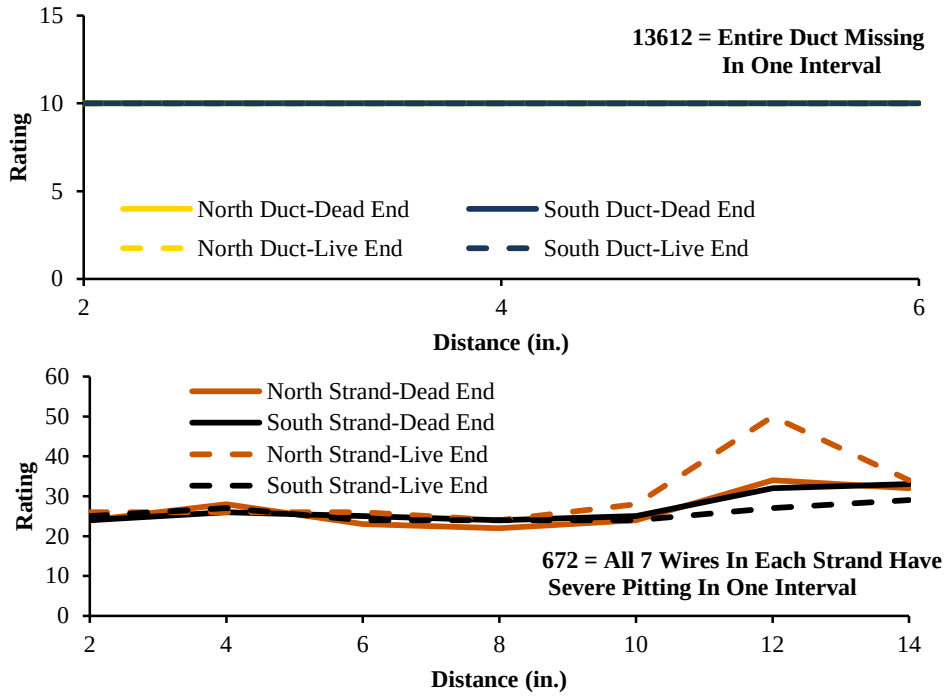

Figure 6.105: Corrosion Rating Plots for Dead and Live End Anchorage Regions of Specimen 5.1

The anchorage components from the live and dead ends had experienced similar damage. So, it can be assumed that the dead end anchorage spray did not make a difference when it came to the damage that was observed. The chloride concentrations further confirm this because the chloride concentrations of the dead end region were below the chloride corrosion limit.

6.2.10 Specimen 5.2: Non-galvanized, Stainless Clad Strand, Two-way Plastic Duct

Figure 6.106: Specimen 5.2 Main Autopsy Region and Grout Vents

Table 6.22: Specimen 5.2 Summary of Main Autopsy Region Corrosion Ratings

Component	Maximum	Total	Generalized
Longitudinal Bars	2	4	0.6
Transverse Bars	5	41	2.9
North Duct	20	220	66
South Duct	10	190	57
North Strands	3	11	1.1
South Strands	4	13	1.3

This specimen received dead end spray exposure during the exposure testing period.

6.2.10.1 Appearance

The surface of Specimen 5.2 had medium scaling on the top surface and on the edges and parts of the ponding area. The ponding area had moderate scaling only on portions of its surface. No cracks were observed at the interface of the backfill mortar and base concrete on either the dead or live end.

The repairs to the cracks from the application of live load on both sides of the live end re-entrant corbel corners were in good repair. No cracks on the dead end re-entrant corbel corners were observed. The ponding area of Specimen 5.2 had 1 large transverse crack that ran from the south side of the specimen to the longitudinal crack over the north tendon and 5 small transverse cracks on the edge of the ponding area (2 on the south side, 2 on the north side and one located at approximately the transverse centerline and on the dead end side of midspan) (Figure 6.107). A longitudinal crack was observed along the location of the north tendon. This crack might have formed because the plastic duct and concrete have different thermal coefficients. Therefore any heating or cooling of the specimen would cause differential shrinkage or expansion between the duct and concrete. The concrete also had decreased cover in this region further exacerbating the cracking. However, this does not explain why the no longitudinal cracking was observed over the south tendon. The average crack width was 0.005 inch. The crack rating for Specimen 5.2 was 0.19. See Figure 6.108 for the crack data from Specimen 5.2.

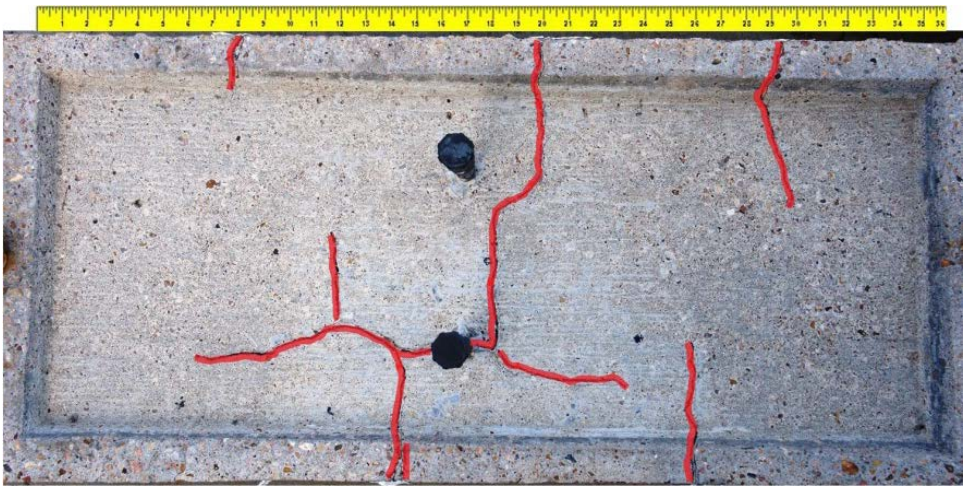

Figure 6.107: Specimen 5.2 Crack Map of Ponding Area

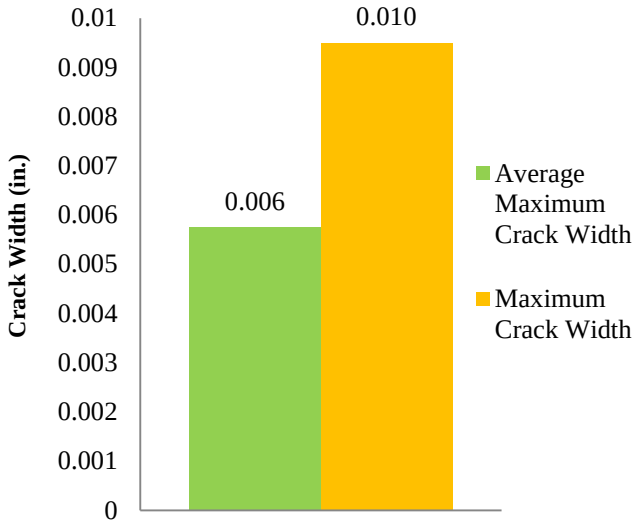

Figure 6.108: Crack Data for Specimen 5.2

6.2.10.2 Longitudinal and Transverse Bars

The north and south longitudinal bars had slight damage from when the bars were extracted from the specimen. No rust stains were evident on either the north or south longitudinal bars. However, light corrosion was observed at approximately midspan of both the north and south longitudinal bars. Figure 6.113 shows the longitudinal bar's

corrosion ratings and Table 6.22 shows the summary of the corrosion ratings for the longitudinal bars.

All transverse bars had damage from when they were extracted from the specimen. All the transverse bars had rust staining at least somewhere over the length of the bar from corrosion of the tie wire used to attach the transverse bars to the longitudinal bars and to attach the duct to the transverse bars. Light corrosion was observed on bars #5 and #6. Moderate corrosion observed on bars #4 and #6 (Figure 6.109). Bar #6 had the highest rating of 17. Bars #1 and #7 had the lowest ratings of 1. This was expected because both of these bars are outside the ponding area with no observed cracks and increased concrete cover. Therefore, no moisture, oxygen, and chlorides would easily reach the bars. Figure 6.113 shows the transverse bar's corrosion ratings and Table 6.22 shows the summary of the corrosion rating for the transverse bars.

Figure 6.109: Moderate Corrosion on Transverse Bar #6 from Specimen 5.2

6.2.10.3 Duct

The entire outer surface of the north duct had a chalky white residue (Figure 6.110). No corrosion staining was observed on the outer or inner surface of the duct. The inner top and bottom surface of the north duct had slight gouges from midspan to the live end of the duct. This indicates that one or more of the strands caused damage either when the

strands were being threaded through the duct or one of the strands or stands were rubbing against the duct when the strands were being stressed. In either case, the integrity of the duct was not compromised. Indications of voids were observed on the top inner surface of the duct along the entire length. No damage was observed on the coupler, grout vent, or heat shrink wrap used to seal the coupler/duct interface. However, the heat shrink wrap did not bond well to the coupler or duct. This might indicate why chloride levels were elevated.

Figure 6.110: Chalky White Residue on North Duct of Specimen 5.2

The entire outer surface of the south duct had a chalky white residue. The inner bottom surface of the north duct had slight gouges over the entire length of the duct. Again, this indicates that one or more of the strands caused damage either when the strands were being threaded through the duct or possible one of the strands or stands were rubbing against the duct when the strands were being stressed. In either case, the integrity of the duct was not compromised. Indications of voids were observed on the top inner surface of the duct along the entire length. The silicone that was used to seal the grout vent to the south duct was found to have debonded from the duct. It is not known if

this happened during extraction or when the concrete was placed. Chloride levels indicate that the latter is the more valid explanation.

Figure 6.113 shows the damage ratings for the ducts and Table 6.22 shows the summary of the damage ratings for the ducts.

6.2.10.4 Grout

No transverse or longitudinal visible cracks were observed during examination of grout from the north and south grouts of Specimen 5.1 but when chloride samples were being taken transverse cracks became evident. No staining of the grout was observed on either the north or south grouts. Small voids in the grout were observed in the flutes along the entire length of the top of the north tendon. The south grout had small voids in the grout on the dead end side of the grout and a large void that ran almost the whole length of the grout's live end side (Figure 6.111). The small voids measured approximately 1.5 inch long and were as wide as the flute width. The coloration of the grout from the north tendon was dark grey at the ends and transitioned to light grey at midspan. A silver crystalline powder was observed on the grout bottom that ran from the dead end quarter point to the live end of the south tendon.

Figure 6.111: Large Void in Grout on Top Live End Side of South Tendon from Specimen 5.2

The chloride concentrations were discussed in depth in Chapter 5. All the chloride concentrations were well above the 0.033% by weight of grout limit for corrosion. See Figure 5.14 for the results of the chloride concentration testing. As expected, the highest

chloride concentration for the north and south tendons were at midspan and were 0.220% and 0.330%, respectively, by weight of grout. As expected, the anchorage regions had the lowest chloride concentrations. This might be because the chlorides would take longer to migrate to the anchorages because the chloride ions would have to travel through the interstitial space between the grout and duct and/or interstitial space between the grout and strand.

6.2.10.5 Strand

As expected, the stainless clad strands of the north and south tendons were essentially defect free. Minimal discoloration was observed on the outer wires of 5 of the 6 strands. The inner wires from the north and south tendons had minimal discoloration as well. Figure 6.112 shows inner and outer wires from a north tendon strand. Figure 6.113 shows the corrosion ratings for the strands and Table 6.22 shows the summary of the corrosion ratings for the strands.

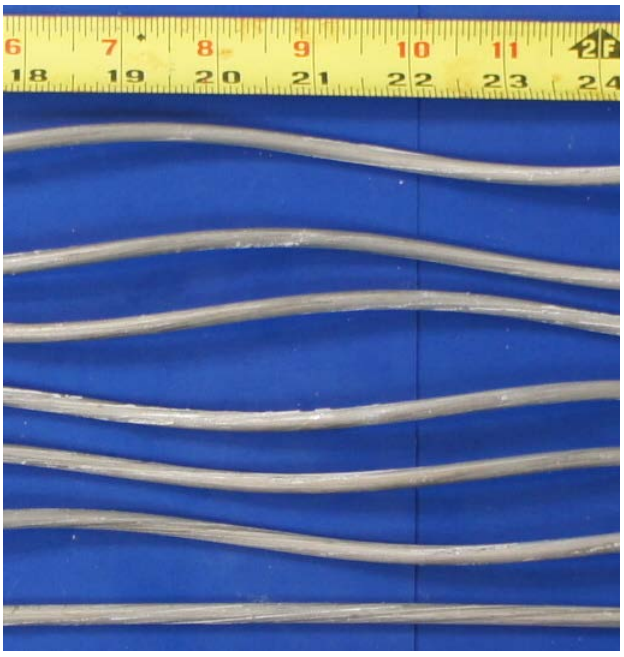

Figure 6.112: Inner and Outer Wires from a North Tendon Strand from Specimen 5.2

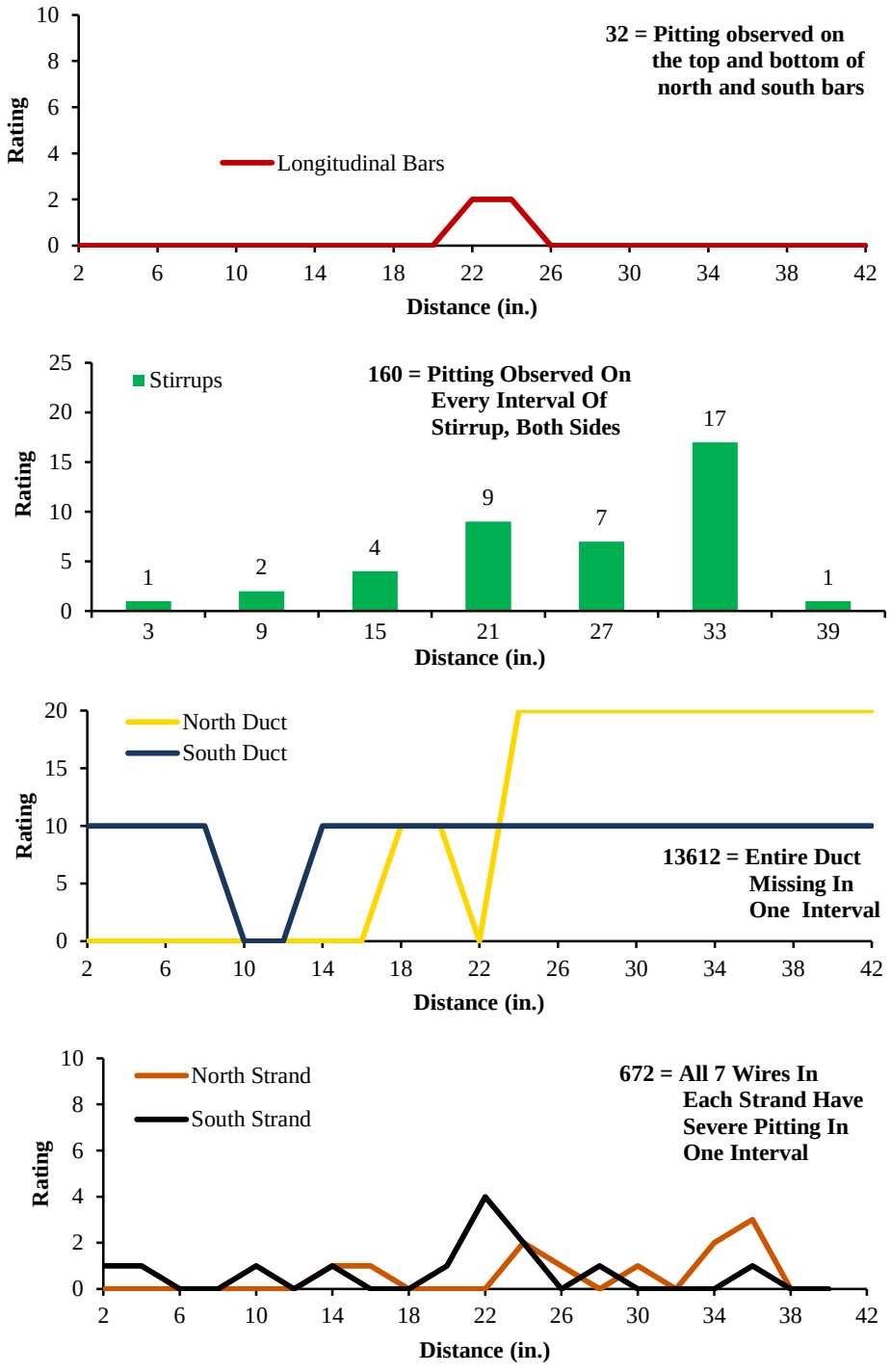

Figure 6.113: Corrosion Rating Plots for Main Autopsy Region of Specimen 5.2

6.2.10.6 Dead and Live End Anchorages

The majority of the epoxy applied to the anchorage from the dead end before the anchorage cavity was backfilled had debonded from the anchorage components of both tendons. The exposed faces of the north and south anchorage plates from the dead end had visible light corrosion in areas where the epoxy had debonded. Light corrosion was observed on the bottom of the embedded portion of the north and south anchorage plates. This corrosion was located in the area away from where the duct was sealed to the anchorage plate and also where the duct was sealed to the anchorage plate (Figure 6.114). The exposed faces of the north and south anchor heads from the dead end had spots of light surface corrosion. The sides of the north and south anchor heads from the dead end had light surface corrosion on the majority of the surface. The unexposed face of the north and south dead end anchor heads had light surface corrosion in a ring outside of where the grout came into contact with the anchor head.

Figure 6.114: Light Corrosion on the Embedded Portion of the North Dead Anchorage Plate from Specimen 5.2

The majority of the epoxy applied to the anchorage heads from the live end before the anchorage cavity was backfilled had debonded from the anchorage components of both tendons. Most of the epoxy applied to the exposed surface of the anchorage plates from the live end before the anchorage cavity was backfilled was still bonded to the surface. The exposed faces of the north and south anchorage plates from the live end had light surface corrosion in a few spots where the epoxy had debonded. The embedded

portion of the north anchorage plate from the live end had light corrosion on the bottom outside the area where the duct connected to the anchorage plate. This corrosion was located in the area away from where the duct connected to the anchorage plate and where the duct connected to the anchorage plate. The embedded portion of the south anchorage from the live end had light corrosion on the bottom outside the area where the duct connected to the anchorage plate and moderate corrosion where the duct connected to the anchorage plate. The exposed faces of the north anchor head from the live end had small spots of light corrosion. The exposed faces of the south anchor head from the live end had light corrosion over the entire face. The sides of the north and south anchor heads from the dead end had light surface corrosion on the majority of the surface. The unexposed face of the north and south live end anchor heads had light surface corrosion in a ring outside of where the grout came into contact with the anchor head.

Table 6.23: Specimen 5.2 Summary of Dead and Live End Anchorage Region Corrosion Ratings

	Dead End Anchorage			**Live End Anchorage**		
Component	Maximum	Total	Generalized	Maximum	Total	Generalized
North Duct	10	10	20	20	30	60
South Duct	0	0	0	40	70	140
North Strands	7	21	6	6	19	5.4
South Strands	3	7	2	8	26	7.4

The north and south ducts from the dead end had slight gouging on one interval. This indicates that one or more of the strands caused damage either when the strands were being threaded through the duct or one of the strands or stands were rubbing against the duct when the strands were being stressed. There was no staining on either duct. There were indications of voids in the grout of the north and south tendon along the length of the top of the duct in the dead end anchorage region from the flutes of the duct.

The north and south ducts from the live end had no gouging. There was no staining on either duct. There were indications of voids in the grout of the north and south tendon

along the length of the top of the duct in the live end anchorage region from the flutes of the duct.

Figure 6.115 shows the damage ratings for the dead and live anchorage region ducts and Table 6.23 shows the summary of the damage ratings for the dead and live anchorage region ducts.

The grout from the north and south dead end tendons had no visible transverse or longitudinal cracks. The grout from both tendons from the dead end had voids and signs of “bubbling” in the area of the flutes of the ducts along the length of the top surface. The segregation was observed in the grout from the north and south dead end tendons.

The grout from the north and south live end tendons had no visible transverse or longitudinal cracks. The grout from both tendons from the live end had voids and signs of “bubbling” in the area of the flutes of the ducts along the length of the top surface. The same silver crystalline powder found on the grout of the south tendon section from the main autopsy region was evident on the grout from the live end of the south tendon.

As expected, the outer and inner wires of the strands from the north and south, dead and live end anchorage regions had discoloration on a few intervals. The wedges from both anchorage regions and both tendons were intact and had light surface corrosion on their outer surface. Figure 6.115 shows the corrosion ratings for the dead and live anchorage region strands and Table 6.23 shows the summary of the corrosion ratings for the dead and live anchorage region strands.

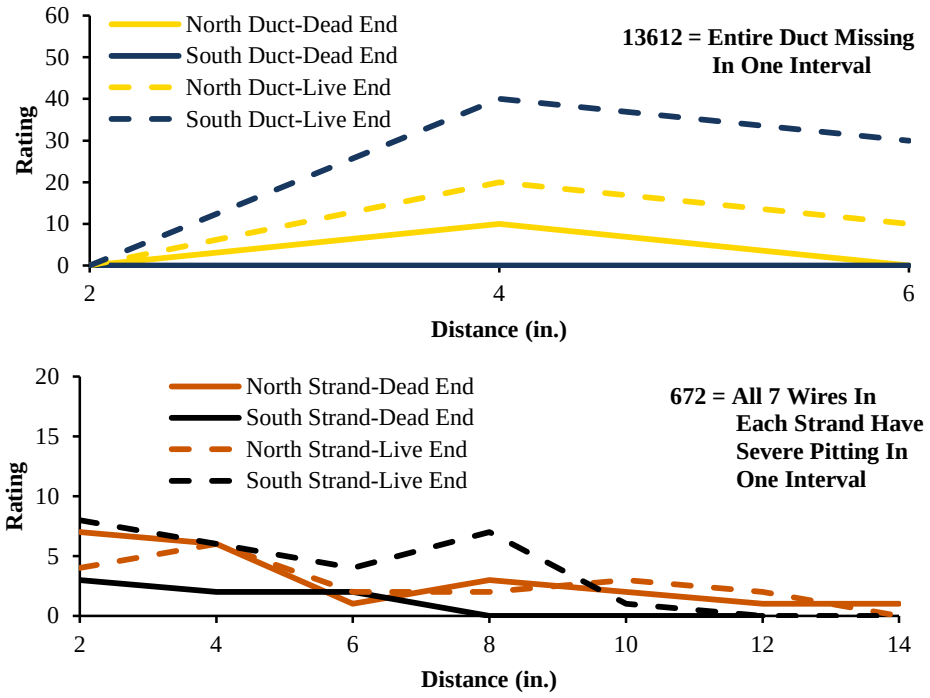

Figure 6.115: Corrosion Rating Plots for Dead and Live End Anchorage Regions of Specimen 5.2

The anchorage components from the live and dead ends had experienced similar damage. So, it can be assumed that the dead end anchorage spray did not make a difference when it came to the damage that was observed. The chloride concentrations further confirm this because the chloride contents of the dead end region were below the chloride corrosion limit.

6.2.11 Specimen 5.3: Non-galvanized Anchorage, Stainless Steel Strand, Two-way Plastic Duct

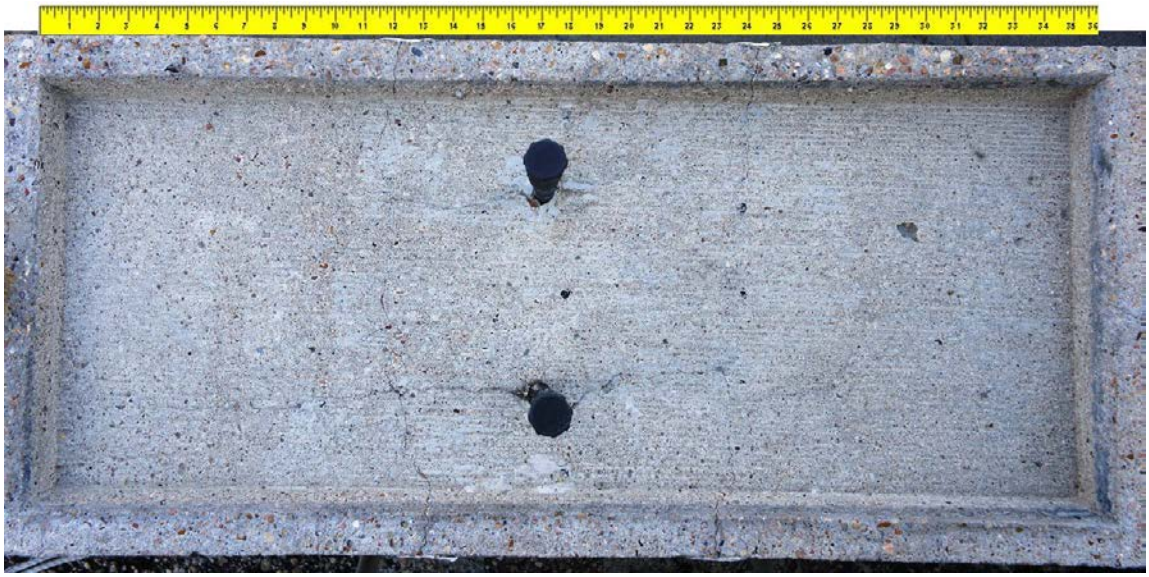

Figure 6.116: Specimen 5.3 Main Autopsy Region and Grout Vents

Table 6.24: Specimen 5.3 Summary of Main Autopsy Region Corrosion Ratings

Component	Maximum	Total	Generalized
Longitudinal Bars	2	9	1.3
Transverse Bars	8	82	5.9
North Duct	40	430	123
South Duct	10	50	14
North Strands	2	5	0.5
South Strands	1	2	0.2

This specimen received dead end spray exposure during the exposure testing period.

6.2.11.1 Appearance

The surface of Specimen 5.3 had medium scaling on the top surface and on the edges of the ponding area. The ponding area was in good repair with only minimal scaling observed (Figure 6.116). There was one medium sized shallow depression

located on the north dead end side of the ponding area where bleed water was trapped between the concrete and formwork during casting. No cracks were observed at the interface of the backfill mortar and base concrete on either the dead or live end.

The repairs to the cracks from the application of live load on both sides of the live and dead end re-entrant corbel corners were in good repair. The ponding area of Specimen 5.3 had 1 large transverse crack that ran from the south side of the specimen to the longitudinal crack over the north tendon and 2 small transverse cracks (one on the south side that ran from the south edge of the ponding area to the location of the south tendon and one that ran from the north edge of the ponding to the location of the north tendon) (Figure 6.117). A longitudinal crack was observed above the location of the north tendon that ran from the dead end side of the ponding area to approximately the live end quarter point (Figure 6.117). This crack might have formed because the plastic duct and concrete have different thermal coefficients therefore any heating or cooling of the specimen would cause differential shrinkage or expansion between the duct and concrete. The concrete also had decreased cover in this region further exacerbating the cracking. However, this does not explain why the no longitudinal cracking was observed over the south tendon. The average crack width was 0.004 inch. The crack rating for Specimen 5.3 was 0.21. See Figure 6.118 for the crack data from Specimen 5.3.

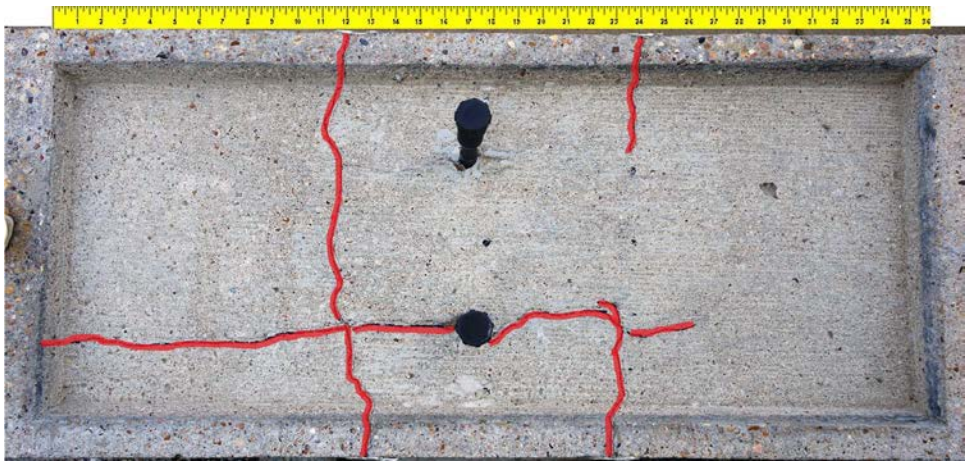

Figure 6.117: Specimen 5.3 Crack Map of Ponding Area

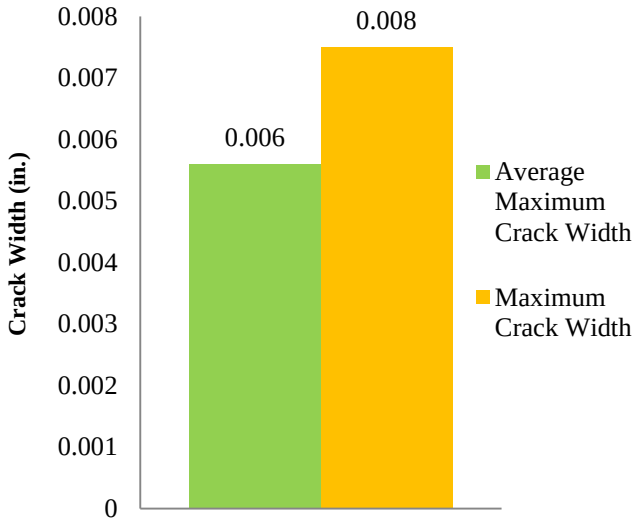

Figure 6.118: Crack Data for Specimen 5.3

6.2.11.2 Longitudinal and Transverse Bars

The north and south longitudinal bars had slight damage from when the bars were extracted from the specimen. Rust stains were also evident at locations where the transverse bars were tied to the longitudinal bars. This staining is from corrosion of the tie wire used to attach the transverse reinforcement to the longitudinal bars and NOT from the longitudinal bar itself. Figure 6.124 shows the longitudinal bar's corrosion ratings and Table 6.24 shows the summary of the corrosion ratings for the longitudinal bars.

All transverse bars had damage from when they were extracted from the specimen. All the transverse bars had rust staining at least somewhere over the length of the bar from corrosion of the tie wire used to attach the transverse bars to the longitudinal bars and to attach the duct to the transverse bars. Light corrosion was observed on at least one interval on all bars and moderate corrosion observed on at least one interval of bars #3 and #4 (Figure 6.119). Bar #3 had the highest rating of 30. Bar #4 had the next highest rating of 17. Bar #7 had the lowest ratings of 4. Figure 6.124 shows the transverse bar's corrosion ratings and Table 6.24 shows the summary of the corrosion rating for the transverse bars.

Figure 6.119: Moderate Corrosion at South Side Corner of Transverse Bar #4 from Specimen 5.3

6.2.11.3 Duct

The entire outer surface of the north duct had a chalky white residue. No corrosion staining was observed on the outer or inner surface of the duct. The inner top surface of the north duct had moderate gouges on the successive intervals on the live end side of midspan. This indicates that one or more of the strands caused damage when the strands were being threaded through the duct because of the curved shape of the stainless steel strand. The bottom inner surface of the north duct had slight gouges starting at the dead end and going to over ¾ of its length and moderate gouges the rest of the length of the bottom inner surface of the duct. This indicates that one or more of the strands caused damage either when the strands were being threaded through the duct or one of the strands or stands were rubbing against the duct when the strands were being stressed. In either case, the integrity of the duct was not compromised. Indications of voids were observed on the top inner surface of the duct along the entire length. No damage was observed on the coupler, grout vent, or heat shrink wrap used to seal the coupler/duct interface. However, the heat shrink wrap did not bond well to the coupler or duct. This

might indicate why chloride levels were elevated. Figure 6.120 shows top outer surface at midspan of the north duct from Specimen 5.3.

Figure 6.120: Top Outer Surface at Midspan of North Duct from Specimen 5.3

The entire outer surface of the south duct had a chalky white residue. The inner bottom surface of the north duct had slight gouges over a few intervals of the duct. Again, this indicates that one or more of the strands caused damage either when the strands were being threaded through the duct or possible one of the strands or stands were rubbing against the duct when the strands were being stressed. In either case, the integrity of the duct was not compromised. Indications of voids were observed on the top inner surface of the duct along the entire length. The silicone that was used to seal the grout vent to the south duct was found to have debonded from the duct. It is not known if this happened during extraction or when the concrete was placed. Chloride levels indicate that the latter is the more valid explanation.

Figure 6.124 shows the damage ratings for the ducts and Table 6.24 shows the summary of the damage ratings for the ducts.

6.2.11.4 Grout

No cracking in the grout could be observed in either tendon because the grout fell apart when the ducts were removed from the tendon due to the curved nature of the

strands (Figure 6.121). Small voids in the grout were observed in the flutes along the entire length of the top of both the north and south tendons. The small voids measured approximately 1.5 inch long and were as wide as the flute width.

Figure 6.121: Grout Falling Apart from North Tendon of Specimen 5.3

The chloride concentrations were discussed in depth in Chapter 5. All the chloride concentrations were well above the 0.033% by weight of grout limit for corrosion. See Figure 5.14 for the results of the chloride concentration testing. As expected, the highest chloride concentration for the north and south tendons were at midspan and were 0.280% and 0.380%, respectively, by weight of grout. As expected, the anchorage regions had the lowest chloride concentrations. This might be because the chlorides would take longer to migrate to the anchorages because the chloride ions would have to travel through the interstitial space between the grout and duct and/or interstitial space between the grout and strand.

6.2.11.5 Strand

The three strands in the north and south tendons had no visible corrosion. Only two outer wires from the strands from the north and south tendons had one interval with slight discoloration and one inner wire from the one of the strands in the south tendon had slight discoloration on one interval. This outcome was expected because of the excellent corrosion resistance properties of stainless steel. Figure 6.122 shows the inner and outer wires of a stainless steel strand from Specimen 5.3. The grout did not adhere well to the strands. Because the grout did not adhere well to the strands, when the tendons were cut the strands retracted into the grout (Figure 6.123). The strands had a highly curved shape (Figure 6.78). Figure 6.124 shows the corrosion ratings for the strands and Table 6.24 shows the summary of the corrosion ratings for the strands.

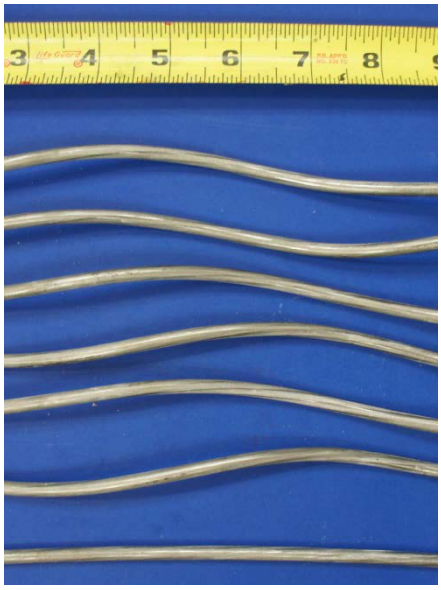

Figure 6.122: Inner and Outer Wires of a Strand from Specimen 5.3

Figure 6.123: Retracted Strands from Specimen 5.3

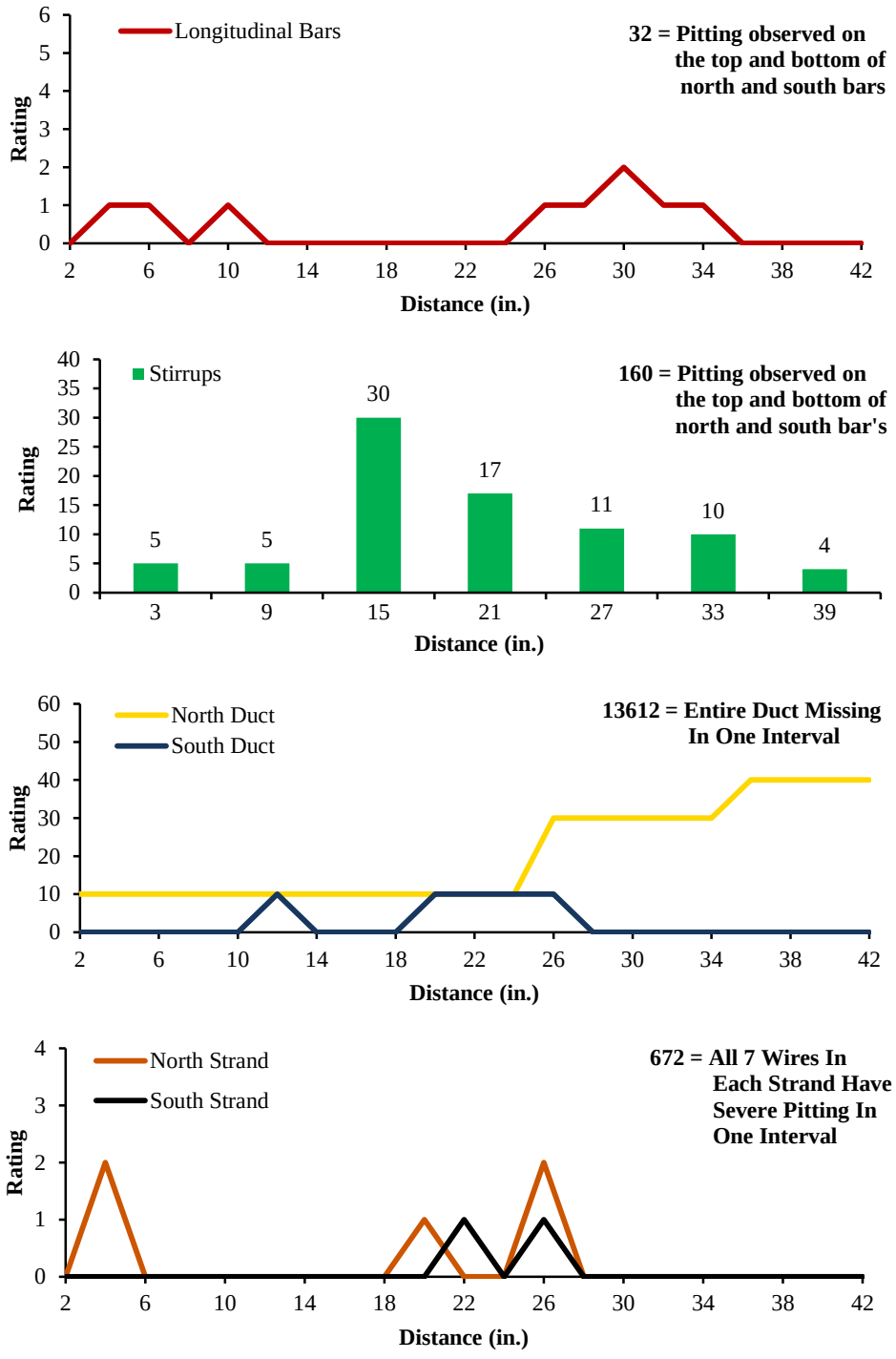

Figure 6.124: Corrosion Rating Plots for Main Autopsy Region of Specimen 5.3

6.2.11.6 Dead and Live End Anchorages

The majority of the epoxy applied to the anchorage components from the dead end before the anchorage cavity was backfilled had debonded from the anchorage components of both tendons. The exposed faces of the north and south anchorage plates from the dead end had visible light corrosion in areas where the epoxy had debonded. Light corrosion was observed on the bottom and top of the embedded portion of the north and south anchorage plates. This light corrosion was observed on the entire surface in the area away from the area where the duct was sealed to the anchorage plate and on the bottom surface where the duct was sealed with duct tape to the anchorage plate. The exposed faces of the north and south anchor heads from the dead end had spots of light surface corrosion. The sides of the north and south anchor heads from the dead end had light surface corrosion on the majority of the surface. The unexposed face of the north and south dead end anchor heads had light surface corrosion in a ring outside of where the grout came into contact with the anchor head.

The majority of the epoxy applied to the anchorage heads from the live end before the anchorage cavity was backfilled had debonded from the anchorage components of both tendons. Most of the epoxy applied to the exposed surface of the anchorage plates from the live end before the anchorage cavity was backfilled was still bonded to the surface (Figure 6.125). The exposed faces of the north and south anchorage plates from the live end had light surface corrosion in a few spots where the epoxy had debonded. The embedded portion of the north anchorage plate from the live end had light corrosion on the bottom outside the area where the duct was sealed to the anchorage plate and where the duct was sealed to the anchorage plate with duct tape. The embedded portion of the south anchorage from the live end had light corrosion on the bottom outside the area where the duct was sealed to the anchorage plate and moderate corrosion where the duct was sealed to the anchorage plate with duct tape. The exposed faces of the north and south anchor heads from the live end had small spots of light corrosion. The sides of the north and south anchor heads from the dead end had light surface corrosion on the majority of the surface. The unexposed face of the north and south live end anchor heads

had light surface corrosion in a ring outside of where the grout came into contact with the anchor head.

Figure 6.125: Exposed Faces of Live End South Anchorage Plate and Anchor Head from Specimen 5.3

Table 6.25: Specimen 5.3 Summary of Dead and Live End Anchorage Region Corrosion Ratings

	Dead End Anchorage			Live End Anchorage		
Component	Maximum	Total	Generalized	Maximum	Total	Generalized
North Duct	10	10	20	10	10	20
South Duct	0	0	0	0	0	0
North Strands	4	6	2	4	8	11
South Strands	3	4	1.3	7	11	3.1

The bottom inside surface of the north duct from the dead end had slight gouging on one interval. This indicates that one or more of the strands caused damage either when the strands were being threaded through the duct or one of the strands or stands

were rubbing against the duct when the strands were being stressed. There was no staining on either duct. There were indications of voids in the grout of the north and south tendon along the length of the top of the duct in the dead end anchorage region from the flutes of the duct.

The bottom inside surface of the north duct from the live end had slight gouging on one interval. There was no staining on either duct. There were indications of voids in the grout of the north and south tendon along the length of the top of the duct in the live end anchorage region from the flutes of the duct.

Figure 6.126 shows the damage ratings for the dead and live anchorage region ducts and Table 6.25 shows the summary of the damage ratings for the dead and live anchorage region ducts.

It could not be determined if the grout from either the north or south duct from either the dead or live end anchorages had transverse or longitudinal cracks because the grout fell apart when the grout was removed from the duct due to the curved nature of the stainless steel strands. The grout from all the tendons in the anchorage regions had voids and signs of “bubbling” in the area of the flutes of the ducts along the length of the top surface. It could not be determined if the grout had segregated because the grout fell apart.

As expected, the outer and inner wires of the strands from the north and south, dead and live end anchorage regions had discoloration on a few intervals. Most of the discoloration was in the region of the wedges. This discoloration might be from heat of the torch when the strands were extracted. The wedges from both anchorage regions and both tendons were intact and had light surface corrosion on their outer surface. Figure 6.126 shows the corrosion ratings for the dead and live anchorage region strands and Table 6.25 shows the summary of the corrosion ratings for the dead and live anchorage region strands.

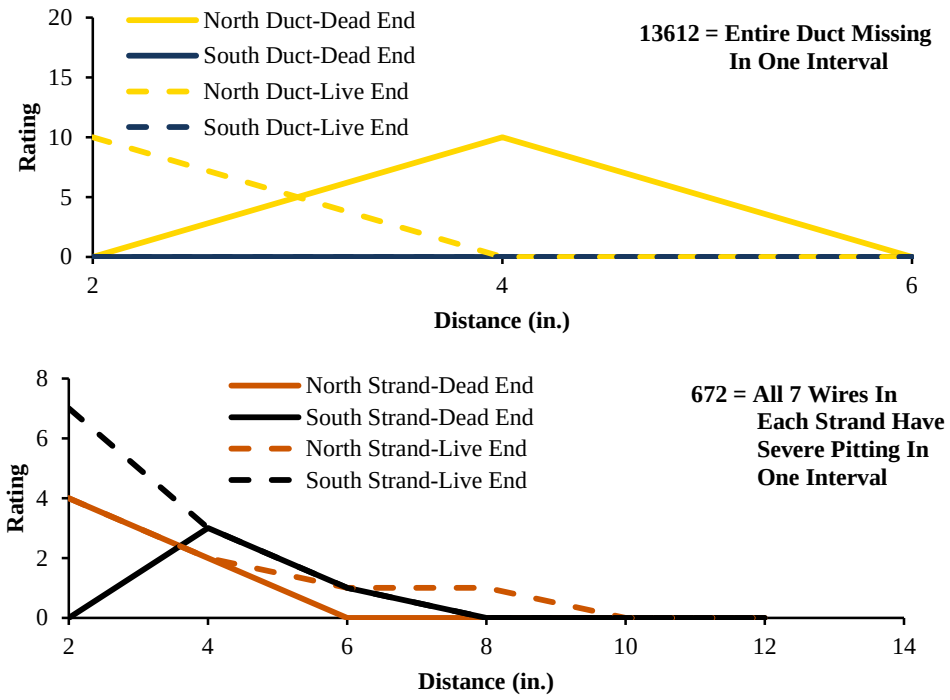

Figure 6.126: Corrosion Rating Plots for Dead and Live End Anchorage Regions of Specimen 5.3

The anchorage components from the live and dead ends had experienced similar damage. So, it can be assumed that the dead end anchorage spray did not make a difference when it came to the damage that was observed. The chloride concentrations further confirm this because the chloride contents of the dead end region were below the chloride corrosion limit.

6.2.12 Specimen 7.2: Non-Galvanized Anchorage, Conventional Strand, Electrically Isolated Tendon

Figure 6.127: Specimen 7.2 Main Autopsy Region and Grout Vents

Figure 6.128: Layout of the Main Autopsy Region of 7-Series Specimens

Table 6.26: Specimen 7.2 Summary of Main Autopsy Region Corrosion Ratings

Component	Maximum	Total	Generalized
Epoxy Coated Longitudinal Bars	6	49	7
Uncoated Longitudinal Bars	24	254	36
Transverse Bars	8	119	8.5
Duct	51.6	121.6	35
Strands	112	1305	124

6.2.12.1 Appearance

The surface of Specimen 7.2 had medium scaling on the top surface and in the ponding area (Figure 6.127). There was dried grout around the grout vents indicating that the vents had overflowed during grouting operations. Rust stains were observed on the north sides of the "wells" that were formed to reduce the concrete cover over the top of the tendon to the same concrete cover as the other specimens (Figure 6.127). Longitudinal cracks were observed at the interface of the backfill mortar and base concrete on the dead and live ends. This indicates that the backfill mortar did not adhere well with the base concrete.

No cracks from the application of live load on both sides of the live and dead end re-entrant corbel corners were observed. Longitudinal cracking on the backfill mortar from the live and dead end anchorage pockets was observed over the top of the grout vent for the anchorage and extended from the top interface to the end interface of the backfill mortar and base concrete (Figure 6.129). This cracking is from not having sufficient concrete cover over the top of the anchorage grout vent. The ponding area of Specimen 7.2 had 1 large transverse crack that ran from the north side to the south side on the dead end side of the ponding area and 8 small transverse cracks (4 on the south side and 4 on the north side) (Figure 6.130). A longitudinal crack was observed and was located on the north side of the "wells". It ran the length of the "wells" (Figure 6.130). This crack is almost certainly due to the expansive nature of the corrosion product from the uncoated longitudinal steel reinforcement that had been added to the specimen for taking AC

impedance readings. However, this does not explain why the no longitudinal cracking was observed on the south side of the "wells" above the similar uncoated bar. The average crack width was 0.006 inch. The crack rating for Specimen 7.2 was 0.46. See Figure 6.131 for the crack data from Specimen 7.2.

Figure 6.129: Cracking in the Backfill Mortar of Specimen 7.2

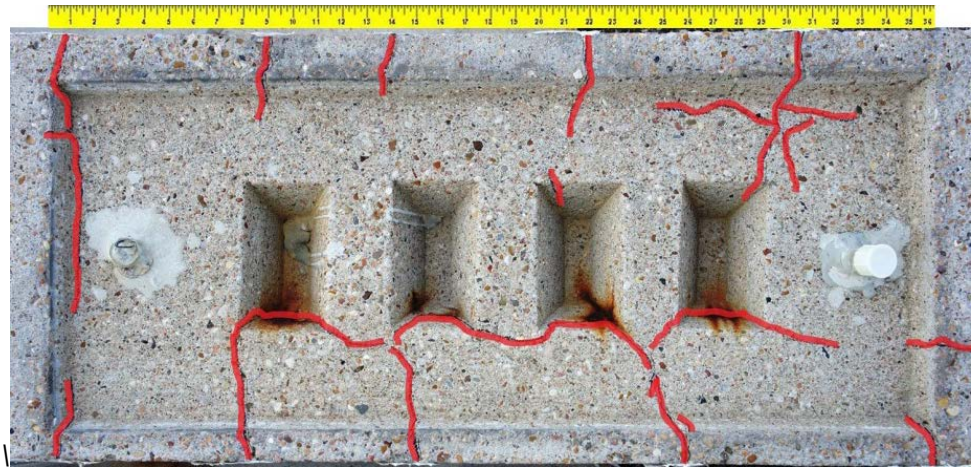

Figure 6.130: Specimen 7.2 Crack Map of Ponding Area

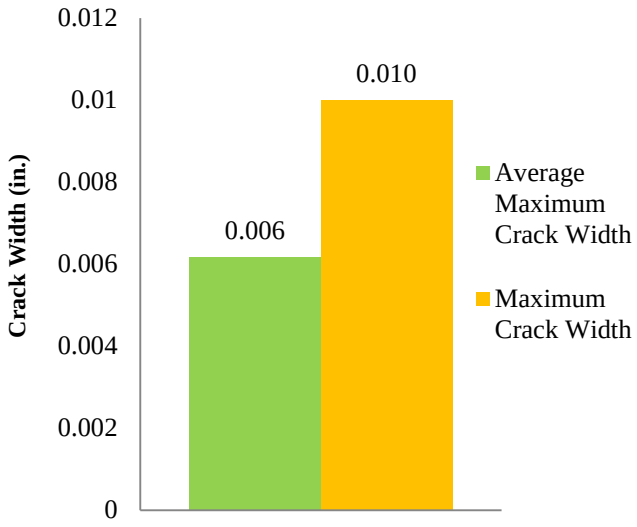

Figure 6.131: Crack Data for Specimen 7.2

6.2.12.2 Longitudinal and Transverse Bars

The north and south epoxy coated longitudinal bars had slight damage from when the bars were extracted from the specimen. The north coated longitudinal bar had no visible signs of corrosion. The south coated longitudinal bar had moderate corrosion and cracks in the epoxy coating located approximately at midspan on the longitudinal rid of the bar (Figure 6.132). Rust stains were also evident at locations where the transverse

bars were tied to the longitudinal bars. This staining is from corrosion of the tie wire used to attach the transverse reinforcement to the longitudinal bars and NOT from the longitudinal bar itself. Figure 6.137 shows the epoxy coated longitudinal bar's corrosion ratings and Table 6.26 shows the summary of the corrosion ratings for the longitudinal bars.

Figure 6.132: Moderate Corrosion and Crack in Epoxy Coating along Longitudinal Rib of South Epoxy Coated Longitudinal Bar of Specimen 7.2

The north and south uncoated longitudinal bars had slight damage from when the bars were extracted from the specimen. The north and south bars had extensive pitting, moderate corrosion, and light corrosion along their lengths (Figure 6.133). The damage to the north bar was much more extensive than the damage to the south bar. This might indicate that the longitudinal crack observed on the north side of the "wells" was present before the bar had corroded. This indicates that moisture, oxygen, and chlorides reached the depth of the bars. The light and moderate corrosion was normally located on intervals adjacent to the areas of pitting. Figure 6.137 shows the uncoated longitudinal bar's corrosion ratings and Table 6.26 shows the summary of the corrosion ratings for the uncoated longitudinal bars.

Figure 6.133: Corrosion Damage to North (Top) and South (Bottom) Uncoated Longitudinal Bars from Specimen 7.2

All transverse bars had damage from when they were extracted from the specimen. All the transverse bars had rust staining at least somewhere over the length of the bar from corrosion of the tie wire used to attach the transverse bars to the longitudinal bars and to attach the duct to the transverse bars. Light corrosion was observed on at least one interval on all bars and moderate corrosion observed on at least one interval of bars #1, #2, #3, and #7. Moderate corrosion was observed on all bars except #3 and #7. Bar #3 had the highest rating of 30. Bar #2 had the next highest rating of 43. Bar #7 had the lowest ratings of 8. Figure 6.137 shows the transverse bar's corrosion ratings and Table 6.26 shows the summary of the corrosion rating for the transverse bars.

6.2.12.3 Duct

The entire outer surface of the duct had a chalky white residue. No corrosion staining was observed on the outer surface of the duct. However, a rust stain was observed near the inner bottom surface of the duct in the dead end grout vent region (Figure 6.134). The bottom inner surface of the duct had slight gouges starting at the dead end at midspan and in the locations of the live and dead end grout vents. This indicates that one or more of the strands caused damage either when the strands were being threaded through the duct or one of the strands or stands were rubbing against the duct when the strands were being stressed. A crack was found on the bottom of the duct near the dead end grout vent of the duct (Figure 6.134). There was no indication that this

crack was caused from the threading or the stressing of the strands. Indications of voids were observed on the top inner surface of the duct along the entire length. No damage was observed on the coupler, grout vent, or heat shrink wrap used to seal the coupler/duct interface. However, the heat shrink wrap did not bond well to the coupler or duct. This might indicate why chloride levels were elevated. Figure 6.137 shows the damage ratings for the ducts and Table 6.26 shows the summary of the damage ratings for the ducts.

Figure 6.134: Rust Stains on Duct (Top) and Crack in Duct (Bottom) Located at the Dead End Grout Vent of Specimen 7.2

6.2.12.4 Grout

No transverse visible cracks were observed during examination of grout. However, a longitudinal crack was observed in the area where a rust stain was observed at the dead end grout vent (Figure 6.135). The tendon had small voids in the grout that ran the length of the tendon. The small voids measured approximately 1.5 inch long and were as wide as the flute width. The coloration on the bottom of the grout from the tendon was light grey at the ends and transitioned to dark grey at midspan. The coloration of the grout on top of the tendon was light grey along the length of the tendon. Portions of strand were visible on the bottom of the grout (Figure 6.135).

Figure 6.135: Rust Stain and Longitudinal Cracking at the Dead End Grout Vent (Left) and Visible Wires on the bottom of the Grout (Right) of Specimen 7.2

The chloride concentrations were discussed in depth in Chapter 5. All the chloride concentrations were above the 0.033% by weight of grout limit for corrosion. See Figure 5.15 for the results of the chloride concentration testing. As expected, the highest chloride concentrations for the tendon were at the dead and live grout vents and were 0.044% and 0.360%, respectively, by weight of grout. Even though the 0.044% chloride concentration is close to the corrosion limit, it was the chloride concentration of the location with the highest corrosion rating for the strands. As expected, the midspan region had the lowest chloride concentration. This might be because this location was at the apex of the tendon and the duct was undamaged in this region.

6.2.12.5 Strand

The damage to the strands was quite extensive but was expected due to the damage to the duct that was observed and the poor bond of the heat shrink to the coupler and duct. Mild pitting was observed on the outer and inner wires of one strand at the location of the dead end grout vent (Figure 6.136). Moderate corrosion was observed on the majority of the outer wire intervals and all the inner wires. Where neither pitting nor moderate corrosion was observed light corrosion was present. This is an indication that moisture, oxygen, and chlorides had reached the strands and corresponds to the chloride concentrations discussed in Chapter 5. The dead end side of the live end grout vent had the lowest rating of 47. As expected, the highest rating of 112 was at the location of the crack in the duct that was observed at the dead end grout vent. Figure 6.137 shows the corrosion ratings for the strands and Table 6.26 shows the summary of the corrosion ratings for the strands.

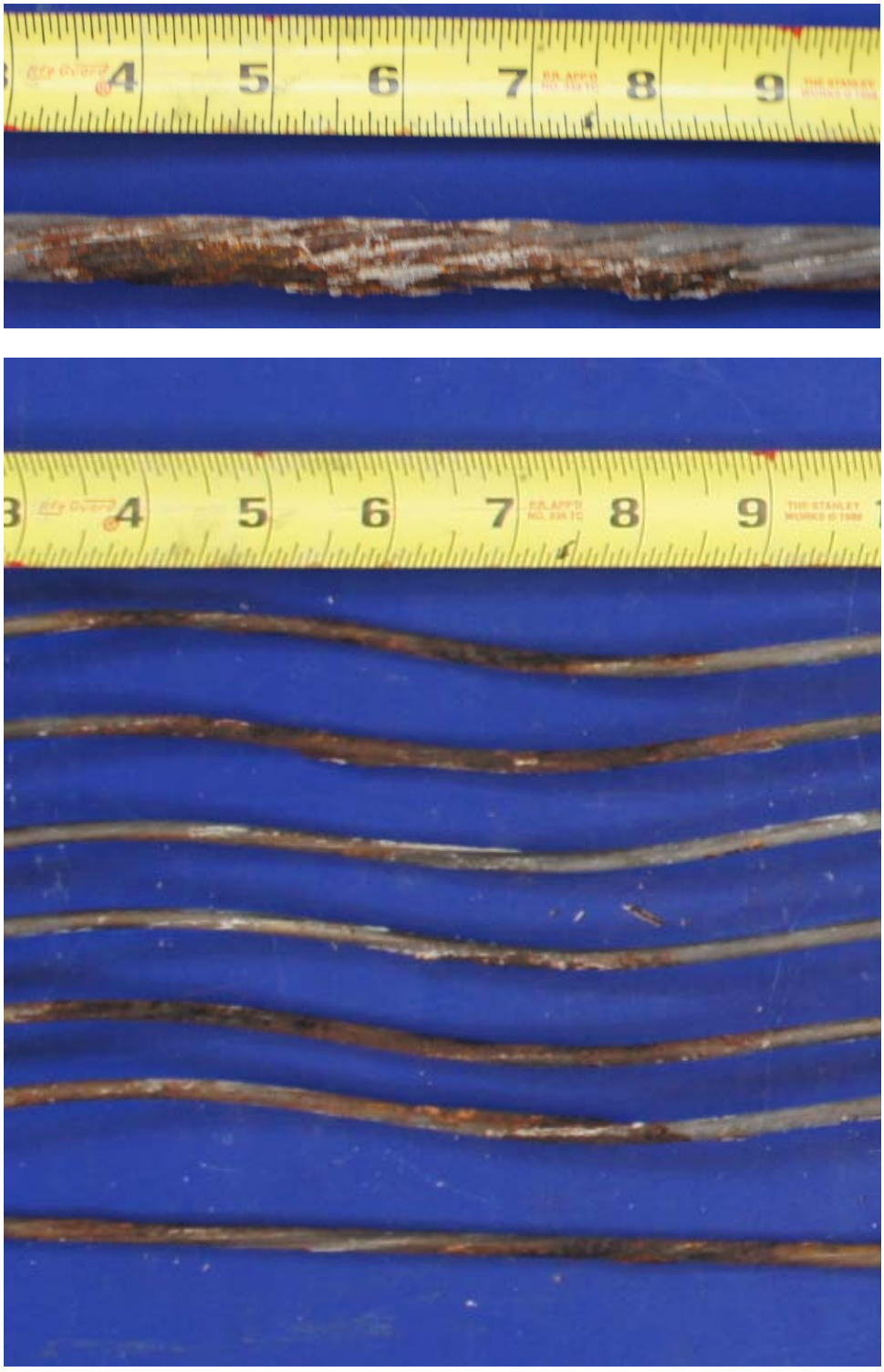

Figure 6.136: Pitting at Dead End Grout Vent of Specimen 7.2

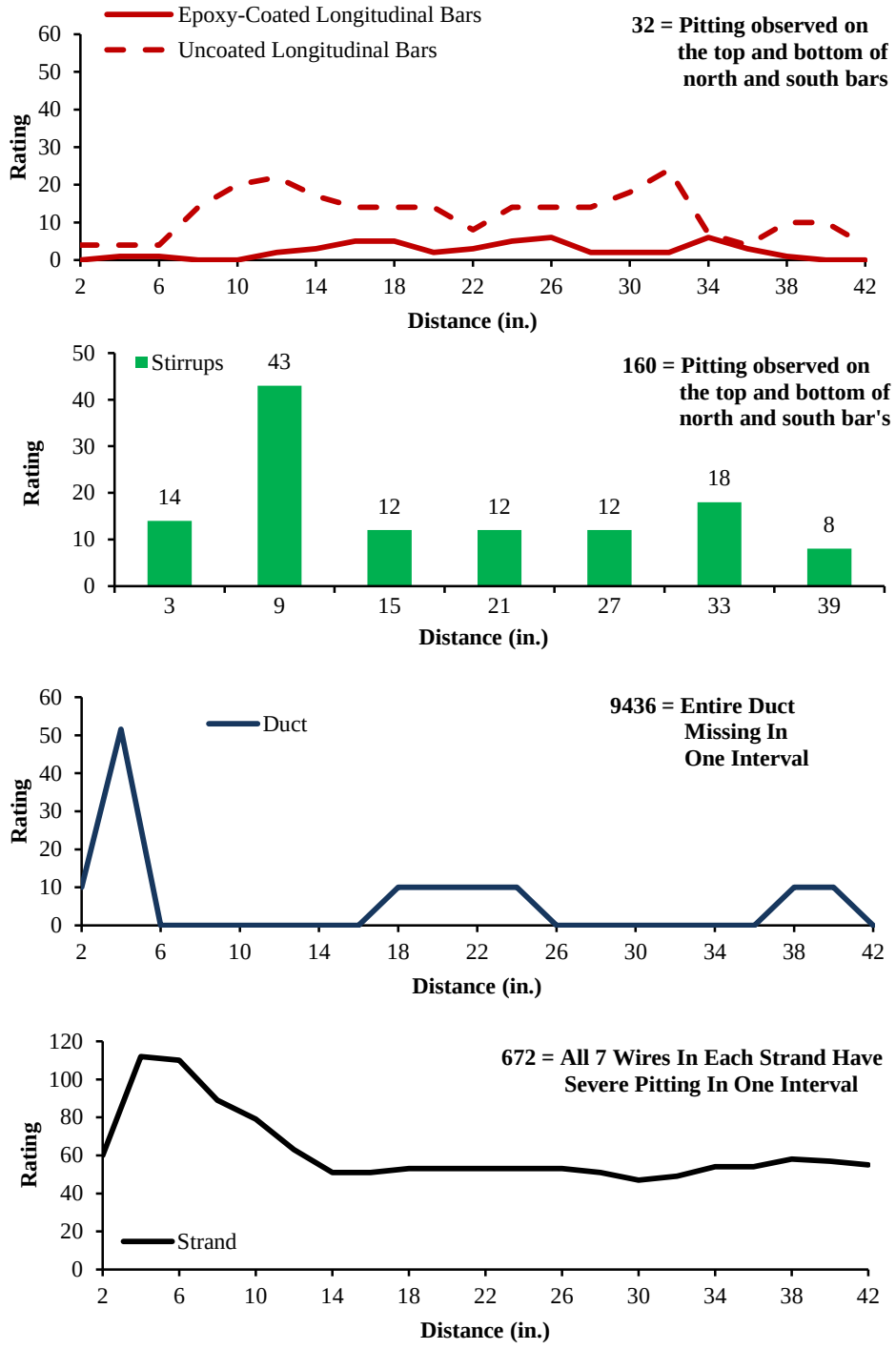

Figure 6.137: Corrosion Rating Plots for Main Autopsy Region of Specimen 7.2

6.2.12.6 Dead and Live End Anchorages

Except for the corrosion damage on their steel parts, the anchorage components from the dead and live anchorage region were in good repair. See Figure 6.138 for a layout of the anchorage components. The dead and live end grout cap was in good repair, except for a cut that the wet saw made in the dead and live end rubber covers when it deviated from a straight line (Figure 6.139). A void in the grout was evident on the inside top surface of the north and south grout caps (Figure 6.139). Rust stains were observed on the exposed and unexposed faces of the lip of the grout caps where the steel retaining ring used to clamp the grout cap to the anchorage plate had corroded (Figure 6.139). The dead and live end steel retaining rings had severe corrosion and pitting over their entire surface (Figure 6.140). The unexposed sides, the sides in contact with the grout cap, of the dead and live end steel retaining rings had greater corrosion damage than the exposed sides. The dead and live end O-ring to seal the grout cap to the insulation plate was intact and in good repair, except for where it was cut by the wet saw. The anchor heads from the live and dead ends had visible signs of corrosion where the wet saw had cut into them, tiny spots of corrosion on the sides and exposed face (face opposite the insulation plate). The dead end unexposed face (face against the anchorage plate) had moderate corrosion over its entire surface and the live end unexposed face had the majority of the moderate corrosion outside the area where the grout from the tendon came into contact with the anchor head (Figure 6.141). The dead and live end insulation plates used to electrically isolate the anchor head from the anchorage plate were in good repair, except for the cut had by the wet saw. Both insulation plates had rust stains from corrosion of the steel retaining ring and anchorage plate (Figure 6.142). The exposed surface (surface in contact with the insulation plate) of the dead and live end anchorage plates had severe corrosion and pitting (Figure 6.143). The embedded surface of the anchorage plate was corrosion free. The bolts used to attach the rubber cover and the anchorage plate were made of stainless steel. Therefore they were corrosion free. Except for one of the bolts, they were relatively easy to extract from the anchorage plate. The

one bolt that could not be extracted had to be cut using a grinder, was from the dead end anchorage, and had been cut by the wet saw (Figure 6.143).

Figure 6.138: Anchorage Components, from Top: Grout Cap, Steel Retaining Ring, Insulation Plate, and Anchorage Plate[2]

Figure 6.139: Rust Stains on Exposed (Left) and Unexposed (Right) Faces of Lip on the Dead End Rubber Cover from Specimen 7.2

Figure 6.140: Severe Corrosion and Pitting on Steel Ring from the Dead End of Specimen 7.2

Figure 6.141: Unexposed Faces of Dead (Left) and Live (Right) End Anchor Heads from Specimen 7.2

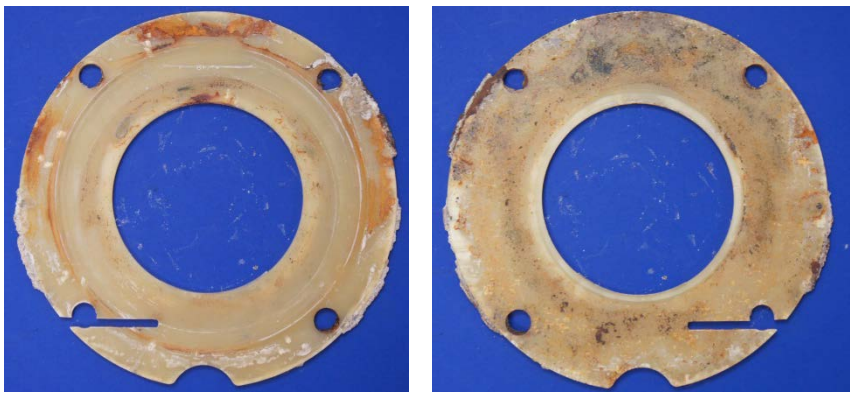

Figure 6.142: Rubber Cover Surface (Left) and Anchor Head Surface of Live End Fiber Glass Barrier from Specimen 7.2

Figure 6.143: Exposed Surface of Dead End Anchorage Plate from Specimen 7.2

This corrosion damage of the anchorage components might be from the salt solution entering the cracks that were observed in the live and dead end backfill mortar. The cracks would have allowed at least moisture and oxygen to infiltrate the anchorage and possible chlorides when the salt solution in the ponding area was being sprayed out. The greater damage to the dead end anchorage components might be from the salt spray from the dripper system entering the crack in the backfill mortar.

Table 6.27: Specimen 7.2 Summary of Dead and Live End Anchorage Region Corrosion Ratings

	Dead End Anchorage			**Live End Anchorage**		
Component	Maximum	Total	Generalized	Maximum	Total	Generalized
Duct	0	0	0	0	0	0
Strands	101	711	158	51	379	84

The outside surface of the dead and live end ducts had a white powder where the duct came into direct contact with the concrete. The ducts in the live and dead end anchorage region had no holes or gouges. However, light scratches were observed on the bottom surface of live and dead end ducts (Figure 6.144). There were no indications of voids in either duct section. Figure 6.147 shows the damage ratings for the dead and live anchorage region ducts and Table 6.27 shows the summary of the damage ratings for the dead and live anchorage region ducts.

Figure 6.144: Light Scratches on the bottom of the Live End Duct Section of Specimen 7.2

No transverse or longitudinal cracks were observed in the grout from either the dead or live end section of the tendon. The grout from both tendon sections in the anchorage regions had small voids along the top surface of the grout (Figure 6.145). There was no sign of segregation of the grout.

Figure 6.145: Small Voids in Grout from Dead End Tendon Section of Specimen 7.2

The outer wires of the dead end section of the tendon had mild pitting, moderate corrosion, light corrosion, and discoloration. The mild pitting was primarily confined to one strand (Figure 6.146). This stand was the strand that was closest to the hole that was observed in the duct section at the dead end grout vent region. This also indicates that moisture, oxygen, and/or chlorides had entered through the hole that was observed in the duct. The inner wires from the dead end section of the tendon had the same damage as the outer wires with the pitting primarily confined to the same strand as the pitting in the

outer wires. The outer and inner wires from the live end fared better with no pitting observed. However, the outer and inner wires had discoloration, moderate, and light corrosion. The corrosion observed on the outer and inner wires from the live end section of the tendon indicates that the heat shrink used to seal the coupler to the duct did not perform as it should have and allowed moisture, oxygen, and/or chlorides into the duct. The wedges were intact and had light surface corrosion. Figure 6.147 shows the corrosion ratings for the dead and live anchorage region ducts and Table 6.27 shows the summary of the corrosion ratings for the dead and live anchorage region ducts.

Figure 6.146: Pitting, Moderate, and Light Corrosion on Inner and Outer Wires from One Strand from the Dead End Section of the Tendon from Specimen 7.2

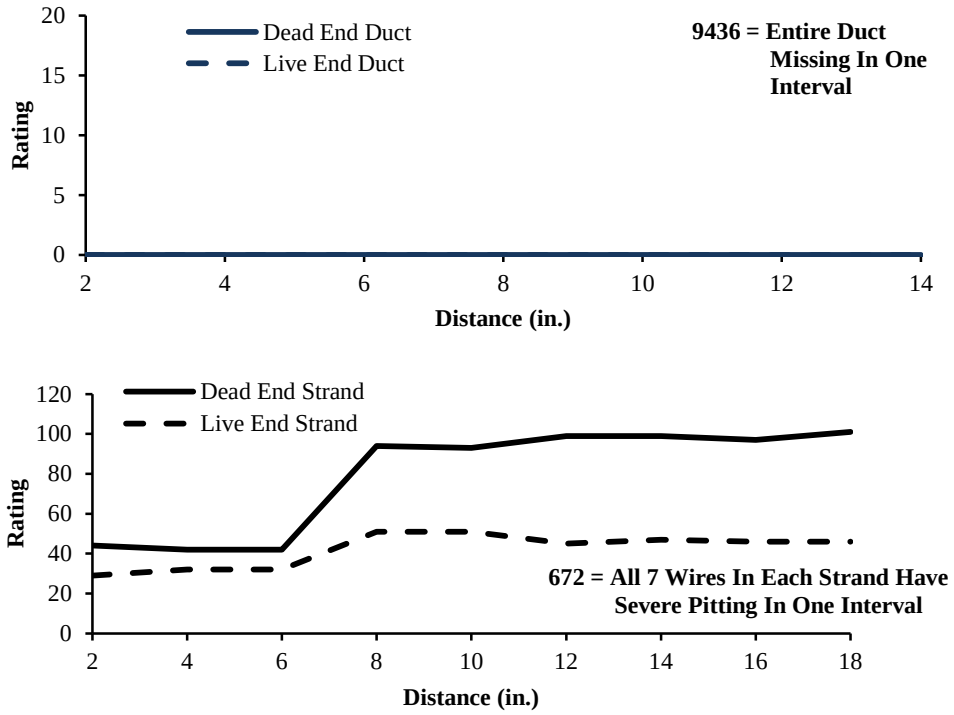

Figure 6.147: Corrosion Rating Plots for Dead and Live End Anchorage Regions of Specimen 7.2

The differential damage between the dead and live end post-tensioning components was from two sources. One source is the spray system where the crack in the backfill mortar exacerbated the infiltration of chlorides to the anchorage components from the spray system. The other source for the differential damage is the crack in the duct. This crack would have allowed moisture, oxygen, and/or chlorides to enter the tendon and induce corrosion.

6.2.13 Specimen 7.3: Non-Galvanized Anchorage, Hot Dip Galvanized Strand, Electrically Isolated Tendon

Figure 6.148: Specimen 7.3 Main Autopsy Region and Grout Vents

Table 6.28: Specimen 7.3 Summary of Main Autopsy Region Corrosion Ratings

Component	Maximum	Total	Generalized
Epoxy Coated Longitudinal Bars	11	77	11
Uncoated Longitudinal Bars	32	306	44
Transverse Bars	16	114	8
Duct	10	110	31
Strands	60	566	54

6.2.13.1 Appearance

The surface of Specimen 7.3 had medium scaling on the edges of the ponding area (Figure 6.148). There was dried grout around the grout vents indicating that the vents had overflowed during grouting operations. Rust stains were observed on the north side of the dead end "well" and in the south side of the transverse crack located at the dead end well (Figure 6.148). Cracks were observed at the interface of the backfill mortar and base concrete on the dead or live ends (Figure 6.149). This indicates that the backfill mortar did not adhere well with the base concrete.

Figure 6.149: Crack at Interface of the Backfill Mortar and Base Concrete at the Live End of Specimen 7.3

No cracks from the application of live load on both sides of the live and dead end re-entrant corbel corners were observed. Longitudinal cracking in the backfill mortar from the live and dead end anchorage pockets was observed over the top of the grout vent for the anchorage and extended from the top interface to the end interface of the backfill mortar and base concrete (Figure 6.149). This cracking is from not having sufficient cover over the top of the anchorage grout vent. The ponding area of Specimen 7.3 had 1 large transverse crack that ran from the north side to the south side on the dead end side of the ponding area and 6 small transverse cracks (3 on the south side and 3 on the north side) (Figure 6.150). Two longitudinal cracks were located on the north side and the south side of the "wells" (Figure 6.150). These cracks are due to the expansive nature of the corrosion product from the uncoated longitudinal steel reinforcement that had been used for taking AC impedance readings. The average crack width was 0.007 inch. The crack rating for Specimen 7.3 was 0.42. See Figure 6.151 for the crack data from Specimen 7.3.

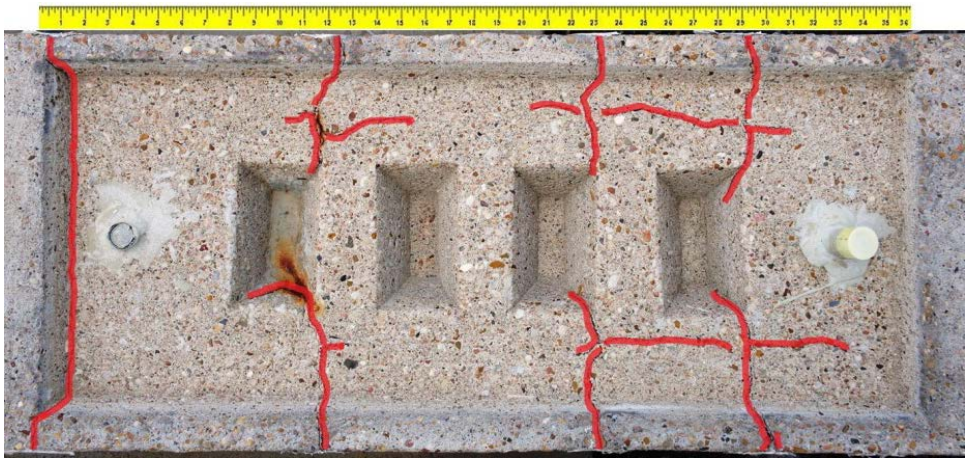

Figure 6.150: Specimen 7.3 Crack Map of Ponding Area

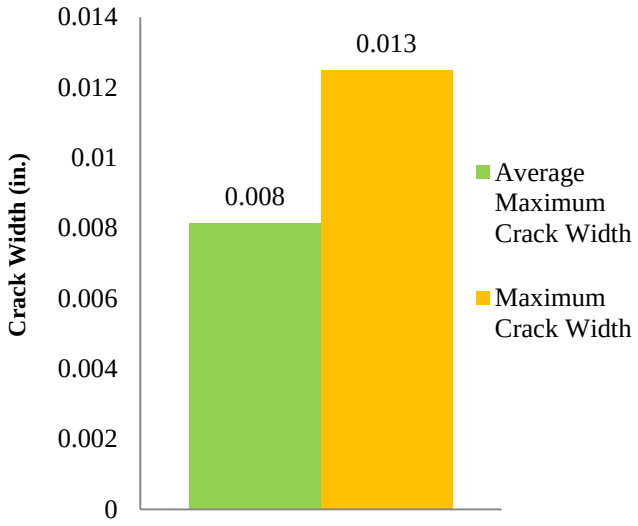

Figure 6.151: Crack Data for Specimen 7.3

6.2.13.2 Longitudinal and Transverse Bars

The north and south epoxy coated longitudinal bars had slight damage from when the bars were extracted from the specimen. The north coated longitudinal bar had one interval with moderate corrosion and two intervals with light corrosion. The south coated longitudinal bar had moderate corrosion on one interval, pitting on one interval, and pitting on 4 successive intervals towards the live end of the bar (Figure 6.152). Rust

stains were also evident at locations where the transverse bars were tied to the longitudinal bars. This staining is from corrosion of the tie wire used to attach the transverse reinforcement to the longitudinal bars and NOT from the longitudinal bar itself. Figure 6.159 shows the epoxy coated longitudinal bar's corrosion ratings and Table 6.28 shows the summary of the corrosion ratings for the longitudinal bars.

Figure 6.152: Pitting on Top of South Longitudinal Epoxy Coated Bar from Specimen 7.3

The north and south uncoated longitudinal bars had slight damage from when the bars were extracted from the specimen. The north and south bars had extensive pitting (Figure 6.153), moderate corrosion, and light corrosion along their lengths. The damage to the north and south bars was located on the same intervals. The light and moderate corrosion was normally located on intervals adjacent to the areas of pitting. The corrosion damage indicates that moisture, oxygen, and chlorides reached the depth of the bars. Figure 6.159 shows the uncoated longitudinal bar's corrosion ratings and Table 6.28 shows the summary of the corrosion ratings for the longitudinal bars.

Figure 6.153: Pitting on North Longitudinal Uncoated Bar from Specimen 7.3

All transverse bars had damage from when they were extracted from the specimen. All the transverse bars had rust staining at least somewhere over the length of the bar from corrosion of the tie wire used to attach the transverse bars to the longitudinal bars and to attach the duct to the transverse bars. All the transverse bars had some form of corrosion damage. Light corrosion was observed on bars #1, #2, and #7. Moderate corrosion was observed on bars #3, #4, #5, and #6. Pitting was observed on bars #3, #5, and #6 (Figure 6.154). Bar #3 had the highest rating of 29 and bar #5 had the second highest rating of 28. Bar #7 had the lowest ratings of 5. Figure 6.159 shows the transverse bar's corrosion ratings and Table 6.28 shows the summary of the corrosion rating for the transverse bars.

Figure 6.154: Pitting on Transverse Bar #3 from Specimen 7.3

6.2.13.3 Duct

The entire outer surface of the duct had a chalky white residue. No corrosion staining was observed on the outer or inner surface of the duct. The bottom inner surface of the duct had slight gouges at the dead end, on the dead end side of midspan, and at midspan to about the live end quarter point. This indicates that one or more of the strands caused damage either when the strands were being threaded through the duct or one of the strands or stands were rubbing against the duct when the strands were being stressed. Regardless of what caused the gouges the integrity of the duct was not compromised. Indications of voids were observed on the top inner surface of the duct along the entire length (Figure 6.155). No damage was observed on the coupler, grout vent, or heat shrink wrap used to seal the coupler/duct interface. However, the heat shrink wrap did not bond well to the coupler or duct. This might indicate why chloride levels were elevated. Figure 6.159 shows the damage ratings for the ducts and Table 6.28 shows the summary of the damage ratings for the ducts.

Figure 6.155: Indications of Voids in Grout on Top Surface of Duct from Specimen 7.3

6.2.13.4 Grout

No transverse visible cracks were observed during examination of the grout. However, when the grout samples were being extracted small transverse cracks were observed (Figure 6.156). Longitudinal cracks were observed. The longitudinal cracks started at a point on the live end side of the dead end grout vent and radiated out to the live end and bisected the tendon (Figure 6.157). These longitudinal cracks might have come from the corrosion of the zinc in the galvanized coating or the tendon could have been impacted by something during the extraction process. No evidence of impact was observed on the duct so the former explanation is the more valid hypothesis. The tendon had small voids in the grout that ran the length of the tendon (Figure 6.157). The small voids measured approximately 1.5 inch long and were as wide as the flute width. The coloration on the bottom of the grout from the tendon was light grey at the ends and transitioned to dark grey at midspan. The coloration of the grout on top of the tendon was light grey along the length of the tendon (Figure 6.157). Portions of strand were visible on the bottom of the grout. The grout adhered well to the strands due to the rough nature of the galvanized coating.

Figure 6.156: Small Transverse Crack in Grout from Specimen 7.3

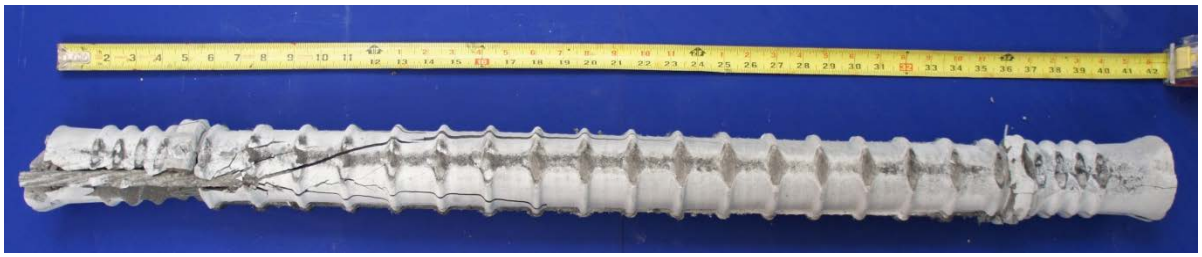

Figure 6.157: Longitudinal Cracking and Small Voids in Grout from Specimen 7.3

The chloride concentrations were discussed in depth in Chapter 5. The majority of the chloride concentrations were well above the 0.033% by weight of grout limit for corrosion. See Figure 5.15 for the results of the chloride concentration testing. As expected, the highest chloride concentrations for the tendon were at the dead and live grout vents and were 0.420% and 0.118%, respectively, by weight of grout. The midspan region had the lowest chloride concentration of 0.032%. This is below the corrosion limit. This might be because this location was at the apex of the tendon and the duct was undamaged in this region.

6.2.13.5 Strand

All the outer and inner wires from the strands had some form of corrosion. Where there was no corrosion, discoloration was observed. The dead end region of two strands received the greatest damage. Mild pitting was observed on the inner and some of the outer wires of one of these strands as well as moderate corrosion (Figure 6.158). The inner and outer wires of the other strand had light to moderate corrosion. The third stand had a few spots of light corrosion on the inner and outer wires. The depletion of the zinc in the galvanized coating is the reason for this corrosion. The depletion of the zinc could have come from corrosion of the zinc or from the strands and wires rubbing together during stressing and/or threading of the strands. The high corrosion ratings in the region of the dead end grout vent indicates that the poor bonding of the shrink wrap to the duct and coupler in that region allowed moisture, oxygen, and/or chlorides to enter the duct. This is an indication that moisture, oxygen, and chlorides had reached the strands and

corresponds to the chloride concentrations discussed in Chapter 5. The live end side of the tendon had the lowest rating of 21. The highest rating of 60 was located close to the dead end grout vent. Figure 6.159 shows the corrosion ratings for the strands and Table 6.28 shows the summary of the corrosion ratings for the strands.

Figure 6.158: Pitting on the Outer Wires of One Strand from Specimen 7.3

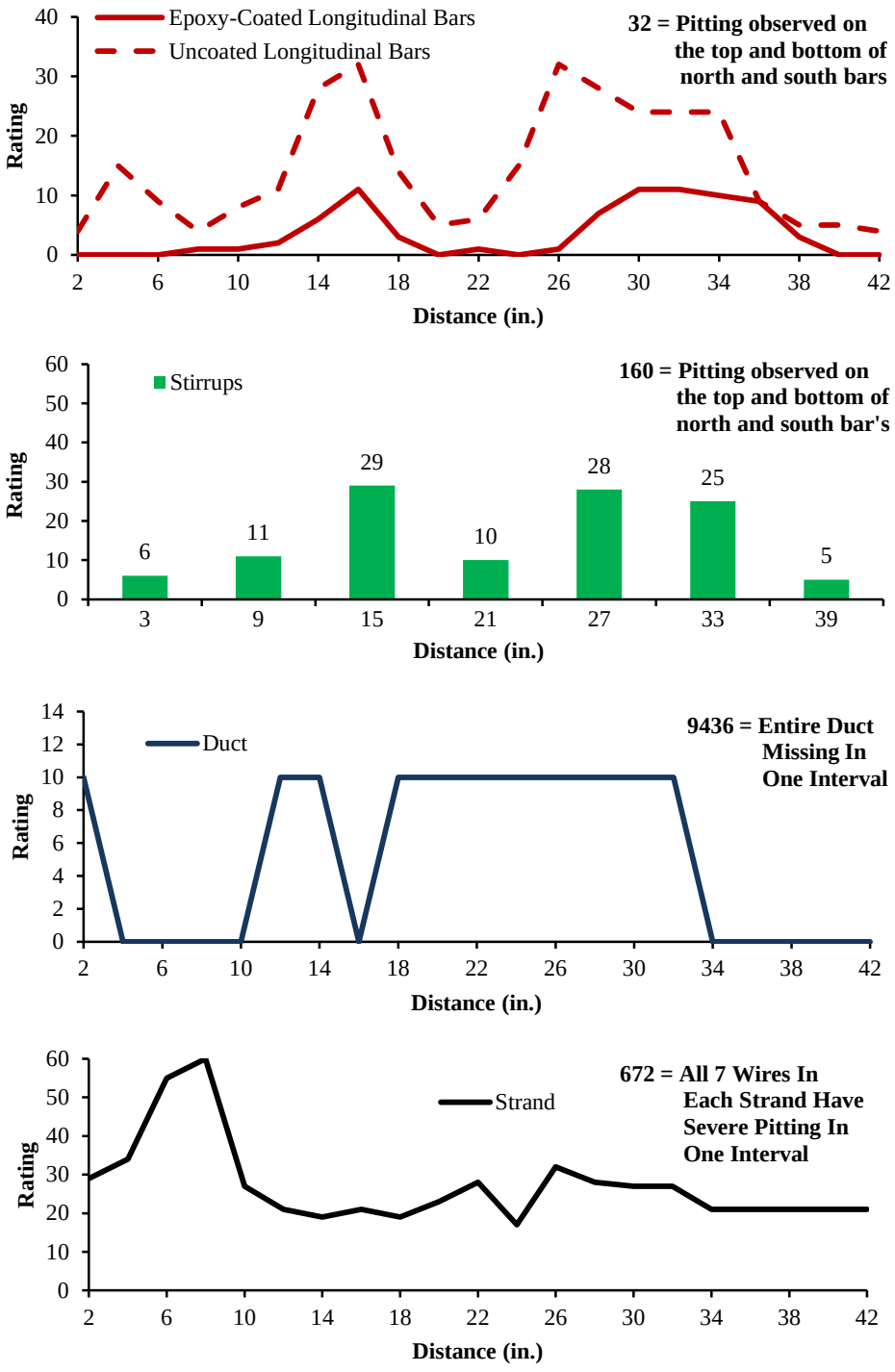

Figure 6.159: Corrosion Rating Plots for Main Autopsy Region of Specimen 7.3

6.2.13.6 Dead and Live End Anchorages

Except for the corrosion damage on their steel parts, the anchorage components from the dead and live anchorage region were in good repair. See Figure 6.128 for a layout of the anchorage components. The dead and live end grout cap was in good repair. A void in the grout was evident on the inside top surface of the north and south grout caps. Rust stains were observed on the exposed face of the lip of the grout caps where the steel retaining ring used to clamp the grout cap to the anchorage plate had corroded. The dead and live end steel retaining rings had severe corrosion and pitting over their entire surface (Figure 6.160). The unexposed sides of the dead and live end steel retaining rings had greater corrosion damage than the exposed sides. The dead and live end O-ring to seal the grout cap to the insulation plate was intact and in good repair. The anchor heads had no visible signs of corrosion of their entire surface. The dead and live end insulation plates used to electrically isolate the anchor head from the anchorage plate were in good repair. Both insulation plates had rust stains from corrosion of the steel retaining ring and anchorage plate. The exposed surface of the dead and live end anchorage plates had severe corrosion over the majority of their surface (Figure 6.161). The embedded surface of the anchorage plate was corrosion free. The bolts used to attach the grout cap and the anchorage plate were made of stainless steel therefore they were corrosion free. Except for the bolts from the dead end, they were relatively easy to extract from the anchorage plate. The bolts from the dead end had to be cut using a grinder.

Figure 6.160: Pitting on Live End Steel Retaining Ring from Specimen 7.3

Figure 6.161: Corrosion on Exposed Face of Dead End Anchorage Plate from Specimen 7.3

Table 6.29: Specimen 7.3 Summary of Dead and Live End Anchorage Region Corrosion Ratings

	Dead End Anchorage			Live End Anchorage		
Component	Maximum	Total	Generalized	Maximum	Total	Generalized
Duct	0	0	0	0	0	0
Strands	34	220	49	29	203	45

The outside surface of the dead and live end ducts had a white powder where the duct came into direct contact with the concrete. The ducts in the live and dead end anchorage region had no holes or gouges. However, light scratches were observed on the bottom surface of live and dead end ducts. There were no indications of voids in either duct section. Figure 6.162 shows the damage ratings for the dead and live anchorage region ducts and Table 6.29 shows the summary of the damage ratings for the dead and live anchorage region ducts.

No transverse or longitudinal cracks were observed in the grout from either the dead or live end section of the tendon. The grout from both tendon sections in the anchorage regions had small voids along the top surface of the grout. There was no sign of segregation of the grout.

The outer and inner wires from the strands of the dead end section of the tendon had discoloration over the majority of their surface. Where discoloration was not evident moderate or light corrosion was observed. The outer and inner wires from the live were in similar condition to the outer and inner wires from the dead end. The majority of their surface had discoloration and where there was no discoloration either moderate or light corrosion was observed. The wedges were intact and had light surface corrosion. Figure 6.162 shows the corrosion ratings for the dead and live anchorage region strands and Table 6.29 shows the summary of the corrosion ratings for the dead and live anchorage region strands.

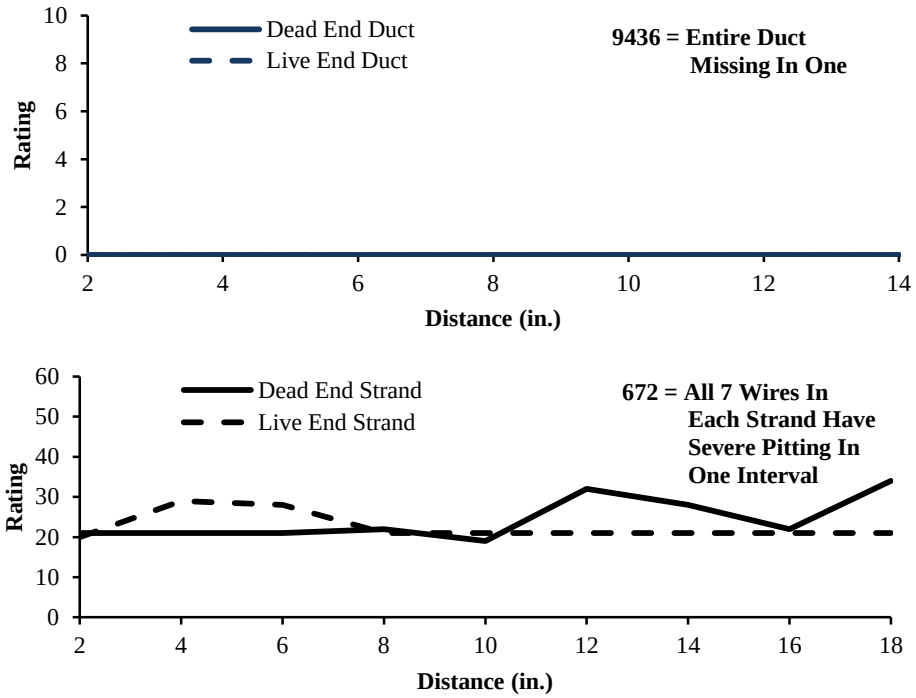

Figure 6.162: Corrosion Rating Plots for Dead and Live End Anchorage Regions of Specimen 7.3

The similar damage to the anchorage components suggests that the dripper system was not a major contributor to the corrosion damage observed, even though the backfill mortar was cracked on the dead end. However, the live end side was cracked as well. So when the ponding area was emptied, the salt solution could have entered the live end and induced corrosion in that region similar to the dead end.

6.2.14 Specimen 7.4: Non-Galvanized Anchorage, Flowfilled Epoxy Coated Strand, Electrically isolated Tendon

Figure 6.163: Specimen 7.4 Main Autopsy Region and Grout Vents

Table 6.30: Specimen 7.4 Summary of Main Autopsy Region Corrosion Ratings

Component	Maximum	Total	Generalized
Epoxy Coated Longitudinal Bars	4	25	3.6
Uncoated Longitudinal Bars	92	309	44
Transverse Bars	8	149	11
Duct	10	10	2.9
Epoxy Coating	48	340	32
Strands	118	1861	177

6.2.14.1 Appearance

The surface of Specimen 7.4 had medium scaling on the top surface, the ponding area, and on the edges of the ponding area (Figure 6.163). There was dried grout around the grout vents indicating that the vents had overflowed during grouting operations. A rust stain was observed on the north side of the live end "well" (Figure 6.163). Cracks

were observed at the interface of the backfill mortar and base concrete on the dead or live ends. This indicates that the backfill mortar did not adhere well with the base concrete.

No cracks from the application of live load on both sides of the live and dead end re-entrant corbel corners were observed. Longitudinal cracking in the backfill mortar from the live and dead end anchorage pockets was observed over the top of the grout vent for the anchorage and extended from the top interface to the end interface of the backfill mortar and base concrete. This cracking is from not having sufficient cover over top of the anchorage grout vent. The ponding area of Specimen 7.4 had 1 large transverse crack that ran from the north side to the south side on the dead end side of the ponding area and 6 small transverse cracks (3 on the south side and 3 on the north side) (Figure 6.164). Multiple longitudinal cracks were located on the north side and the south side of the "wells" (Figure 6.164). These cracks are due to the expansive nature of the corrosion product from the uncoated longitudinal steel reinforcement that had been used for taking AC impedance readings. The average crack width was 0.005 inch. The crack rating for Specimen 7.4 was 0.35. See Figure 6.165 for the crack data from Specimen 7.4.

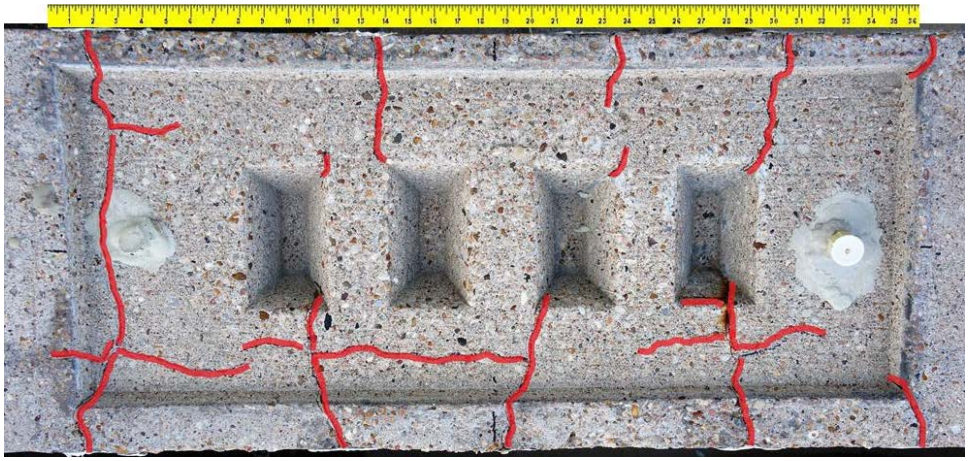

Figure 6.164: Specimen 7.4 Crack Map of Ponding Area

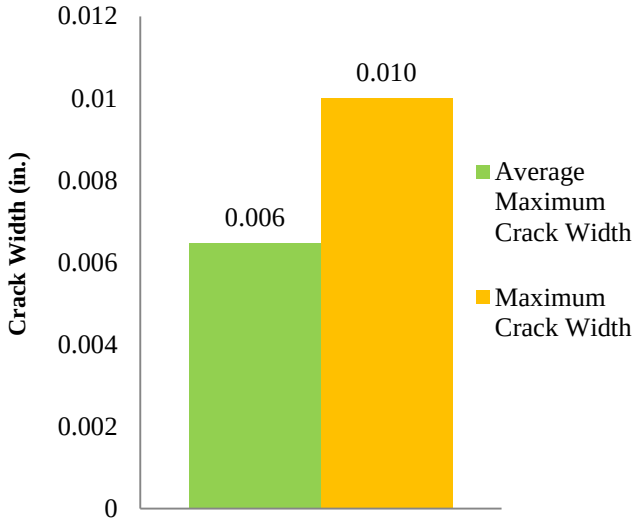

Figure 6.165: Crack Data for Specimen 7.4

6.2.14.2 Longitudinal and Transverse Bars

The north and south epoxy coated longitudinal bars had slight damage from when the bars were extracted from the specimen. The north and south coated longitudinal had rust stains where the transverse bars were tied to the coated longitudinal bars. This staining is from corrosion of the tie wire used to attach the transverse reinforcement to the longitudinal bars and NOT from the longitudinal bar itself. Figure 6.172 shows the epoxy coated longitudinal bar's corrosion ratings and Table 6.30 shows the summary of the corrosion ratings for the longitudinal bars.

The north and south uncoated longitudinal bars had slight damage from when the bars were extracted from the specimen. The north bar had extensive pitting, moderate corrosion, and light corrosion along its length. The south bar had some pitting, light to moderate corrosion, and appreciable cross sectional area loss due to pitting on the live end of the bar (Figure 6.166). This indicates that moisture, oxygen, and chlorides reached the depth of the bars. Figure 6.172 shows the uncoated longitudinal bar's corrosion ratings and Table 6.30 shows the summary of the corrosion ratings for the longitudinal bars.

Figure 6.166: Appreciable Cross Sectional Area Loss due to Pitting on the South Coated Longitudinal Bar from Specimen 7.4

All transverse bars had damage from when they were extracted from the specimen. All the transverse bars had rust staining at least somewhere over the length of the bar from corrosion of the tie wire used to attach the transverse bars to the longitudinal bars and the duct. All the transverse bars had some form of corrosion damage, expect bar #3. Light corrosion was observed on bars #2, #6, #5, and #7. Moderate corrosion was observed on bars #1, #4, #6, and #7. Pitting was observed on bar #1 (Figure 6.167). Bar #1 had the highest rating of 41. Bar #5 had the lowest ratings of 6. Figure 6.172 shows the transverse bar's corrosion ratings and Table 6.30 shows the summary of the corrosion rating for the transverse bars.

Figure 6.167: Pitting on Transvers Bar #1 from Specimen 7.4

6.2.14.3 Duct

The entire outer surface of the duct had a chalky white residue. No corrosion staining was observed on the outer or inner surface of the duct. The bottom inner surface of the duct had slight gouges at midspan (Figure 6.168). This indicates that one or more of the strands caused damage either when the strands were being threaded through the duct or one of the strands or stands were rubbing against the duct when the strands were being stressed. Regardless of what caused the gouges, the integrity of the duct was not compromised. Indications of voids were observed on the top inner surface of the duct along the entire length. No damage was observed on the coupler, grout vent, or heat shrink wrap used to seal the coupler/duct interface. However, the heat shrink wrap did not bond well to the coupler or duct. This might indicate why chloride levels were elevated. Figure 6.172 shows the damage ratings for the ducts and Table 6.30 shows the summary of the damage ratings for the ducts.

Figure 6.168: Gouge on the Bottom Inner Surface of the Duct from Specimen 7.4

6.2.14.4 Grout

No visible transverse or longitudinal cracks were observed during examination of the grout. The tendon had small voids in the grout that ran the length of the tendon. The small voids measured approximately 1.5 inch long and were as wide as the flute width. The coloration on the bottom of the grout from the tendon was light grey at the live end and transitioned to dark grey at the dead end (Figure 6.169). The coloration of the grout on top of the tendon was light grey along the length of the tendon. Portions of strand were visible on the bottom of the grout. The grout did not adhere well to the strands due to the smooth surface of the epoxy coating.

Figure 6.169: Variation of Color on the Bottom of the Grout from Specimen 7.4

The chloride concentrations were discussed in depth in Chapter 5. The majority of the chloride concentrations were above the 0.033% by weight of grout limit for corrosion. See Figure 5.15 for the results of the chloride concentration testing. As expected, the highest chloride concentrations for the tendon were at the dead and live grout vents and were 0.139% and 0.350%, respectively, by weight of grout. The midspan region had the lowest chloride concentration of 0.029%. This is below the corrosion limit. This might be because this location was at the apex of the tendon and the duct was undamaged

6.2.14.5 Strand

The epoxy coating on the strands had minor scratches and gouging over the majority of its surface (Figure 6.170). One tiny hole was observed on the live end of one of the strands. The holes, gouges, and scratches might be from the stressing process or from the threading of the strands through the duct. In either case, except for the hole, the integrity of the coating was not compromised. Figure 6.172 shows the damage ratings for

the epoxy coating and Table 6.30 shows the summary of the damage ratings for the epoxy coating.

Figure 6.170: Scratches and Gouges in Epoxy Coating of a Strand form Specimen 7.4

The epoxy coated strand did not perform as well as had been expected. All the outer and inner wires from the strands had some form of corrosion over their entire length (Figure 6.171). Mild pitting was observed somewhere on every outer and inner wire. One inner wire had mild pitting along its entire length. Another inner wire had mild pitting over half of its length and the rest of the length had light corrosion. The third inner wire had mild pitting on a small portion of its length and light corrosion on the rest of it length. The outer wires had mild pitting and light to moderate corrosion. This corrosion might be from two sources. One source could be that the paint stripper used to remove the epoxy coating in the autopsies could have been mildly corrosive. The other reason could be that the corrosion existed before the strands were flow filled with epoxy. The live end side of the tendon had the lowest rating of 21. The highest rating of 60 was located close to the dead end grout vent. Figure 6.172 shows the corrosion ratings for the strands and Table 6.30 shows the summary of the corrosion ratings for the strands.

Figure 6.171: Mild Pitting and Moderate Corrosion on Inner Wire from a Specimen 7.4 Strand

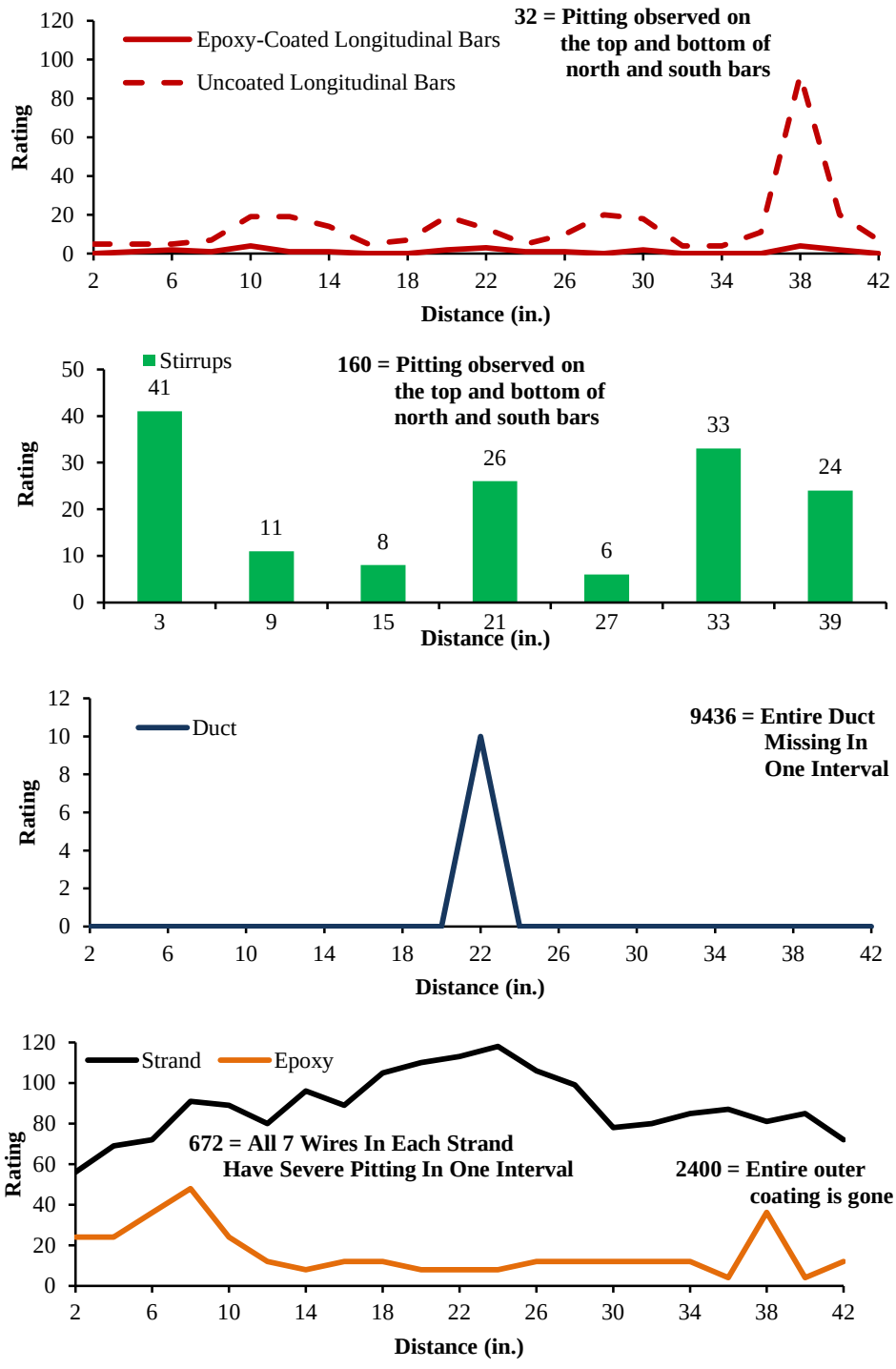

Figure 6.172: Corrosion Rating Plots for Main Autopsy Region of Specimen 7.4

6.2.14.6 Dead and Live End Anchorages

Except for the corrosion damage on their steel parts, the anchorage components from the dead and live anchorage region were in good repair. See Figure 6.138 for a layout of the anchorage components. The dead and live end grout cap was in good repair with signs of minimal damage from when the anchorage was extracted from the specimen. A void in the grout was evident on the inside top surface of the north and south grout caps. Rust stains were observed on the exposed and unexposed face of the lip of the grout caps where the steel retaining ring used to clamp the grout cap to the anchorage plate had corroded (Figure 6.173). The dead and live end steel retaining rings had severe corrosion and pitting over their entire surface. The damage done by corrosion was greater on the dead end retaining ring than on the live end retaining ring. The dead and live end O-ring used to seal the grout cap to the insulation plate was intact and in good repair. The dead and live end anchor heads had light corrosion on their exposed faces and moderate corrosion on their unexposed faces (Figure 6.174). The dead and live end insulation plates used to electrically isolate the anchor head from the anchorage plates had split where the anchor head had pressed against it (Figure 6.175). The anchor heads were not the proper anchor heads for this system and instead of primarily bearing on the anchorage plate it pressed primarily on the insulation plate damaging the insulation plate. Both insulation plates had rust stains from corrosion of the steel retaining ring and anchorage plate. The exposed surface of the dead end anchorage plate had severe corrosion over the majority of their surface. The exposed surface of the live end anchorage plate had severe corrosion over approximately 40% of its surface. The embedded surface of the anchorage plate was corrosion free. The bolts used to attach the grout cap and the anchorage plate were made of stainless steel therefore they were corrosion free. Except for the three bolts from the dead end, they were relatively easy to extract from the anchorage plate. The three bolts from the dead end had to be cut using a grinder.

Figure 6.173: Rust Stains on Lip of Live End Group Cap from Specimen 7.4

Figure 6.174: Moderate Corrosion on Unexposed Face of the Dead End Anchor Head from Specimen 7.4

Figure 6.175: Split in Dead End Insulation Plate from Specimen 7.4

Table 6.31: Specimen 7.4 Summary of Dead and Live End Anchorage Region Corrosion Ratings

	Dead End Anchorage			Live End Anchorage		
Component	Maximum	Total	Generalized	Maximum	Total	Generalized
Duct	0	0	0	0	0	0
Epoxy	36	141	31	24	109	24
Strands	22	176	39	35	276	61

The outside surface of the dead and live end ducts had a white powder where the duct came into direct contact with the concrete. The ducts in the live and dead end anchorage region had no holes or gouges. However, light scratches were observed on the bottom surface of live and dead end ducts. There were no indications of voids in either duct section. Figure 6.177 shows the damage ratings for the dead and live anchorage region ducts and Table 6.31 shows the summary of the damage ratings for the dead and live anchorage region ducts.

No transverse or longitudinal cracks were observed in the grout from either the dead or live end section of the tendon. The grout from both tendon sections in the

anchorage regions had small voids along the top surface of the grout. There was no sign of segregation of the grout.

The epoxy coating on the strands from the dead and live end sections of the tendon had scratches over the majority of the length of the strand. Gouges were observed on a few intervals of the epoxy coating on the strand in live and dead end sections of the tendon. The region of the epoxy coating that was in the anchor head could not be rated because the epoxy coating had melted due to heating of the anchor head to facilitate the removal of the strands from the anchor head.

The outer and inner wires from the strands of the dead end section of the tendon had discoloration over the majority of their surface. Light corrosion was observed on the majority of the remaining intervals of the inner and outer wires that did not have discoloration. The outer wires from the live end had light corrosion over the majority of their lengths. The remaining intervals had discoloration. The inner wires had light corrosion over their entire length. The dead end wedges were intact and had light surface corrosion. The live end wedges were intact and had moderate surface corrosion (Figure 6.176). Figure 6.177 shows the corrosion ratings for the dead and live anchorage region strands and Table 6.31 shows the summary of the corrosion ratings for the dead and live anchorage region strand.

Figure 6.176: Moderate Corrosion on a Live End Wedge from Specimen 7.4

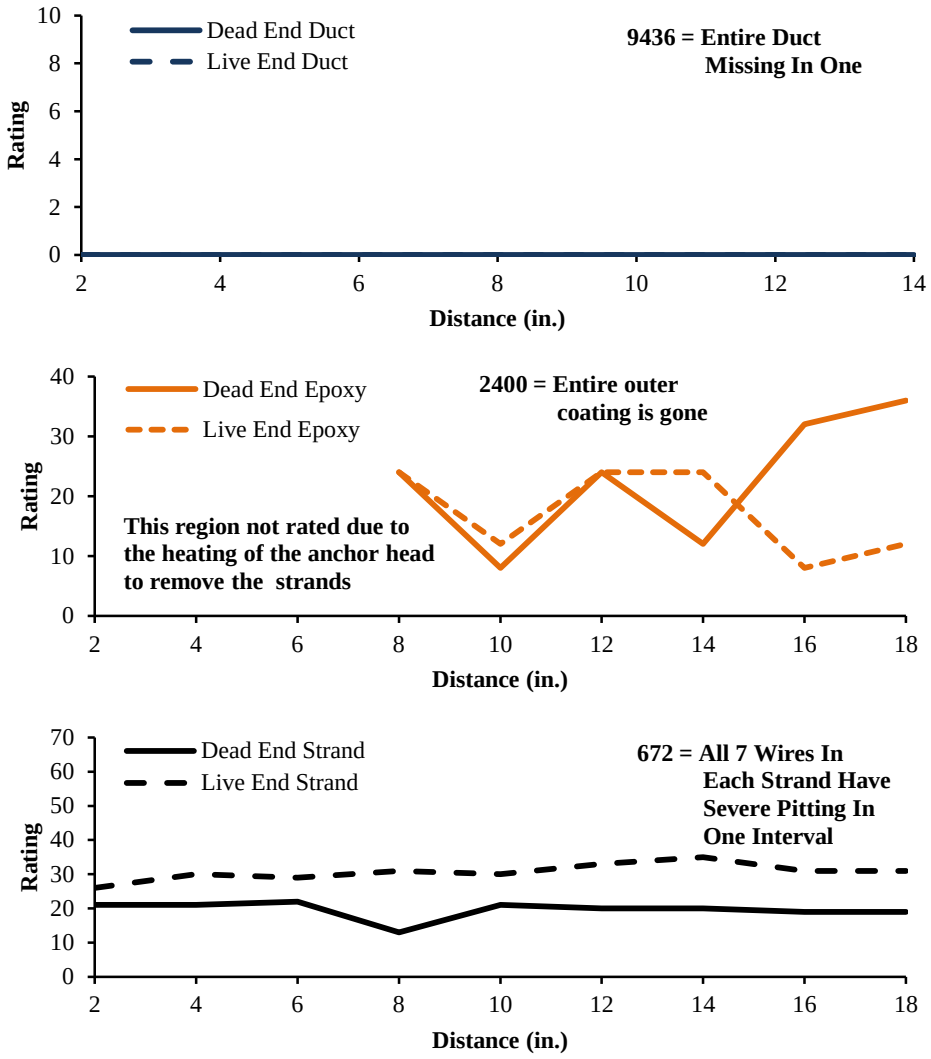

Figure 6.177: Corrosion Rating Plots for Dead and Live End Anchorage Regions of Specimen 7.4

The differential damage between the dead and live end post-tensioning components was from the spray system but the crack in the backfill mortar exacerbated the infiltration of chlorides to the anchorage components from the spray system. This crack would have allowed moisture, oxygen, and/or chlorides to enter the tendon and induce corrosion.

CHAPTER 7

Analysis of Results

7.1 Overall Observations from Forensic Analysis

7.1.1 Specimen Appearance and Cracking

Medium scaling was observed on the all the specimen's top concrete surface and the edges of the ponding area. A few of the specimens had bleed water voids on the bottom of the ponding area. Cracking at the interface between the backfill mortar and the base concrete was present on the majority of the dead and/or live ends of most of the specimens. Corrosion staining was observed in the area of at least one of the grout vents on all the specimens with galvanized duct, in the "wells" of the fully encapsulated specimens, on specimen 4.4 over top of the north uncoated steel reinforcement, and where a tie wire had corroded on Specimen 3.3.

The majority of the transverse cracks observed on the specimens were wider than when the live load was applied. All the longitudinal cracks observed were not noted immediately after live load application. Some of the specimens had cracks at the re-entrant corbel corners that had not been noted immediately after live load application. Some of the specimens with repaired re-entrant corbel corner cracks and with new re-entrant corbel corner cracks had efflorescence or evidence of water seeping from the cracks. This was an indication that moisture had infiltrated the specimen at these locations.

See Figure 7.1 for the crack ratings for all the specimens. Most of the specimens had a crack rating above the crack rating of 0.27, which is from a fictitious specimen with one transvers crack the width of the specimen (18 inches) and an average crack width of 0.015 inch. Specimens 1.3, 4.1, 5.2, and 5.3 were the specimens below the 0.27 crack rating. All these specimens had either 0.6 inch stainless clad or stainless steel strands. The average crack ratings for duct type were 0.26, 0.44, and 0.43 for galvanized duct, plastic duct, and non-prestress specimens, respectively. The specimens with plastic duct

had the highest average crack rating. The specimens with plastic duct all had longitudinal cracking whereas the specimens with galvanized duct did not. This would account for the higher average crack rating. The longitudinal cracking in the plastic duct specimens might be from the vastly different thermal coefficients of the plastic duct and concrete, which would have induced expansive stresses on the concrete thus inducing longitudinal cracking along the duct. Even though the galvanized duct had extensive corrosion damage, the corrosion damage did not cause further longitudinal cracking in these specimens. This might have happened because the bleed water voids in the grout allowed the corrosion product, which occupies a greater volume than the metal that produced it, to expand into the void instead of imposing transverse tensile stresses on the concrete. The non-prestressed Specimens 4.3 and 4.4 had the second highest average crack rating for two reasons. One reason, the specimens were not prestressed which resulted in the specimens having a applied Dywidag bar live load that was lower than the prestressed specimens and instead of the cracks opening wider during loading more transverse cracks formed[1]. The other reason is Specimen 4.4 had longitudinal cracking due to corrosion of the uncoated longitudinal reinforcement inducing transverse tensile stress on the concrete.

In the specimens with galvanized duct, Specimens 1.1 and 1.4 had an average crack rating of 0.46 whereas Specimens 1.3 and 4.1 had an average crack rating of 0.065. The quite different crack ratings between these two groups of specimens has to do with the amount of prestressing force that had to be applied to the specimens before they would crack. Specimen 1.3 and 4.1 had 0.6 inch strand whereas Specimens 1.1 and 1.4 had 0.5 inch strand. This resulted in a higher prestressing force in the former and therefore a higher live load was needed to crack the specimens. After the first crack/cracks appeared in Specimens 1.1 and 1.4 live loading was stopped. Stopping the loading at this level resulted in narrower and fewer cracks compared to the Specimens 1.1 and 1.4[1]. Therefore, since the cracks had very little growth on all the specimens, the crack ratings at the end of exposure were considerably less for Specimens 1.3 and 4.1. The cracks had

very little growth or shrinkage because the railroad springs did as they had been intended. They decreased the effects of creep and shrinkage on the prestressing.

For the specimens with plastic duct, Specimens 2.3, 3.3, and 5.1 had an average crack rating of 0.63 whereas Specimens 5.2 and 5.3 had an average crack rating of 0.20. The reason for this large difference is similar to the difference in the two groups with the galvanized duct. The strands in Specimens 5.2 and 5.3 had 0.6 inch strands whereas Specimens 2.3, 3.3, and 5.1 had 0.5 inch strands. Therefore, the prestressing force in the 0.6 inch strands was higher, which resulted in the live load for cracking being greater in Specimens 2.3 and 5.1. Also, during live load application the loading was stopped when cracking first appeared which resulted in narrower and fewer transverse cracks[1]. Therefore, since the cracks had very little growth on all the specimens, the crack rating at the end of exposure was considerably less for Specimens 5.2 and 5.3. The cracks had very little growth or shrinkage because of the railroad springs did as they had been intended. They decreased the effects of creep and shrinkage on the prestressing. Specimen 3.3 had the highest crack rating of 0.72. This might be due to the decreased modulus of elasticity due to the copper cladding. Copper has a lower modulus of elasticity. The decreased modulus of elasticity would have made the copper clad strands less resistant to the live load. Therefore, the live load, which was the same as the live load of the conventional strands, would have caused wider cracks, thus increasing the crack rating. The longitudinal cracking observed in the specimens with plastic duct was predominantly over the coupled duct and not over the continuous duct. The local effect of the couplers would reduce the effective cover and made that side more susceptible to longitudinal cracking.

The specimens with EIT's had an average crack rating 0.41. This is a lower average crack rating than the average crack rating of Specimens 2.3, 3.3, and 5.1. Even though the EIT specimens had longitudinal cracking from corrosion of the uncoated reinforcement used to facilitate taking AC impedance readings, the increased concrete cover over the duct might have restrained the longitudinal cracking due to the differences

in thermal coefficient. The longitudinal cracking from the corrosion of the uncoated reinforcement raised the crack ratings to higher than the average crack ratings of the specimens with galvanized duct.

The non-prestressed Specimens 4.3 and 4.4 had the second highest average crack rating of 0.43. As mentioned previously, the high cracking ratings for these specimens were so high because the specimens were not prestressed which resulted in the specimens having an applied Dywidag bar live load that was lower than the prestressed specimens. Instead of the cracks opening wider during loading more transvers cracks formed[1]. Specimen 4.4 had a higher crack rating than Specimen 4.3 because of the longitudinal cracking caused by the corrosion of the uncoated longitudinal bars.

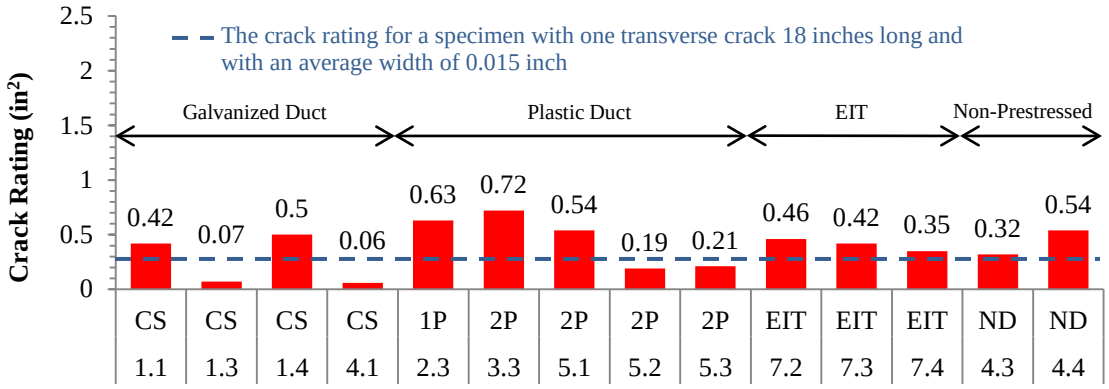

Duct Type:

CS – Galvanized Corrugated Steel Duct

1P - 1 Way Plastic Duct

2P – 2 Way Plastic Duct

EIT – Electrically Isolated Tendon

ND – No Duct (No Prestressing)

Figure 7.1: Crack Ratings

7.1.2 Longitudinal and Transverse Bars

The overall condition of the epoxy coated steel bars was quite good. Where there was corrosion, the corrosion was mild and contained in small areas. However, there were a few areas with pitting. The corrosion usually occurred at places where the epoxy

coating had been damaged either by handling or where the other components might have cracked the epoxy coating during the placement of concrete. Discoloration was the major form of corrosion that had been observed. The areas with discoloration usually occurred where the epoxy coated tie wire that was used to connect the transverse reinforcement to the longitudinal bars or the duct to the transverse reinforcement had corroded. The epoxy coated ties were corroded because of two reasons. One reason is the cut ends of the wires had not been coated with epoxy to protect them from corroding. The other reason is the epoxy coating had rubbed off during the handling of the reinforcement cage either during placement of the concrete or inserting the completed cage in the formwork. The longitudinal uncoated steel reinforcement in Specimen 4.4 had extensive corrosion damage in the regions of the transverse cracks. The damage ranged from mild corrosion to pitting. However, there was no appreciable cross sectional area loss on the uncoated bars. These exposure tests clearly showed the benefit of epoxy coated bars.

Figure 7.2 shows the longitudinal and transverse bars generalized corrosion ratings and crack ratings for each specimen. There was a slight correlation between the crack and corrosion ratings of the longitudinal and transverse bars, the higher the crack rating the higher the corrosion rating. Generally, the location of the corrosion and discoloration observed on the epoxy coated bars was located in the vicinity of the transverse cracks. For Specimen 4.4, the high crack rating corresponds to the high rating for the uncoated longitudinal steel reinforcement. As mentioned previously, the expansive stresses from the corrosion of the longitudinal steel reinforcement might have caused the longitudinal cracking observed in Specimen 4.4. The 7-series specimens had the highest corrosion ratings for longitudinal and transverse bars. This might be because the specimens were larger and therefore the reinforcement cages were larger. As size of a reinforcement cage goes up the stability of the cage goes down. Since the stability of the cage was less, the chance of the epoxy coating of the bars being damaged increased when the cage was being handled. The epoxy coating being damaged would have increased the corrosion

rating because the underlying reinforcement at the damaged coating would have had no protection from corrosion.

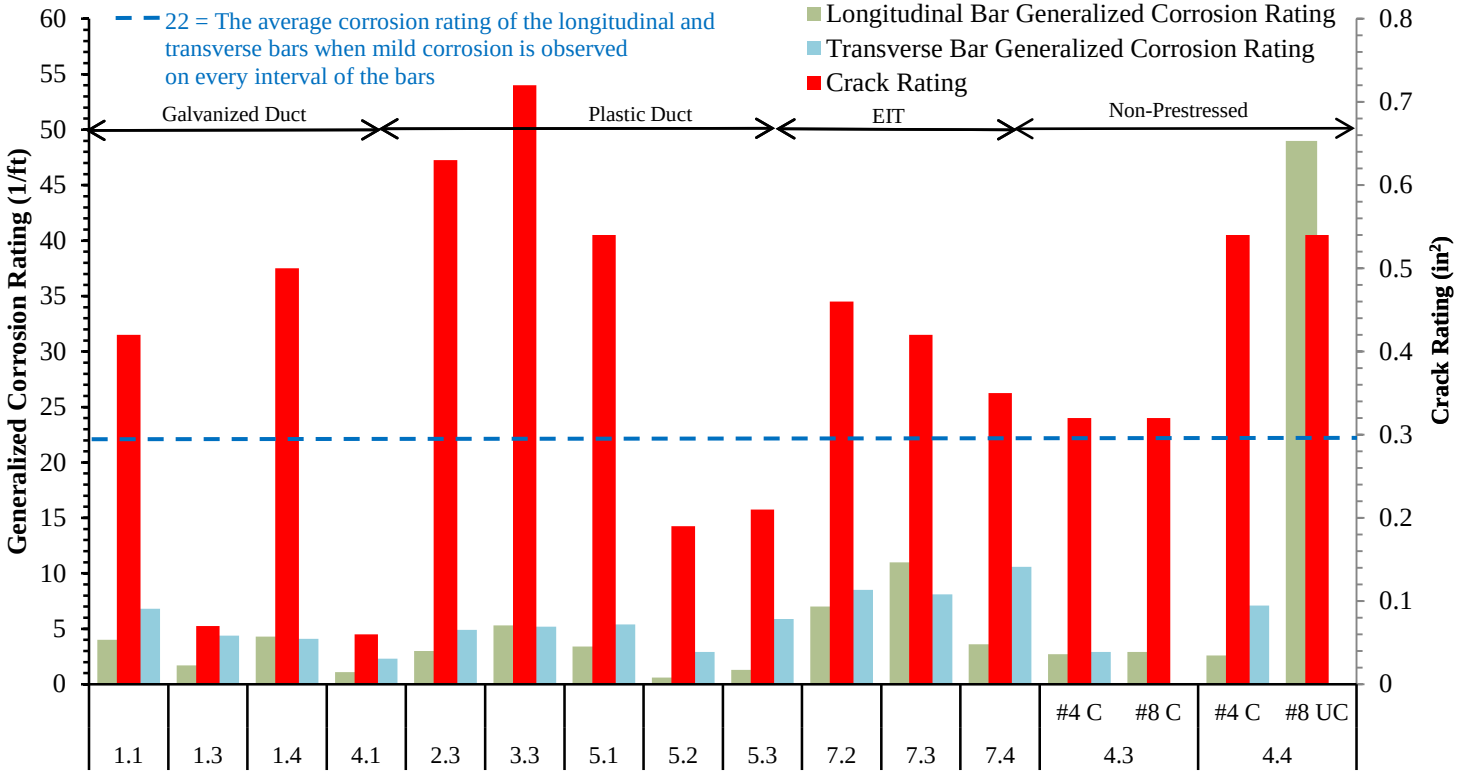

C – Epoxy Coated Longitudinal Bars

UC – Uncoated Steel Longitudinal Bars

Figure 7.2: Longitudinal and Transverse Bars Generalized Corrosion Ratings and Crack Ratings

7.1.3 Duct

The galvanized corrugated steel ducts did not hold up well under the corrosive environment that they had experienced. At locations of bleed water voids in the grout, the galvanized duct had substantial area loss and severe corrosion. In areas without area loss, pitting and moderate corrosion was observed over large portions of the duct. Also, the areas with the most damage were at locations in close proximity to the specimen's transverse cracks. The average corrosion rating for the galvanized duct was 3400.

Slight gouging was observed on the inside of all the specimens with plastic duct. These slight gouges were either from the strand being threaded through the duct and/or the strands rubbing against the duct during stressing. Specimen 5.3 had the highest average generalized damage rating for plastic duct of 69. These ducts contained stainless steel strands, which were highly curved and the curved nature of the strands would have easily gouged the duct during threading through the duct. The average damage rating for all the plastic ducts was 31. This is far below the average corrosion rating of the galvanized duct. This is an indication that the plastic duct is far superior to the galvanized duct in highly aggressive environments. The average damage rating for the plastic ducts from the conventionally post-tensioned specimens was 35. The average damage rating from the EIT specimens was 23.

Except for Specimen 7.2, none of the plastic ducts had observed holes or cracks. This indicates that the high chloride levels found in the tendons of the plastic ducts did not come from a defect in the duct except for Specimen 7.2 that had a crack at the location of the dead end grout vent. The seal of the heat shrink wrap to the duct and coupler was observed to be inadequate to keep out contaminants in the north duct and the 7-series specimen's duct. Also, the couplers used to connect the two halves of the north duct and to connect the sections of the 7-series specimen's duct did not provide an adequate seal to keep out contaminants. The silicone used to attach the grout vents to the south ducts was found to be loose on all specimens. All of these factors would have

provided a path for chlorides to enter the ducts and explain the elevated chloride concentrations that had been observed in the grout from the specimens with plastic duct.

7.1.4 Grout

The condition of the grout varied from specimen to specimen and at times from tendon to tendon. The specimens that were grouted earlier in the fabrication process had grout that was in poorer condition than the specimens that had been grouted later. The grout from the earlier specimens had grout that had greater variations in color, were rough to the touch, and broke apart easily when the duct was removed from the tendon. These characteristics suggest that pump pressure during grouting of the tendon was not well maintained. The specimens fabricated later had less color variations, had a smooth texture, and the grout was tougher to break when the duct was removed from the tendon. Also, there were color variations in the grout between tendons of the same specimens with plastic duct. The north tendons, which were the spliced tendons, generally had greater color variations than the south tendons, which were continuous. This suggests that the pressure in the north tendon was harder to maintain during grouting of the tendon. The vast majority of voids present on top of the grout in all tendons were generally small. However, large voids were usually present at the apex of the galvanized ducts. Some of the grout had partial strands visible on the bottom, suggesting that the grout did not consolidate well around the strands. The bond between the grout and the strand varied from strand type to strand type. For the most part, the majority of the chloride concentrations were well above the chloride concentration believed critical for corrosion of 0.033% by weight of grout. The exceptions were at the apex of the ducts from Specimens 7.4 and 7.3. Combined with the uniform discoloration and/or corrosion of the strands, the high chloride concentrations suggests that chlorides had entered the grout and reached the strands and proceeded to travel along the interstices of the strand and/or the interstitial space between the stand and the grout.

7.1.5 Strand

Most of the corrosion observed on the outer wires of the conventional strands was light. Where no corrosion was observed some discoloration was present. However, mild pitting was observed only on the outer wires of one strand from Specimen 7.2. The pitting was located at the dead end grout vent where a crack in the duct had been observed. The inner wires of the conventional strands had greater corrosion damage with moderate corrosion along many of the intervals and with minimal pitting. The hot dip galvanized strand had similar damage as the conventional strand. The outer wires on the galvanized strand had signs that the zinc and underlying steel was corroding and the inner wires showed signs of the steel corroding where the galvanized coating had not covered the underlying steel in the interstitial space between the outer and inner wire. The outer and inner wires of the copper clad strands had a very dark brown discoloration along the length of the wires. Also, occasional tiny reddish colored spots were observed on the copper clad wires. Other than very few spots of discoloration and corrosion, the inner and outer wires of the stainless clad and stainless steel strands were faultless. The flowfilled epoxy coated strand did not perform as expected. The inner and outer wires had corrosion ranging from mild pitting to light corrosion over the majority of their lengths. This corrosion might have been from the paint stripper used to remove the epoxy coating in the autopsy process or the corrosion may have existed before the strand was coated. The latter might be the more valid reason because the half-cell potentials taken during the exposure testing suggest that corrosion had already existed before the stripper was applied.

7.1.6 Anchorages

The conventionally post-tensioned systems showed signs of damage on all components. All the anchorage plates had light corrosion on their outer surface where the epoxy coating had not adhered well. On the embedded portion of the anchorage plates, corrosion was most prominent on the underside of the anchorage plate and where duct tape was used to attach and seal the plastic duct to the anchorage plate. This

suggests that moisture, oxygen, and/or chlorides had infiltrated to this region where a possible void had formed during casting. On specimens that did not use duct tape to seal the duct to the anchorage plate, no corrosion was evident. The ducts from the anchorage regions showed similar damage to their counter parts from the main autopsy region. The condition of the grout was similar to the grout from the main autopsy region but with smaller voids and had chloride concentrations ranging from slightly above to well above the corrosion threshold. The damage to the strands was most evident in the region of the anchor head. The wedges were intact and had either light or moderate corrosion.

The fully encapsulated systems had greater damage to its components than the conventionally post-tensioned systems. In fairness to the system manufacturers who ordinarily install these systems on projects, the EIT systems were installed by the same graduate students who installed all systems. The more complex EIT system might require more care and experience in the installation than the other systems. The steel retaining rings from all specimens had pitting, moderate corrosion, and light corrosion on all surfaces. The anchorage plate had pitting, severe corrosion, and moderate corrosion on the exposed face. The embedded faces were corrosion free. The ducts from the anchorage regions were in similar condition to the duct sections from the main autopsy region. The strands showed similar damage to the strands from the main autopsy region. The wedges were intact and some had either light or moderate surface corrosion.

Except for the 7-series specimens, the presence of the dripper system did not seem to have much of an effect on the anchorage components. This suggests that the damage observed in the anchorage regions might be from another source. The path of salt water solution, moisture, and oxygen was more than likely from the cracks that had been observed at the interface of the backfill mortar and the base concrete. The salt water solution could have entered the cracks when the ponding area was emptied after the wet exposure cycle. The 7-series specimens had greater damage to the dead end anchorage region, which was the end exposed to the dripper system. This might be from the cracking observed in the backfill mortar of the anchorage pockets allowing chlorides to

infiltrate deeper into the mortar than the uncracked backfill mortar from the conventionally post-tensioned specimens.

7.2 Analysis of Variables

7.2.1 Strand Type

A direct comparison of the different strand types cannot be made because of the corrosion properties of the different metals. Figure 7.4 shows the generalized corrosion rating for the strands and the maximum chloride concentration plotted together and organized by strand type. The maximum chloride concentration for all the tendons was well above the threshold for corrosion.

Of the tendons with conventional strand, Specimen 7.2 had the highest corrosion rating but did not have the highest chloride concentration. The crack in the duct undoubtedly was the major contributor to this highly localized corrosion. The south tendon of Specimen 2.3 had the highest chloride concentration of the tendons with conventional strand. The tendons with conventional strands that had the lowest corrosion rating were the south tendons of Specimens 1.1 and 1.4. Both of these tendons had chloride concentrations around the median for the chloride concentrations of the tendons with conventional strands. The tendon with conventional strand that had the lowest chloride concentration was the north tendon of Specimen 1.4 and had a corrosion rating around the median for the conventional strands. Since the highest chloride concentration does not correspond to the highest corrosion rating, it can be assumed that corrosion rating is not dependent on chloride concentration once the threshold for corrosion is met for conventional strands.

The corrosion ratings for the north and south tendons with copper clad strand were identical. However, the chloride concentration for the north tendon was lower than the south tendon. Like the conventional strands, this suggests that the corrosion rating for copper clad strand is independent of chloride concentration.

The hot dip galvanized strand had a corrosion rating similar to the conventional strands. There was no other tendon to compare the corrosion rating to. Therefore, a determination cannot be made if different levels of chloride concentration would affect the corrosion rating of hot dip galvanized strands.

The corrosion rating for all the tendons with stainless clad strands were relatively the same. The highest corrosion rating was from the south tendon of Specimen 1.3 and the lowest corrosion rating was from the north tendon of the same specimen. The corrosion ratings from the north and south tendons of Specimen 5.2 were nearly equal. The tendon with stainless clad strands with the highest corrosion rating had the lowest chloride concentration of the tendons with stainless clad strands. Like the previous strand types, the corrosion rating seems to be independent of chloride concentration.

The corrosion ratings for the stainless steel strands were nearly equal. Even though there was minimal discoloration, the stainless steel strands were essentially in same condition as when they were installed, with no visible defects. The tendons with stainless steel strands had varying chloride concentrations. The strands from the south tendon of specimen had the lowest corrosion rating but the highest chloride content of the tendons with stainless steel strands. Again, like the previous strand types, the corrosion rating seems to be independent of chloride concentration.

The flowfilled epoxy coated strands had the highest corrosion rating of all the strands and could be compared to the conventional strand because the strands were the same as the conventional strands but with an epoxy coating. This strand type did not perform as initially expected. However, there is a question of when the corrosion was initiated. Did the corrosion exist at time of installation of the strands or did the paint stripper used to remove the epoxy coating cause the corrosion. To determine if the paint stripper was the cause of the corrosion observed on the flowfilled epoxy coated strands, a simple experiment was run. A sample of conventional strand wires was treated in the same manner that had been used to strip the epoxy from the flowfilled epoxy coated strand. Two wires from a conventional strand were lightly polished, covered with paint

stripper, and encased in aluminum foil for seven days. After seven days, the wires were examined for any corrosion that would be similar to that observed on the flowfilled epoxy coated strand. There was no corrosion on the wires and this differed greatly from the flowfilled epoxy coated strand. Figure 7.3 shows the appearance of the wires before and after seven days of exposure to the paint stripper. This observation indicates that the paint stripper was not the cause of the corrosion observed on the flowfilled epoxy coated strand.

The chloride concentration for the grout in the tendon with epoxy coated strands was around the median of the chloride concentrations for the grouts in the tendons with conventional strands. This indicates, again, that the corrosion rating was independent of the chloride content.

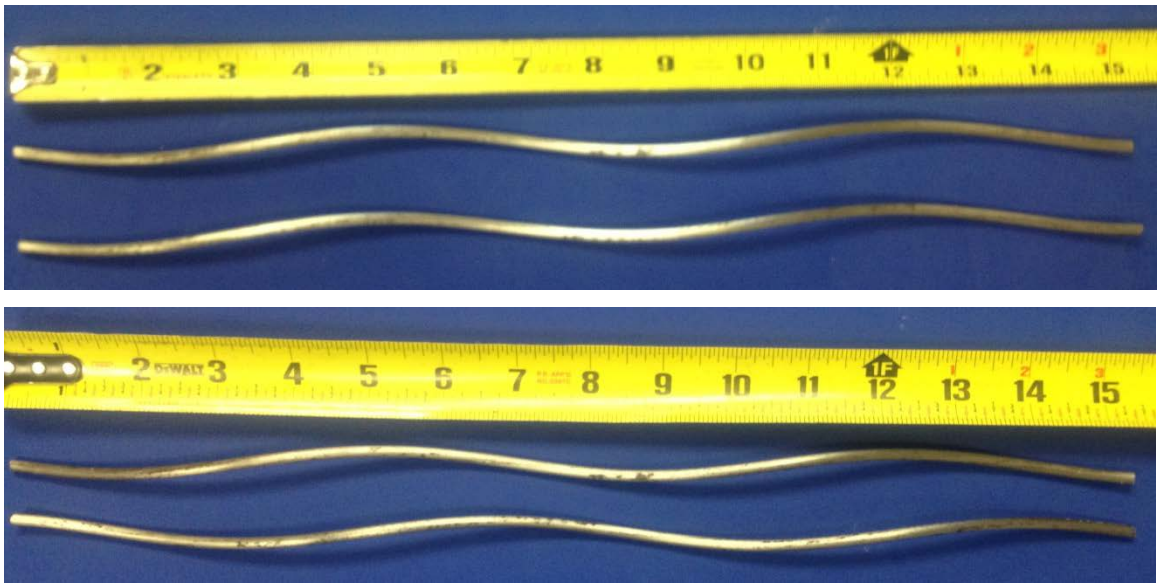

Figure 7.3: Conventional Wires Before (Top) and After (Bottom) Exposure to Paint Stripper

The average strand generalized corrosion ratings are plotted with crack ratings for each specimen in Figure 7.5 and are organized according to strand type. There is no correlation between corrosion rating and crack rating for each strand type. In the case of the strands, a high crack rating does not mean that the corrosion rating will be high as well.

All tendons had sufficient chloride concentrations to induce corrosion. The stainless steel and stainless clad strands performed the best in resisting corrosion. The copper clad strands were the next highest performer. For the conventional strand, there was no discernible difference in the corrosion ratings between the strands in galvanized duct and the strands in plastic duct. The hot dip galvanized and conventional strands were essentially undamaged, except for the strands from Specimen 7.2. Surprisingly, the flowfilled epoxy coated strands performed the worst. However, it is not sure when or how this corrosion was initiated. The chloride concentrations clearly show that the seal and coupling methods for the plastic duct are not adequate. The performance of the EIT system at keeping out chlorides was poor and indicates that the system as constructed is not worth the extra cost.

The role that grout plays in mitigating corrosion cannot be neglected. Grout quality was not rated in this research. Much more effective grouting was displayed in the Project 0-4562 specimens than the earlier Project 0-1405 specimens in this series. The grout quality varied somewhat from specimen to specimen and tendon to tendon. The tendons were grouted with a hand pump instead of the industry standard electric pump[1]. The voids would have been possibly eliminated or made smaller if an electric pump had been used. Regardless of grout quality, grout can be cracked under service loads, because the grout is not prestressed, and the cracks create a pathway for chlorides to reach the strands.

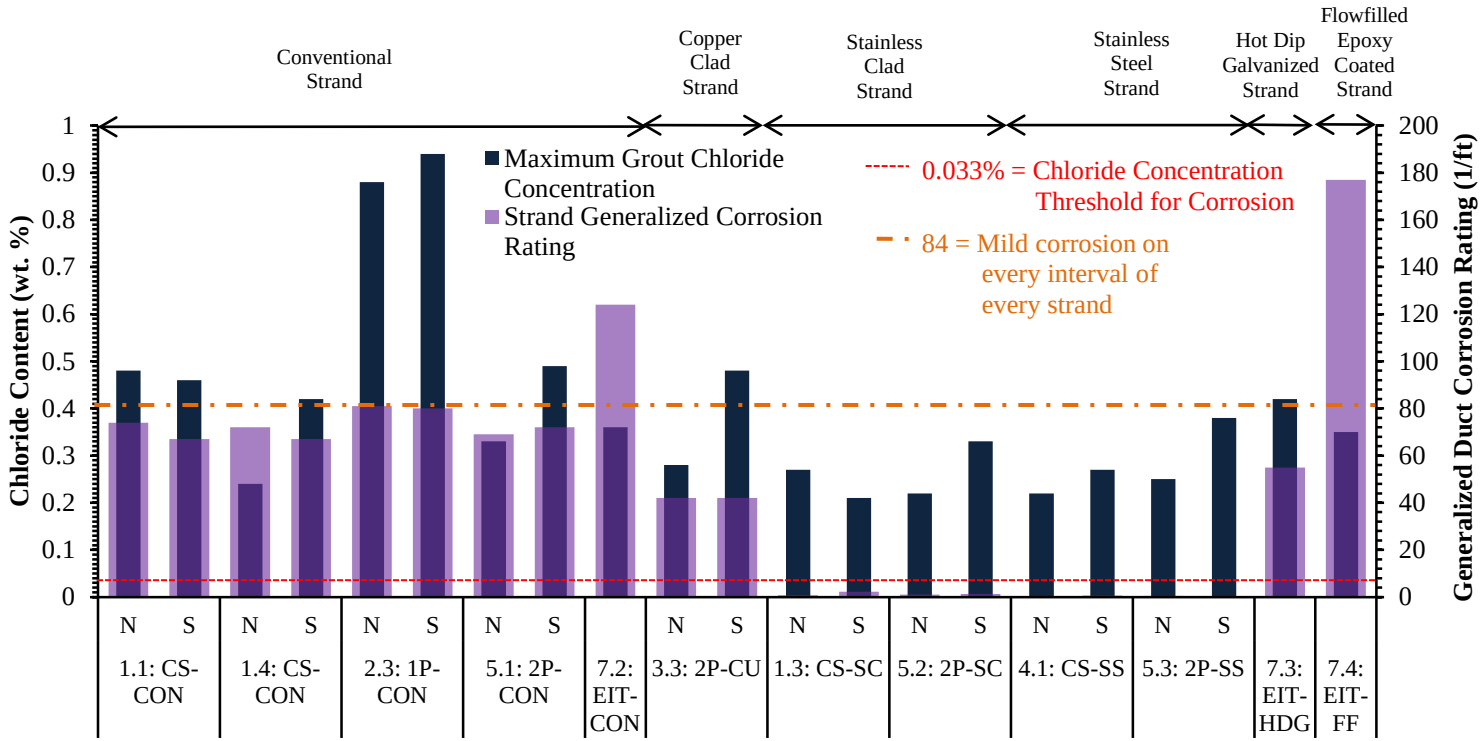

N – North Tendon
S – South Tendon

CON – Conventional Strand
CU – Copper Clad Strand
SC – Stainless Clad Strand

SS – Stainless Steel Strand
HDG – Hot Dip Galvanized Strand
FF – Flowfilled Epoxy Coated Strand

CS – Galvanized Corrugated Steel Duct
1P – One-way Plastic Duct
2P – Two-way Plastic Duct

EIT – Electrically Isolated Tendon

Figure 7.4: Generalized Strand Corrosion Ratings and Maximum Tendon Chloride Content

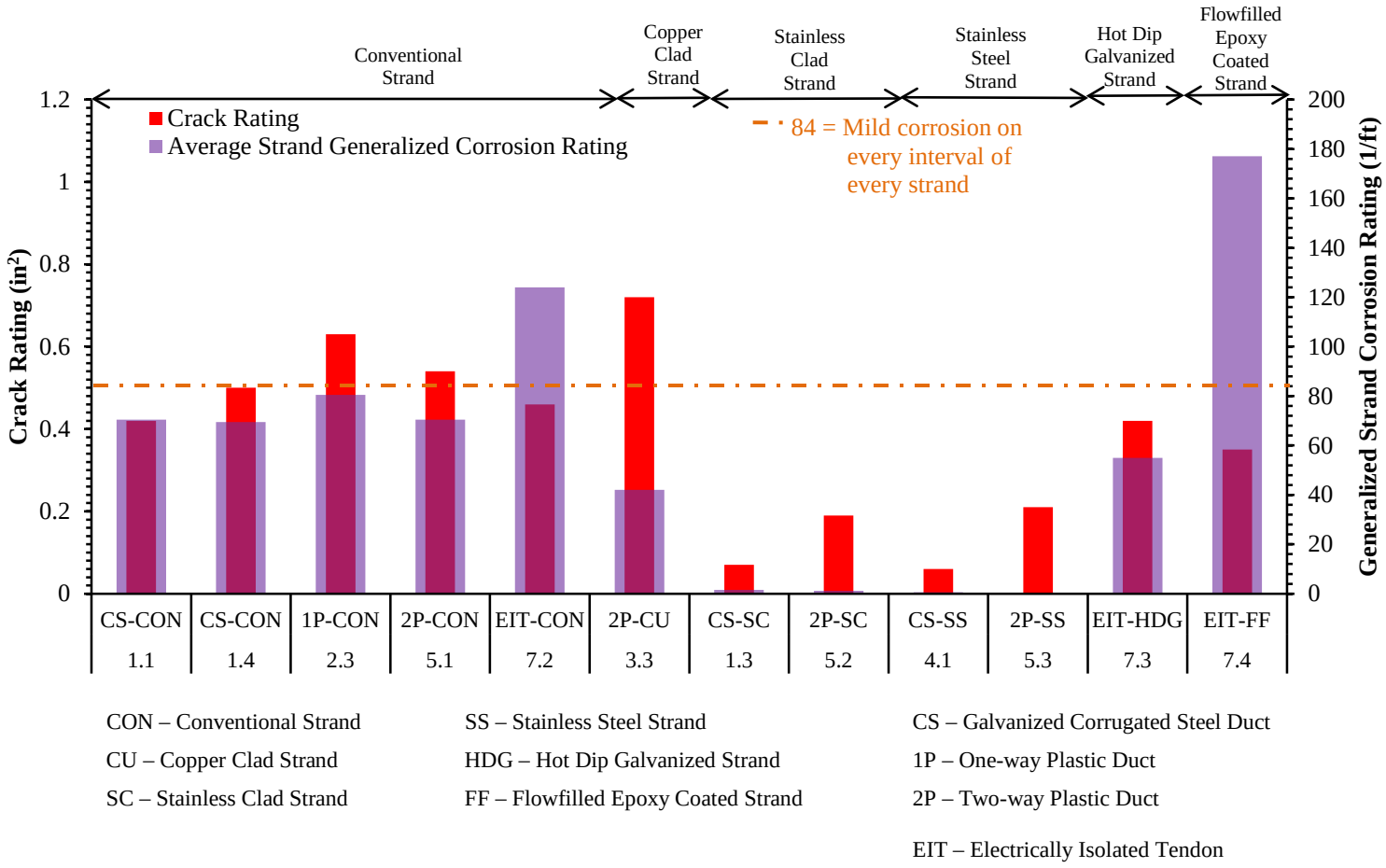

Figure 7.5: Average Generalized Strand Corrosion Rating and Crack Rating

7.2.2 Duct Type

The specimens that had been autopsied contained four different duct types: two-way plastic duct, one-way plastic duct, galvanized corrugated steel duct, and another one-way plastic duct. The plastic duct came from two different vendors. One of the one-way ducts and the two way duct came from GTI. The other one-way duct came from VSL. The one-way duct from VSL was used in the EIT specimens. Figure 7.6 shows the generalized duct corrosion/damage ratings plotted with the maximum chloride concentration for each tendon.

There was a slight correlation between the corrosion ratings of the galvanized ducts to the maximum chloride concentrations. In general the higher the chloride concentrations in the grout the higher corresponded to the corrosion ratings for the galvanized duct. Surprisingly, the highest maximum chloride concentration was not from grout encased in galvanized duct but from grout encased in one-way plastic duct. On average, the chloride concentrations in the tendons encased in plastic duct were higher than in the tendons encased in galvanized duct. This is almost certainly due to the poor seal of the heat shrink wrap and the coupler used to connect the duct of the spliced ducts and the loose silicone around the grout vents in the continuous duct. The higher chloride concentrations in the grouts encased in plastic duct are certainly disconcerting. The poor seals on the plastic duct would have allowed chlorides to enter the tendon sooner than the galvanized duct because the chlorides would not be able to enter the tendon until corrosion created a hole in the galvanized duct. There is no correlation between the damage rating to the plastic duct and the chloride concentrations of the tendons. However, there is a correlation between the type of grout vent used and the chloride concentration of the tendon. When plastic ducts from the same specimens are compared the ducts with the researcher installed grout vents consistently had higher chloride contents than the manufacturer installed grout vents. This indicates that far more

attention must be given to the overall integrity of the plastic duct system during fabrication.

Figure 7.7 shows the average generalized duct corrosion/damage ratings plotted with the crack rating for each specimen. For the galvanized ducts there was a definite correlation between the corrosion rating and the crack rating. For the majority of the specimens with galvanized duct, the higher crack ratings correspond to the higher duct corrosion ratings. In the autopsy it was noted that Specimen 1.1 had larger voids in the grout than the grout from the tendons in Specimen 1.4. This would suggest that both the number and size of voids and the number and size of the cracks contributed to the corrosion damage observed on the ducts.

The damage ratings for all of the plastic ducts were very low. Except for the duct from Specimen 7.2, the damage observed on the interior of the plastic ducts was gouging from the stressing and/or threading of the strands, which did not penetrate the duct walls. Specimen 7.2 had a through crack observed in the region around the dead end grout vent. This crack gave it the third highest damage rating of the plastic duct. The specimens with the highest damage rating of the plastic ducts were from the Specimens 5.2 and 5.3, which contained stainless clad and stainless steel strands, respectively. The highly curved nature of these strands caused gouging on the interior that would explain the elevated plastic duct damage ratings. Specimen 7.3 had a fairly elevated plastic duct damage rating similar to Specimen 7.2. This might be because of the size of the duct and not the curvature of the strand. The diameter of the one-way VSL duct was smaller than either of the GTI duct types. This would have caused the strands to gouge the duct more easily during threading than the GIT ducts. The possible reason for the duct from Specimen 7.4 having a low damage rating is the epoxy coating on the strand acted as a buffer between the strand and the duct, therefore protecting the duct from being gouged as much as the other 7-series specimens. No matter what the damage rating was, the condition of the plastic ducts were not affected by the amount of chlorides at the level of the ducts due to the transverse or longitudinal cracks that had been observed.

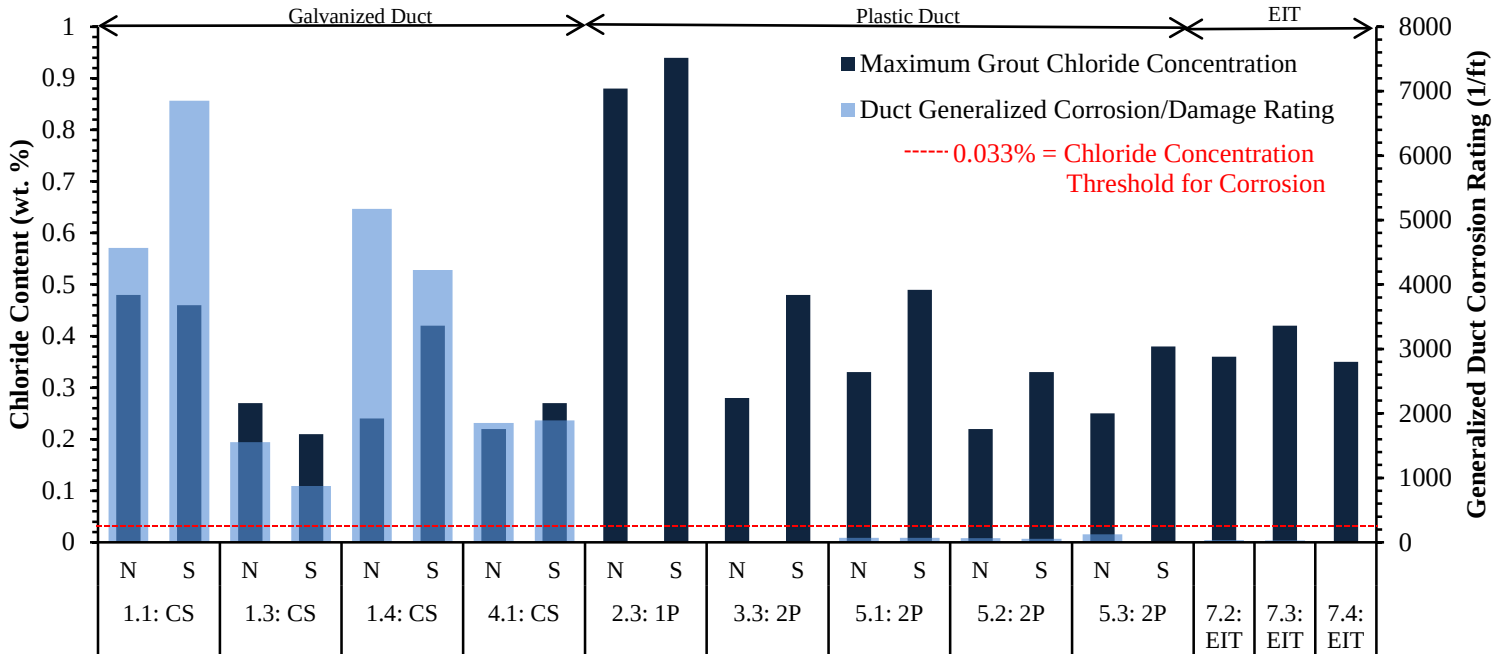

CS – Galvanized Corrugated Steel Duct

1P– One-way Plastic Duct

2P – Two-way Plastic Duct

EIT – Electrically Isolated Tendon

Figure 7.6: Generalized Duct Corrosion/Damage Rating and Maximum Chloride Concentration

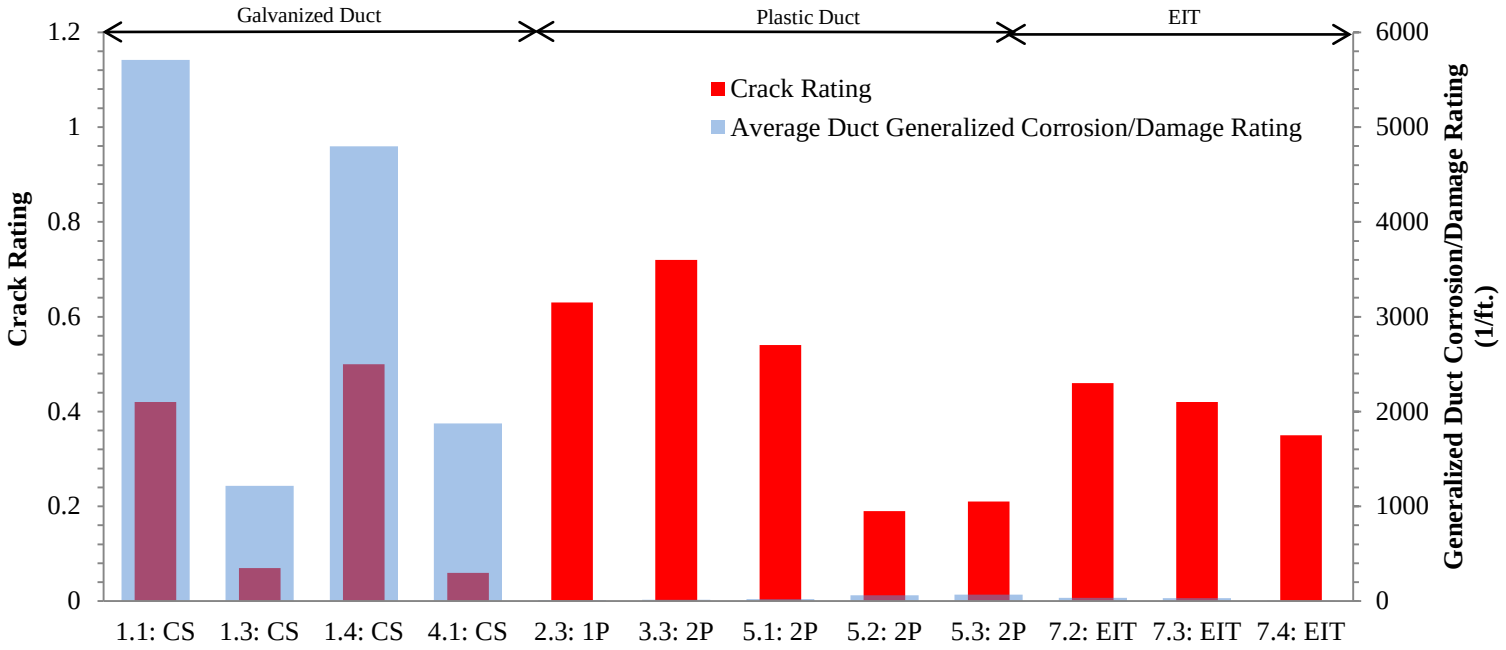

CS – Galvanized Corrugated Steel Duct

1P– One-way Plastic Duct

2P – Two-way Plastic Duct

EIT – Electrically Isolated Tendon

Figure 7.7: Average Generalized Duct Corrosion/Damage Rating and Crack Rating

Except for Specimen 7.2, the integrity of the plastic ducts away from the splices and vents was intact at time of autopsy. The damage observed on Specimen 7.2 was more than likely from when the ducts were installed in the reinforcement cage. Even though high chloride concentrations were observed in the grouts encased in plastic duct, plastic duct can be a more effective barrier against chloride infiltration than galvanized duct if the points of infiltration can be properly sealed. The couplers, grout vents, and heat shrink wrap need to have a positive water tight seal to the duct. If a positive water tight seal can be formed, then the plastic duct can be an effective barrier against chloride infiltration even in a high chloride environment. Such water tight seals are routinely used in PVC water supply systems where solvents or pipe threads are used in the connection process. It is imperative that such a positive water tight seal be developed for the plastic ducts. The current grout vents used on plastic duct are threaded and "welded" to the duct or coupler (Figure 7.8).

Figure 7.8: Threaded Grout Vent "Welded" to Plastic Duct (Top) and Cut Away of Slip-on Coupler with "Welded" Threaded Grout Vent

7.2.3 Coupler Type

No couplers were attached to the tendons encased in galvanized ducts. Two types of couplers were used to connect the sections of ducts that encased the north tendons of conventional post-tensioned specimens: GIT snap-on and GTI slip-on. The ducts from the fully encapsulated specimens had VSL snap-on couplers.

Figure 7.9 shows the grout chloride concentration in the tendon at the location of each coupler. The highest grout chloride concentration was found in the duct with a GTI snap-on coupler. This was expected since during the autopsy grout was seen in the space between the duct and the coupler past the seal of the coupler. This indicates that the seal was not water tight and was the access point for chloride infiltration. The lowest grout chloride concentration was at the dead end coupler of Specimen 7.2. This was the region in which the duct had been cracked. There is no definitive reason for the low chloride concentration in the region of the cracked duct. On average the heat shrink wrapped GTI slip-on couplers had the lowest grout chloride concentration but the concentrations were still well above the corrosion threshold. The couplers and heat shrink for the 7-series specimens did not perform as well as expected. Most of the grout chloride concentrations were well above the corrosion threshold. The high grout chloride concentrations support the corrosion observed on the strands during the autopsies.

Figure 7.10 shows the grout chloride concentrations at midspan for specimens that contained two tendons encased in plastic duct. All the grout chloride concentrations were above the corrosion threshold. The south tendons, which were encased in continuous ducts that had grout vents attached by project staff during manufacture, had grout chloride concentrations that were consistently higher than the north tendon, which were encased in a coupled duct with a manufacture installed grout vent on the coupler. While both ducts allowed excessive amounts of chlorides into the tendon, the continuous duct, with the researcher installed grout vent, performed the worst. This reaffirms the corrosion observed in the strands during the autopsies.

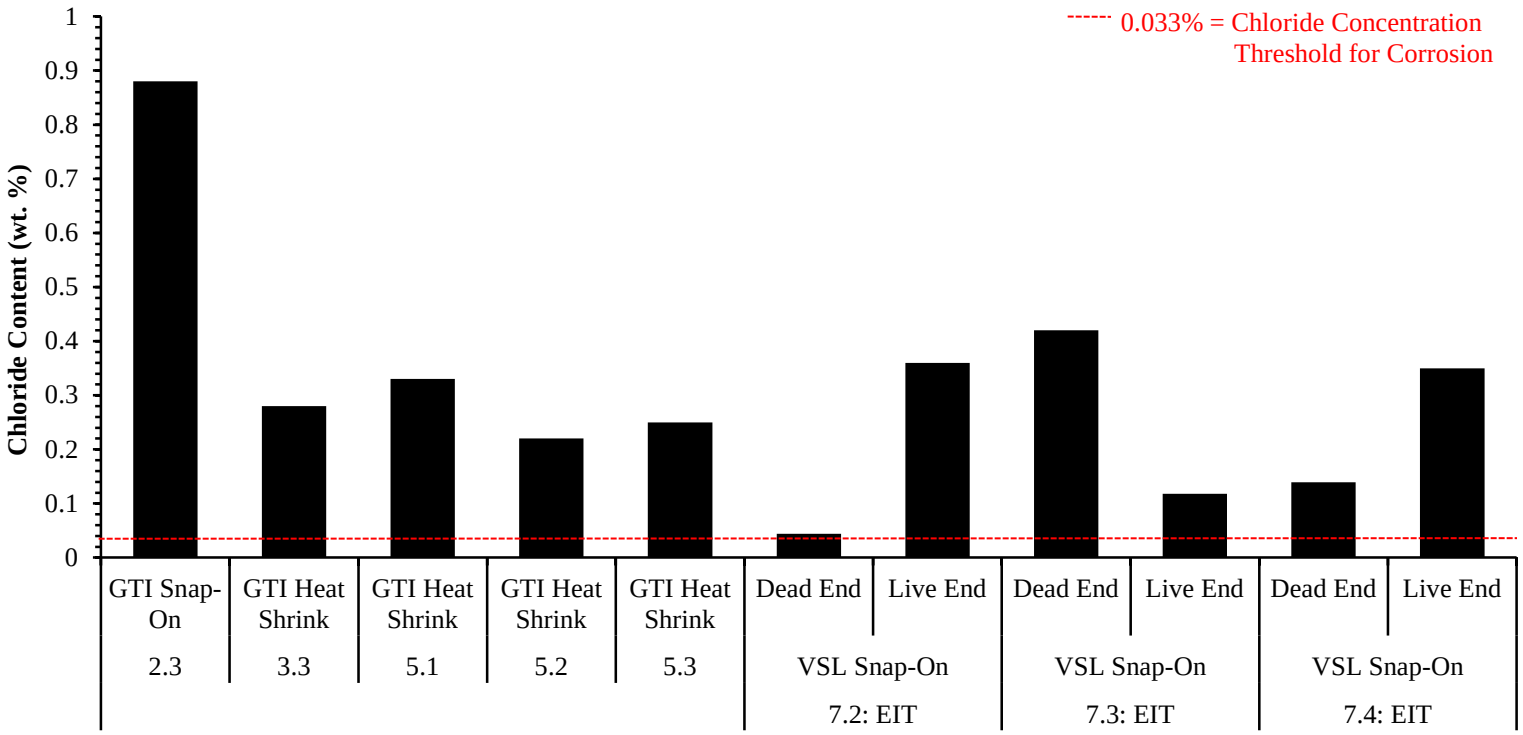

Figure 7.9: Grout Chloride Concentrations at Coupler Location

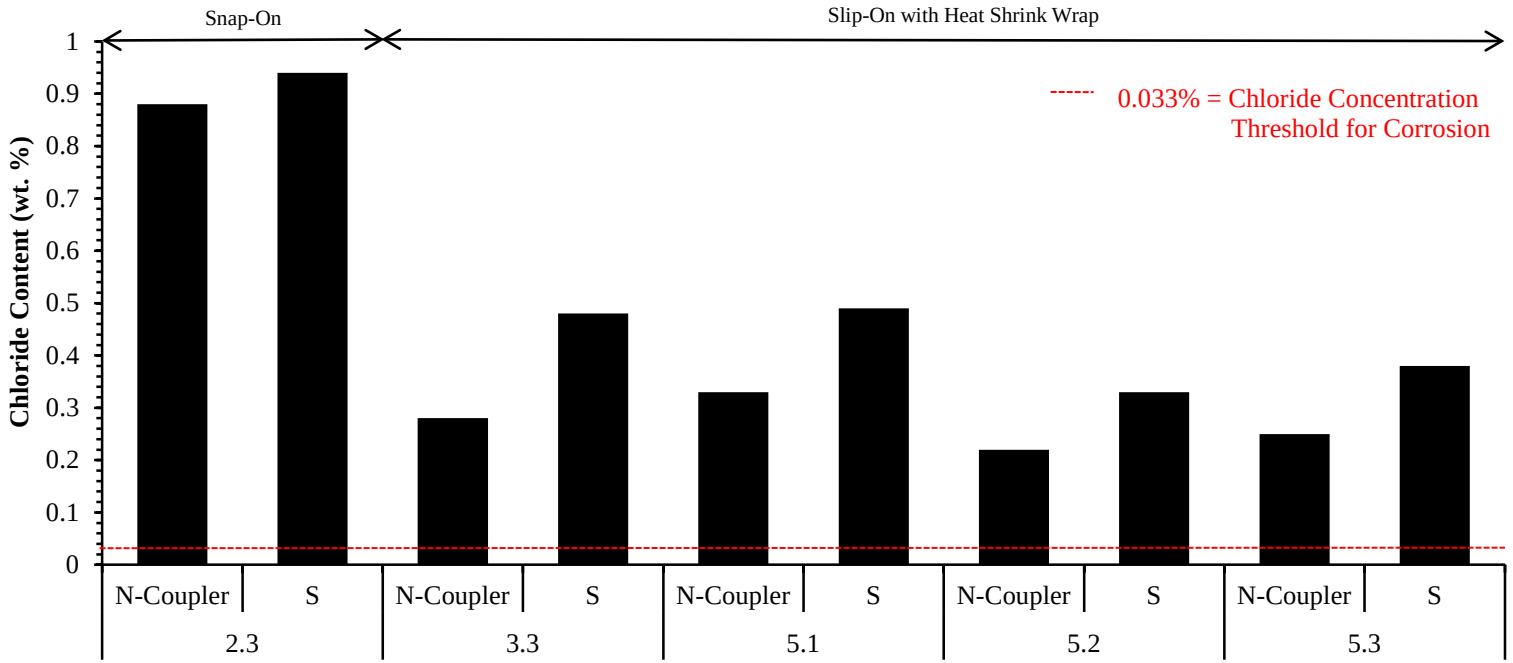

Figure 7.10: Grout Chloride Concentrations at Midspan for Specimens with Two Plastic Ducts

7.2.4 Anchorage Type

Of the specimens autopsied in this series, only Specimens 1.4 and 5.1 had galvanized anchorage plates. Duct tape was not used to seal the ducts to the anchorage plates for Specimens 1.1, 1.3, 1.4, and the 7-series specimens. All of these did not have visible signs of corrosion on the embedded portion of the anchorage plate but all did have visible corrosion of the exposed face of the anchorage plate. Duct tape was used to seal the ducts to the anchorage plates of the remainder of the specimens and all had visible signs of corrosion on the bottom of embedded portion and the exposed face of the anchorage plates. However, the corrosion of Specimen 5.1 was less severe and not as wide spread. In general, all the non-galvanized anchorage plates had visible signs of corrosion.

Specimens 1.1 and 1.4 both had conventional strands, galvanized duct, and duct tape was not used to seal the ducts to the anchorage plates. Therefore, they will be used to compare the effects of bearing type on the other components within the anchorage region of the specimens. Specimen 5.1 will not be used because it had its dead end sprayed with salt water solution and it contained plastic ducts. As mentioned previously, the anchorage plates from both specimens had no visible signs of corrosion on their embedded portions. However, the visible corrosion on the exposed faces of the anchorage plates from Specimen 1.1 was more wide spread than the visible corrosion on the exposed faces of the anchorage plates from Specimen 1.4 (Figure 7.11). This is because the zinc in the galvanized coating acted as a sacrificial coating as it was intended. The zinc acts as a sacrificial coating when used with steel because it is the more active metal on the galvanic scale. The level of corrosion in the ducts from the dead end anchorage regions of Specimens 1.1 and 1.4 were essentially the same. However, the level of corrosion on the strands was greater on the strands from Specimen 1.1 than 1.4. This might suggest that the zinc coating on the duct and anchorage acted as a sacrificial anode for the strand.

Figure 7.11: Corrosion on Exposed Faces of Galvanized (Left) and Non-Galvanized (Right) Anchorage Plates

In all, the galvanized anchorage plates from Specimen 1.4 performed better than the non-galvanized anchorage plates from Specimen 1.1. However, caution must be taken before deciding on using galvanized anchorage plates because it is not clearly understood how the galvanized coating will affect the steel components of the system. The level of corrosion on the non-galvanized anchorage plates was not severe enough to effect structural integrity after six years of aggressive exposure.

7.2.5 Fully Encapsulated System

Specimens 7.2, 7.3, and 7.4 had electrically isolated tendons. Except for the grout chloride concentrations at midspan, grout chloride concentrations were well above the corrosion threshold. The grout chloride concentrations at midspan were very near to the corrosion threshold (Figure 5.15) and were much lower than the grout chloride concentrations at midspan of the conventional post-tensioning system with plastic ducts (Figures 5.13 and 5.14). The chloride concentrations at midspan of these tendons should be the lowest because the duct was not breached at this location and midspan is the highest point on the duct. The ducts in the conventionally post-tensioned specimens with plastic ducts had either a researcher installed grout vent or a coupler with a manufacturer installed grout vent at midspan. The corrosion ratings for the epoxy coated steel reinforcement were a little higher than the conventionally post-tensioned specimens

(Figure 7.2). This might be due to the amount of cracking caused by corrosion of the uncoated reinforcement that had been used for the AC impedance monitoring that had been observed on the specimens. Specimen 7.2 had the highest corrosion rating of the conventional strands. This is due to the crack that was observed in the duct from the region of the dead end grout vent. The strand corrosion ratings from Specimens 7.3 and 7.4 were elevated as well. This indicates that the fully encapsulated system did not perform as intended and allowed moisture, oxygen, and chlorides into the tendon. The moisture that was observed when the tendons were cut from the anchorage plates reinforces the idea that the ducts and its components allowed moisture into the system. Even with the cracked duct in specimen 7.2, the ducts had relatively low damage ratings. Since, Specimens 7.3 and 7.4 had elevated chloride concentrations without cracked ducts, the couplers and heat shrink did not prevent the infiltration of chlorides into the tendon.

The theory behind the electrically isolated tendon is valid but if the system is not installed correctly and the duct is breached than the extra cost to purchase and install it is wasted. Even though the researchers took the time and care to try to install the components correctly, there were still issues with the couplers and heat shrink not performing as intended and a portion of a duct was still cracked. In a field environment, where this type of system would be installed, the installers probably would not take as much time or care to install the system as the researchers did. In defense of the fully encapsulated system, when it is installed in Europe, professional post-tensioning system installers are ordinarily used whereas in the U.S. on smaller projects generally it would be the general contractor that would install this system.

7.3 Comparison of Monitoring and Forensic Data

7.3.1 Half-Cell Potential

7.3.1.1 Half-Cell Potential Data vs. Observed Corrosion Damage

Figure 7.12 shows the corrosion ratings for longitudinal and transverse bars plotted with the final average half-cell potential for each specimen. Expect for Specimens 5.3,

7.2, and 7.3, all the specimens had final average half-cell potentials more negative than the 90% chance of corrosion half-cell potential[18]. The three exceptions had final average half-cell potentials in corrosion uncertain range. Corrosion of the coated steel bars was observed to some extent on the longitudinal and transverse bars. Therefore, the half-cell potential readings were helpful in determining if corrosion had existed in the specimen before the autopsies had been performed. However, as mentioned in Chapter 5, the half-cell readings are not an accurate means of predicting the severity of corrosion. The variance of the corrosion ratings for the bars supports that half-cell potential are not an accurate indicator for the severity of corrosion.

Figure 7.13 shows the generalized duct corrosion rating plotted with average final half-cell potential for each specimen with galvanized duct. Only the specimens with galvanized duct are shown because half-cell potential readings would not be an accurate indicator of plastic duct damage. For all the specimens with galvanized ducts, the average final half-cell potentials were more negative than the half-cell potential limit for 90% chance of corrosion. Figure 7.12 shows that while the specimens with plastic ducts had half-cell potential readings indicating corrosion or the uncertainty of corrosion, the half-cell potential readings from the specimens with galvanized duct were more negative than the half-cell potential readings from the plastic duct. This is a good indicator that the corrosion of the galvanized duct might have made the half-cell potential readings more negative.

Figure 7.14 shows the corrosion ratings for the strands plotted with the average final half-cell potentials for each specimen organized by strand type. All the tendons with conventional and flowfilled epoxy coated strands had average final half-cell potentials either more negative than the half-cell potential for greater than 90% chance of corrosion or in the corrosion uncertain range. Since all these strands types had some form of corrosion observed on them the half-cell potential readings were a good indicator of corrosion. However, there was no correlation between the half-cell potential readings and the corrosion rating as mentioned previously.

As mentioned in Chapter 5, the boundaries for corrosion from Reference 18 are not a good indicator of corrosion for the novel strands. Therefore, the active corrosion potentials from the LPR testing in Reference 13 were used as indicators of corrosion for the novel strands. The tendons with copper clad strand had low corrosion ratings and the two strands had equal corrosion ratings. However, the average final half-cell potentials were not even close to being equal. The north tendon was more negative than the active corrosion potential from the LPR testing and the south tendon was less negative than the active corrosion potential from the LPR testing. The wires of the strands had a very dark brown patina on them that is a passivation product and wires from both tendons had tiny reddish spots on a few locations.

All tendons with stainless clad strands had average final half-cell potentials more negative than the active corrosion potential from LPR testing. All the strands had minimal discoloration and a few spots of light corrosion not from the underlying strands. The highly negative average half-cell potentials might be from the passivation of the stainless cladding and not from corrosion the steel core.

Like the tendons with stainless clad strand, three of the four tendons with stainless steel strands had average final half-cell potentials more negative than the active corrosion potential determined from LPR testing. The other tendon had an average final half-cell potential that was less negative than to the active corrosion potential from LPR testing. The strands had minimal discoloration and no visible signs of corrosion. The highly negative average half-cell potentials might be from the passivation of the stainless steel.

The tendon with hot dip galvanized strand had an average final half-cell potential substantially less than the active corrosion potential determined from LPR testing and in the uncertainty range from Reference 18. The strands had discoloration and light to moderate corrosion. The average final half-cell potential being substantially less than the active corrosion potential but in the uncertainty range can be explained. When the zinc had been depleted enough for the steel to start corroding the potential would have become less negative to around the potential for corrosion of steel.

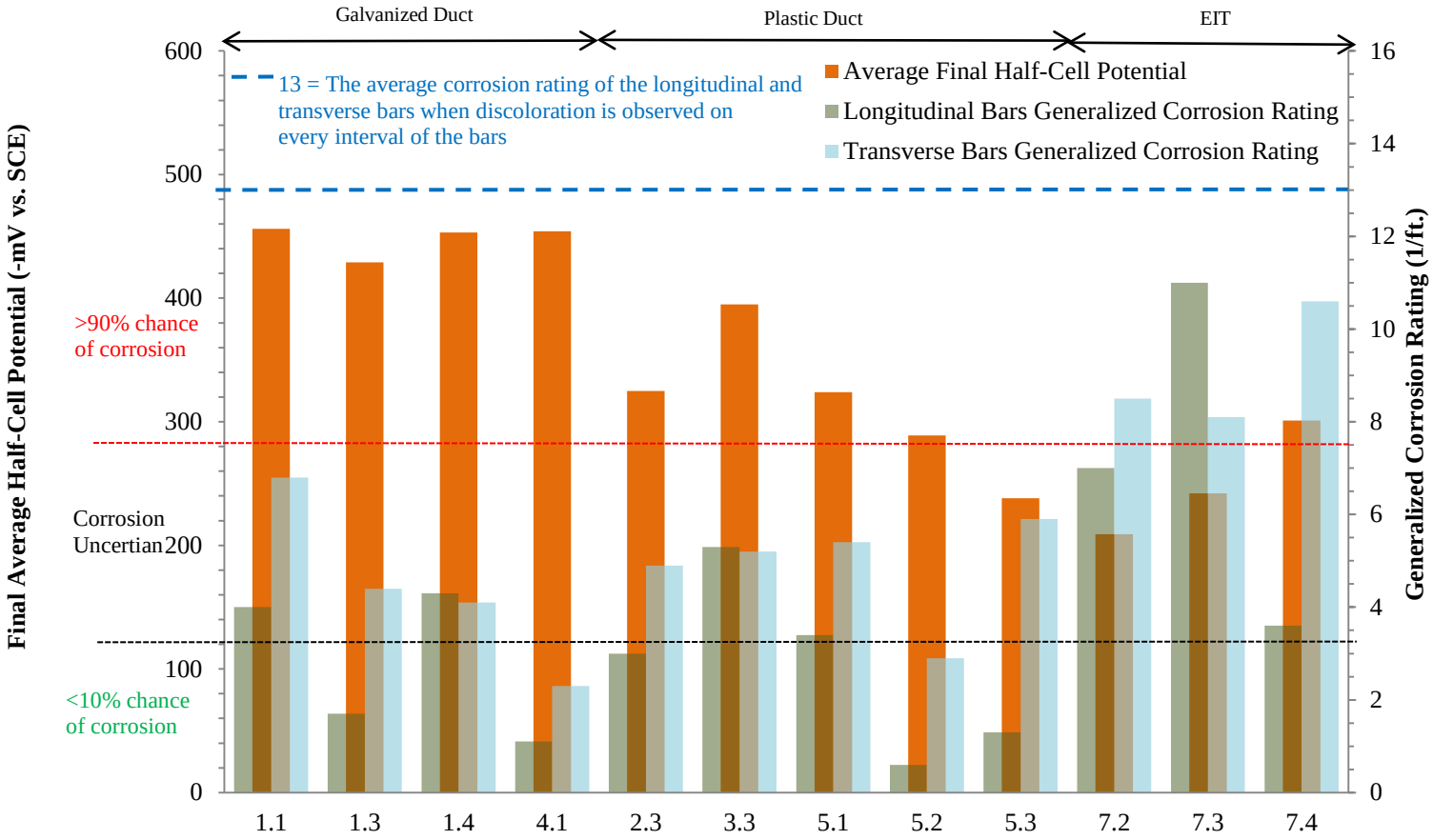

Figure 7.12: Longitudinal and Transverse Bars Generalized Corrosion Ratings and Average Final Half-Cell Potential

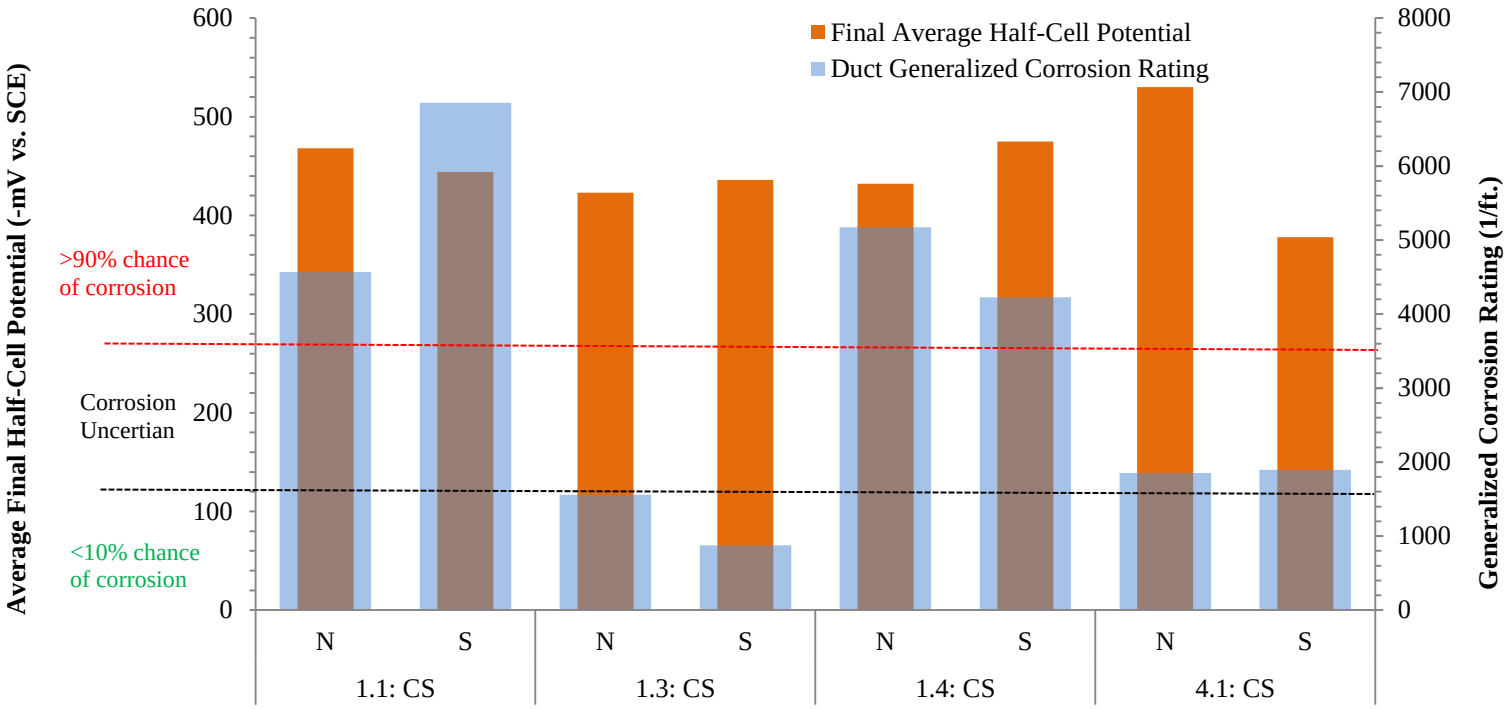

Figure 7.13: Generalized Duct Corrosion Rating and Average Final Half-Cell Potential

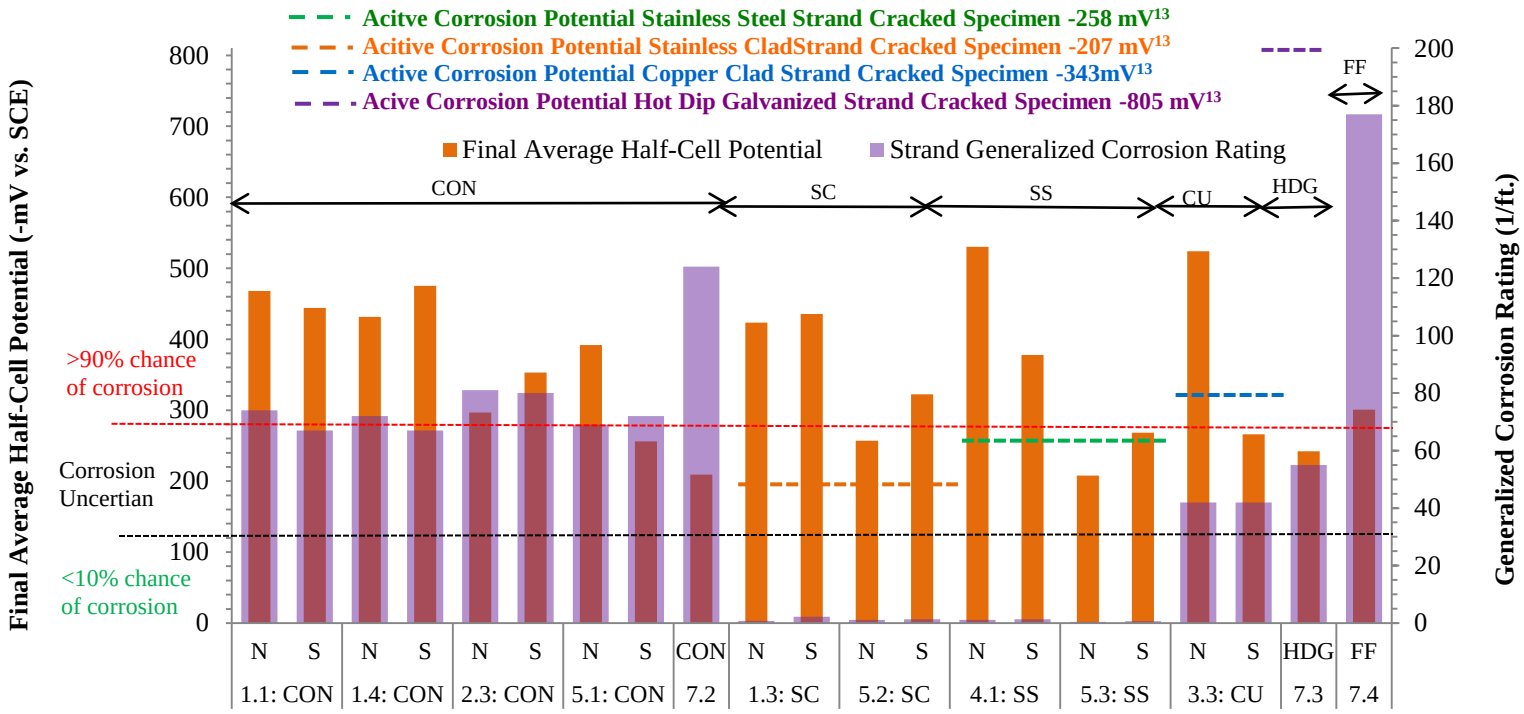

Figure 7.14: Generalized Strand Corrosion Ratings and Average Final Half-Cell Potential

Even though the half-cell potential method from reference 18 successfully predicted corrosion in the specimens, it could not make a valid prediction for corrosion in just the strands. It could not accurately predict corrosion in just the strands for a number a reasons. One, not all the strands were made of the same metal. Two, the epoxy coated steel reinforcement had some corrosion. Finally, the galvanized duct had corroded. The first reason is a contributing factor because every metal has a different corrosion potential in different environments. The final two reasons make the testing method invalid because the corroding of either or both of the epoxy coated steel bars and/or the galvanized duct would have interfered with the true half-cell potential of the strands. For these reasons, further research needs to be done to develop an effective way to predict corrosion in post-tensioned structures in a non-destructive manner.

7.3.1.2 Time to Corrosion vs. Observed Corrosion Damage

In Chapter 5, corrosion was assumed to be initiated when the most negative half-cell potential was more negative than the half-cell potential for 90% chance of corrosion from Reference 18 for the conventional and flowfilled epoxy coated strand. For the novel strands, the days to onset of corrosion was determined by using the active corrosion potentials from LPR testing done in Reference 13.

Figure 7.15 shows the generalized longitudinal and transverse bar corrosion rating plotted with days to onset of corrosion for each specimen. There is not much of a correlation between corrosion rating of the longitudinal and transverse bars and days to the onset of corrosion. However, the bars with the highest corrosion ratings seemed to have the lowest days to onset of corrosion.

Figure 7.16 shows the average generalized duct corrosion rating plotted with days to the onset of corrosion for each specimen. The specimens with galvanized ducts had the lowest days to onset of corrosion and the highest corrosion ratings. However, there was much variability to the corrosion rating. Therefore, correlation cannot be made to the severity of corrosion and days to onset of corrosion. The specimens with plastic ducts

had a lot of variability with the days to onset of corrosion. There is no correlation between days to the onset of corrosion and damage rating of the plastic ducts.

Figure 7.17 shows the generalized strand corrosion rating plotted with day to onset of corrosion for each tendon. The tendons with conventional and epoxy coated strands generally had the lowest days to onset of corrosion and the highest corrosion ratings. Not much variability was seen between the days to onset of corrosion and corrosion rating so a determination cannot be made if lower days to onset of corrosion correlated to higher corrosion ratings. The tendons with copper clad strand had equal corrosion ratings but a large gap between days to onset of corrosion. The stainless clad tendons had relatively equal corrosion ratings but the days to onset of corrosion were different between the tendons encased in galvanized duct and the tendons encased in plastic duct. The days to onset of corrosion was higher in the tendons encased in plastic duct for the tendons with stainless clad strand. The tendons with stainless steel strands were similar to the tendons with stainless clad. The corrosion ratings were essentially the same between tendons but the days to onset of corrosion differed between duct types. The tendons encased in plastic ducts had higher days to corrosion than the tendons encased in galvanized ducts. There were no other tendons with hot dip galvanized strands so a comparison cannot be made between strands types. However, the galvanized stand can be compared to conventional strands with regards to days to onset of corrosion. The tendon with hot dip galvanized strand had a longer time to days to onset of corrosion than the tendons with conventional strand.

From this data, a correlation can be made with regards to days to onset of corrosion and the corrosion ratings for galvanized duct. In general, corrosion was initiated in the tendons encased in galvanized ducts before corrosion was initiated in the tendons encased in plastic ducts. This means that the galvanized ducts probably started corroding before the strand or epoxy coated steel reinforcement started corroding. For the tendons with plastic duct the initiation of corrosion was effected by the corrosion of the epoxy coated steel reinforcement.

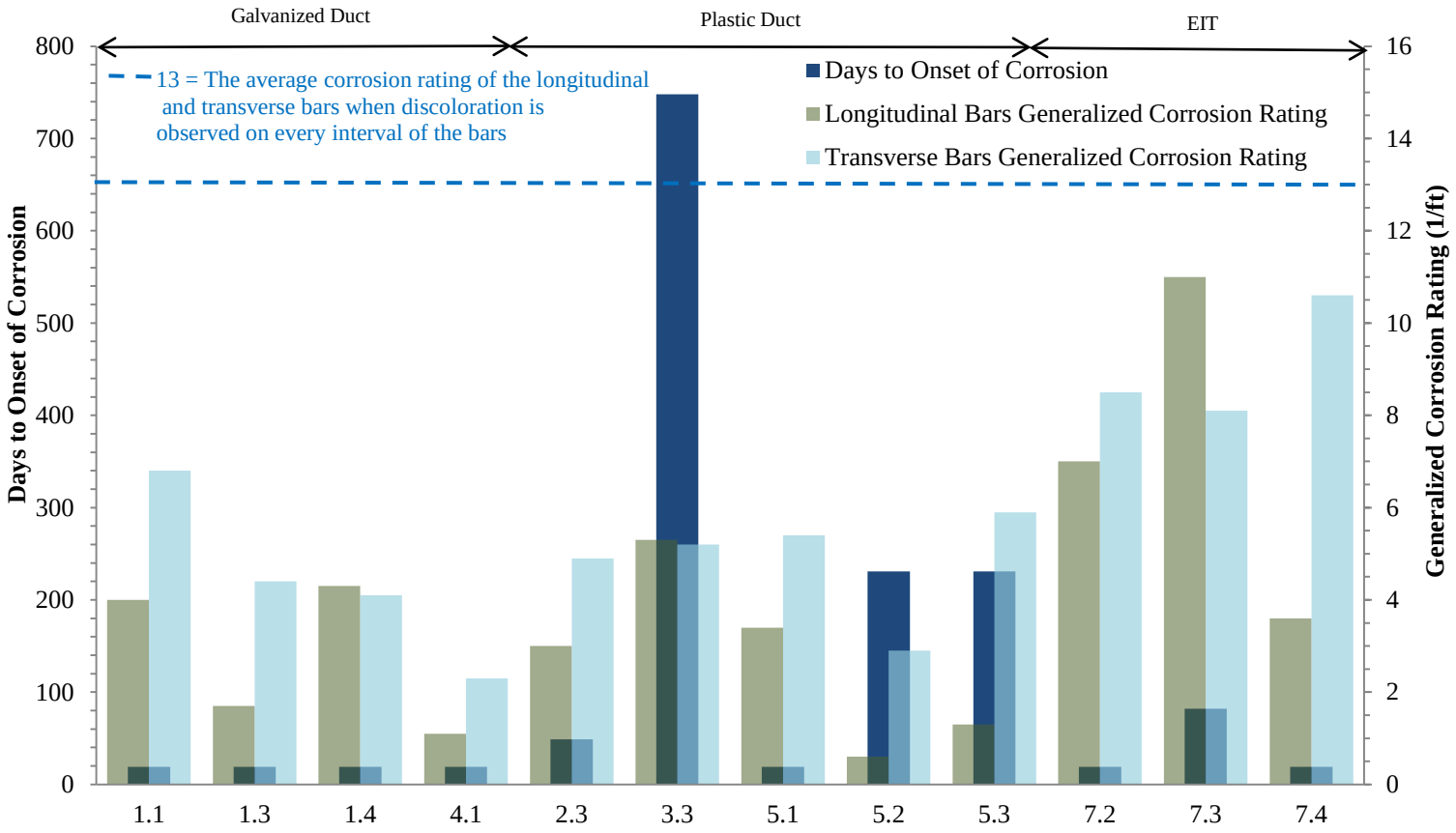

Figure 7.15: Generalized Longitudinal and Transverse Bar Corrosion Rating and Days to the Onset of Corrosion

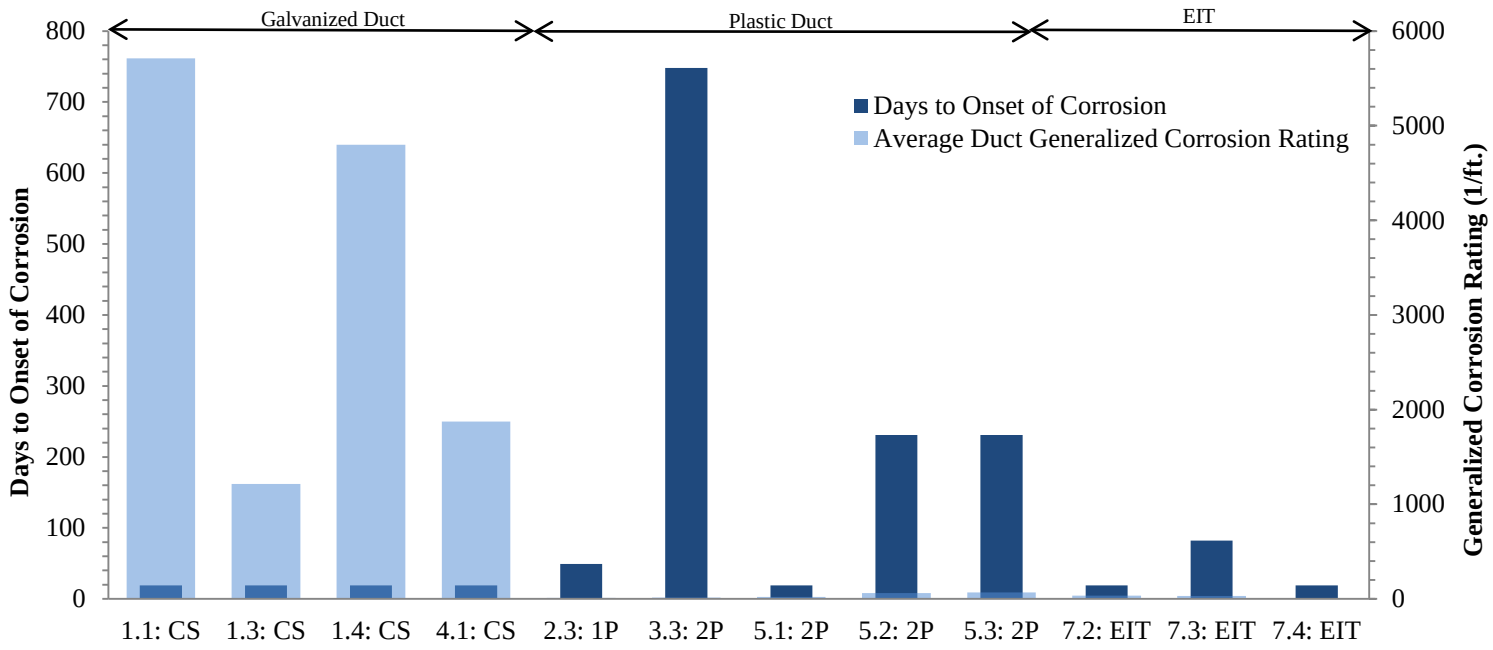

Figure 7.16: Generalized Duct Corrosion/Damage Rating and Days to the Onset of Corrosion

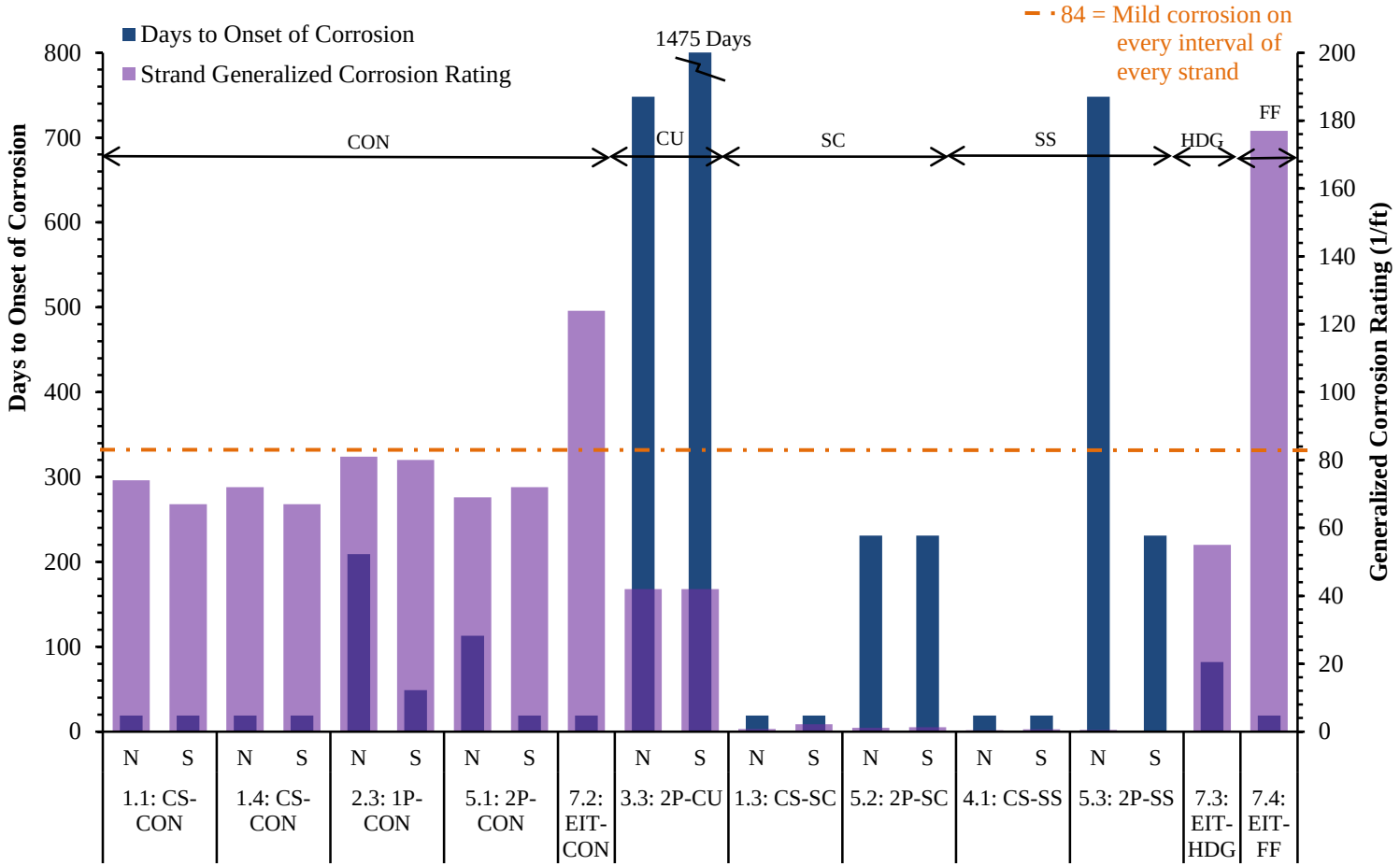

Figure 7.17: Generalized Strand Corrosion Rating and Days to the Onset of Corrosion

7.3.2 AC Impedance Data

Water tightness and electrical isolation of a tendon can be monitored for an electrically isolated tendon by measuring the AC impedance. However, AC impedance does not directly indicate the presence or the probability of corrosion in a tendon. As mentioned in Chapter 5, moisture infiltration can be detected in a tendon if the measured resistance has a 30% or greater drop[19]. Figure 7.18 shows the resistance vs. time for Specimens 7.2, 7.3, and 7.4. The first drop in resistance for all specimens was at 25 days of exposure. This corresponds to the days to the onset of corrosion for both Specimens 7.2 and 7.4, which had 19 days to onset of corrosion. Specimen 7.3 had 82 days to onset of corrosion. At least for Specimens 7.2 and 7.4, the first resistance drops suggest that corrosion was initiated approximately the same time.

In general, a low specific resistance indicates that the duct has been breached[19]. Therefore specific resistance might be used to ascertain if there is damage to a duct. However, given the questionable monitorability of Specimens 7.2, 7.3, and 7.4, specific resistance will not be discussed.

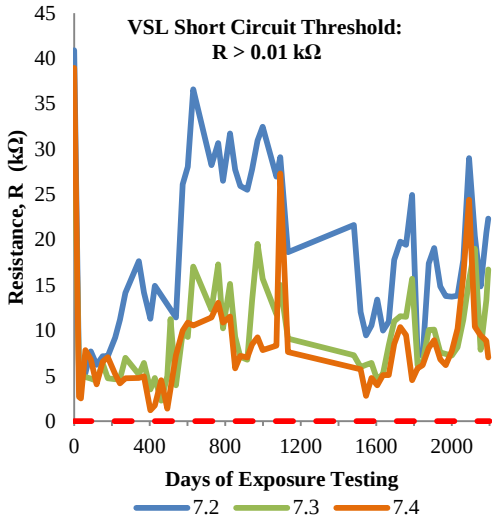

Figure 7.18: Resistance vs. Time for Specimens 7.2, 7.3, and 7.4

7.3.3 Chloride Penetration Data

The reason that concrete samples for chloride concentration testing were taken at a depth of one inch from the bottom surface of the ponding area is because the longitudinal and transverse bars were located at a depth of approximately one inch from the bottom surface of the ponding area. These chloride concentrations would represent the chloride concentrations at the depth of the bars. Figure 7.19 shows the generalized longitudinal and transverse bar corrosion rating plotted with the chloride concentration at a one inch depth for each specimen.

Except for Specimens 1.4, 4.1, and 4.4, all specimens had chloride concentrations at a one inch depth considerably higher than the corrosion threshold from Reference 5. Specimens 1.4, 4.1, and 4.4 had chloride concentrations very near the corrosion threshold. Specimen 4.1 had the lowest chloride concentration, the lowest transverse bar corrosion rating, and the second lowest longitudinal bar corrosion rating. Specimen 4.1 also had the lowest crack rating (Figure 7.2). As expected, the uncoated longitudinal bars from Specimen 4.4 had the highest corrosion rating. However, Specimen 4.4 had a chloride concentration at the corrosion threshold. The 7- series specimens had some of the highest chloride concentrations and generally had the highest corrosion ratings. In general, the higher the chloride concentration the higher the corrosion rating. However, since the specimens were cracked, the bars would have experienced greater concentrations of chlorides with cracks than what was present in the concrete. The chloride concentrations to which the bars might have been exposed at the locations of the cracks are probably better represented by the chloride concentration from Specimen 2.3. Specimen 2.3 had the highest chloride concentration and its corrosion ratings were around the average.

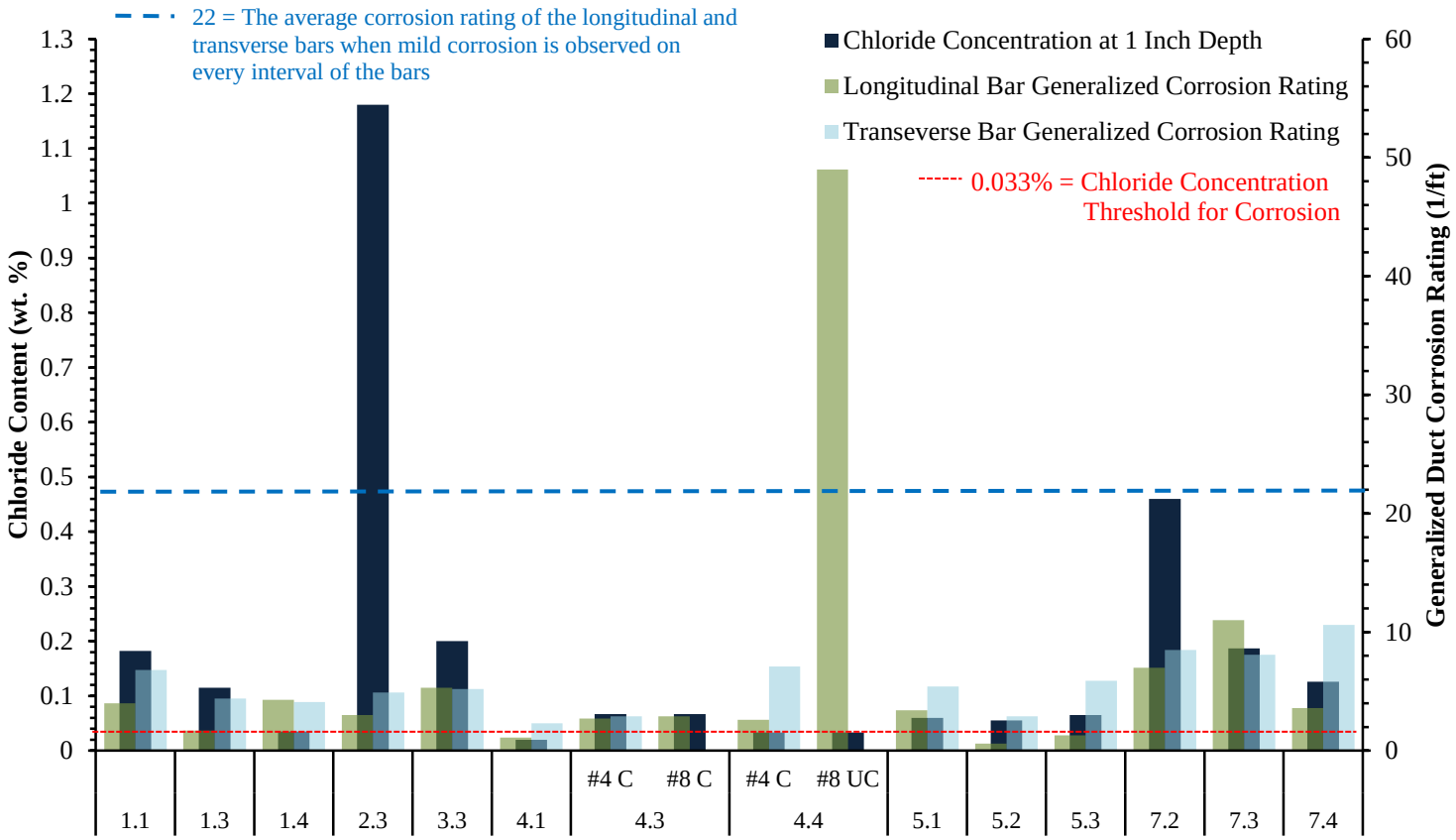

Figure 7.19: Generalized Longitudinal and Transverse Bars Corrosion Rating and Chloride Concentration at One Inch Depth

7.4 Comparison to Project 0-4562 Four Year Forensic Findings

7.4.1 Appearance

The condition of the 6 year and 4 year autopsied specimens was similar. All the specimens had limited rust staining around the grout vents of specimens containing galvanized ducts. Some of the specimens from both autopsy periods had additional cracks form in the re-entrant corbel corner after the application of live load. Some of the specimens from both autopsy periods had efflorescence around the cracks of the re-entrant corbel corner. All the specimens from both autopsy periods had medium scaling on the top surface and the bottom surface of the ponding area. Some of the specimens from both autopsy periods had small shallow bleed water voids in the ponding area. See Figure 7.20 for the typical condition of the ponding area for a 4 year and 6 year autopsied specimen.

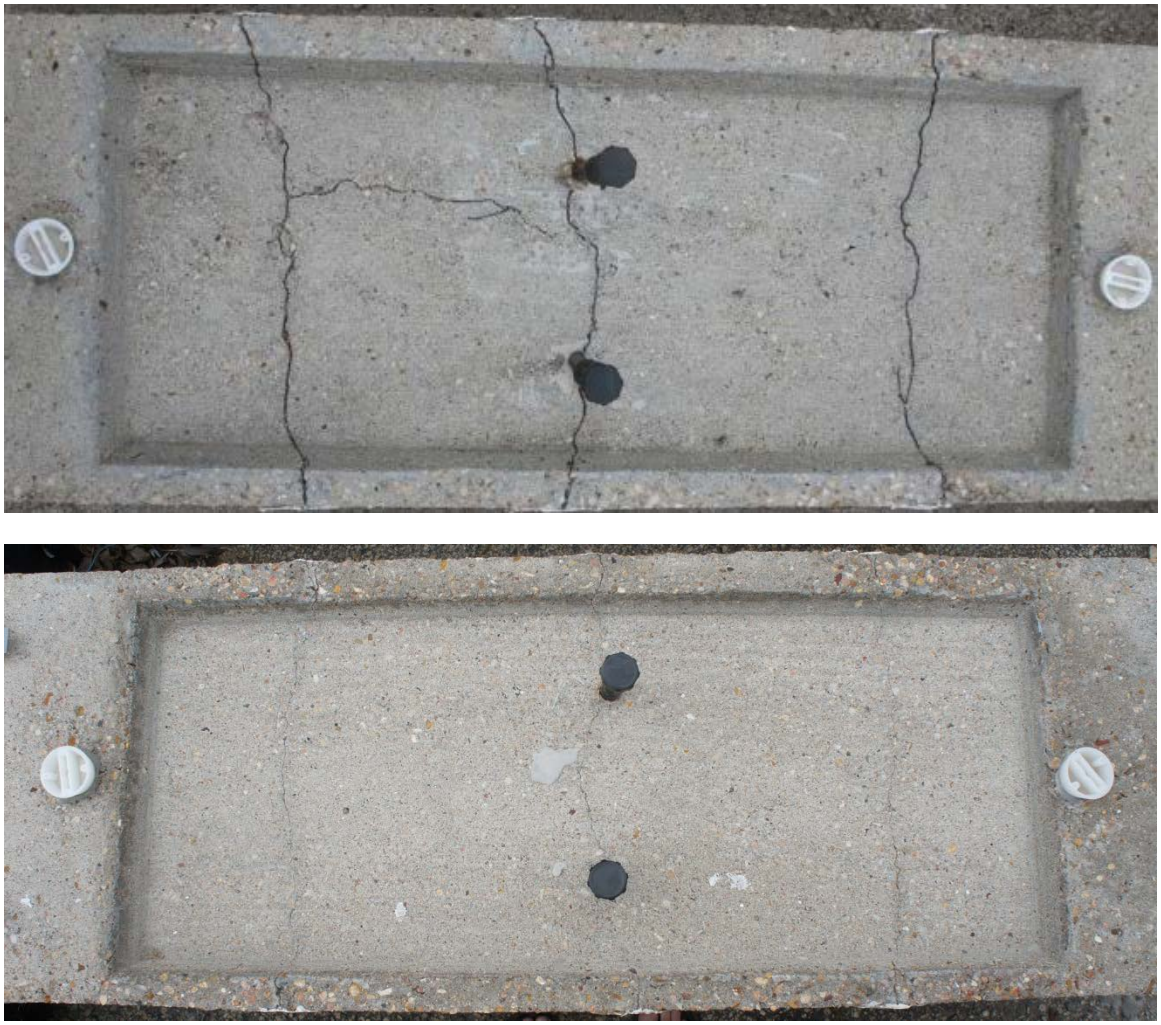

Figure 7.20: Typical Condition of Ponding Area for a 4 Year[2] (Top) and 6 Year (Bottom) Specimen

7.4.2 Longitudinal and Transverse Bars

The longitudinal and transverse bars from both autopsy periods had epoxy coated steel reinforcement. The condition of the bars was similar for both autopsy periods. Discoloration was found on all bars. Minimal moderate and light corrosion was found on some of the bars. Pitting was observed on very few bars. Generally, the corrosion was limited to areas in which the epoxy coating had been breached. Normally, the epoxy coating had been breached at curves in the bar and points where separate bars had touched. For the most part, the condition of the epoxy coating remained intact and

prevented widespread corrosion. The good condition of the longitudinal and transverse bars from the 4 year and 6 year autopsy periods is an indication that there is great value in using epoxy coated steel reinforcement in aggressive environments. The overall condition of the bars from the 6 year autopsy period was better than the overall condition of the 4 year autopsy period. This was unexpected. The overall condition of the 6 year autopsy period bars were expected to be worse than the overall condition of the 4 year autopsy period due to the longer exposure to chlorides. This discrepancy might because the 6 year autopsy period had more specimens with plastic duct and had two specimens that had no post-tensioning components. Therefore, transverse reinforcement would have had less staining on them decreasing the corrosion rating, thus decreasing the average corrosion rating for the transverse bars. Figure 7.21 shows a typical bar from the 4 year and 6 year autopsy period.

Figure 7.21: Typical Longitudinal Bar from 4 Year[2] (Top) and 6 Year (Bottom) Autopsy Period

7.4.3 Ducts

The condition of the galvanized ducts for the 6 year and 4 year autopsy periods were similar. All the galvanized ducts from both autopsy periods had holes on top of the ducts caused by corrosion. These holes were normally located at voids in the grout and at the locations of transverse cracks in the concrete. The majority of the ducts from both autopsy periods had pitting observed on their bottom inner surface. Moderate and light corrosion was observed on the outer and inner surfaces of all ducts from both autopsy periods. However, the 6 year autopsy specimens had somewhat more corrosion damage

than the 4 year autopsy specimens with larger holes where voids in the grout were located. The increase in damage over the 2 year period was approximately 15%. This was expected because the galvanized duct from the 6 year autopsy period were exposed to chlorides longer than the galvanized duct from the 4 year autopsy period See Figure 7.22 a typical galvanized duct from the 4 year and 6 year autopsy period.

Figure 7.22: Typical Galvanized Duct from 4 year[2] (Right) and 6 Year (Left) Autopsy Periods

The condition for the plastic ducts from both autopsy periods was similar. All the ducts had gouging observed from threading and/or stressing the strands. However, the one-way plastic ducts from the 4 year autopsy period had substantially more gouging than the one-way duct from the 6 year autopsy period. This can be contributed to the diameters of the duct. The one-way ducts' diameters from the 4 year autopsy period were smaller. The smaller diameter of the duct would have increased the chance of the strands rubbing against the duct during threading or stressing.

7.4.4 Grout

The grout condition from both autopsy periods varied form specimen to specimen. Both autopsy periods had grouts that had little variation in color, were smooth to the touch, and resilient against breaking. Also both autopsy periods had grouts that were rough to the touch, had large variations in color, and easily broke apart. The quality of grout improved in the specimens that had been grouted later. Grouts from both autopsy

periods had small voids on the top portion of the grout and some had large voids on the top portion of the grout. Strands were visible on the bottom of the grout from both study periods. The grout from galvanized ducts for both autopsy periods had rust stains from the corrosion of the duct. Most of the chloride concentrations were well above the corrosion threshold of 0.033% by weight for both study periods. However, if the chloride concentrations from like ducts are compared from both autopsy periods, the average 6 year autopsy chloride concentrations were approximately 19% greater than the average chloride concentrations from the 4 year autopsy period. This is expected because of the increased exposure time would have allowed more chlorides to accumulate in the grout. Figure 7.23 shows the typical grout from plastic ducts for both autopsy periods.

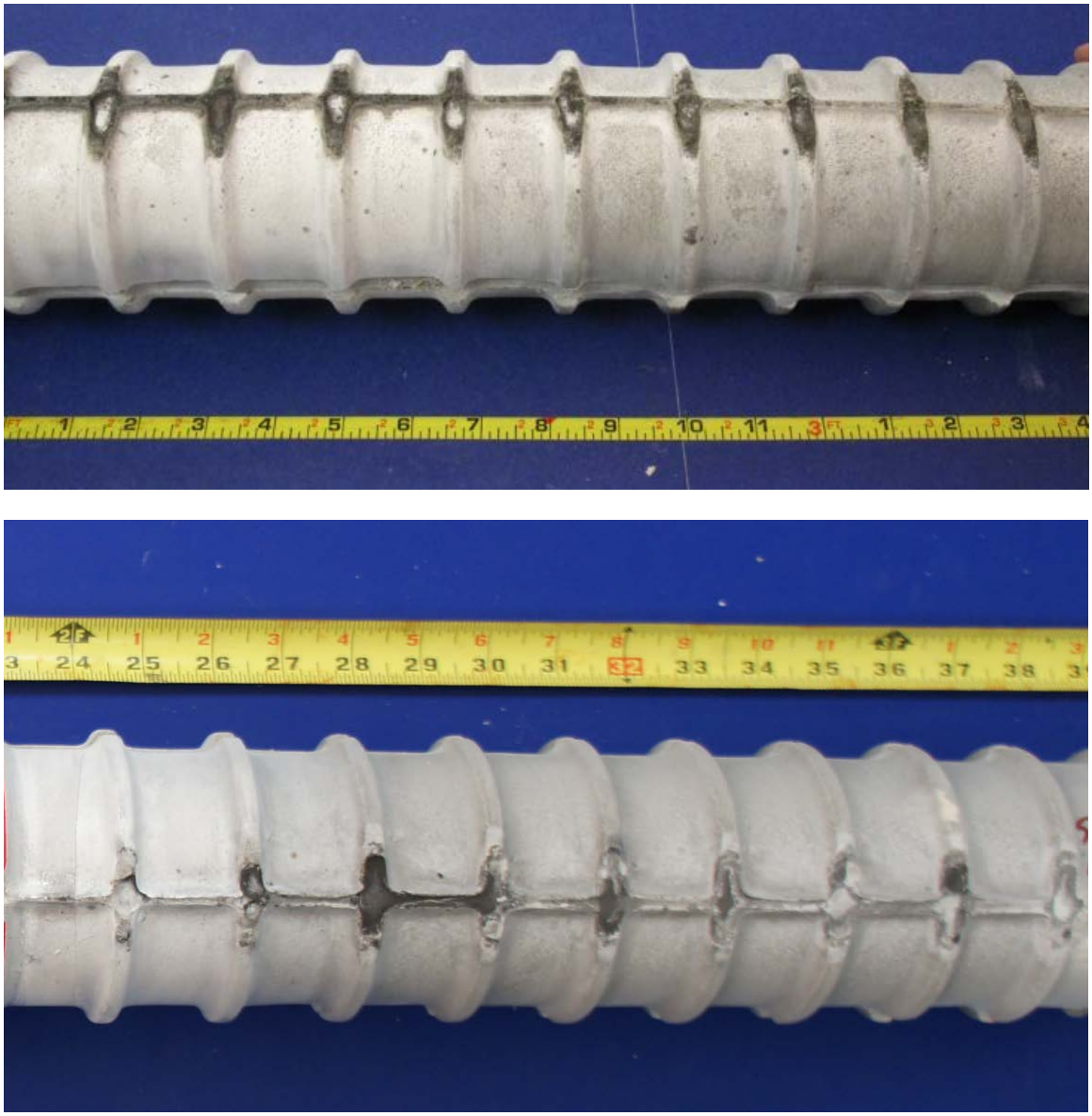

Figure 7.23: Typical Grout from Plastic Duct for 4 Year[2] (Top) and 6 Year (Bottom) Autopsy Periods

7.4.5 Strands

The conventional strands from both autopsy periods showed discoloration and spots of light corrosion on their outer strands and to some degree the corrosion on the inner wires was more severe. However, the corrosion on the inner and outer wires of the

6 year autopsy period was somewhat more widespread and pitting was observed on some of the wires. There was approximately a 220% increase in corrosion damage to the conventional strands over the two year period between autopsies. The condition of the hot dip galvanized strands from both autopsy periods was somewhat similar, with the strands from the 6 year having greater and more widespread damage. There was approximately 240% increase in corrosion damage to hot dip galvanized over the two year period between autopsies. The copper clad strands from both autopsy periods had a very dark brown patina on them and the patina did not change during the 2 year period between autopsies. There was no difference in the condition of the stainless steel strands from the 4 and 6 year autopsy periods. No specimens from the 4 year autopsy period contained either stainless clad or flowfilled epoxy coated strands. Figure 7.24 shows a typical conventional strand from the 4 year and 6 year autopsy periods.

Figure 7.24: Typical Conventional Strand from 4 Year[2] (Top) and 6 Year (Bottom) Autopsy Periods

7.4.6 Anchorages

The condition of the anchorage components from both autopsy periods was similar in condition. The anchorage plates from both autopsy periods had corrosion on the underside of the embedded portion. The ducts from both autopsy periods had somewhat similar damage with the galvanized ducts having a little more widespread and little more severe corrosion. The strands from the 4 year autopsy period were to some extent similar to the strands from the 6 year period. The strands from the 6 year period had a little more widespread and a little more severe corrosion damage. The conventional strands had a 50% increase in the corrosion damage over the 2 year period. The copper clad and the

stainless steel strands had no increase in corrosion damage over the two year period. The hot dip galvanized strands had a 37% increase in damage over the two year period. No specimens from the 4 year autopsy period contained either stainless clad or flowfilled epoxy coated strands. The wedges from both autopsy periods were somewhat intact with observed light corrosion. Figure 7.25 shows the typical anchorage from both autopsy periods.

Figure 7.25: Typical Anchorage from 4 Year[2] (Left) and 6 Year (Right) Autopsy Periods

7.4.7 Corrosion Ratings

Figure 7.26 shows the generalized corrosion ratings for various components of the 4 and 6 year autopsy periods. Because the 4 year autopsy period did not contain stainless

clad or flowfilled epoxy coated strands, these strand types will not be evaluated in this section. The corrosion ratings of the epoxy coated steel reinforcing bars from the 4 year autopsy period were higher than the corrosion ratings for the 6 year autopsy period. This might be due to the 6 year autopsy period had more specimens with plastic ducts and having two specimens that had no post-tensioning components. Therefore, transverse reinforcement would have had less staining on them decreasing the corrosion rating, thus decreasing the average corrosion rating for the transverse bars. This might be the same reason why the 6 year autopsy period longitudinal bars had an average corrosion rating less than 4 year autopsy period. The 6 year autopsy period average corrosion rating for the galvanized duct was higher than the 4 year autopsy period. This was expected because the ducts from the 6 year autopsy period would have been exposed to chlorides longer than the 4 year autopsy period galvanized ducts. The average damage rating for plastic ducts for the 6 year autopsy period was substantially lower than the 4 year autopsy period. As mentioned previously, this can be contributed to the diameters of the duct. The one-way duct's diameter from the 4 year autopsy period was smaller. The smaller diameter of the duct would have increased the chance of the strand rubbing against the duct during threading or stressing. The average corrosion ratings for conventional and hot dip galvanized strands were substantially higher for the 6 year autopsy period than the 4 year period. This can be contributed to the increased length of time that the strands were exposed to moisture, oxygen and chlorides. The average corrosion ratings from both periods for the stainless steel strands were nearly the same. This was expected because stainless steel is very resistant to corrosion in a high chloride environment. The average corrosion ratings of the copper clad strand for both periods had identical corrosion ratings. Therefore, the copper clad strand was not affected by the high chloride environment during the additional 2 years of aggressive exposure.

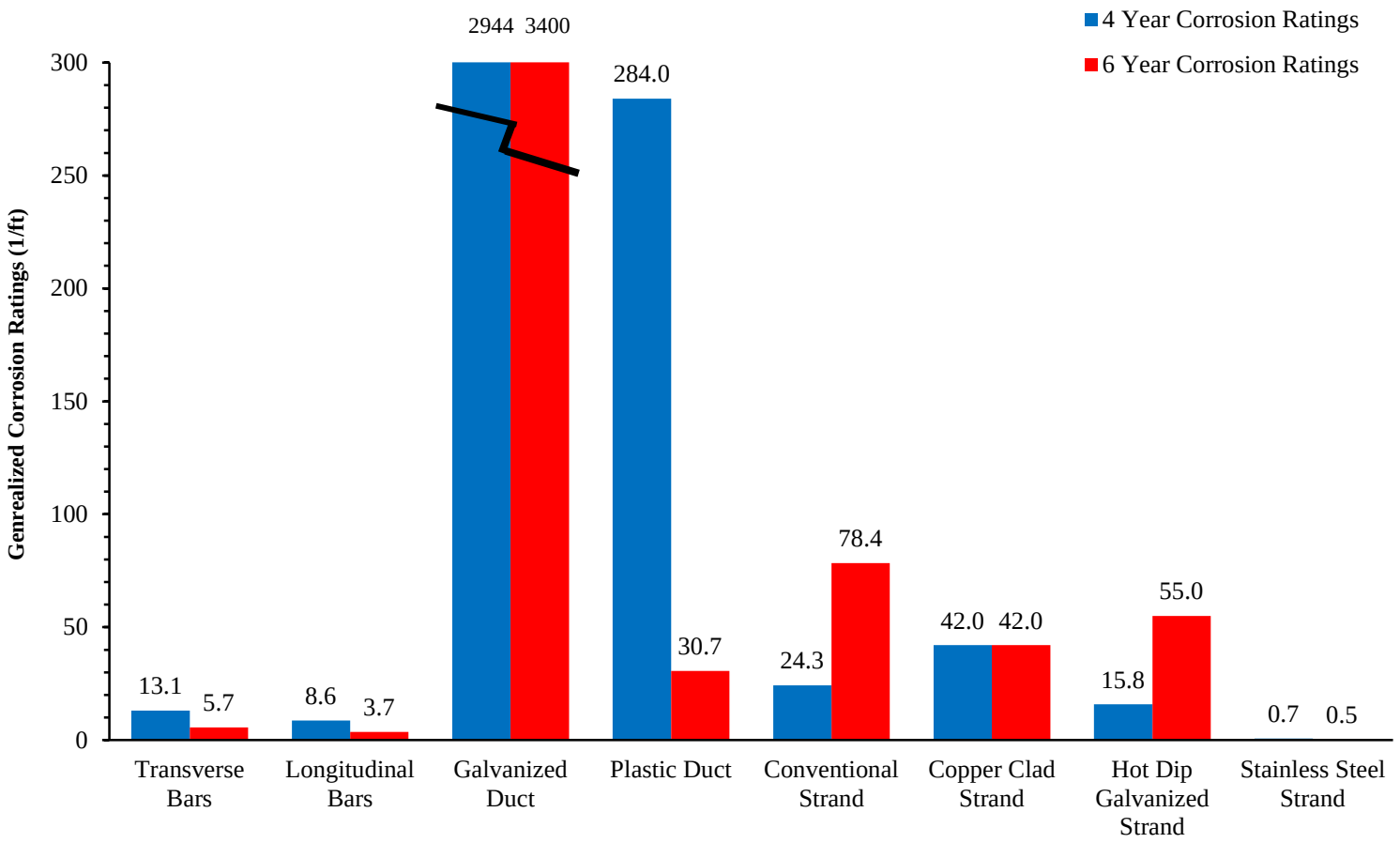

Figure 7.26: 4 and 6 Year Generalized Corrosion Ratings for Most Components of Project 0-4562

7.5 Comparison with Project 0-1405 Forensic Findings

Twenty-seven large scale large beam specimens were construction, exposure tested, and autopsied for a portion of TxDOT Project 0-1405. The first set of beams started exposure testing in 1998 and the last set of beams were autopsied in 2006. Project 0-1405 was the predecessor of Project 0-4562. Because of this the lessons learned in Project 0-1405 were used to refine the corrosion resistance of the Project 0-4562 specimens and to decrease the interaction of the variables of Project 0-4562. The results from Reference 5 are used herein to compare the results of this study. Reference 5 autopsied 12 of the Project 0-1405 specimens after 3.5 to 4.5 years of exposure[5].

7.5.1 Appearance

The appearances of Project 0-1405 specimens were dismal. Moderate to severe rust staining was found on the tops of most of the specimens. Surface cracking observed on some of the specimens was from flexural loading but much of the wide cracks were due to tensile stresses caused by internal corrosion of the uncoated reinforcement and galvanized duct. These cracks allowed the chlorides from the ponding area to easily infiltrate the concrete. The chlorides then could easily spread to other portions of the specimens where no flexural cracks were observed.

The exterior condition of the Project 0-4562 specimens was much improved over the condition of the Project 0-1405 specimens. Limited rust staining was observed and normally was contained around the grout vents of the specimens with galvanized duct. Of the specimens with galvanized duct the majority of the specimens had no visible longitudinal cracking. Figure 7.27 shows the typical external appearance of specimens from both projects. The switch to epoxy coated reinforcement was very significant in preserving external appearance.

Figure 7.27: Typical Specimen from Project 0-1405[5] (Top) and Project 0-4562 (Bottom)

7.5.2 Longitudinal and Transverse Bars

The specimens from Project 0-1405 contained uncoated steel longitudinal and transverse bars. These bars were seriously damaged due to corrosion over the majority of the autopsy region. The steel bars had substantial cross-sectional area loss due to this corrosion, particularly in the partially prestressed specimens. The wider crack widths in the latter were found to have influenced the corrosion of the bars.

Project 0-4562 used epoxy coated longitudinal and transverse bars. Minimal discoloration, light to moderate corrosion, and on some occasion mild pitting were observed along the length of the bars. All in all, the epoxy coating remained intact and hindered further corrosion of the bars. There was a reduction of almost 100% in the average corrosion rating of transverse reinforcement of Project 0-1405 compared to Project 0-4562. There was also a reduction of 95% in the average corrosion rating of longitudinal reinforcement of Project 0-1405 compared to Project 0-4562. This indicates that the use of epoxy coated bars in an aggressive environment is very effective. Figure 7.28 shows typical longitudinal bars from both projects.

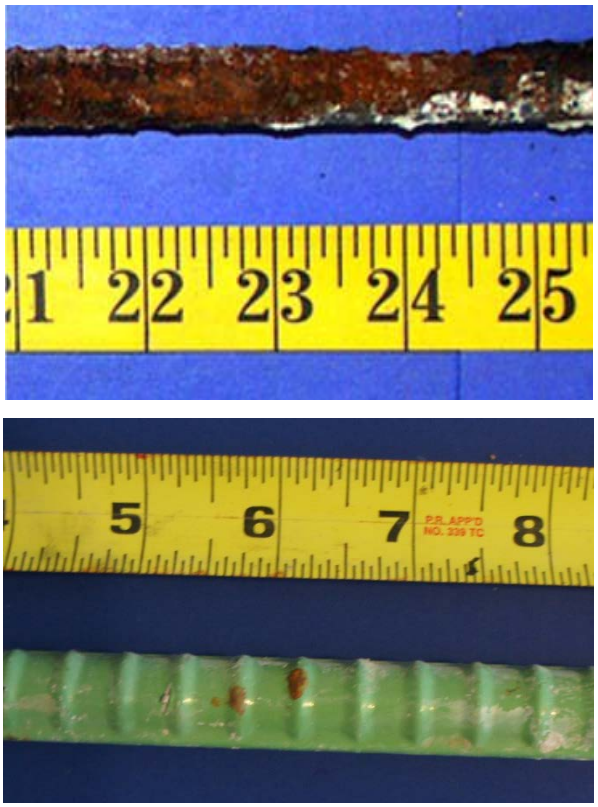

Figure 7.28: Typical Bar Longitudinal Bar from Project 0-1405[5] (Top) and Project 0-4562 (Bottom)

7.5.3 Ducts

Pitting and area loss was observed in the galvanized steel ducts from Project 0-1405. The worst corrosion occurred at locations where large bleed water voids had formed in the grout. The splices using heat shrink and "industry standard" (duct tape) did not perform well. This created a path for chlorides to infiltrate the duct at the splices. Reference 5 did not include any specimens with plastic duct.

The corrosion observed on the galvanized duct from both projects was comparable. Like Project 0-1405, the galvanized ducts from Project 0-4562 had severe corrosion at the locations of bleed water voids in the grout and at the locations of transverse cracks. However, there was a 400% increase in galvanized duct corrosion damage in the Project 0-4562 specimens. The average corrosion ratings for galvanized duct were 677 and 3400

for Project 0-1405 and Project 0-4562, respectively. Project 0-1405 used level of prestress and live load as variables for the project. This would have caused the flexural cracks to vary widely from specimen to specimen and would have caused less damage to some of the ducts. Therefore the average corrosion rating would be less. Figure 7.29 shows a typical galvanized duct from both projects. The similar damage to the galvanized ducts from both projects indicates that the testing conditions were fairly consistent, except that the improved grouting in Project 0-4562 resulted in fewer large bleed water voids and less loss of duct area.

Figure 7.29: Typical Galvanized Steel Duct from Project 0-1405[5] (Top) and Project 0-4562 (Bottom)

7.5.4 Grout

One of the test variables for Project 0-1405 was grout type and grouting procedures. The ducts were grouted using different grout types and both industry standard and "poor" grouting techniques. Voids or indications of porosity were observed in all tendons. It was found that improved grouting techniques improved grout quality. However, the improvement was countered by underdesigned and obsolete grout mixes.

The grout for Project 0-4562 was prebagged and injected into the duct using a hand pump. Grout quality varied from specimen to specimen. Compared to Project 0-1405 the voids in the grout were much smaller and primarily limited to the flutes of the duct. Segregation was observed in some of the grouts. This suggests that the pressure was not uniform during the injection of the grout. However, the quality of the grout was greatly improved over the grout from Project 0-1405 and the area of voids substantially less. The

average corrosion ratings for galvanized duct were 677 and 3400 for Project 0-1405 and Project 0-4562, respectively. Project 0-1405 used level of prestress and live load as variables for the project. This would have caused the flexural cracks to vary widely from specimen to specimen and would have caused less damage to some of the ducts. Therefore the average corrosion rating would be less.

7.5.5 Strands

The corrosion damage observed on the conventional strands of Project 0-1405 was substantial. Pitting and cross sectional area loss was commonplace. Some strands even fractured during the autopsy process. The non-flowfilled epoxy coated strand was found to not be in much better shape. Damage to the coating allowed corrosive contaminates to enter and migrate down the strand. The galvanized strand was substantially corroded and pitted. However, the galvanized strand did not begin to corrode till much later than the other strand types.

Since copper clad, stainless, and stainless clad strands were not evaluated in Project 0-1405, they will not be discussed in this section. The conventional strands from Project 0-4562 had far less damage. The strands showed discoloration and spots of light corrosion on their outer wires and to some degree the corrosion on the inner wires was more severe. The galvanized strand from Project 0-4562 had far less damage, with discoloration and light to moderate corrosion on the inner and outer wires of the strand. The flowfilled epoxy coated strand did not perform as well as expected. The inner and outer wires had corrosion ranging from mild pitting to light corrosion over the majority of their lengths. The average corrosion ratings for all the strands from Project 0-1405 and the like strands from Project 0-4562 were 124 and 83, respectively. This is approximately a 50% reduction in corrosion damage. The improved grout condition and plastic duct helped mitigate the damage that the strands experienced. Figure 7.30 shows a typical strand from Project 0-1405 and Project 0-4562.

Figure 7.30: Typical Conventional Strand from Project 0-1405[5] (Top) and Project 0-4562 (Bottom)

7.5.6 Corrosion Ratings

Figure 7.31 shows the average corrosion ratings for common components from both projects. Reference 5 did not evaluate plastic ducts. Therefore, only the four galvanized ducts from Project 0-4562 that had been autopsied at 6 years of exposure were considered for comparison. The damage to the epoxy coated bars for Project 0-4562 was much less damaged than the uncoated bars from Project 0-4562. The average 6 year conventional strand corrosion rating from Project 0-4562 was somewhat lower than Project 0-1405. This might be due to the better condition of the grout for Project 0-4562.

Average duct corrosion rating for Project 0-4562 was substantially higher than the average duct corrosion rating for Project 0-1405. Project 0-1405 used level of prestress and live load as variables for the project. This would have caused the flexural cracks to

vary widely from specimen to specimen and would have caused less damage to some of the ducts. Therefore the average corrosion rating would be less. On the other hand, the transverse crack widths were approximately equal for each specimen and caused the ducts to have approximately the same level of damage.

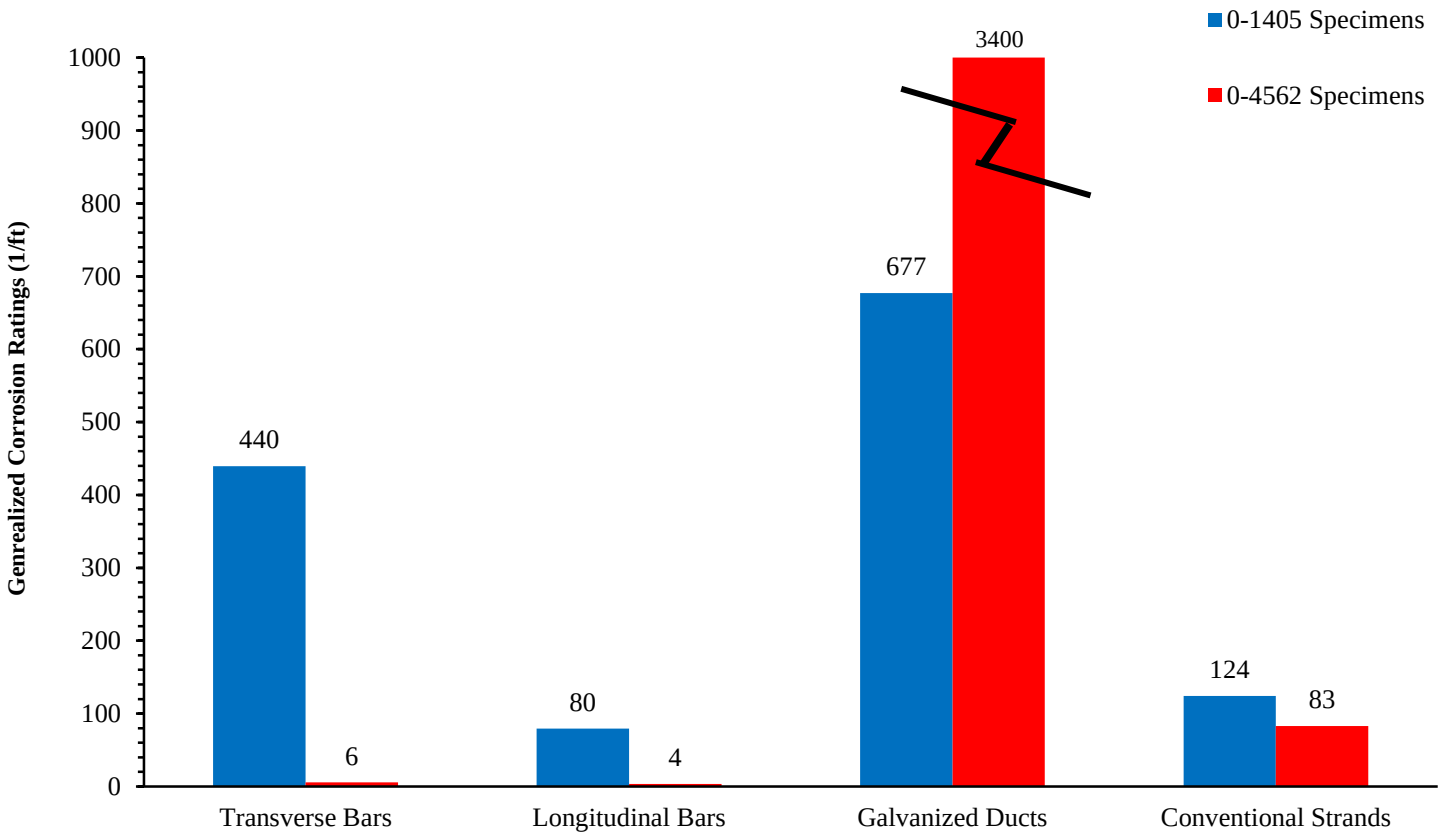

Figure 7.31: Generalized Corrosion Ratings for All Components of Project 0-1405 and Project 0-4562 among Specimens with Galvanized Steel Ducts

CHAPTER 8

Cost and Service Life Analysis

8.1 Cost Analysis

All the content in this section comes from cost analysis conducted in Reference 2 with additional cost analysis done by the author on stainless steel and flowfilled epoxy coated strands.

8.1.1 Rationale

The service life of a bridge could be extended by the new corrosion resistant post-tensioned materials evaluated in this series and in Reference 2 if the materials were properly implemented. The service life of a bridge would be extended by delaying or eliminating the onset of corrosion. Even though the materials might extend the life of a bridge, there are additional costs that must be taken into account. Each of the main project variables' additional costs are presented and analyzed in this chapter. Quantities from a typical segmental bridge were used in the analysis.

8.1.2 Methodology

Based on the size and scope of a structure, unit costs can vary extensively for post-tensioning materials. Because of this, Reference 2 chose to analyze the cost for the FM 2031 Gulf Coast Intracoastal Waterway (GIWW) bridge in Matagorda, Texas to attain a uniform comparison (Figure 8.1). The structure has three spans of 680 feet overall length of cast-in-place post-tensioned segmental box girders and 19 additional precast prestressed concrete girder approach spans. The bridge was put into service in 2009[26]. TxDOT provided the post-tensioning material quantities[27]. Only longitudinal post-tensioning materials were considered for the three post-tensioned spans to simplify the comparison. Table 8.1 shows the quantities used in the analysis. Grout vents, plugs, or any other support items were not considered.

Figure 8.1: FM 2031 Bridge over GIWW in Matagorda, Texas[2]

Table 8.1: Matagorda GIWW Bridge Longitudinal Post-Tensioning Quantities[2]

Item	Quantity	Unit
2” Duct	2720	Ft.
3” Duct	9891	Ft.
4” Duct	18180	Ft.
2” Coupler	176	Each
3” Coupler	783	Each
4” Coupler	1452	Each
7-Strand Anchorage	8	Each
12-Strand Anchorage	88	Each
19-Strand Anchorage	160	Each
0.6” 7-Wire Strand	267400	Ft.

The costs for each duct and anchorage type examined in this chapter were acquired from a post-tensioning supplier. Post-tensioning suppliers and the Federal Highway Administration were used to estimate the cost of the strands. The estimates for strand and duct were given in unit cost per foot. Coupler cost estimates were given in cost per coupler. A package price was given for the anchorage. The package consisted of

anchorage plate, anchor head, and corresponding number of wedges. The Swiss Franc cost of the electrically isolated tendons (EIT) had to be converted to US dollars at the market exchange rate at 5:00 PM EST on Friday, November 12, 2010[2]. The cost had to be converted to US dollars because at that time the EIT was not available in the US and prices were obtained from a supplier in Switzerland. Shipping, handling, and profit mark-up by the post-tensioning suppliers were excluded. Installation labor was assumed to be equal for all materials.

8.1.3 Cost Data and Analysis

The official published construction cost of the bridge was $16 million[29]. This price was defined as the baseline cost. The percent increase in total construction cost for each combination of strand, duct, and anchorage shown in Figure 8.2 was based on the cost estimates acquired in Reference 2 and by the writer of this series.

Figure 8.2 shows that there is a clear correlation between increased protection and the cost of construction. As the level of protection increases the cost of construction goes up. Non-galvanized anchorage plates were less expensive than galvanized anchorage plates. Post-tensioned systems with galvanized duct were more economical than the ones with plastic ducts. The most expensive post-tensioning system was the fully encapsulated (EIT). The cost of the strands increased as the level of corrosion resistance increased. This is assuming that the corrosion observed in the flowfilled epoxy coated strand in the autopsied specimens was an anomaly. If the Matagorda bridge were constructed with stainless steel strand and electrically isolated tendons the total increase in construction would have been approximately 8.4%. This was the highest increase in construction cost. The total increase in construction cost, regardless of components, was less than 10%. Duct and anchorage types had less of an effect than strand type on the cost of construction.

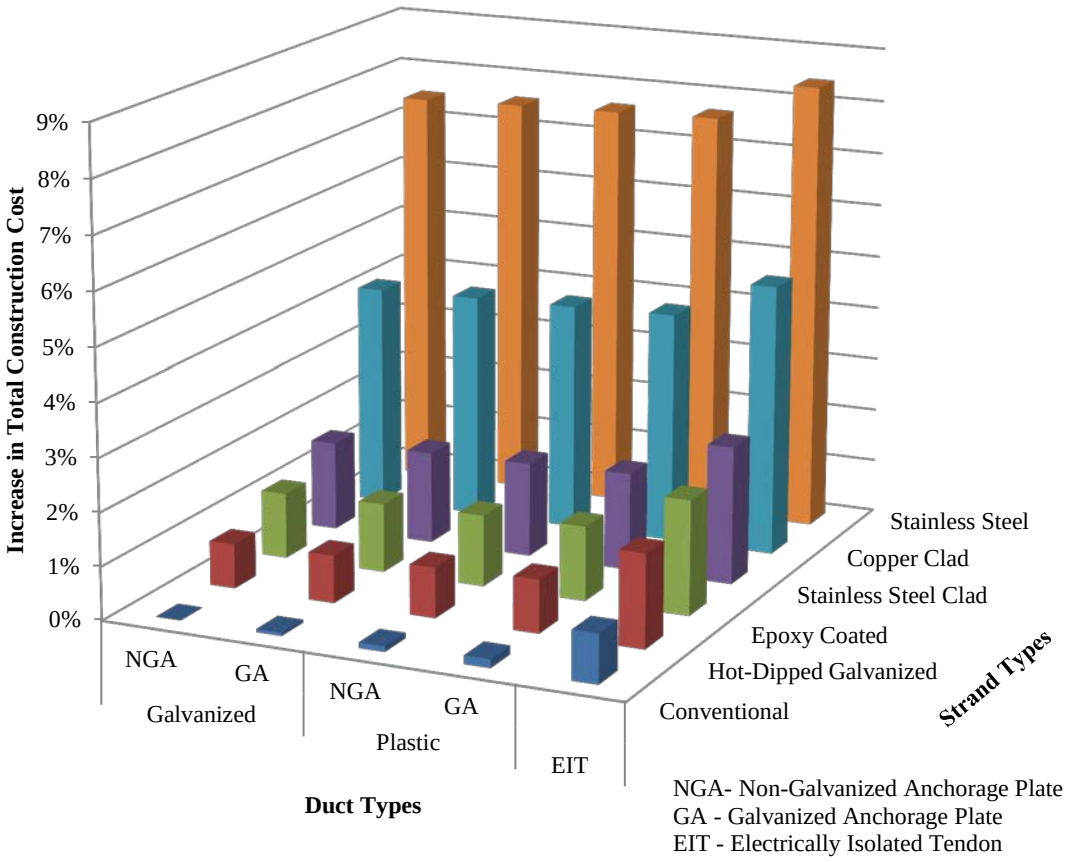

Figure 8.2: Percent Increase of Total Construction Cost for Each Project Variable[2]

To better illustrate the effect of duct and anchorage plates on cost of construction, Figure 8.3 shows the percent increase in construction cost based on conventional strand with different anchorage and duct types. The incremental increase in cost for galvanized anchorage plates and plastic ducts were approximately 0.05% and 0.10%, respectively. Because of the increased number and complexity of components, the increase in construction cost of the fully encapsulated EIT post-tensioning system was substantially higher with an increase in cost of approximately 0.9%.

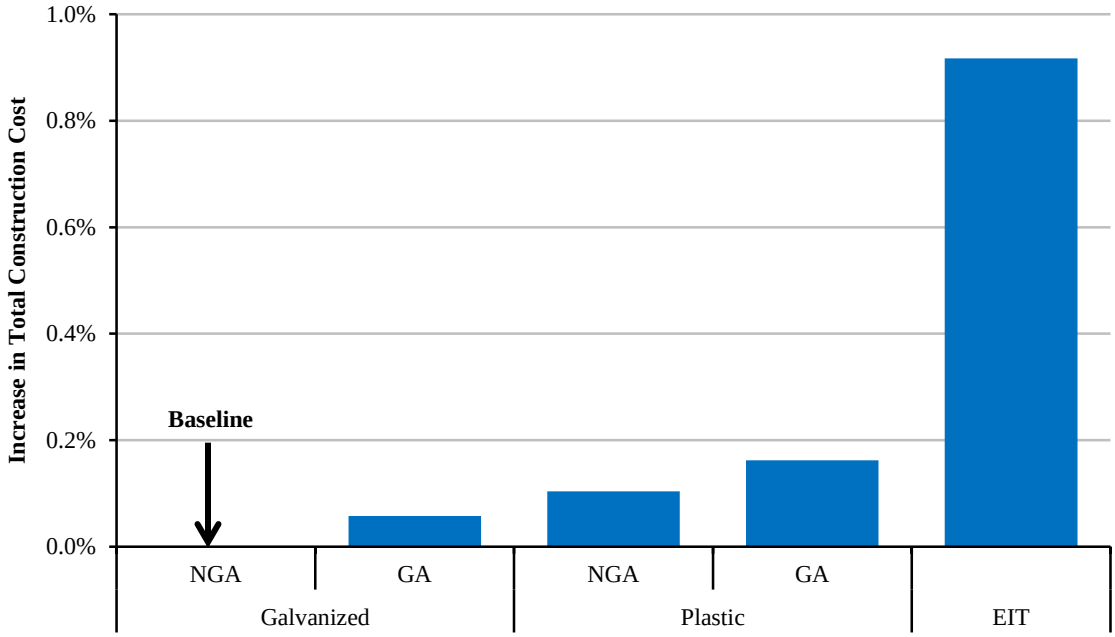

NGA- Non-Galvanized Anchorage Plate
GA - Galvanized Anchorage Plate
EIT - Electrically Isolated Tendon

Figure 8.3: Percent Increase in Construction Cost for Conventional Strand[2]

Repair and maintenance cost of a bridge over its lifetime are important considerations when considering the total cost of the bridge. Lifetime maintenance costs might be reduced and service life increased if more durable components are used in construction, even though these components would result in marginally higher construction costs. To illustrate this, a simple numerical example will be considered and some assumptions made. One assumption is a bridge would cost 8% more to construct with stainless steel strands than the same bridge using conventional strands. Another assumption is the service life of the bridge would increase from 50 to 100 years. According to Reference 30, a reasonable cost estimate for the annual maintenance of a bridge is 1% of the construction cost. If 100 is treated as a unitless construction cost, than the total cost of the bridge with conventional strands, including maintenance, would be: 100 + 50*1 per year = 150. Spread over the 50 year service life of the structure, this would be a cost of 3 per year. For the bridge with stainless steel strands: 108+100*1per

year=208. In this case, the total cost per year would be 2.08. This is a 31% decrease in lifetime costs for a bridge with stainless steel strands.

Real costs and the effect of inflation must be considered for a true life cycle cost analysis. More importantly, the question of how post-tensioning materials increase the service life of a bridge needs to be answered. Reference 30 tried to answer these questions by performing life cycle cost analysis from the macrocell corrosion tests done in References 5 and 8. Reference 30 was able to compute lifetime costs on a random structure by making the assumption that a decrease in corrosion rate corresponds to a proportional decrease in maintenance cost. Additionally, the corrosion rating system does not differentiate between strand types. An example of this is the corrosion ratings for copper clad strand which had the same corrosion rating regardless of duct type and the amount of years of exposure the strands experienced. The next section in this chapter tries to answer how duct and strand type affect the service life.

8.2 Service Life Analysis

8.2.1 Rationale

As the bridges in the US age and the cost to replace or maintain them increase substantially, the designer has an obligation to think about how they might be able to increase the service life and lower the maintenance costs of these bridges. The post-tensioning components studied in Project 0-4562 might be the answer to increasing the service life of a post-tensioned bridge and in some aspects decrease the cost of maintaining a post-tensioned bridge. There were some assumptions made in the previous section about how different post-tensioning materials might affect the service life of a bridge. The section will calculate a better approximation of the service life of a bridge using the post-tensioning materials studied in Project 0-4562.

8.2.2 Methodology

Some assumptions were made in calculating the estimated service life of a bridge using the materials evaluated in Project 0-4562. One assumption is that the mechanical

properties for the strands studied were all equivalent. The research conducted in Reference 13 found that the copper clad, stainless clad, stainless steel, and hot dip galvanized strands were found to not the meet the mechanical qualifications to be used as prestressing strands as outlined in Reference 15. This deficiency might be able to be overcome if the strand manufactures can improve the mechanical properties of these strand types to meet those standards. Several manufactures declared that this would be possible if enough quantity demand could be assured. The other assumption was that the couplers for the plastic duct could be improved to provide a positive water tight seal. This assumption is reasonable because the couplers manufactured now have improved substantially with regards to their water tightness and plastic pipe has been used in water transmission applications. The last assumption made was that a bridge with a post-tensioning system containing conventional strands and galvanized duct would have a service life of 50 years. Extensive surveys of the durability of current post-tensioned concrete in place and segmental bridges show that this is reasonable[36].

The contribution of the strand types to the service life was evaluated using the weight loss from passive corrosion testing performed in Reference 13. This is a better approximation of how the strand types will contribute to the service life of a bridge in an aggressive environment than the corrosion ratings from this thesis or from Reference 2 because the weight loss from the passive corrosion testing is quantitative whereas the corrosion ratings from the autopsies are qualitative and primarily based on observations and not measurements. To evaluate the contribution of the duct types, the average corrosion rating for galvanized ducts came from this series and the average damage rating for plastic ducts came from Reference 2. These two ratings were chosen because they were the highest values and thus least conservative in the two studies.

To determine the contribution of strand type to service life, the weight loss of the conventional strand from the passive testing was used as a baseline value and was divided by the weight loss of a given strand type to get a unit value for that strand type. To get the contribution of duct type to service life, the corrosion rating of the galvanized duct

was used as a baseline and was divided by the damage rating from the plastic duct and its own corrosion rating to get a unit value. The unit value for a strand type was summed with the unit value for a duct type. These combined unit values were then divided by the unit value from sum of conventional strand and the galvanized duct unit values. This combined unit value was then multiplied by 50 years to get a service life based on a service life of 50 years for a post-tensioning system with conventional strand and galvanized duct.

Example:

Service life of Bridge with hot dip galvanized strand and plastic duct

Weight loss of conventional strand from passive corrosion testing = W_{con}=10.13[13]

Weight loss of hot dip galvanized strand form passive corrosion testing = W_{gal} = 2.03[13]

Galvanized duct corrosion rating = C_{gal} =3400

Plastic duct damage rating = C_{pla} =284[2]

Convention strand unit value = $U_{cons} = W_{con} / W_{con} = 1$

Galvanized duct unit value = $U_{gal} = C_{gal} / C_{gal} = 1$

Hot dip galvanized strand unit value = $U_{gals} = W_{con} / W_{gal} = 5$

Plastic duct unit value = $U_{pla} = C_{gal} / C_{pla} = 12$

Sum of hot dip galvanized strand and plastic duct unit values = $U_{gp} = U_{gals} + U_{pla} = 17$

Sum of conventional strand and galvanized duct unit values = $U_{cg} = U_{cons} + U_{gal} = 2$

Combined unit value = $U_{comgp} = U_{gp} / U_{cg} = 8.5$

Service life with conventional strand and galvanized duct = SL_{cg} = 50 yrs.

Service life with galvanized strand and plastic duct = $SL_{gp} = U_{comgp} * SL_{cg}$ = 424 yrs.

8.2.3 Service Life and Analysis

Figure 8.4 shows the estimated service life for a post-tensioned bridge containing various combinations of post-tensioning components.

The strands encased in plastic duct showed substantial increase in service life when compared to the same strands encased in galvanized duct. The stainless steel, stainless clad, and copper clad strands had essentially the same service life when encased in the

same duct type. These strands had an average service life of 263 years when encased in galvanized duct and 537 years when encased in plastic duct. The hot dip galvanized strand tripled the service life when encased in galvanized duct and increased the service life to 424 years when encased in plastic duct. The post-tensioning system with flowfilled epoxy coated strands had the highest overall estimated service life of 721 years and when encased in galvanized duct had the highest estimated service life of 447 years when compared to the other strands encased in the same duct type.

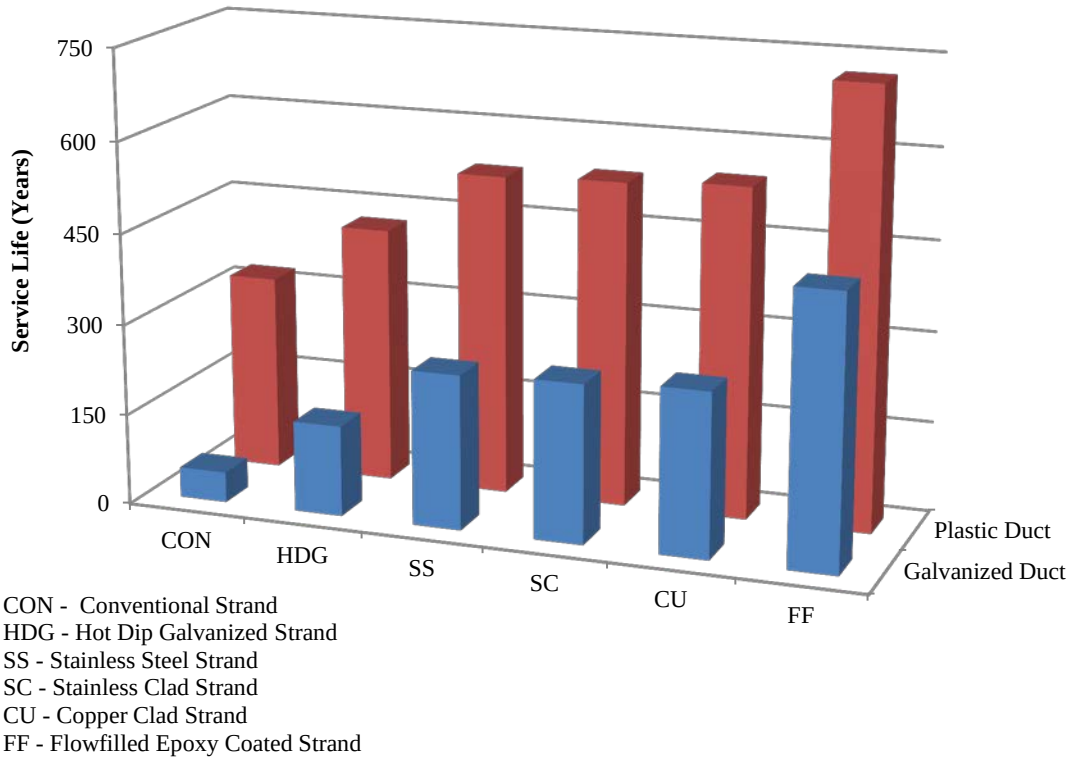

Figure 8.4: Service Life Estimate for a Bridge with Various Post-Tensioning Components

The results might seem excessive. However, the results do show that as the level of protection and the corrosion resistance of the strands go up, the service life of a bridge

would increase appreciably. If the service life increases then the cost of construction can be spread out over a longer span saving the customer money. Also, the research done in Reference 30 assumes that as corrosion resistance of the strands goes up the cost of maintenance would go down[30]. It should be noted that masonry bridges are still in service that were constructed by the Romans in antiquity. These structures were designed so that its elements would only experience compressive loads and that there would be no ferrous materials. That is why they are still in existence today. These service life estimates should NOT be used to estimate the service life of a structure because other factors might affect the service life of a structure as well. They simply indicate the relative effects of different post-tensioned system materials. Factors like the type of conventional reinforcement used (uncoated or epoxy coated), concrete quality, and type and quality of grout can affect the service life of a structure.

CHAPTER 9

Design Recommendations

9.1 Crack Control

The most severe damage to the longitudinal bars, transverse bars, and galvanized steel ducts was located near or at the locations of flexural cracks and longitudinal splitting cracks over the ducts. Nevertheless, chlorides will still migrate through the pore space of the concrete to the depth of the reinforcement, regardless if the post-tensioned elements of a structure are uncracked. This would greatly delay the onset and spread of corrosion but not stop it. Adequate cover of dense, nonporous concrete should always be used. Fully prestressed elements of a structure will have minimal flexural cracking if loads are below the design service loads. This is why it is recommended that post-tensioned elements of a structure be fully prestressed in an aggressive environment. Segmental construction should never use dry joints and tendon ducts should be positively sealed at joints.

9.2 Epoxy Coating of Mild Reinforcement

The use of epoxy coated reinforcement greatly reduced the secondary cracking due to expansion of corroding reinforcement. Coated bars should always be used in aggressive environments. The minimal corrosion observed on the epoxy coated steel reinforcement normally occurred at locations where it had come into contact with another component or the epoxy coating had been damaged in some fashion. The epoxy bars should be handled with the knowledge that the epoxy coating can be damaged to a point where the underlying steel is exposed. Defects that might arise during handling should be repaired with the appropriate repair compound before placement of concrete. A few of the instances of coating damage were caused by the epoxy coated tie wire used to attach bars and duct in assembly of the reinforcement cage. Therefore, to minimize

damage to the epoxy coating, it is recommended that the ties used to attach components to the coated bars be a robust plastic tie. It is recommended that the epoxy coated steel reinforcement meet the relevant ASTM standard and the epoxy coating meet the applicable TxDOT standard for thickness.

9.3 Duct Type

Due to the fairly wide spread corrosion of the galvanized duct, it is recommended that galvanized duct not be used in an aggressive environment. The greatly improved durability of the plastic ducts prevented the majority of the ducts from getting damaged during casting and post-tensioning and in the highly aggressive chloride exposure. Therefore, it is recommended that they always be used in aggressive environments. It must be noted that the continuous ducts with researcher installed grout vents allowed chlorides to infiltrate the duct through the poor quality vent seal. Therefore, all grout vents should be installed on couplers where specific provisions are made for the grout hose to have a positive water tight connection. Current grout vents are “welded” to the plastic duct or coupler as shown in Figure 7.7. As shown in Chapter 8, plastic ducts when used with conventional strands and non-galvanized anchorages increase the construction cost by only 0.1%. However, Chapter 8 also shows that the service life can be significantly increased when plastic ducts are used with conventional strands. Therefore, the extra construction cost can be spread over a longer service life and maintenance costs would be less, thus saving the customer money.

9.4 Coupler Type

Breaches in the seals between the ducts and the couplers and the poor bond of the heat shrink to the coupler or duct allowed chlorides to enter the plastic duct. All coupling of ducts must be positive water tight connections. The installation of the couplers and their components should be supervised by an inspector certified by ASBI, the Post-Tensioning Institute, or some equivalent thereof. TxDOT Standard Specification for pressure testing of the duct should be followed. It is recommended for internal

longitudinal ducts in segmental construction, that the duct couplers be installed at segment joints and a sealant applied to the inside of the couplers to protect the tendon from chloride infiltration. The sealant should be robust enough to maintain a seal during construction and sufficiently durable in a high alkaline environment throughout the service life of the bridge.

9.5 Grout Type

Due to the use of a hand pump to inject the grout into the duct of these small specimens, the grout was not always well consolidated and some large voids were observed. An anti-bleed and/or thixotropic grout should be used for internally bonded post-tensioned tendons. It should be mentioned that the prebagged grout used in the current study might have been contaminated with chlorides at a level very near the chloride limit before the grout was placed in the tendons. Therefore, it is recommended that the chloride levels of any grout used be considerably less than the chloride concentration threshold for corrosion. It is also recommended that the chloride concentration of the grout be determined before the grout is injected into the duct. TxDOT Standard Specification should be followed for the injection of grout into ducts.

9.6 Strand Type

The majority of the strands had minimal damage. Strand type should be chosen on the following criteria: cost, mechanical properties, availability, and contractor familiarity. The mechanical testing done in Reference 13 indicated that the mechanical properties of the copper clad, stainless clad, and stainless steel strand did not meet any of the Reference 15 specifications and the hot dip galvanized strand did not meet the mechanical specifications from Reference 15 for 270 ksi strands. However, the copper clad, stainless clad, and stainless steel strands showed great corrosion resistant properties in Reference 13 and this study. Therefore, it is recommended that the mechanical properties of these strands be improved to meet Reference 18 specifications before they are used in any post-tensioned structures. If flowfilled epoxy coated strand is chosen,

before coating the strand with flowfilled epoxy, the strand should be cleaned of all corrosion and/or dirt. It is recommended that the bare ends of the strands be coated with epoxy immediately after cutting to protect from the corrosion. Due to the corrosion observed on the conventional and hot-dip galvanized strands in this study, it is recommended that they be encased in an anti-bleed and/or thixotropic grout within water tight plastic duct if these strands are to be used in an aggressive environment. TxDOT specifications should be followed when installing and stressing strands. As shown in Chapter 8, the cost of using flowfilled epoxy with non-galvanized anchorages and plastic duct increases the cost of construction by 1.3%. However, if the corrosion observed in the flowfilled epoxy coated strand of this study is an anomaly, the service life of a bridge would increase very significantly. Therefore, the extra cost of construction can be spread over a longer time span and overall save the customer money. Like the flowfilled epoxy coated strands, the copper clad, stainless clad, and stainless steel strands increased the cost to a bridge. However, they also could increase the service life substantially and the increased construction cost would be spread over a longer time span, thus saving the customer money.

9.7 Anchorage Regions

The backfill mortar for the majority of the anchorage pockets had debonded from the base concrete and the resulting cracks allowed chlorides to enter the anchorage region. However, the majority of the chloride concentrations of the backfill mortar were below the corrosion threshold. This shows that the backfill mortar was well consolidated and performed as intended. However, the cracks at the interface of the backfill mortar and base concrete indicated that the primer and the epoxy was not installed correctly. These cracks also allowed moisture, oxygen, and/or chlorides to enter the anchorage region and cause corrosion. Therefore, it is recommended that all anchorage regions be detailed so the chance of chloride exposure is kept to a minimum. It is also

recommended that the manufacturer's specifications should be followed when applying the primer and epoxy and the placement of the backfill mortar.

9.8 Electrically Isolated Systems

The performance of the fully encapsulated specimens performed as well as the conventional specimens but certainly not as well as expected. This is possibly because of the inexperience of the research crew in assembling the more complex components. The AC impedance data suggested that the ducts were not water tight. The moisture that had been observed in the duct when the tendon was being cut from the anchorage plate and the chloride concentration of the grout supports the AC impedance data. The observed moisture and chloride concentrations came from poor bonding of the heat shrink to the duct and coupler and the poor seal of the coupler to the duct for all but one coupler region. The outlier is the duct that had a crack in the region of one of the couplers. For all the prior reasons, it is recommended that fully encapsulated systems be installed under the supervision of a certified inspector and personnel familiar with the system. The use of this system in a bridge may increase the service life of the bridge.

9.9 Half-Cell Potential Measurements

The presence of corrosion in some elements was able to be indicated by the half-cell potential measurements. However, the readings were not able to indicate which components were corroding and to what extent they had corroded. To accurately evaluate the corrosion in post-tensioned elements further research needs to be conducted in the area on non-destructive corrosion testing of post-tensioned elements.

9.10 AC Impedance

This method is only valid for electrically isolated tendons. If the tendons are properly installed and the correct monitoring equipment is used, this procedure would provide a straightforward means of determining the systems soundness. Nevertheless, to establish its reliability further testing needs to be conducted.

9.11 Chloride Content

The probability of corrosion for an unprotected component is high at a location with a chloride concentration of the concrete or grout that is above the corrosion threshold for that material. Chloride concentrations are not an accurate means of predicting corrosion in an element with epoxy coated reinforcement and/or plastic duct that is undamaged. Chloride concentrations cannot accurately predict the level or severity of corrosion.

CHAPTER 10

Summary, Conclusions, and Recommendations for Future Testing

10.1 Summary

Fourteen specimens were exposed to 6 years of aggressive recurring ponded salt solution exposure. Seven of these specimens had their dead end anchorage region sprayed with salt solution for 6 hours once a month. After the wet exposure cycle, non-destructive monitoring was conducted consisting of: half-cell potential measurements, AC impedance measurements (specimens with electrically isolated tendons), and periodic visual inspections. At the end of exposure testing, concrete and grout samples were taken to test for chloride concentration. After 6 years of exposure testing, the specimens were autopsied and all reinforcing components from the ponding area and the dead end anchorage regions from all specimens were examined for corrosion. The specimens that received the salt solution spray also had components from their live end anchorage region examined for corrosion.

10.2 Conclusions

10.2.1 Specimens

The reduced size of the specimens worked well compared to the Project 0-1405 specimens. All the specimens had medium scaling on the top surface and the edges of the ponding area of the specimens. The majority of the anchorage region backfill mortar had debonded from the base concrete. Some of the corbel re-entrant corners had cracks that had not been present at time of live load application. The repairs to the cracks in the corbel re-entrant corners that had been present immediately after live load were in good repair. However, some of the repairs had signs of efflorescence and moisture around the repair.

10.2.2 Strand Type

In general, the strands had low levels of corrosion. The high chloride concentrations in the grouts indicate that chlorides were able to migrate through the grout at the level of the strands. The level of corrosion in the strands from the anchorage regions was similar to the level of corrosion in the ponding area. Some strand types did not meet some of the Reference 15 requirements for the yield and ultimate strengths of grades 250 and 270 strand types.

10.2.2.1 Conventional Strand

The outer wires of the conventional strands had light corrosion and where no corrosion was present discoloration was observed. The observed corrosion on the inner wires was more severe than the outer wires with more incidences of moderate corrosion and minimal pitting. The condition of the strands from the anchorage region was similar to the condition of the strands from the ponding region. The mechanical properties of this strand type met Reference 15 specifications[13]. Chapter 8 showed that encasing conventional strands in plastic ducts instead of galvanized ducts and anchoring against non-galvanized anchorage plates would result in an approximately 0.1% increase in construction cost of a bridge. However, this combination would result in a substantial increase in service life.

10.2.2.2 Hot Dip Galvanized Strand

The outer wires on the galvanized strand had signs of the zinc and underlying steel corroding and the inner wires showed signs of the steel corroding where the galvanized coating had not covered the underlying steel, specifically the interstitial space between the outer and inner wire. The condition of the strands in the anchorage regions was similar to the condition of the strands from the ponding area. The bond of the grout to the strand was very strong due to the rough nature of the galvanized coating. This increased the effort that it took to remove the grout. The mechanical properties were only sufficient enough to meet the grade 250 specifications for yield and ultimate strengths from Reference 15[13]. Chapter 8 showed that, the use of hot dip galvanized strands

encased in plastic duct instead of galvanized duct with non-galvanized anchorage plates would result in an increase of the construction cost by 0.9%. However, this would increase the service life considerably.

10.2.2.3 Copper Clad Strand

The outer and inner wires of the copper clad strands had a very dark brown discoloration along the length of the wires. Also, occasional tiny reddish colored spots were observed on the copper clad wires. The strands in the anchorage region were similar to the condition of strands from the ponding region. All in all the strands performed well in regards to their corrosion resistant properties. The mechanical properties of these strands were not sufficient to meet any of the specifications of Reference 15[13] for yield and ultimate strengths of both grades 250 and 270 strand types. Chapter 8 showed that when copper clad strands are encased in plastic duct instead of galvanized duct and were anchored against non-galvanized anchorage plates, the cost of construction would increase by approximately 4.3%. However, the service life would be lengthened immensely.

10.2.2.4 Stainless Steel Strand

A few spots of discoloration and light corrosion were observed on the stainless steel strands. Other than those few spots the strands were in immaculate condition. Staining was greater in the end regions. This is more than likely because the anchor heads had to be heated to extract the strands. The strands retracted into the grout after cutting the specimens apart. This was due to the poor bond between the grout and strand. The mechanical properties of these strands were not sufficient to meet any of the specifications of Reference 15[13] for yield and ultimate strengths of both grades 250 and 270 strand types. Chapter 8 showed that when stainless steel strands are encased in plastic duct instead of galvanized duct and were anchored against non-galvanized anchorage plates, the cost of construction would increase by approximately 7.7%. However, the service life would be lengthened immensely.

10.2.2.5 Stainless Clad Strand

The condition of the stainless clad strands was similar to the condition of the stainless steel strands with a few spots of discoloration and light corrosion. The heat treatment of the anchor heads to remove the strand might have caused the discoloration that had been observed in the strands from the anchorage region. The grout bonded better with the stainless clad strands than it did with the stainless strands. The mechanical properties of these strands were not sufficient to meet any of the specifications of Reference 15[13] for yield and ultimate strengths of both grades 250 and 270 strand types. Chapter 8 showed that when stainless clad strands are encased in plastic duct instead of galvanized duct and were anchored against non-galvanized anchorage plates, the cost of construction would increase by approximately 1.8%. However, the service life would be lengthened immensely.

10.2.2.6 Flowfilled Epoxy Coated Strand

The flowfilled epoxy coated strand did not perform as well as initially expected. The inner and outer wires had corrosion ranging from mild pitting to light corrosion over the majority of their lengths. There seems to be two possibilities for the origin of this very light corrosion and mild pitting. The first of these is that this corrosion might have been induced by the paint stripper used to remove the epoxy. However, the experiment that was performed on two lightly polished wires from a conventional strand exposed to the paint stripper for seven days showed no further corrosion or pitting on the wires. This indicated that the second possibility was more likely. That is that the corrosion probably existed before the strand was coated. The condition of the epoxy coating was good with a tiny hole, slight scratches, and slight gouges.

The underlying strand is the same as the conventional strand so the mechanical properties were equivalent to the conventional strand. Therefore, the strands met all Reference 15 mechanical specifications[13]. Chapter 8 showed that when flowfilled epoxy coated strands are encased in plastic duct instead of galvanized duct and were anchored against non-galvanized anchorage plates, the cost of construction would increase by approximately 1.4%. However, the service life would be lengthened immensely. This is

assuming that the corrosion that had been observed during this study was an anomaly and the strand would have had the same corrosion resistances as indicated in Reference 13.

10.2.3 Duct Type

10.2.3.1 Galvanized Steel Duct

The galvanized corrugated steel ducts did not hold-up well under the corrosive environment experienced. At locations of bleed water voids in the grout, the galvanized duct had substantial area loss and severe corrosion. In areas without area loss, pitting and moderate corrosion was observed over large portions of the duct. Also, the areas with the most damage were at locations in close proximity to the specimen's transverse cracks.

10.2.3.2 Plastic Duct

Slight gouging was observed in the interior of all the plastic ducts. These slight gouges were either from the strand being threaded through the duct and/or the strands rubbing against the duct during stressing. Even with these scratches and gouges, the integrity of the duct was not compromised. However, chloride concentrations were very elevated in the continuous ducts. This suggests that grout vents should be an integral part of the coupler and for utmost water tightness grout hoses should have a positive attachment to the grout vent. The grout chloride concentration in the coupled one-way duct was approximately twice that of the grout chloride concentrations in the coupled two-way ducts. This indicates that the snap-on coupler on the one-way duct had not been as water tight as the heat shrink wrapped slip-on coupler of the two-way ducts. The bleed water voids in the grout encased in the one-way ducts were slightly larger than the bleed water voids in the grout encased in two-way ducts. This indicates that the two-way ducts were somewhat more efficient at allowing air to escape during grouting operations than the one-way ducts. Most of the plastic coupled ducts had longitudinal cracking in the concrete above the duct. This was from the reduced concrete cover over the coupler and the vastly different thermal coefficients of the plastic coupler/duct and concrete. Chapter 8 showed that the cost of construction would increase by varying amounts depending on

the strand type and type of anchorage plate used. For example, a bridge using conventional strands anchored against galvanized anchorage plates and encased in plastic ducts would have a 0.2% increase in construction cost. However, the service life would increase substantially no matter what strand type was used.

10.2.4 Coupler Type

All of the plastic ducts with couplers had grout chloride concentrations well above the corrosion threshold. This indicates that the seals of the mechanical snap-on couplers were inadequate and the bond of the heat shrink for the slip-on couplers was not sufficient enough to keep out chlorides.

10.2.5 Anchorage Type

In this limited time of exposure there was no significant difference between the performance of the galvanized and non-galvanized anchorage plates. The quality of the backfill mortar and the bond of the backfill mortar to the base concrete had a more significant role in the protection of the anchorage region than the anchorage plates did.

10.2.6 Fully Encapsulated System

Except for the region with mild pitting, the corrosion of the conventional strands in the electrical isolated tendons was similar to corrosion of the conventional strands in the conventional post-tensioning system. Except for the apex of the duct, the grout chloride concentrations were well above the corrosion threshold. At the apex of the duct the chloride concentrations were very near to the corrosion threshold. These chloride concentrations suggest that the poor bond of the heat shrink and poor seal of the coupler had allowed chlorides to enter the duct. When the tendon was being cut from the anchorage plate moisture was observed. This supports the AC impedance data that suggested that the integrity of the duct had breached in some fashion. Chapter 8 showed that, the cost of using this system on a bridge would increase the cost of a bridge by appreciable amounts depending on the strand type. No analysis was done on how this system would affect the service life of a bridge.

10.2.7 Accuracy of Non-Destructive and Destructive Measurements

10.2.7.1 Half-Cell Potential Measurements

The half-cell potential readings were capable of predicting the presence of corrosion. However, the readings were not able to predict the severity of the corrosion or which component was corroding.

10.2.7.2 AC Impedance

The AC impedance data suggests that the electrically isolated tendons were not monitorable and at least that moisture had entered the duct. Moisture entering the duct was confirmed when moisture was observed in the duct when the tendon was cut from the anchorage plate. AC impedance measurements can also indicate that a duct might have lost integrity. However, since the monitorability was in question it cannot be definitively said that the AC impedance data indicated that the ducts had lost integrity.

10.2.7.3 Concrete Chloride Samples

The majority of the concrete chloride concentrations from the ponding area at the level of the epoxy coated bars were above the corrosion threshold and all bars had some form of corrosion. However, chloride concentrations cannot accurately predict the severity of the corrosion.

10.3 Recommendations for Future Testing

- Due to the corrosion of the uncoated Dywidag bars used to apply external load, it is recommended that the Dywidag bars be epoxy coated. This will allow the Dywidag bars to be safely and more easily removed.
- To track the infiltration of the chlorides into the specimen and possibly into the duct, it is recommended that a dye be used in the salt solution. The dye should not affect how the chlorides react with metals and/or add any additional chlorides to the solution.
- Grout mixes need to continue to be developed that minimize bleed water voids. Controlling the amount of chlorides in a grout needs to be

paramount because the grout should not be the first source of chlorides that a tendon experiences.

- The chloride concentration of the grout should be determined before exposure testing begins. The grout in this study did not have its chloride concentration determined until the end of exposure testing. Therefore, no baseline for the chloride concentration existed.
- A study needs to be done on how to minimize the cracking in a post-tensioned element from the effect of the different thermal coefficients between the plastic duct and the concrete.
- There is a need to improve the current non-destructive testing methods and develop improved non-destructive testing methods for post-tensioned elements.
- The mechanical properties of the strands that did not meet Reference 15 mechanical specifications but had excellent corrosion resistant properties need to be improved to take advantage of their corrosion resistant properties.

APPENDIX A

All Project 0-4562 specimens are listed below. The naming system outlined in Chapter 2 is used to identify the specimens.

Casting Group	Specimen Name	Specimen Identification
T	T.1	TEST-GA-CON-CS-CG-T
	T.2	TEST-NGA-CON-CS-CG-T
1	1.1	NGA-CON-CS-CG-1
	1.2	NGA-CU-CS-CG-1
	1.3	NGA-SC-CS-CG-1
	1.4	GA-CON-CS-CG-1
2	2.1	NGA-FF-CS-CG-2
	2.2	NGA-HDG-CS-CG-2
	2.3	NGA-CON-1P-CG-2
	2.4	NGA-CU-1P-CG-2
3	3.1	NGA-CON-2P-CG-3
	3.2	NGA-HDG-2P-CG-2
	3.3	NGA-CU-2P-CG-3
	3.4	NGA-HDG-1P-CG-3
4	4.1	NGA-SS-CS-CG-4
	4.2	NGA-SS-1P-CG-4
	4.3	Comparison-Epoxy-4
	4.4	Comparison-Uncoated-4
5	5.1	GA-CON-2P-CG-5
	5.2	NGA-SC-2P-CG-5
	5.3	NGA-SS-2P-CG-5
6	6.1	NGA-EG-CS-CG-6
	6.2	NGA-EG-1P-CG-6
	6.3	NGA-EG-2P-CG-6
7	7.1	EIT-CON-CG-7
	7.2	EIT-CON-CG-7
	7.3	EIT-HDG-CG-7
	7.4	EIT-FF-CG-7

= 4 year Autopsy Specimens

= 4 year Autopsy Specimens

Appendix B

Listed below are all the material suppliers for the Project 0-4562 specimens.

Material	Supplier	Contact
Bearing Plates	VSL USA	Jordan Stephenson jstephenson@vsl.net 817-545-4807
Galvanized Steel Duct		
PT Plus Plastic Duct and Couplers		
Hot Dip Galvanized Strand*		
0.6" Strand Anchor Heads		
Wedges		
EIT Systems*	VSL Switzerland	Hans-Rudolf Ganz hansrudolf.ganz@vsl.com
76mm One-Way Ribbed Plastic Duct*	GTI	Joe Harrison joe.harrison@gti-usa.com 281.240.0550
76mm Couplers*		
85mm Two-Way Ribbed Plastic Duct*		
85mm Coupler*		
Stainless Strand*	Techalloy	Jim Beitz jbeitz@techalloy.com 815.923.2131
Stainless Clad Strand*	DSI	Ron Bonomo ron.bonomo@dsiamerica.com
Copper Clad Strand*	Copperweld	Milton Lamb mlamb@copperweld.com info@copperweld.com
Epoxy Coated Strand*	Sumiden Wire	Steve Yoshida stevey@sumiden.com
Type V Epoxy*	Unitex	Susan Wintz 816.231.7700
Epoxy Coated Rebar	ABC Coating	Mary Boyette 972.937.9841 orders@abccoatingtx.com
Concrete	Capitol Aggregates	Ron Taff

* - Material Donated to Research Project

References

1. Ahern, M.E., “Design and Fabrication of a Compact Specimen for Evaluation of Corrosion Resistance of New Post-Tensioning Systems,” M.S. Thesis, The University of Texas at Austin, May 2005.

2. McCool, Gregory E., “ Evaluation of Corrosion Resistance of New and Upcoming Post-Tensioning Materials After Long-Term Exposure Testing,” M.S. Thesis, The University of Texas at Austin, December 2010.

3. Mac Lean, Sean, “Comparison of the Corrosion Resistance of New and Innovative Prestressing Strand Types used in the Post Tensioning of Bridges,” M.S. Thesis, The University of Texas at Austin, May 2008.

4. Kalina, Ryan D., “Comparative Study of the Corrosion Resistance of Different Prestressing Strand Types for use in Post-Tensioning of Bridges,” M.S. Thesis, The University of Texas at Austin, May 2009.

5. Salas, R.M., “Accelerated Corrosion Testing, Evaluation, and Durability Design of Bonded Post-Tensioned Concrete Tendons,” Ph.D. Dissertation, The University of Texas at Austin, August 2003.
6. Schokker, A.J., “Improving Corrosion Resistance of Post-Tensioned Substructures Emphasizing High-Performance Grouts,” Ph.D. Dissertation, The University of Texas at Austin, May 1999.

7. Turco, G.P., “Durability Evaluation of Post-Tensioned Concrete Beam Specimens After Long-Term Aggressive Exposure Testing,” M.S. Thesis, The University of Texas at Austin, August 2007.

8. West, J.S., “Durability Design of Post-Tensioned Bridge Substructures,” Ph.D. Dissertation, The University of Texas at Austin, May 1999.

9. Summer, Eric, VSL Regional Director, Phone interview and email correspondence, May 2012.

10. Rowan, Robert, Owner Robt. L. Rowan, Phone Interview, May 2012.

11. Harrison, Joe, GTI representative, Phone interview, May 2012.

12. Texas, Department of Transportation, “Standard Specifications for Construction and Maintenance of Highways, Streets, and Bridges,” 2004.

13. Kalina, Ryan, Mac Lean, Sean and Breen, J.E., “Comparative Study of Mechanical and Corrosion Resistance Properties of Bridge Post-Tensioned Strands," Center for Transportation Research Bureau of Engineering Research, The University of Texas at Austin, August 2011

14. ASTM, “Standard Test Method for Testing of Wire Ropes and Strand,” ASTM A 931, American Society for Testing and Materials, Philadelphia, PA, 2002.

15. ASTM, “Standard Specification for Steel Strand, Uncoated Seven-Wire for Prestressed Concrete,” ASTM A 416/A 416M, American Society for Testing and Materials, Philadelphia, PA, 2006.

16. ASTM, “Standard Test Method for Determining Effects of Chemical Admixtures on the Corrosion of Embedded Steel Reinforcement in Concrete Exposed to Chloride Environments,” ASTM G109-07, American Society for Testing and Materials, Philadelphia, PA, 2007.

17. ACI Committee 222, “Corrosion of Metals in Concrete” (ACI 222R-01), American Concrete Institute, Farmington Hills, MI, 2001.

18. ASTM, “Standard Test Method for Corrosion Potentials of Uncoated Reinforcing Steel in Concrete,” ASTM C876-09, American Society for Testing and Materials, Philadelphia, PA, 2009.

19. fib Bulletin 33, “Durability of Post-Tensioning Tendons,” Fèdèration Internationale du Bèton, Lausanne, Switzerland, 2006.

20. Elsener, B., “Monitoring of Electrically Isolated Post-Tensioning Tendons,” Structural Concrete: Journal of the fib, Vol. 6, No. 3, September 2005

21. Ganz, H.R., Email Correspondence, November 5, 2010.

22. ASTM, “Standard Test Method for Acid-Soluble Chloride in Mortar and Concrete,” ASTM C 1152/C1152M-04, American Society for Testing and Materials, Philadelphia, PA, 2004.

23. Bundesamt für Strassen, “Massnahmen zur Gewährleistung der Dauerhaftigkeit von Spanngliedern in Kunstbauten,” ASTRA Richtlinie 12 010, 2007.

24. ACI Committee 201, “Guide for Conducting a Visual Inspection of Concrete in Service” (ACI 201.1R-08), American Concrete Institute, Farmington Hills, MI, 2001.

25. SIKA, “SikaGrout 300 PT Product Specification,” Sika Concrete Restoration Systems.

26. Frank, D., “FM 2031 Bridge, GIWW,” U.S. Coast Guard Office of Waterways Management: Bridge Program Division, Presentation to U.S. Department of Homeland Security, August 14, 2009.

27. Turco, G.P., Email Correspondence, October 15, 2010.

28. Corven, J. and Moreton, A, “Post-Tensioning Tendon Installation and Grouting Manual,” Federal Highway Administration, Tallahassee, FL, May 26, 2004.

29. Van Lunduyt, D., "The Gulf Intracoastal Waterway Bridge at Matagorda, Texas," Aspire: The Concrete Bridge Magazine, Winter 2010, pp. 20-23.

30. Grau, K.A., "Survey of Costs, Economic Analysis, and Design Guidelines for Corrosion Protection Methods for Post-Tensioned Concrete Bridges," M.S. Thesis, The University of Texas at Austin, May 2005.

31. Bongers, Michiel P.H, Koch, Gerhardus H., Payer, J.H., Thompson, Neil G., Virmani, Y. Paul, *"Corrosion Costs and Prevention Strategies in the United States"*, NACE International, Houtson, Texas, 2002.

32. Standing Committee on Structural Safety, *"Seventh Report of the Committee"*, July 1987.

33. Corven Engineering, Inc.,*"New Directions of Florida Post-Tensioned Bridges"*, Florida Department of Transportation, Tallahassee, FL, February, 2002.

34. Montemor, M. F., Simoes, A.M.P., Ferreira, M.G.S., "*Chloride-induced corrosion on reinforcing steel: from the fundamentals to the monitoring techniques"*, Cement and Concrete Composites 25, Elsevier, 2003.

35. Jones, Denny A., *"Principles and Prevention of Corrosion"*, Prentice Hall, Upper Saddle River, NJ, 1996.

36. Pielstick, Brett, *"Durability Survey of Segmental Concrete Bridges"*, 3rd Edition, American Segmental Bridge Institute, Buda, TX, 2007